UNIVERSITY OF CALIFORNIA
RIVERSIDE

Regulation of Hippocampal Synapse Formation and Function by Astrocytic Ephrin-B1: From Early Postnatal Development to Adulthood

A Dissertation submitted in partial satisfaction
of the requirements for the degree of

Doctor of Philosophy

in

Neuroscience

by

Amanda Quetran Nguyen

December 2019

Dissertation Committee:
Dr. Iryna M. Ethell, Chairperson
Dr. Peter W. Hickmott
Dr. Andre Obenaus

The Dissertation of Amanda Quetran Nguyen is approved:

_____

_____

_____

Committee Chairperson

University of California, Riverside

Acknowledgements

The work described in this doctoral dissertation could only be completed due to the efforts of many. First and foremost, I would like to express my deepest gratitude to my advisor, Dr. Iryna Ethell, who has supported me throughout my graduate study. Her patience, guidance, encouragement, and dedication to my scientific career have been with me during my time at UC Riverside. Dr. Ethell gave me the opportunity and the freedom to explore my own research interests. She would challenge me both scientifically and intellectually while still providing the support I needed. Thank you, Dr. Ethell, for always supporting me and helping me grow as a scientist and as a person!

I would also like to express my deepest appreciation to my committee members, Drs. Andre Obenaus and Peter Hickmott. Over the years, they have provided tremendous helpful guidance and feedback on my work. In collaboration with Dr. Obenaus, I learned how to do extracellular field recordings at Loma Linda University, starting my career as an electrophysiologist. Without Dr. Hickmott, I never would have mastered blind whole-cell patch recordings! The wealth of knowledge between these two is immense. Thank you for always encouraging me even when I had my doubts.

I would like to thank my lab members (and the Razak lab) for all their support through the years. Their constant support, morning Starbucks runs, tea times, interesting (and sometimes odd) musings kept me going and made my experience so unforgettable. I would like to thank a few people in particular: Dr. Jordan Koeppen, thank you for choosing me from all the rotating students to work on the ephrin project with you! You've been there since day one, teaching me the bread and butter of the lab. Dr. Teresa

Wen, thank you for always keeping me in the loop of the world when I'd sometimes forget there is more to life than lab. Dr. Anna Kulinich, thank you for always supporting me and having so much confidence in me. Dr. Patricia Pirbhoy, thank you for sharing your wealth of knowledge of all things with me. Arnold Palacios, thanks for keeping the lab together and functioning (and the undergraduates in line). Maham Rais, thank you for always letting me vent when I needed it most. I'd like to also thank all the undergraduates that have worked with me; without this team a lot of this work would still be unprocessed and unanalyzed. It has been an absolute pleasure working with you all.

Lastly, for their endless support and encouragement, I would like to thank my family. My parents Minh Nguyen and Mychan Pham raised me and always believed in me even when they did not quite understand everything I was doing. I would not be here without their endless support, care, and love. Thank you to my brothers, Steve Nguyen and Kevin Nguyen, who always kept me entertained. I would also like to thank my number one supporter and partner, Justin Alan Bass. Thank you for keeping me grounded. It has been a long journey and your constant presence, patience, support, encouragement, and unwavering love kept me going and now I am finally done! My family, this would not have been possible without each and every one of you.

The text of this dissertation and figures in part is a reprint of the material as it appears in Journal of Neuroscience, 2018. The co-author Iryna M. Ethell listed in that publication directed and supervised the research which forms the basis for Chapter 3 of this dissertation. I collaborated and co-authored with Jordan Koeppen to characterize the

synaptic changes following astrocytic ephrin-B1 deletion during adulthood. I collected the electrophysiology data, including extracellular field recordings and whole-cell patch clamp recordings. As well, I isolated hippocampal synaptosomes to probe for AMPA-receptor subunits, GluR1 and GluR2, using western blot analysis. Jordan Koeppen characterized excitatory pre- and post-synaptic changes identified by vGlut1 and PSD-95 expression and dendritic spine labeling.

The citation is as follows:

Koeppen J, Nguyen AQ, Nikolakopoulou AM, Garcia M, Hanna S, Woodruff S, Figueroa Z, Obenaus A, Ethell IM. 2018. Functional consequences of synapse remodeling following astrocyte-specific regulation of ephrin-B1 in adult hippocampus. Journal of Neuroscience. 5710-5726.

ABSTRACT OF THE DISSERTATION

Regulation of Hippocampal Synapse Formation and Function by Astrocytic Ephrin-B1: From Early Postnatal Development to Adulthood

by

Amanda Quetran Nguyen

Doctor of Philosophy, Graduate Program in Neuroscience
University of California, Riverside, December 2019
Dr. Iryna M. Ethell, Chairperson

Neurons communicate with each other through synaptic connections. During development, it is essential that synapses undergo structural and functional modification. Improper development of neural connections can lead to neurodevelopmental disorders such as autism and intellectual disabilities. The synapse development process is comprised of three major steps: synaptogenesis, synapse pruning, and synapse stabilization. This refined process involves several key players, including astrocytes that come into close association with synapses, forming a tripartite complex with the pre- and postsynaptic structures. This association allows astrocytes to monitor and alter synaptic functions. Astrocytes communicate with synapses through either secreted factors or contact-mediated interactions. Release of specific astrocyte-derived gliotransmitters can affect both the structure and function of neurons. Besides affecting synaptogenesis and function, astrocytes are also involved in pruning of unnecessary synapses through

contact-mediated phagocytosis; however, the exact “eat me” signal is still not known. My research investigates the role of astrocytic ephrin-B1 regulation of hippocampal synapses during early postnatal development, adulthood, and learning and memory consolidation. Ephrin-B1 is a membrane bound protein that acts as a ligand for EphB receptors, allowing for bi-directional signaling through cell-cell interactions. Astrocyte-neuronal interactions may allow astrocytes expressing ephrin-B1 to find and engulf synapses that are marked for removal by targeting unoccupied EphB receptors. Therefore, hippocampal circuitry may be modulated through the Eph/ephrin interaction between neuron and astrocytes. My studies indicate that astrocytic ephrin-B1 is a negative regulator of synapse formation. During early postnatal development, astrocytic ephrin-B1 is essential for proper excitatory/inhibitory (E/I) circuit formation, as loss of astrocytic ephrin-B1 resulted in enhanced excitatory function of CA1 pyramidal cells and diminished inhibitory function. Dysregulation of E/I balance impaired sociability and increased repetitive behaviors. In contrast, in adulthood astrocytic ephrin-B1 maintains synapse numbers. Ablation of astrocytic ephrin-B1 in adulthood resulted in increased excitatory synaptogenesis, particularly of immature synapses. Overabundance of immature synapses reduced CA1 pyramidal cell excitatory function. Interestingly, astrocytic ephrin-B1 functions in an activity dependent manner, specifically modulating synapse formation on activated neurons during learning and memory consolidation and recall. Together, these results suggest that astrocytic ephrin-B1 influences hippocampal circuits by restricting synapse formation.

Table of Contents

List of Figures

Chapter 1

Chapter 2

List of Tables

List of Abbreviations

AAV: adeno-associated virus

ACM: astrocyte-conditioned medium

ACSF: artificial cerebral spinal fluid

AMPA: α-Amino-3-hydroxy-5-methyl-4-isoxazolepropionic acid

AMPAR: AMPA receptor

ASD: autism spectrum disorder

ATP: adenosine-5'-triphosphate

BDNF: brain derived neurotrophic factor

CA1: *Cornu Ammonis* 1 region of the hippocampus

Ca^{2+}: calcium ions

CA3: *Cornu Ammonis* 3 region of the hippocampus

Cre: Cre recombinase

CS: conditioned stimulus

D-AP5: D-(-)-2-Amino-5-phosphonopentanoic acid

DAPI: 4′,6-diamidino-2-phenylindole

DG: dentate gyrus

DiI: 1,1′-dioctadecyl-3,3,3′,3′-tetramethylindocarbocyanine perchlorate

DNA: deoxyribonucleic acid

E/I: excitatory/inhibitory

E: embryonic day

Efnb1: ephrin-B1

EphA R: ephrin A receptor

EphB R: ephrin B receptor

EPSC: excitatory postsynaptic current

ERT2: estrogen receptor 2

fEPSP: field excitatory postsynaptic potential

FV: fiber volley

GABA: γ-Aminobutyric acid

$GABA_A$: GABA receptor α5 subunit

GAD65: glutamic acid decarboxylase 65

GAPDH: glyceraldehyde-3-phosphate dehydrogenase

GFAP: glial fibrillary acidic protein

GFP: green fluorescent protein

GLAST: glutamate-aspartate transporter

GLT1: glucose transporter 1

GluA1: glutamate ionotropic receptor AMPR type subunit 1

GluA2/3: glutamate ionotropic receptor AMPR type subunit 2/3

HDAC: histone deacetylase

HRP: horseradish peroxidase

I/O: input-output

IP: intraperitoneally

IPSC: inhibitory postsynaptic current

KO: knock-out

LTD: long-term depression

LTP: long-term potentiation

mEPSC: miniature EPSC

Mg^{2+}: magnesium ions

mIPSC: miniature IPSC

NBQX: 2,3-dihydroxy-6-nitro-7-sulphamoyl-benzo(F)quinoxaline

NMDA: N-methyl-D-aspartate receptor

NMDAR: NMDA receptor

NO: nitric oxide

NR1: NMDA receptor subunit 1

NR2B: NMDA receptor subunit 2B

OE: overexpression

P: postnatal day

PBS: phosphate-buffered saline

PCR: polymerase chain reaction

PFA: paraformaldehyde

PKC: protein kinase C

PPF: paired-pulse facilitation

PPI: paired-pulse inhibition

PS: population spike

PSD95: postsynaptic density 95

PV: parvalbumin

RGC: retinal ganglion cells

S1: mouse stranger 1

S2: mouse stranger 2

SC: Schaffer collaterals

SO: stratum oriens layer of the hippocampus

SP: stratum pyramidale layer of the hippocampus

SPARC: secreted protein acidic and rich in cysteine

SR: stratum radiatum layer of the hippocampus

SLM: stratum lacunosum-moleculare layer of the hippocampus

TAM: tamoxifen

TBS: tris-buffered saline

TGF-β: transforming growth factor β

TNF-α: tumor necrosis factor-α

TSP: thrombospondin

TTX: tetrodotoxin

US: unconditioned stimulus

VGAT: vesicular GABA transporter

vGlut1: vesicular glutamate transporter 1

VP: viral particles

WT: wild-type

Chapter 1 : Introduction

1.1 Synapse Development

The synapse development process, which occurs prenatally through adulthood, is a series of growth and remodeling. Synapse development is comprised of three different stages: synaptogenesis, synapse pruning, and synapse stabilization. Synaptogenesis is a multi-step process of forming new synapses that involves the coordination of cell morphological changes (Garner et al., 2002). Synaptogenesis involves ligand-receptor interactions and intracellular signaling cascades that instruct synapse formation. During this process, one neuron will receive thousands of synaptic inputs. Since not all synapses are necessary, the synapse pruning phase commences. During synapse pruning, exuberant synaptic connections are eliminated allowing for increased efficiency of neuronal transmission and to ensure establishment of an organized functional circuitry (Cowan et al., 1984; Luo and O'Leary, 2005). Synaptic pruning is not random; weakly reinforced, redundant, or undesirable connections are pruned away while more active synapses are reinforced. Informed by our experience, neural activity drives the synapse strengthening and maturation through the pre- and post-synaptic differentiation, thus establishing refined neural circuits. Even after the formation and maturation of neuronal circuits, the synaptic connections remain plastic, which refers to their ability to undergo structural and functional changes. Through synaptic plasticity, strength between two connecting neurons can undergo changes based on the fluctuations in neuronal activity and the environment. While synapses are highly plastic and can frequently change during early development, synaptic plasticity is less frequent, but is still observed in the adult brain (Yasumatsu et al., 2008). Synaptic plasticity is regulated through several mechanisms,

including the modulation of both post-synaptic receptors and pre-synaptic release of neurotransmitters that can undergo short- or long-term changes. Short-term plasticity refers to changes that can occur up to milliseconds to minutes as seen during depression or facilitation of neurotransmitter release (Abbott and Regehr, 2004). Long-term plasticity are changes in synaptic strength that persist over a span of hours, days, weeks, or even months. These longer term changes can be observed at the level of a single synapse, a cell, or a circuit (Abraham, 2003). Cellular form of long-term plasticity can be observed in a form of long-term potentiation (LTP) or long-term depression (LTD), which are suggested to underlie learning and memory.

1.2 Learning & Memory

The hippocampus is essential for the formation of new memories and life-long learning (Milner et al., 1998; Neves et al., 2008) due to its highly plastic nature. The landmark paper by Scoville and Milner (1957) first described the hippocampus as a region necessary for formation of new memories, detailing their findings from a patient known by his initials, H.M. Patient H.M. underwent bilateral hippocampal removal for treatment of intractable epilepsy. Following this treatment, patient H.M. experienced a permanent loss of ability to encode new information into long-term memory. From here, a plethora of studies have gone on to show how the hippocampus is essential for learning and memory. The hippocampus has a very conserved trisynaptic circuit, comprised of three major cell groups: granule cells in the dentate gyrus (DG), pyramidal cells in the CA3, and pyramidal cells in the CA1. The trisynaptic circuit begins at the entorhinal

cortex providing the major cortical input into the hippocampus. The entorhinal cortex sends its strongest projections via the performant pathway to the DG region; the DG projects to the CA3 region via the mossy fiber pathway; the CA3 projects to the CA1 region via the Schaffer Collateral pathway; then finally the CA1 projects back to the entorhinal cortex, completing the loop (Knierim, 2015). These circuits of the hippocampus remain plastic throughout life, allowing for life-long learning (May, 2011; Lovden et al., 2013). As such, hippocampal synapses must undergo constant synapse formation, pruning, and restructuring. Despite the plethora of studies, there are still many unknown factors that contribute to learning and memory.

1.3 Astrocytes

Astrocytes, star-shaped glial cells, are more than just support players in brain processing. Astrocytes are well equipped and uniquely positioned to engage in a dynamic two-way communication with neurons. The partnership between neurons and astrocytes takes place across the nervous system and has been found to be essential for the formation, maintenance, and remodeling of the brain connectivity. The importance of this association can be seen from early prenatal effects of glial cells on neuronal migration and differentiation to glial effects in diseases. Astrocytes have a multitude of functions, ranging from organizing and maintaining brain structure and function to modulating information processing and signal transduction in the brain by influencing synapse functions in the central nervous system (Barker and Ullian, 2010). Astrocytes can

regulate synapse development and plasticity via contact-mediated interactions with neurons and through astrocytic secretion factors.

1.3.1 Astrocyte gliotransmission

During the synaptogenic period, astrocytes have been found to produce and secrete factors that promote synaptogenesis (Eroglu and Barres, 2010). These glial cells also contribute to the pruning and clearing processes of unwanted axons and synapses by phagocytosis (Chung et al., 2013). In addition, astrocytes are able to regulate synapse plasticity through the secretion of growth-promoting and growth-inhibiting molecules (Bezzi and Volterra, 2001; Perea and Araque, 2007; Henneberger et al., 2010). Neuronal signaling to astrocytes is also important in the regulation of synapse development. Astrocytes are highly sensitive to changes in neuronal activity and can respond to changes in neurotransmitter release at synapses by generating elevations of intracellular Ca^{2+} concentrations, which can result in gliotransmission and signaling back to neurons (Fellin and Carmignoto, 2004). Astrocytes, like neurons, have the ability to package and release transmitters. The release of gliotransmitters is Ca^{2+} dependent: vesicle fusion and exocytosis are triggered by intracellular cascades of Ca^{2+} and involves SNARE formation (Zhang et al., 2004; Montana et al., 2006; Li et al., 2008; Liu et al., 2011). Gliotransmitters encompass a large number of neuroactive molecules, such as amino acids (D-serine, glutamate, GABA), ATP, neurotrophins (BNDF), cytokines (interleukins, interferons, tumor necrosis factors alpha), and growth factors (Sanzgiri et al., 1999; Fields and Stevens, 2000; Hussy et al., 2000; Snyder and Kim, 2000; Bezzi and

Volterra, 2001; Bergami et al., 2008; Blum et al., 2008; Liu et al., 2008; Fujita et al., 2009). Regarding astrocytes, the major gliotransmitters are glutamate, D-serine, and ATP. With increased research in astrocytic signaling, a variety of other factors have been found to be released, such as GABA, hevin, nitric oxide (NO), and thrombospondin. Release of these astrocytic factors have been found to be involved in modifying synaptic structure, and pre- and post-synaptic function (Table 1.1).

Neurons can form synapses in a glia-free environment depending on the cell type. In some studies, glial-free neuronal cultures through immunopanning or fluorescence-activated cell sorting can form numerous synaptic connections (Steinmetz et al., 2006). Others, such as retinal ganglion cells (RGC; Ullian et al., 2001), motoneurons (Ullian et al., 2004), and cerebellar Purkinje cells (Buard et al., 2010) can only form few connections. However, synapse number can be increased when glial cells are present in rat and mouse RGCs cultures. (Pfrieger and Barres, 1997; Nagler et al., 2001; Ullian et al., 2001; Steinmetz et al., 2006), Purkinje cells (Buard et al., 2010), motoneurons (Ullian et al., 2004), and in cortical (Hu et al., 2007) and hippocampal neurons (Tournell et al., 2006; Boehler et al., 2007). Purified rodent RGCs have been used to investigate the role of astrocyte in synaptogenesis; cultured RGCs can be immunopurified and cultured in the absence of astrocytes, and therefore are ideal for studying the role of astrocytes in synapse formation (Meyer-Franke et al., 1995). RGCs can be cultured from postnatal rodent retina by using specific antibodies for surface antigens on RGCs. These neurons can grow and survive for several weeks while making contacts with each other. However, few synapses are formed in the cultures that exhibit little spontaneous synaptic activity,

whereas the treatment of RGCs with astrocyte-condition medium (ACM) induces synaptogenesis providing a perfect system to study the role of astrocyte-derived factors in synapse formation (Pfrieger and Barres, 1997). With the use of embryonic hippocampal and cortical neurons, astrocytes are required for correct neuronal differentiation and survival (Banker, 1980). This provides evidence that astrocytic secreted-factors are involved with synapse formation and function.

The first proteins that were identified as key synaptogenic secreted factors by astrocytes belong to a family of thrombospondins (TSPs; Christopherson et al., 2005). TSPs are extracellular matrix proteins that mediate cell-cell and cell-matrix interactions. There are five mammalian TSPs, though only two TSP isoforms have currently been found to be secreted by astrocytes. It was first shown by Christopherson et al. (2005) that by the addition of purified TSP protein to cultured neurons, there was an increase in synapse numbers comparable to ACM, whereas immunodepletion of TSPs from ACM greatly reduced the synaptogenic activity of ACM. In vivo, mice lacking expression of TSP1/2 developed significantly fewer cerebral cortical excitatory synapses. It should be noted that there is a correlation with the timing of normal synapse formation and the levels of astrocytic-derived TSP1/2 release. Due to the expression times of TSP1/2, the authors proposed that it acts as a permissive switch that controls the timing of synaptogenesis during a specific postnatal window. Interestingly, in these studies TSP induced the formation of ultrastructurally normal synapses that were presynaptically active, but postsynaptically silent. This study suggests that astrocytes must also secrete

additional factors that are necessary for the postsynaptic differentiation and production of functional synapses.

More recently, secreted protein acidic, rich in cysteine (SPARC) family protein and SPARC-like protein hevin has been identified as another synaptogenic protein that is secreted by astrocytes (Kucukdereli et al., 2011). Hevin is highly expressed in developing and mature astrocytes and localized to synaptic clefts (Johnston et al., 1990; Lively and Brown, 2008). Kucukdereli et al. (2011) shows that in RGCs culture, hevin is able to induce ultrastructurally normal synapses and regulates synapse size. Hevin, however, only accounts for some of the astrocytic synaptogenic effects. When RGC cultures are treated with conditioned TSP1/2 double null astrocytes plus hevin, hevin is unable to increase the synapse number, as if the culture were treated with TSP1/2. Additionally, hevin-depleted ACM prepared by conditioned TSP1/2 double-null astrocytes resulted in a lack of any significant synaptogenic activity. From these results, Kucukdereli et al. (2011) looked also at SPARC due to hevin's inability to compensate for the lack of TSP in ACM as there might be an inhibitory factor to synapse formation. SPARC is a secreted protein highly homologous to hevin, but unlike hevin, SPARC is not synaptogenic; SPARC antagonizes hevin. When RGCs were treated with both hevin and SPARC, the synaptogenic activity of hevin is diminished. On the contrary, when RGCs are cocultured with TSP and SPARC, SPARC did not antagonize the synaptogenic activity of TSP, therefore SPARC's inhibitory effect is specific to hevin-induced synaptogenesis. These findings demonstrate that astrocytes can provide both stimulation of synapse formation and inhibition of synaptogenesis by releasing anti-synaptogeneic protein SPARC. It

should be noted that under long-term culturing conditions, RGC survival did not differ between RGC's cultured alone or with hevin or SPARC. However, when both SPARC and hevin are present, neurite outgrowth and branching are promoted (Kucukdereli et al., 2011). In hevin null mice, synaptic connections in the superior colliculus had impaired formation and maturation; SPARC null mice exhibited accelerated formation of synapses in the superior colliculus. Taken together, hevin and SPARC are able to control the rate and the extent of synapse formation and maturation in the brain.

Insertion of AMPA receptors into postsynaptic sites can produce functional synapses. Astrocytes are able to strongly regulate the distribution of AMPA receptors within neurons. In cultured RGCs in the presence of astrocytes, there is a three-fold increase in the surface level of AMPA receptor subunits along with a correlative increase in synaptic strength (Allen et al., 2012). It was found that glypican 4 and glypican 6 are astrocyte-secreted signals that are sufficient to induce functional synapses in purified RGC neurons. When glypican 4 and 6 are depleted from ACM, there is significant reduction in the medium to induce postsynaptic activity. Glypican 4 and 6 increase the surface level and synaptic clustering of AMPA receptors which specifically contain the GluA1 subunit. Glypican 4 deficient mice have defective synapse formation due to decreased amplitude of excitatory synaptic currents in the hippocampus during early postnatal development, as well, exhibit reduced recruitment of GluA1 to synapses. These data identify glypicans as a family of novel astrocyte-derived molecules that are necessary and sufficient to promote glutamate receptor clustering and receptivity and induce the formation of post-synaptically functioning CNS synapses.

1.3.2 Astrocytic contact with neurons

At the tripartite synapse, astrocytic processes extend thousands of fine processes and come into close contact with synaptic sites, where a single astrocyte can contact up to 140,000 synapses (Bushong et al., 2002). It is not surprising to see astrocytes can directly contact the pre- and post-synaptic sites and therefore affect synapse development (Table 1.2). Astrocytes express a variety of cell adhesion molecules and proteins that activate signaling pathways at the pre- and post-synaptic neuron. Barker et al. (2008) cultured RGC from 17 day old embryos (E17) and cultured them together with postnatal RGCs in the presence of ACM (Barker et al., 2008). Interestingly, the E17 RGC failed to receive synapses from postnatal RGC under these conditions; however, at E19, when astrocytes typically begin to appear in the retina, the RGCs responded to ACM. When E17 RGC are co-cultured with astrocytes, there are increased synapses at the RGCs. This provides evidence that astrocytes provide a contact-mediated signal to allow for young neurons to receive synapses. Contact by astrocytes signals for the partitioning out of neurexin from dendrites as neurexin is a synaptic adhesion molecule that inhibits synapse formation (Barker et al., 2008). Similarly, Hama et al. (2004) found in cultured hippocampal neurons, astrocytic contact promotes synaptogenesis specifically at excitatory synapses. Using microisland cultures of neuron only or neuron plus astrocyte, both supplemented with ACM, neurons with astrocytes in the microisland resulted in increased synapse numbers, activity of presynaptic release sites, and the amplitude of autaptic EPSCs. Hama et al. (2004) suggested that through integrin-mediated protein kinase C (PKC) signaling promoted synaptogenesis; contact with astrocytes activated neuronal integrin

receptors, which would lead to activation of neuronal PKC. In addition to excitatory synapses, contact with astrocytes have been found to affect the development of inhibitory synapses. When developing neurons are co-cultured with astrocytes, the amplitude and density of $GABA_A$ currents significantly increases (Liu et al., 1996). Particularly, neuronal cell bodies that were in contact with astrocytes exhibited greater increases in amplitude and density of $GABA_A$ current. This contact-dependent increase in GABAergic synaptic activity required calcium signaling in astrocytes. Interesting, γ-protocadherin have been shown to affect both excitatory and inhibitory synaptogenesis, particularly in the spinal cord (Garrett and Weiner, 2009). γ-protocadherin mediate homophilic adhesion; developing neurons with astrocytes not expressing γ-protocadherin have decreased synaptogenesis. However, if neurons are more mature, neurons co-cultured with astrocytes without γ-protocadherin, will still be able to form synapses as normal. This implicates that astrocytic γ-protocadherin is essential for promoting excitatory and inhibitory synaptogenesis during critical developmental periods.

Including affecting synapse formation, astrocytes may drive loss of synapses as well. Indeed, electron microscopy studies have implicated astrocytes in trans-endocytosis between hippocampal neurons and astrocytes, such that astrocytes may be engulfing synapses through trans-phagocytosis. Through gene expression analysis, Cahoy et al. (2008) found a plethora of genes in astrocytes implicated in engulfment and phagocytosis. The phagocytic genes can be categorized into three pathways: (1) genes controlling for actin cytoskeleton rearrangement which allows for increased membrane dynamics for phagocytes to surround cellular debris, (2) genes involved in the integrin

pathway to regulate the genes involved in actin skeleton rearrangement, and (3) genes involved in recognition of cellular debris and engulfment. Chung et al. (2013) showed directly astrocyte-mediated pruning of synapses by performing an engulfment assay. Astrocytes were cultured in the presence of synaptosomes, which are isolated nerve terminals, and engulfment of the synaptosomes by astrocytes was determined by a pH-sensitive dye, pHrodo. Astrocyte-mediated synapse elimination involved two phagocytic receptors, multiple EGF-like–domains 10 (MEGF10) and MER receptor tyrosine kinase (MERTK). Astrocytes deficient with either resulted in greater defects in astrocytic synapse engulfment. Chung et al. (2013) also showed in vivo MEGF10 and MERTK is essential, taking advantage of the retinogeniculate system, where RGCs form excessive synapses with neurons in the dorsal lateral geniculate nucleus then these excessive synapses are later pruned and refined during later postnatal development. RGCs were fluorescently labeled and imaged and found RGCs in mice deficient in both MEGF10 and MERTK failed to refine their connections resulting in excessive functional synapses. Synapse elimination by astrocytes is dependent on neural activity, as blocking spontaneous retinal waves with intraocularly injected epibatidine in both eyes reduced astrocyte-mediated phagocytosis of synaptic inputs from both eyes. However, blocking of one eye induces a preferential engulfment of weaker, silent synapses. This preferential engulfment was reduced with deficiency of MEGF10 and MERTK. Although astrocytes are involved in the pruning of synapses, the exact “eat me” signals are still not yet understood, particularly during the developmental process.

1.4 Ephrins

Ephrins are a membrane-bound protein that act as a ligand for ephrin receptors (Eph), which activate a series of intracellular signals that play an important role in the interactions between pre- and post-synaptic neurons. Membrane anchorage of ephrin/Eph implies signaling is mediated by cell-to-cell contacts (Davis et al., 1994). Ephrins fall into two subclasses based on structural characteristics and binding affinities: ephrin-As and ephrin-Bs with EphA and EphB receptors. Class ephrin-A consists of five members (ephrin-A1-5) and are tethered to the membrane through a glycosylphosphatidyl inositol (GPI) anchor and preferentially interact with EphA receptors. However, EphAs and ephrin-As are known to be a bit promiscuous and some may bind to the B class counterparts. Ephrin-Bs, on the other hand, possess transmembrane domains with high affinity for EphB receptors. Following cell-cell contact, ephrin ligands bind to Eph receptors resulting in signaling, which follows a receptor tyrosine model. Eph-ephrin interactions have a unique feature: upon binding Eph-ephrins can facilitate bi-directional signaling. There is the classical “forward” signaling where there is a signal transmitted into the Eph receptor expressing cell. As well, there is a “reverse” signal where the signal is transmitted into the ephrin expressing cell (Bush and Soriano, 2009; Sloniowski and Ethell, 2012; Xu and Henkemeyer, 2012). Cell-cell contact between Eph-ephrins have been shown to play a prominent role to mediate cell adhesion or repulsion, and are implicated in axon guidance, cell migration and proliferation, and synaptogenesis, particularly at excitatory synapses (Dalva et al., 2000; Henkemeyer et al., 2003; Murai et al., 2003; Kayser et al., 2006; Egea and Klein, 2007; Kayser et al., 2008).

Eph/ephrin interaction requires cell-cell contact. Upon contact Eph/ephrin signaling generates both attraction and repulsion signals to help guide migrating neuronal axons and cells to their appropriate targets as well as neuronal cell proliferation and synaptogenesis. The initiation of Eph/ephrin signaling occurs with clustering of the Eph/ephrin complexes for both forward (Davis et al., 1994; Stein et al., 1998) and reverse signaling (Cowan and Henkemeyer, 2002; Davy and Soriano, 2005). Mechanistically, Eph/ephrin signaling controls local cytoskeletal dynamics by regulating actin cytoskeleton and associated cell-matrix adhesions. Specifically, Eph/ephrin signaling modulates Rho-family GTPases, such as Rac1, Cdc42, and RhoA, which are the molecular switches regulating reorganization of the actin skeleton (Hall and Nobes, 2000; Ridley, 2001; Irie and Yamaguchi, 2002; Kullander and Klein, 2002; Penzes et al., 2003). It is interesting to note the paradoxal role of Eph/ephrin signaling in both cellular adhesion and repulsion. The complexity provided by Eph/ephrin signaling allows for diverse functional consequences.

1.4.1 EphA-Ephrin-A

EphA and ephrin-A have been shown to be important regulators for excitatory synaptogenesis and spine formation (Murai et al., 2003; Zhou et al., 2012) and can affect behaviors associated with neuropsychiatric disorders (Carmona et al., 2009; Arnall et al., 2010; Wurzman et al., 2015). To affect synapse formation, EphA signaling has been shown to promote actin-based remodeling of dendritic spines (Zhou et al., 2012). Signaling through EphA activates actin filament depolymerizing factor coffin and alters

F-actin distribution in spines. Interestingly, however, EphA not only induces spine elongation, but is also involved in spine retraction (Zhou et al., 2012). Recently, there have been many studies that have looked at the link between BDNF signaling and EphA/ephrin-A signaling. Ephrin-A5 is expressed at the hippocampal CA1-CA3 pyramidal axons and have been found to regulate synapse development and function. At the presynaptic side, ephrin-A5 promotes BDNF-induced synapse formation through potentiation of TrkB signaling, which augments the activation of PI3 kinase/AKT pathway to promote for survival (Gottschalk et al., 1999; Marler et al., 2008). Interestingly, on the postsynaptic side, binding of postsynaptic EphA5 receptors to presynaptic ephrin-A5 can disrupt BDNF-induced synaptogenesis (Bi et al., 2011). In regard to inhibitory neurons, EphA7 has been shown to be required for stabilization of synaptic terminals in parvalbumin-positive basket cells in the hippocampus. Deletion of EphA7 in adult animals resulted in loss of basket cell innervations and impaired long-term potentiation (LTP). In inhibitory neurons, EphA7 may be inducing gephyrin clustering through PI3 kinase/AKT-mTOR signaling (Beuter et al., 2016). However, EphA3 has been found to be a negative regulator for inhibitory neurons: activation of EphA3 through NCAM binding and ephrin-A5 induced clustering of EphA3, then subsequent autophosphorylation of EphA3, resulted in stimulation of RhoA signaling for GABAergic growth cone repulsion (Sullivan et al., 2016).

1.4.2 EphB-Ephrin-B

Neuronal EphBs and ephrin-Bs have been shown to be required for many processes involved in dendritic spine filopodial motility, spine formation and recruitment to synapses, recruitment of glutamate receptors to synapses, maturation of pre- and post-synapses, and affecting synapse function and plasticity (Hruska and Dalva, 2012; Sloniowski and Ethell, 2012; Kania and Klein, 2016). Ephrin-Bs are expressed both pre- and post-synaptically; with their ability to allow for bi-directional signaling, understanding their exact function is complicated.

EphB/Ephrin-B signaling at the synapse have been shown to be involved with presynaptic differentiation and function. To test the role of ephrin-B signaling at the synapse, heterologous co-culture systems containing non-neuronal cells is transfected with a putative postsynaptic inducer that are then plated onto neuronal culture. After some time, the ability of the putative inducer to form and organize hemi-synapses is then tested. It has been shown that EphB2 is able to induce functional presynaptic release sites on axons from contact of EphB2-transfected non-neuronal cells, suggesting a presynaptic role for ephrin-Bs (Kayser et al., 2006). It was revealed that ephrin-B1 and ephrin-B2 are required for normal EphB2-dependent synaptic formation (McClelland et al., 2009). The ability for inducing functional presynaptic release is due to the recruitment of syntenin-1, which clusters synaptic vesicles (McClelland et al., 2009). The synaptic behavior and plasticity can also be controlled by ephrin-Bs, which have been shown to modulate LTP. At the mossy fiber terminals in the hippocampus, activation of ephrin-B3 through treatment with EphB2 receptor bodies leads to enhanced synaptic transmission

(Contractor et al., 2002). This enhanced synaptic transmission is suggested to be due to ephrin-B3 signaling to recruit more neurotransmitter vesicles to the presynaptic zone (Grunwald et al., 2001; Grunwald et al., 2004; Lim et al., 2008).

Postsynaptically, EphB/ephrin-B signaling can also affect synaptic plasticity, spinogenesis, glutamate receptor recruitment, and synapse density (Dalva et al., 2000; Ethell et al., 2001; Contractor et al., 2002; Henkemeyer et al., 2003; Grunwald et al., 2004; McClelland et al., 2010; Xu et al., 2011). The first evidence of EphB signaling in dendritic spine formation was exhibited in culture, EphB2 triggered phosphorylation and clustering of heparin sulfate proteoglycan syndecan-2 at postsynaptic sites (Ethell et al., 2001). Syndecan-2 is involved in the maturation of dendritic spines. Inhibition of EphB2 by a dominant-negative inhibitor results in impaired syndecan-2 induced spine formation such that dendritic protrusions appeared immature. Further, deletion of EphB1, 2, and 3 receptors resulted in failure to form spines in vitro and development of abnormal headless, or small-headed spines in vivo (Henkemeyer et al., 2003). However, when ephrin-B2 is provided to neurons in culture, there is reduced number of filopodia-like protrusions, and increased number of spines that appeared more mature (Henkemeyer et al., 2003), indicating EphB/ephrin-B signaling may be involved in the maturation and stabilization of spines. Indeed, in cultured hippocampal neurons, ephrin-Bs regulate the maturation of dendritic spines by controlling the transition of filopodia to spines by recruiting GIT1 to sites of ephrin-B signaling (Segura et al., 2007). Recruitment of GIT1 to ephrin-B sites leads to additional recruitment of machinery necessary for remolding actin cytoskeleton underlying spine morphogenesis. To control synapse density, ephrin-

B3 has been implicated in a competitive model for surviving synapses (McClelland et al., 2010). Ephrin-B3 functions as a competitive signal where neurons with more ephrin-B3 enable them to receive more synapses, demonstrated in a heterogenotypic co-culture of neurons either expressing ephrin-B3 or no ephrin-B3. Cultures with 10% wild-type neurons and 90% ephrin-B3 null neurons, wild-type neurons made more synapses than normal. This survival with ephrin-B3 may be mediated by EphB2. Therefore, neurons with higher levels of ephrin-B3 can generate more synaptic connections than neurons with less ephrin-B3 expression (McClelland et al., 2010).

Functionally, ephrin-Bs have been found to regulate LTP at the postsynaptic side and stabilize and/or recruit of AMPA and NMDA receptors. Deletion of postsynaptic ephrin-B2 at CA1 pyramidal neurons have significantly reduced LTP; potentiation through ephrin-B2 may rely on interactions with EphA4, as ablation of presynaptic EphA4 results in reduction in the early phases of LTP (Grunwald et al., 2004). Modulation of this synaptic strength may be due to ephrin-B's effects on AMPA and NMDA receptors. Activation of ephrin-B2 signaling has been shown to reduce AMPA receptor internalization in cultured neurons (Essmann et al., 2008). Ephrin-B2 may affect retention of AMPA receptors by interacting with GRIP1, which allows AMPA receptors to be stabilized and retained at the surface (Essmann et al., 2008). Activation of Eph-ephrin signaling has also been shown to affect phosphorylation of a serine residue on GluA1 AMPA receptor subunit, which affects the trafficking of this subunit. Increased activation of Eph/ephrin signaling through EphB2 results in increased surface AMPA (Hussain et al., 2015). Ephrin-B signaling can also antagonize internalization processes

for the GluR2 subunit by inhibiting PKC function (Chung et al., 2003; Essmann et al., 2008). Along with affecting AMPA receptor stabilization, NMDA receptor expression is also affected. Dalva et al. (2000) showed that ephrin-B binding to postsynaptic EphB2 results in clustering of the Eph receptor and the NR1 NMDA receptor subunit. Activation of EphBs also result in phosphorylation and recruitment of the NR2B subunit (Takasu et al., 2002; Nolt et al., 2011). This recruitment of NR1 and phosphorylation of NR2B to the surface may also affect the function of NMDA receptors, and indeed, EphB2 signaling enhanced the ability of NMDA receptor to regulate the influx of calcium (Takasu et al., 2002).

1.5 The ephrin link between astrocytes and neurons

Besides neurons, astrocytes have also been found to express certain Ephs and ephrins. Ephrin-A3 has been shown to be highly expressed in astrocytes (Murai et al., 2003; Carmona et al., 2009). Astrocytes expressing ephrin-A3 has been shown to regulate spine morphogenesis, glutamate transport, and LTP at CA1-CA3 synapses by interacting with dendritic EphA4 receptors (Murai et al., 2003; Carmona et al., 2009; Filosa et al., 2009). Activation of EphA4 with ephrin-A3 binding induces spine retraction (Murai et al., 2003). However, deletion of astrocytic ephrin-A3 results in abnormal, elongated spines, with reduced LTP (Carmona et al., 2009; Filosa et al., 2009). Along with synaptic changes, due to the bi-directional nature of ephrins, these null-ephrin-A3 astrocytes have increased levels of glutamate transporters. Deficits in LTP may be due to more efficient removal of glutamate from the synaptic cleft, which therefore reduces the activation of

glutamate receptors. It has also been shown with ephrin-Bs, there is increased expression in astrocytes after injury (Wang et al., 2005; Goldshmit et al., 2006; Du et al., 2007; Ren et al., 2013; Nikolakopoulou et al., 2016). My lab has shown that ephrin-B1 is expressed in reactive astrocytes. Reactive astrocytes resemble developing astrocytes and re-express many genes involved in synapse development, including ephrin-B1. In an injury model, astrocytes become reactive and have increased ephrin-B1 levels after injury. Along with this model, there is increased synaptic loss. However, targeted ablation of ephrin-B1 from adult astrocytes accelerates synapse recovery. These studies suggest that astrocytic ephrin-B1 may act as a negative regulator of synaptogenesis and mediates pruning of existing synapses through its interaction with neuronal EphB receptors.

1.6 Conclusion

With the findings that connect astrocytes to neurodevelopment (Molofsky et al., 2012), researchers are now looking towards astrocytes as a contributor in neurodevelopmental and psychiatric disorders. Astrocytic dysfunctions are implicated in synapse pathologies associated with neurodevelopmental disorders (Ballas et al., 2009; Jacobs et al., 2010; Lioy et al., 2011; Higashimori et al., 2016). Improper neurodevelopment can lead to such disorders as Rett syndrome, Fragile X Syndrome, autism and even psychiatric disorders such as schizophrenia. It is therefore essential to study the relationship between astrocytes and neurons, specifically at how astrocytes regulate synaptic connections, and therefore the developing brain. My research presents

the essential role of astrocytic ephrin-B1 in maintaining synapse formation during both early development and adulthood (Fig. 1.1).

References

Abbott, L.F., and Regehr, W.G. (2004). Synaptic computation. *Nature* 431(7010)**,** 796-803. doi: 10.1038/nature03010.

Abraham, W.C. (2003). How long will long-term potentiation last? *Philos Trans R Soc Lond B Biol Sci* 358(1432)**,** 735-744. doi: 10.1098/rstb.2002.1222.

Albrecht, D., Lopez-Murcia, F.J., Perez-Gonzalez, A.P., Lichtner, G., Solsona, C., and Llobet, A. (2012). SPARC prevents maturation of cholinergic presynaptic terminals. *Mol Cell Neurosci* 49(3)**,** 364-374. doi: 10.1016/j.mcn.2012.01.005.

Allen, N.J., Bennett, M.L., Foo, L.C., Wang, G.X., Chakraborty, C., Smith, S.J., et al. (2012). Astrocyte glypicans 4 and 6 promote formation of excitatory synapses via GluA1 AMPA receptors. *Nature* 486(7403)**,** 410-414. doi: 10.1038/nature11059.

Arnall, S., Cheam, L.Y., Smart, C., Rengel, A., Fitzgerald, M., Thivierge, J.P., et al. (2010). Abnormal strategies during visual discrimination reversal learning in ephrin-A2(-/-) mice. *Behav Brain Res* 209(1)**,** 109-113. doi: 10.1016/j.bbr.2010.01.023.

Ballas, N., Lioy, D.T., Grunseich, C., and Mandel, G. (2009). Non-cell autonomous influence of MeCP2-deficient glia on neuronal dendritic morphology. *Nat Neurosci* 12(3)**,** 311-317. doi: 10.1038/nn.2275.

Banker, G.A. (1980). Trophic interactions between astroglial cells and hippocampal neurons in culture. *Science* 209(4458)**,** 809-810. doi: 10.1126/science.7403847.

Barker, A.J., Koch, S.M., Reed, J., Barres, B.A., and Ullian, E.M. (2008). Developmental control of synaptic receptivity. *J Neurosci* 28(33)**,** 8150-8160. doi: 10.1523/JNEUROSCI.1744-08.2008.

Barker, A.J., and Ullian, E.M. (2010). Astrocytes and synaptic plasticity. *Neuroscientist* 16(1)**,** 40-50. doi: 10.1177/1073858409339215.

Beattie, E.C., Stellwagen, D., Morishita, W., Bresnahan, J.C., Ha, B.K., Von Zastrow, M., et al. (2002). Control of synaptic strength by glial TNFalpha. *Science* 295(5563)**,** 2282-2285. doi: 10.1126/science.1067859.

Bergami, M., Santi, S., Formaggio, E., Cagnoli, C., Verderio, C., Blum, R., et al. (2008). Uptake and recycling of pro-BDNF for transmitter-induced secretion by cortical astrocytes. *J Cell Biol* 183(2)**,** 213-221. doi: 10.1083/jcb.200806137.

Beuter, S., Ardi, Z., Horovitz, O., Wuchter, J., Keller, S., Saha, R., et al. (2016). Receptor tyrosine kinase EphA7 is required for interneuron connectivity at specific subcellular compartments of granule cells. *Sci Rep* 6**,** 29710. doi: 10.1038/srep29710.

Bezzi, P., Carmignoto, G., Pasti, L., Vesce, S., Rossi, D., Rizzini, B.L., et al. (1998). Prostaglandins stimulate calcium-dependent glutamate release in astrocytes. *Nature* 391(6664)**,** 281-285. doi: 10.1038/34651.

Bezzi, P., and Volterra, A. (2001). A neuron-glia signalling network in the active brain. *Curr Opin Neurobiol* 11(3)**,** 387-394. doi: 10.1016/s0959-4388(00)00223-3.

Bi, C., Yue, X., Zhou, R., and Plummer, M.R. (2011). EphA activation overrides the presynaptic actions of BDNF. *J Neurophysiol* 105(5)**,** 2364-2374. doi: 10.1152/jn.00564.2010.

Blum, A.E., Joseph, S.M., Przybylski, R.J., and Dubyak, G.R. (2008). Rho-family GTPases modulate Ca(2+) -dependent ATP release from astrocytes. *Am J Physiol Cell Physiol* 295(1)**,** C231-241. doi: 10.1152/ajpcell.00175.2008.

Boehler, M.D., Wheeler, B.C., and Brewer, G.J. (2007). Added astroglia promote greater synapse density and higher activity in neuronal networks. *Neuron Glia Biol* 3(2)**,** 127-140. doi: 10.1017/s1740925x07000440.

Buard, I., Steinmetz, C.C., Claudepierre, T., and Pfrieger, F.W. (2010). Glial cells promote dendrite formation and the reception of synaptic input in Purkinje cells from postnatal mice. *Glia* 58(5)**,** 538-545. doi: 10.1002/glia.20943.

Bush, J.O., and Soriano, P. (2009). Ephrin-B1 regulates axon guidance by reverse signaling through a PDZ-dependent mechanism. *Genes Dev* 23(13)**,** 1586-1599. doi: 10.1101/gad.1807209.

Bushong, E.A., Martone, M.E., Jones, Y.Z., and Ellisman, M.H. (2002). Protoplasmic astrocytes in CA1 stratum radiatum occupy separate anatomical domains. *J Neurosci* 22(1)**,** 183-192.

Caberoy, N.B., Alvarado, G., Bigcas, J.L., and Li, W. (2012). Galectin-3 is a new MerTK-specific eat-me signal. *J Cell Physiol* 227(2)**,** 401-407. doi: 10.1002/jcp.22955.

Cahoy, J.D., Emery, B., Kaushal, A., Foo, L.C., Zamanian, J.L., Christopherson, K.S., et al. (2008). A transcriptome database for astrocytes, neurons, and oligodendrocytes: a new resource for understanding brain development and function. *J Neurosci* 28(1)**,** 264-278. doi: 10.1523/jneurosci.4178-07.2008.

Carmona, M.A., Murai, K.K., Wang, L., Roberts, A.J., and Pasquale, E.B. (2009). Glial ephrin-A3 regulates hippocampal dendritic spine morphology and glutamate transport. *Proc Natl Acad Sci U S A* 106(30)**,** 12524-12529. doi: 10.1073/pnas.0903328106.

Christopherson, K.S., Ullian, E.M., Stokes, C.C., Mullowney, C.E., Hell, J.W., Agah, A., et al. (2005). Thrombospondins are astrocyte-secreted proteins that promote CNS synaptogenesis. *Cell* 120(3)**,** 421-433. doi: 10.1016/j.cell.2004.12.020.

Chung, H.J., Steinberg, J.P., Huganir, R.L., and Linden, D.J. (2003). Requirement of AMPA receptor GluR2 phosphorylation for cerebellar long-term depression. *Science* 300(5626)**,** 1751-1755. doi: 10.1126/science.1082915.

Chung, W.S., Clarke, L.E., Wang, G.X., Stafford, B.K., Sher, A., Chakraborty, C., et al. (2013). Astrocytes mediate synapse elimination through MEGF10 and MERTK pathways. *Nature* 504(7480)**,** 394-400. doi: 10.1038/nature12776.

Contractor, A., Rogers, C., Maron, C., Henkemeyer, M., Swanson, G.T., and Heinemann, S.F. (2002). Trans-synaptic Eph receptor-ephrin signaling in hippocampal mossy fiber LTP. *Science* 296(5574)**,** 1864-1869. doi: 10.1126/science.1069081.

Cotrina, M.L., Lin, J.H., Alves-Rodrigues, A., Liu, S., Li, J., Azmi-Ghadimi, H., et al. (1998). Connexins regulate calcium signaling by controlling ATP release. *Proc Natl Acad Sci U S A* 95(26)**,** 15735-15740. doi: 10.1073/pnas.95.26.15735.

Cowan, C.A., and Henkemeyer, M. (2002). Ephrins in reverse, park and drive. *Trends Cell Biol* 12(7)**,** 339-346. doi: 10.1016/s0962-8924(02)02317-6.

Cowan, W.M., Fawcett, J.W., O'Leary, D.D., and Stanfield, B.B. (1984). Regressive events in neurogenesis. *Science* 225(4668)**,** 1258-1265. doi: 10.1126/science.6474175.

Crawford, D.C., Jiang, X., Taylor, A., and Mennerick, S. (2012). Astrocyte-derived thrombospondins mediate the development of hippocampal presynaptic plasticity in vitro. *J Neurosci* 32(38)**,** 13100-13110. doi: 10.1523/JNEUROSCI.2604-12.2012.

Dalva, M.B., Takasu, M.A., Lin, M.Z., Shamah, S.M., Hu, L., Gale, N.W., et al. (2000). EphB receptors interact with NMDA receptors and regulate excitatory synapse formation. *Cell* 103(6)**,** 945-956.

Davis, S., Gale, N., Aldrich, T., Maisonpierre, P., Lhotak, V., Pawson, T., et al. (1994). Ligands for EPH-related receptor tyrosine kinases that require membrane

attachment or clustering for activity. *Science* 266(5186)**,** 816-819. doi: 10.1126/science.7973638.

Davy, A., and Soriano, P. (2005). Ephrin signaling in vivo: look both ways. *Dev Dyn* 232(1)**,** 1-10. doi: 10.1002/dvdy.20200.

Diniz, L.P., Almeida, J.C., Tortelli, V., Vargas Lopes, C., Setti-Perdigao, P., Stipursky, J., et al. (2012). Astrocyte-induced synaptogenesis is mediated by transforming growth factor beta signaling through modulation of D-serine levels in cerebral cortex neurons. *J Biol Chem* 287(49)**,** 41432-41445. doi: 10.1074/jbc.M112.380824.

Du, J., Fu, C., and Sretavan, D.W. (2007). Eph/ephrin signaling as a potential therapeutic target after central nervous system injury. *Curr Pharm Des* 13(24)**,** 2507-2518. doi: 10.2174/138161207781368594.

Egea, J., and Klein, R. (2007). Bidirectional Eph-ephrin signaling during axon guidance. *Trends Cell Biol* 17(5)**,** 230-238. doi: 10.1016/j.tcb.2007.03.004.

Eroglu, C., and Barres, B.A. (2010). Regulation of synaptic connectivity by glia. *Nature* 468(7321)**,** 223-231. doi: 10.1038/nature09612.

Essmann, C.L., Martinez, E., Geiger, J.C., Zimmer, M., Traut, M.H., Stein, V., et al. (2008). Serine phosphorylation of ephrinB2 regulates trafficking of synaptic AMPA receptors. *Nat Neurosci* 11(9)**,** 1035-1043. doi: 10.1038/nn.2171.

Ethell, I.M., Irie, F., Kalo, M.S., Couchman, J.R., Pasquale, E.B., and Yamaguchi, Y. (2001). EphB/syndecan-2 signaling in dendritic spine morphogenesis. *Neuron* 31(6)**,** 1001-1013. doi: 10.1016/s0896-6273(01)00440-8.

Fellin, T., and Carmignoto, G. (2004). Neurone-to-astrocyte signalling in the brain represents a distinct multifunctional unit. *J Physiol* 559(Pt 1)**,** 3-15. doi: 10.1113/jphysiol.2004.063214.

Fields, R.D., and Stevens, B. (2000). ATP: an extracellular signaling molecule between neurons and glia. *Trends Neurosci* 23(12)**,** 625-633. doi: 10.1016/s0166-2236(00)01674-x.

Filosa, A., Paixao, S., Honsek, S.D., Carmona, M.A., Becker, L., Feddersen, B., et al. (2009). Neuron-glia communication via EphA4/ephrin-A3 modulates LTP through glial glutamate transport. *Nat Neurosci* 12(10)**,** 1285-1292. doi: 10.1038/nn.2394.

Frischknecht, R., Heine, M., Perrais, D., Seidenbecher, C.I., Choquet, D., and Gundelfinger, E.D. (2009). Brain extracellular matrix affects AMPA receptor lateral mobility and short-term synaptic plasticity. *Nat Neurosci* 12(7)**,** 897-904. doi: 10.1038/nn.2338.

Fuentes-Medel, Y., Ashley, J., Barria, R., Maloney, R., Freeman, M., and Budnik, V. (2012). Integration of a retrograde signal during synapse formation by glia-secreted TGF-beta ligand. *Curr Biol* 22(19)**,** 1831-1838. doi: 10.1016/j.cub.2012.07.063.

Fujita, T., Tozaki-Saitoh, H., and Inoue, K. (2009). P2Y1 receptor signaling enhances neuroprotection by astrocytes against oxidative stress via IL-6 release in hippocampal cultures. *Glia* 57(3)**,** 244-257. doi: 10.1002/glia.20749.

Garner, C.C., Zhai, R.G., Gundelfinger, E.D., and Ziv, N.E. (2002). Molecular mechanisms of CNS synaptogenesis. *Trends Neurosci* 25(5)**,** 243-251. doi: 10.1016/s0166-2236(02)02152-5.

Garrett, A.M., and Weiner, J.A. (2009). Control of CNS synapse development by {gamma}-protocadherin-mediated astrocyte-neuron contact. *J Neurosci* 29(38)**,** 11723-11731. doi: 10.1523/JNEUROSCI.2818-09.2009.

Goldshmit, Y., McLenachan, S., and Turnley, A. (2006). Roles of Eph receptors and ephrins in the normal and damaged adult CNS. *Brain Res Rev* 52(2)**,** 327-345. doi: 10.1016/j.brainresrev.2006.04.006.

Gomez-Casati, M.E., Murtie, J.C., Rio, C., Stankovic, K., Liberman, M.C., and Corfas, G. (2010). Nonneuronal cells regulate synapse formation in the vestibular sensory epithelium via erbB-dependent BDNF expression. *Proc Natl Acad Sci U S A* 107(39)**,** 17005-17010. doi: 10.1073/pnas.1008938107.

Gottschalk, W.A., Jiang, H., Tartaglia, N., Feng, L., Figurov, A., and Lu, B. (1999). Signaling mechanisms mediating BDNF modulation of synaptic plasticity in the hippocampus. *Learn Mem* 6(3)**,** 243-256.

Grunwald, I.C., Korte, M., Adelmann, G., Plueck, A., Kullander, K., Adams, R.H., et al. (2004). Hippocampal plasticity requires postsynaptic ephrinBs. *Nat Neurosci* 7(1)**,** 33-40. doi: 10.1038/nn1164.

Grunwald, I.C., Korte, M., Wolfer, D., Wilkinson, G.A., Unsicker, K., Lipp, H.P., et al. (2001). Kinase-independent requirement of EphB2 receptors in hippocampal synaptic plasticity. *Neuron* 32(6)**,** 1027-1040.

Hall, A., and Nobes, C.D. (2000). Rho GTPases: molecular switches that control the organization and dynamics of the actin cytoskeleton. *Philos Trans R Soc Lond B Biol Sci* 355(1399)**,** 965-970. doi: 10.1098/rstb.2000.0632.

Hama, H., Hara, C., Yamaguchi, K., and Miyawaki, A. (2004). PKC signaling mediates global enhancement of excitatory synaptogenesis in neurons triggered by local contact with astrocytes. *Neuron* 41(3)**,** 405-415.

Henkemeyer, M., Itkis, O.S., Ngo, M., Hickmott, P.W., and Ethell, I.M. (2003). Multiple EphB receptor tyrosine kinases shape dendritic spines in the hippocampus. *J Cell Biol* 163(6)**,** 1313-1326. doi: 10.1083/jcb.200306033.

Henneberger, C., Papouin, T., Oliet, S.H., and Rusakov, D.A. (2010). Long-term potentiation depends on release of D-serine from astrocytes. *Nature* 463(7278)**,** 232-236. doi: 10.1038/nature08673.

Higashimori, H., Schin, C.S., Chiang, M.S., Morel, L., Shoneye, T.A., Nelson, D.L., et al. (2016). Selective Deletion of Astroglial FMRP Dysregulates Glutamate Transporter GLT1 and Contributes to Fragile X Syndrome Phenotypes In Vivo. *J Neurosci* 36(27)**,** 7079-7094. doi: 10.1523/jneurosci.1069-16.2016.

Hruska, M., and Dalva, M.B. (2012). Ephrin regulation of synapse formation, function and plasticity. *Mol Cell Neurosci* 50(1)**,** 35-44. doi: 10.1016/j.mcn.2012.03.004.

Hu, R., Cai, W.Q., Wu, X.G., and Yang, Z. (2007). Astrocyte-derived estrogen enhances synapse formation and synaptic transmission between cultured neonatal rat cortical neurons. *Neuroscience* 144(4)**,** 1229-1240. doi: 10.1016/j.neuroscience.2006.09.056.

Hussain, N.K., Thomas, G.M., Luo, J., and Huganir, R.L. (2015). Regulation of AMPA receptor subunit GluA1 surface expression by PAK3 phosphorylation. *Proc Natl Acad Sci U S A* 112(43)**,** E5883-5890. doi: 10.1073/pnas.1518382112.

Hussy, N., Deleuze, C., Desarmenien, M.G., and Moos, F.C. (2000). Osmotic regulation of neuronal activity: a new role for taurine and glial cells in a hypothalamic neuroendocrine structure. *Prog Neurobiol* 62(2)**,** 113-134.

Ikeda, H., and Murase, K. (2004). Glial nitric oxide-mediated long-term presynaptic facilitation revealed by optical imaging in rat spinal dorsal horn. *J Neurosci* 24(44)**,** 9888-9896. doi: 10.1523/jneurosci.2608-04.2004.

Irie, F., and Yamaguchi, Y. (2002). EphB receptors regulate dendritic spine development via intersectin, Cdc42 and N-WASP. *Nat Neurosci* 5(11)**,** 1117-1118. doi: 10.1038/nn964.

Jacobs, S., Nathwani, M., and Doering, L.C. (2010). Fragile X astrocytes induce developmental delays in dendrite maturation and synaptic protein expression. *BMC Neurosci* 11**,** 132. doi: 10.1186/1471-2202-11-132.

Johnston, I.G., Paladino, T., Gurd, J.W., and Brown, I.R. (1990). Molecular cloning of SC1: a putative brain extracellular matrix glycoprotein showing partial similarity to osteonectin/BM40/SPARC. *Neuron* 4(1)**,** 165-176. doi: 10.1016/0896-6273(90)90452-l.

Jones, E.V., Bernardinelli, Y., Tse, Y.C., Chierzi, S., Wong, T.P., and Murai, K.K. (2011). Astrocytes control glutamate receptor levels at developing synapses through SPARC-beta-integrin interactions. *J Neurosci* 31(11)**,** 4154-4165. doi: 10.1523/jneurosci.4757-10.2011.

Kania, A., and Klein, R. (2016). Mechanisms of ephrin-Eph signalling in development, physiology and disease. *Nat Rev Mol Cell Biol* 17(4)**,** 240-256. doi: 10.1038/nrm.2015.16.

Kayser, M.S., McClelland, A.C., Hughes, E.G., and Dalva, M.B. (2006). Intracellular and trans-synaptic regulation of glutamatergic synaptogenesis by EphB receptors. *J Neurosci* 26(47)**,** 12152-12164. doi: 10.1523/JNEUROSCI.3072-06.2006.

Kayser, M.S., Nolt, M.J., and Dalva, M.B. (2008). EphB receptors couple dendritic filopodia motility to synapse formation. *Neuron* 59(1)**,** 56-69. doi: 10.1016/j.neuron.2008.05.007.

Knierim, J.J. (2015). The hippocampus. *Curr Biol* 25(23)**,** R1116-1121. doi: 10.1016/j.cub.2015.10.049.

Kucukdereli, H., Allen, N.J., Lee, A.T., Feng, A., Ozlu, M.I., Conatser, L.M., et al. (2011). Control of excitatory CNS synaptogenesis by astrocyte-secreted proteins Hevin and SPARC. *Proc Natl Acad Sci U S A* 108(32)**,** E440-449. doi: 10.1073/pnas.1104977108.

Kullander, K., and Klein, R. (2002). Mechanisms and functions of Eph and ephrin signalling. *Nat Rev Mol Cell Biol* 3(7)**,** 475-486. doi: 10.1038/nrm856.

Li, D., Ropert, N., Koulakoff, A., Giaume, C., and Oheim, M. (2008). Lysosomes are the major vesicular compartment undergoing Ca2+-regulated exocytosis from cortical astrocytes. *J Neurosci* 28(30)**,** 7648-7658. doi: 10.1523/jneurosci.0744-08.2008.

Lim, B.K., Matsuda, N., and Poo, M.M. (2008). Ephrin-B reverse signaling promotes structural and functional synaptic maturation in vivo. *Nat Neurosci* 11(2)**,** 160-169. doi: 10.1038/nn2033.

Lioy, D.T., Garg, S.K., Monaghan, C.E., Raber, J., Foust, K.D., Kaspar, B.K., et al. (2011). A role for glia in the progression of Rett's syndrome. *Nature* 475(7357)**,** 497-500. doi: 10.1038/nature10214.

Liu, H.T., Toychiev, A.H., Takahashi, N., Sabirov, R.Z., and Okada, Y. (2008). Maxi-anion channel as a candidate pathway for osmosensitive ATP release from mouse astrocytes in primary culture. *Cell Res* 18(5)**,** 558-565. doi: 10.1038/cr.2008.49.

Liu, Q.Y., Schaffner, A.E., Li, Y.X., Dunlap, V., and Barker, J.L. (1996). Upregulation of GABAA current by astrocytes in cultured embryonic rat hippocampal neurons. *J Neurosci* 16(9)**,** 2912-2923.

Liu, T., Sun, L., Xiong, Y., Shang, S., Guo, N., Teng, S., et al. (2011). Calcium triggers exocytosis from two types of organelles in a single astrocyte. *J Neurosci* 31(29)**,** 10593-10601. doi: 10.1523/jneurosci.6401-10.2011.

Lively, S., and Brown, I.R. (2008). The extracellular matrix protein SC1/hevin localizes to excitatory synapses following status epilepticus in the rat lithium-pilocarpine seizure model. *J Neurosci Res* 86(13)**,** 2895-2905. doi: 10.1002/jnr.21735.

Lovden, M., Wenger, E., Martensson, J., Lindenberger, U., and Backman, L. (2013). Structural brain plasticity in adult learning and development. *Neurosci Biobehav Rev* 37(9 Pt B)**,** 2296-2310. doi: 10.1016/j.neubiorev.2013.02.014.

Luo, L., and O'Leary, D.D. (2005). Axon retraction and degeneration in development and disease. *Annu Rev Neurosci* 28**,** 127-156. doi: 10.1146/annurev.neuro.28.061604.135632.

Marler, K.J., Becker-Barroso, E., Martinez, A., Llovera, M., Wentzel, C., Poopalasundaram, S., et al. (2008). A TrkB/EphrinA interaction controls retinal axon branching and synaptogenesis. *J Neurosci* 28(48)**,** 12700-12712. doi: 10.1523/JNEUROSCI.1915-08.2008.

May, A. (2011). Experience-dependent structural plasticity in the adult human brain. *Trends Cogn Sci* 15(10)**,** 475-482. doi: 10.1016/j.tics.2011.08.002.

McClelland, A.C., Hruska, M., Coenen, A.J., Henkemeyer, M., and Dalva, M.B. (2010). Trans-synaptic EphB2-ephrin-B3 interaction regulates excitatory synapse density by inhibition of postsynaptic MAPK signaling. *Proc Natl Acad Sci U S A* 107(19)**,** 8830-8835. doi: 10.1073/pnas.0910644107.

McClelland, A.C., Sheffler-Collins, S.I., Kayser, M.S., and Dalva, M.B. (2009). Ephrin-B1 and ephrin-B2 mediate EphB-dependent presynaptic development via

syntenin-1. *Proc Natl Acad Sci U S A* 106(48)**,** 20487-20492. doi: 10.1073/pnas.0811862106.

Meyer-Franke, A., Kaplan, M.R., Pfrieger, F.W., and Barres, B.A. (1995). Characterization of the signaling interactions that promote the survival and growth of developing retinal ganglion cells in culture. *Neuron* 15(4)**,** 805-819. doi: 10.1016/0896-6273(95)90172-8.

Milner, B., Squire, L.R., and Kandel, E.R. (1998). Cognitive neuroscience and the study of memory. *Neuron* 20(3)**,** 445-468.

Molofsky, A.V., Krencik, R., Ullian, E.M., Tsai, H.H., Deneen, B., Richardson, W.D., et al. (2012). Astrocytes and disease: a neurodevelopmental perspective. *Genes Dev* 26(9)**,** 891-907. doi: 10.1101/gad.188326.112.

Montana, V., Malarkey, E.B., Verderio, C., Matteoli, M., and Parpura, V. (2006). Vesicular transmitter release from astrocytes. *Glia* 54(7)**,** 700-715. doi: 10.1002/glia.20367.

Murai, K.K., Nguyen, L.N., Irie, F., Yamaguchi, Y., and Pasquale, E.B. (2003). Control of hippocampal dendritic spine morphology through ephrin-A3/EphA4 signaling. *Nat Neurosci* 6(2)**,** 153-160. doi: 10.1038/nn994.

Murphy, S. (2000). Production of nitric oxide by glial cells: regulation and potential roles in the CNS. *Glia* 29(1)**,** 1-13.

Nagler, K., Mauch, D.H., and Pfrieger, F.W. (2001). Glia-derived signals induce synapse formation in neurones of the rat central nervous system. *J Physiol* 533(Pt 3)**,** 665-679. doi: 10.1111/j.1469-7793.2001.00665.x.

Neves, G., Cooke, S.F., and Bliss, T.V. (2008). Synaptic plasticity, memory and the hippocampus: a neural network approach to causality. *Nat Rev Neurosci* 9(1)**,** 65-75. doi: 10.1038/nrn2303.

Nikolakopoulou, A.M., Koeppen, J., Garcia, M., Leish, J., Obenaus, A., and Ethell, I.M. (2016). Astrocytic Ephrin-B1 Regulates Synapse Remodeling Following Traumatic Brain Injury. *ASN Neuro* 8(1)**,** 1-18. doi: 10.1177/1759091416630220.

Nishiyama, H., Knopfel, T., Endo, S., and Itohara, S. (2002). Glial protein S100B modulates long-term neuronal synaptic plasticity. *Proc Natl Acad Sci U S A* 99(6)**,** 4037-4042. doi: 10.1073/pnas.052020999.

Nolt, M.J., Lin, Y., Hruska, M., Murphy, J., Sheffler-Colins, S.I., Kayser, M.S., et al. (2011). EphB controls NMDA receptor function and synaptic targeting in a

subunit-specific manner. *J Neurosci* 31(14)**,** 5353-5364. doi: 10.1523/JNEUROSCI.0282-11.2011.

Parpura, V., Basarsky, T.A., Liu, F., Jeftinija, K., Jeftinija, S., and Haydon, P.G. (1994). Glutamate-mediated astrocyte-neuron signalling. *Nature* 369(6483)**,** 744-747. doi: 10.1038/369744a0.

Penzes, P., Beeser, A., Chernoff, J., Schiller, M.R., Eipper, B.A., Mains, R.E., et al. (2003). Rapid induction of dendritic spine morphogenesis by trans-synaptic ephrinB-EphB receptor activation of the Rho-GEF kalirin. *Neuron* 37(2)**,** 263-274. doi: 10.1016/s0896-6273(02)01168-6.

Perea, G., and Araque, A. (2007). Astrocytes potentiate transmitter release at single hippocampal synapses. *Science* 317(5841)**,** 1083-1086. doi: 10.1126/science.1144640.

Pfrieger, F.W., and Barres, B.A. (1997). Synaptic efficacy enhanced by glial cells in vitro. *Science* 277(5332)**,** 1684-1687. doi: 10.1126/science.277.5332.1684.

Pyka, M., Wetzel, C., Aguado, A., Geissler, M., Hatt, H., and Faissner, A. (2011). Chondroitin sulfate proteoglycans regulate astrocyte-dependent synaptogenesis and modulate synaptic activity in primary embryonic hippocampal neurons. *Eur J Neurosci* 33(12)**,** 2187-2202. doi: 10.1111/j.1460-9568.2011.07690.x.

Ren, Z., Chen, X., Yang, J., Kress, B.T., Tong, J., Liu, H., et al. (2013). Improved axonal regeneration after spinal cord injury in mice with conditional deletion of ephrin B2 under the GFAP promoter. *Neuroscience* 241**,** 89-99. doi: 10.1016/j.neuroscience.2013.03.010.

Ridley, A.J. (2001). Rho GTPases and cell migration. *J Cell Sci* 114(Pt 15)**,** 2713-2722.

Sanzgiri, R.P., Araque, A., and Haydon, P.G. (1999). Prostaglandin E(2) stimulates glutamate receptor-dependent astrocyte neuromodulation in cultured hippocampal cells. *J Neurobiol* 41(2)**,** 221-229.

Scoville, W.B., and Milner, B. (1957). Loss of recent memory after bilateral hippocampal lesions. *J Neurol Neurosurg Psychiatry* 20(1)**,** 11-21. doi: 10.1136/jnnp.20.1.11.

Segura, I., Essmann, C.L., Weinges, S., and Acker-Palmer, A. (2007). Grb4 and GIT1 transduce ephrinB reverse signals modulating spine morphogenesis and synapse formation. *Nat Neurosci* 10(3)**,** 301-310. doi: 10.1038/nn1858.

Serrano, A., Haddjeri, N., Lacaille, J.C., and Robitaille, R. (2006). GABAergic network activation of glial cells underlies hippocampal heterosynaptic depression. *J Neurosci* 26(20)**,** 5370-5382. doi: 10.1523/jneurosci.5255-05.2006.

Sloniowski, S., and Ethell, I.M. (2012). Looking forward to EphB signaling in synapses. *Semin Cell Dev Biol* 23(1)**,** 75-82. doi: 10.1016/j.semcdb.2011.10.020.

Snyder, S.H., and Kim, P.M. (2000). D-amino acids as putative neurotransmitters: focus on D-serine. *Neurochem Res* 25(5)**,** 553-560. doi: 10.1023/a:1007586314648.

Stein, E., Lane, A.A., Cerretti, D.P., Schoecklmann, H.O., Schroff, A.D., Van Etten, R.L., et al. (1998). Eph receptors discriminate specific ligand oligomers to determine alternative signaling complexes, attachment, and assembly responses. *Genes Dev* 12(5)**,** 667-678. doi: 10.1101/gad.12.5.667.

Steinmetz, C.C., Buard, I., Claudepierre, T., Nagler, K., and Pfrieger, F.W. (2006). Regional variations in the glial influence on synapse development in the mouse CNS. *J Physiol* 577(Pt 1)**,** 249-261. doi: 10.1113/jphysiol.2006.117358.

Stellwagen, D., and Malenka, R.C. (2006). Synaptic scaling mediated by glial TNF-alpha. *Nature* 440(7087)**,** 1054-1059. doi: 10.1038/nature04671.

Sullivan, C.S., Kumper, M., Temple, B.S., and Maness, P.F. (2016). The Neural Cell Adhesion Molecule (NCAM) Promotes Clustering and Activation of EphA3 Receptors in GABAergic Interneurons to Induce Ras Homolog Gene Family, Member A (RhoA)/Rho-associated protein kinase (ROCK)-mediated Growth Cone Collapse. *J Biol Chem* 291(51)**,** 26262-26272. doi: 10.1074/jbc.M116.760017.

Takasu, M.A., Dalva, M.B., Zigmond, R.E., and Greenberg, M.E. (2002). Modulation of NMDA receptor-dependent calcium influx and gene expression through EphB receptors. *Science* 295(5554)**,** 491-495. doi: 10.1126/science.1065983.

Tournell, C.E., Bergstrom, R.A., and Ferreira, A. (2006). Progesterone-induced agrin expression in astrocytes modulates glia-neuron interactions leading to synapse formation. *Neuroscience* 141(3)**,** 1327-1338. doi: 10.1016/j.neuroscience.2006.05.004.

Tran, M.D., and Neary, J.T. (2006). Purinergic signaling induces thrombospondin-1 expression in astrocytes. *Proc Natl Acad Sci U S A* 103(24)**,** 9321-9326. doi: 10.1073/pnas.0603146103.

Ullian, E.M., Harris, B.T., Wu, A., Chan, J.R., and Barres, B.A. (2004). Schwann cells and astrocytes induce synapse formation by spinal motor neurons in culture. *Mol Cell Neurosci* 25(2)**,** 241-251. doi: 10.1016/j.mcn.2003.10.011.

Ullian, E.M., Sapperstein, S.K., Christopherson, K.S., and Barres, B.A. (2001). Control of synapse number by glia. *Science* 291(5504)**,** 657-661. doi: 10.1126/science.291.5504.657.

Wang, Y., Ying, G.X., Liu, X., Wang, W.Y., Dong, J.H., Ni, Z.M., et al. (2005). Induction of ephrin-B1 and EphB receptors during denervation-induced plasticity in the adult mouse hippocampus. *Eur J Neurosci* 21(9)**,** 2336-2346. doi: 10.1111/j.1460-9568.2005.04093.x.

Wolosker, H., Blackshaw, S., and Snyder, S.H. (1999). Serine racemase: a glial enzyme synthesizing D-serine to regulate glutamate-N-methyl-D-aspartate neurotransmission. *Proc Natl Acad Sci U S A* 96(23)**,** 13409-13414. doi: 10.1073/pnas.96.23.13409.

Wurzman, R., Forcelli, P.A., Griffey, C.J., and Kromer, L.F. (2015). Repetitive grooming and sensorimotor abnormalities in an ephrin-A knockout model for Autism Spectrum Disorders. *Behav Brain Res* 278**,** 115-128. doi: 10.1016/j.bbr.2014.09.012.

Xu, N.J., and Henkemeyer, M. (2012). Ephrin reverse signaling in axon guidance and synaptogenesis. *Semin Cell Dev Biol* 23(1)**,** 58-64. doi: 10.1016/j.semcdb.2011.10.024.

Xu, N.J., Sun, S., Gibson, J.R., and Henkemeyer, M. (2011). A dual shaping mechanism for postsynaptic ephrin-B3 as a receptor that sculpts dendrites and synapses. *Nat Neurosci* 14(11)**,** 1421-1429. doi: 10.1038/nn.2931.

Yang, Y., Ge, W., Chen, Y., Zhang, Z., Shen, W., Wu, C., et al. (2003). Contribution of astrocytes to hippocampal long-term potentiation through release of D-serine. *Proc Natl Acad Sci U S A* 100(25)**,** 15194-15199. doi: 10.1073/pnas.2431073100.

Yasumatsu, N., Matsuzaki, M., Miyazaki, T., Noguchi, J., and Kasai, H. (2008). Principles of long-term dynamics of dendritic spines. *J Neurosci* 28(50)**,** 13592-13608. doi: 10.1523/jneurosci.0603-08.2008.

Zhang, J.M., Wang, H.K., Ye, C.Q., Ge, W., Chen, Y., Jiang, Z.L., et al. (2003). ATP released by astrocytes mediates glutamatergic activity-dependent heterosynaptic suppression. *Neuron* 40(5)**,** 971-982. doi: 10.1016/s0896-6273(03)00717-7.

Zhang, Q., Pangrsic, T., Kreft, M., Krzan, M., Li, N., Sul, J.Y., et al. (2004). Fusion-related release of glutamate from astrocytes. *J Biol Chem* 279(13)**,** 12724-12733. doi: 10.1074/jbc.M312845200.

Zhou, L., Jones, E.V., and Murai, K.K. (2012). EphA signaling promotes actin-based dendritic spine remodeling through slingshot phosphatase. *J Biol Chem* 287(12)**,** 9346-9359. doi: 10.1074/jbc.M111.302802.

Zhuo, M., Small, S.A., Kandel, E.R., and Hawkins, R.D. (1993). Nitric oxide and carbon monoxide produce activity-dependent long-term synaptic enhancement in hippocampus. *Science* 260(5116)**,** 1946-1950. doi: 10.1126/science.8100368.

Figures

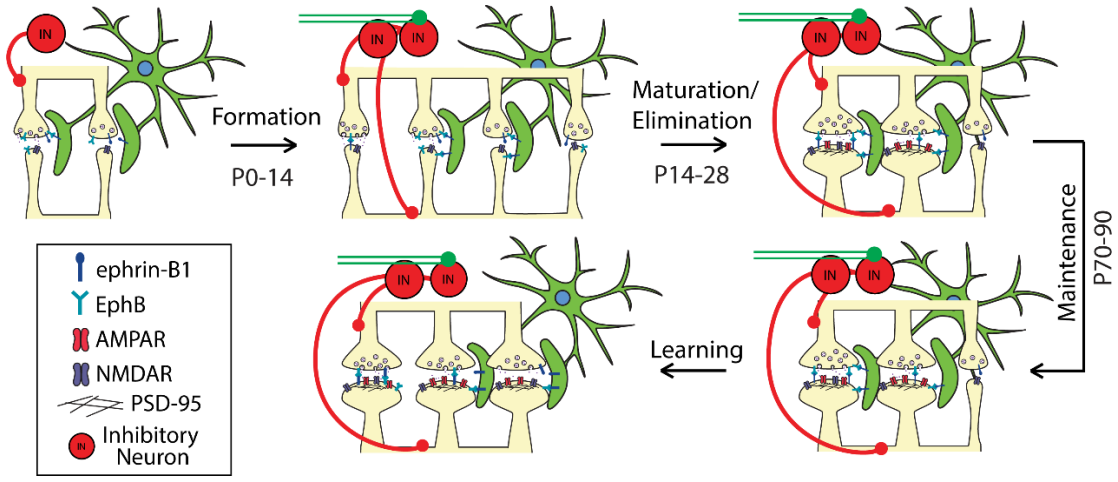

Figure 1.1 Model depicting astrocytic involvement in synapse development from early postnatal development to adulthood, to learning in adulthood. During early postnatal development (P0-28), synaptogenesis initially occurs saturating the number of synapses; however, elimination occurs to refine the circuitry and allow for maturation of necessary synapses. Synapses are maintained during adulthood (P70-90). During learning, immature synapses become potentiated and mature into functional synapses. Astrocytes play a role in these processes by releasing specific gliotransmitters and/or contact specific synapses to modulate synapse formation, elimination, or maturation. Specifically, with Eph/ephrin signaling, astrocytic ephrin-B1 may locate neuronal EphB receptors to refine synaptic circuitry by eliminating unnecessary, non-functional, synapses.

Tables

Table 1.1 Astrocytic secretion factors essential for synaptic modifications.

Secreted Factors	Assay	Role in Synapse Development	References
ATP	Culture	Heterosynaptic depression	Cotrina et al. (1998); Zhang et al. (2003)
BDNF	In vitro/ In vivo	Induces excitatory synapse formation	Gomez-Casati et al. (2010)
D-Serine	Culture	Metaplasticity of synaptic transmission LTP	Wolosker et al. (1999); Yang et al. (2003)
GABA	In vitro	Modulation of heterosynaptic depression	Serrano et al. (2006)
Glutamate	Culture	Synaptic plasticity	Parpura et al. (1994); Bezzi et al. (1998)
Glypican-4, 6	Culture/In vitro	Increases synaptic AMPARs Induces glutamatergic synapse formation	Allen et al. (2012)
Hevin	Culture	Induces glutamatergic synapse formation	Kucukdereli et al. (2011)
NO	In vitro	LTP Long-term presynaptic facilitation	Zhuo et al. (1993); Murphy (2000) Ikeda and Murase (2004)
S100β	In vitro/In vivo	LTP	Nishiyama et al. (2002)
SPARC	Culture	Decreases synaptic AMPARs Inhibits maturation of presynaptic cholinergic terminals	Jones et al. (2011); Albrecht et al. (2012)
TGF-β	Culture/In vitro	Induces glutamatergic synapse formation; regulates synapse maturation	Diniz et al. (2012); Fuentes-Medel et al. (2012)
Thrombospondin (TSP-1/-2)	Culture/In vivo	Neuronal development and neuronal repair, synaptogenesis Inhibits presynaptic release at glutamatergic synapses Increases post-synaptic glycine receptors; decrease post-synaptic AMPARs Activated by Gabapentin R a2o-1	Christopherson et al. (2005); Tran and Neary (2006) Crawford et al. (2012)
TNF-α	In vitro	Regulation of synaptic connectivity Increases synaptic AMPARs; decreases synaptic $GABA_AR$s	Beattie et al. (2002); Stellwagen and Malenka (2006)

Table 1.2 Astrocytic contact-mediated factors involved in synapse development.

Contact-mediated Factors	In vivo/vitro/ culture (assay)	Role in Synapse Development	References
ECM	Culture & in vitro	Stabilizes AMPA receptors at synapses	Frischknecht et al. (2009); Pyka et al. (2011)
Ephrin A/B	In vitro & in vivo	Modulate dendritic spine dynamics Activated by Eph A/B	Murai et al. (2003); Carmona et al. (2009) Ethell et al. (2001)
Mac-2 (Lgals3)	In vitro	Synaptic pruning via phagocytosis Activated by MerTK	Caberoy et al. (2012)
γ-Protocadherins	in vitro & in vivo	Induces glutamatergic and GABAergic synapse formation	Garrett and Weiner (2009)

Chapter 2 : Astrocytic ephrin-B1 controls excitatory-inhibitory balance in the developing hippocampus

Abstract

Astrocytes are implicated in synapse formation and elimination that are associated with developmental refinements of neuronal circuits and related behaviors. Astrocyte dysfunctions are also linked to synapse pathology associated with neurodevelopmental disorders and neurodegenerative diseases. Although several astrocyte-derived secreted factors are implicated in synaptogenesis, the role of contact-mediated glial-neuronal interactions in synapse formation and elimination is still unknown. Previous studies suggest that the membrane-bound ephrin-B1 expressed in astrocytes may influence trans-synaptic interaction between neuronal ephrin and its EphB receptors, affecting synapse formation *in vitro* and synapse maintenance in the adult hippocampus. In this study, I examined whether the loss or overexpression of astrocytic ephrin-B1 during early postnatal development (P14-P28) would affect synapse formation and maturation in the developing hippocampus *in vivo*. I found enhanced excitation of CA1 pyramidal neurons in astrocyte-specific ephrin-B1 knock-out (KO), which coincided with a greater vGlut1/PSD95 co-localization, higher number of dendritic spines and enhanced evoked AMPAR and NMDAR excitatory postsynaptic currents (EPSCs) in CA1 neurons of KO mice compared to wild-type (WT) mice. In contrast, evoked inhibitory postsynaptic currents (IPSC) were reduced in CA1 neurons of KO mice. Although I observed an overall increase in number of vGAT/gephyrin-positive puncta, reduced vGlut1-positive boutons onto parvalbumin (PV) inhibitory neurons and lower PV cell numbers in the CA1 hippocampus of KO mice may contribute to reduced inhibition and higher excitation of CA1 neurons. Finally, dysregulation of excitatory/inhibitory (E/I) balance in KO mice

most likely underlies impaired sociability and increased repetitive behaviors observed in these mice.

2.1 Introduction

Synapses are the building blocks of neuronal networks functioning as fundamental information-processing units in the brain (Südhof and Malenka, 2008; Mayford et al., 2012). Excitatory glutamatergic synapses are specialized cell-cell connections that facilitate neuronal activity, which is also fine-tuned by a complex network of inhibitory inputs from γ-aminobutyric acid (GABA) expressing interneurons. Synapse development involves activity-mediated formation, pruning, and maturation of specific synapses that are important in establishing neural circuits. Improper synapse development that leads to imbalance between excitatory and inhibitory (E/I) synaptic activity is linked to several neurologic disorders, including autism spectrum disorders (ASD; (Gao and Penzes, 2015; Lee et al., 2017) and epilepsy (Fritschy, 2008; Bonansco and Fuenzalida, 2016). Thus, investigations of the mechanisms underlying excitatory and inhibitory synapse development may contribute to an understanding of the pathophysiological mechanisms of the brain disorders.

Astrocytes are able to control the connectivity of neuronal circuits by regulating formation, pruning, and maturation of synapses by either secretion of numerous gliotransmitters or through direct contact with synapses. Astrocytes produce and secrete several factors that promote synaptogenesis, such as thrombospondin (Christopherson et al., 2005), hevin (Kucukdereli et al., 2011) and glypican (Allen et al., 2012), whereas the release of gliotransmitters such as glutamate (Fellin et al., 2004), D-serine (Henneberger et al., 2010), and TNF-α (Beattie et al., 2002; Stellwagen and Malenka, 2006) can modulate synaptic functions. Astrocytic processes are also suggested to modulate synapse

number and function through the direct contacts with dendritic spines and presynaptic boutons (Araque et al., 1999; Ullian et al., 2001; Hama et al., 2004; Clarke and Barres, 2013; Allen and Eroglu, 2017). The direct contacts of astrocytes with synapses may also regulate synapse elimination (Chung et al., 2013).

EphB receptor tyrosine kinases and their ephrin-B ligands are membrane-associated proteins that play an important role in regulating a variety of cell-cell interactions during development including axons guidance (Zimmer et al., 2003), and synaptogenesis (Dalva et al., 2000; Ethell et al., 2001; Henkemeyer et al., 2003; Moeller et al., 2006; Segura et al., 2007). EphB/ephrin-B interactions upon cell-cell contact result in bidirectional signaling, activating forward signaling in the Eph-expressing cell and reverse signaling in the ephrin-expressing cell (Bush and Soriano, 2009; Sloniowski and Ethell, 2012; Xu and Henkemeyer, 2012). The trans-synaptic Eph/ephrin-B interactions can promote postsynaptic spine formation and maturation during development (Henderson et al., 2001; Henkemeyer et al., 2003; Kayser et al., 2006). EphB receptors are shown to directly interact with NMDARs and are important for the recruitment and retention of NMDARs at the synaptic site and modulating the function of NMDARs (Dalva et al., 2000; Henderson et al., 2001; Kayser et al., 2006; Nolt et al., 2011). EphBs can also regulate the localization of AMPARs by interacting with adaptor proteins and regulating intracellular signaling cascades (Kayser et al., 2006; Hussain et al., 2015). Together, EphB/ephrinB signaling influences both synapse formation and maturation by regulating glutamate receptors at the post-synaptic sites.

My previous study suggests that the changes in ephrin-B1 levels in astrocytes may influence trans-synaptic interactions between neuronal ephrin-B and its EphB receptors, affecting synapse formation *in vitro* and synapse maintenance in the adult hippocampus *in vivo* (Koeppen et al., 2018). In this study, I examined whether the deletion of astrocytic ephrin-B1 during early postnatal development (P14-P28) would affect synapse formation and maturation in the developing hippocampus *in vivo*. I observed enhanced excitation of CA1 pyramidal neurons in astrocyte-specific ephrin-B1 knock-out (KO) using field recordings, which is most likely a result of an increase in number of excitatory synapses and enhanced evoked AMPAR and NMDAR excitatory postsynaptic currents (EPSCs) in CA1 neurons of KO mice compared to wild-type (WT) mice. Additionally, I observed reduced vesicular glutamate transporter (vGlut1)-positive boutons onto parvalbumin (PV) inhibitory neurons and lower PV cell numbers in the CA1 hippocampus of KO mice suggesting changes in inhibitory circuits as well. In addition, evoked inhibitory postsynaptic currents (IPSC) were reduced in CA1 hippocampal neurons of KO mice compared to WT. Enhanced E/I balance in CA1 neurons of KO mice manifested itself in increased repetitive behaviors and reduced sociability. Together, my findings suggest that astrocytic ephrin-B1 influences the development of hippocampal circuits during early postnatal period, E/I balance, and animal behaviors by regulating synapse development.

2.2 Materials & Methods

2.2.1 Mice

ERT2-Cre^{GFAP} (B6.Cg-Tg(*GFAP*-cre/ERT2)505Fmv/J RRID: IMSR_JAX:012849) male mice were crossed with *ephrin-B1*$^{flox/+}$ (129S-*Efnb1*$^{flox/+}$/J female mice, RRID: IMSR_JAX:007664) female mice to obtain ERT2-Cre^{GFAP}*ephrin-B1*$^{flox/y}$ (KO), or ERT2-Cre^{GFAP} (WT) male mice (Fig. 2.1A). Young WT and KO littermates received tamoxifen at postnatal age (P) 14 intraperitoneally (IP; 0.5 mg in 5 mg/ml of 1:9 ethanol/sunflower seed oil solution) once a day for 5 consecutive days. There were no detectable changes in ephrin-B1 levels in astrocytes or neurons in ERT2-Cre^{GFAP}*ephrin-B1*$^{flox/y}$ non-injected or injected with sunflower seed oil without tamoxifen as previously reported (Nikolakopoulou et al., 2016). To confirm specific ablation of ephrin-B1 in astrocytes, ephrin-B1 immunoreactivity was analyzed in ERT2-Cre^{GFAP}*ephrin-B1*$^{flox/y}$ (KO) and ERT2-Cre^{GFAP} (WT) mice (Fig. 2.2A). Ephrin-B1 immunoreactivity was observed in cell bodies and dendrites of CA1 neurons but not hippocampal astrocytes of tamoxifen-treated KO mice (Fig. 2.2A). There were no changes in ephrin-B1 levels in astrocytes and neurons of tamoxifen-treated WT mice. PCR analysis of genomic DNA isolated from mouse tails was used to confirm genotypes. Mice were maintained in an AAALAC accredited facility under 12-h light/dark cycle and fed standard mouse chow. All mouse studies were done according to NIH and Institutional Animal Care and Use Committee guidelines; animal welfare assurance number A3439-01 is on file with the Office of Laboratory Animal Welfare (OLAW).

2.2.2 Immunohistochemistry

Animals were anesthetized with isoflurane and transcardially perfused with 0.9% NaCl followed by fixation with 4% paraformaldehyde in 0.1 M phosphate-buffered saline (PBS), pH 7.4. Brains were post-fixed overnight with 4% paraformaldehyde in 0.1 M PBS and 100 μm coronal brain sections were cut with a vibratome. Excitatory presynaptic boutons were labeled by immunostaining against vesicular glutamate transporter 1 (vGlut1) using rabbit anti-vGlut1 antibody (0.25 mg/ml, Invitrogen 482400, RRID: AB_2533843), excitatory postsynaptic sites were identified with mouse anti-postsynaptic density-95 (PSD95) antibody (1.65 μg/ml, Invitrogen MA1-045, RRID: AB_325399). Inhibitory neurons were detected with mouse anti-glutamic acid decarboxylase 65 (GAD65) antibody (10 μg/ml, BD Pharmingen 559931, RRID: AB_397380). Parvalbumin (PV)-positive cells were identified with mouse anti-PV antibody (6 μg/ml, Sigma-Aldrich P3088, RRID: AB 477329). Inhibitory pre-synaptic sites were detected with vesicular GABA transporter (vGAT) using rabbit anti-vGAT antibody (1:100, Synaptic Systems 131002, RRID: AB_887871). Inhibitory post-synaptic sites were detected with gephyrin using mouse anti-gephyrin antibody (1:500, Synaptic Systems 147111, RRID: AB_887719). Astrocytes were identified by immunolabeling against glial fibrillary acidic protein (GFAP) using mouse anti-GFAP antibody (1:500, Sigma-Aldrich G3893, RRID: AB_477010), and ephrin-B1 levels were detected by immunostaining with goat anti-ephrin-B1 antibody (20 μg/ml, R&D Systems AF473, RRID: AB_2293419). Secondary antibodies used were Alexa Fluor 594-conjugated donkey anti-mouse IgG (4 mg/ml, Molecular Probes A-21203, RRID: AB_141633),

Alexa Fluor 647-conjugated donkey anti-rabbit IgG (4 mg/ml, Molecular Probes A-31573, RRID: AB_2536183), Alexa Fluor 647-conjugated donkey anti-goat IgG (4 mg/ml, Molecular Probes A-21447, RRID: AB_141844), or Alexa Fluor 488-conjugated donkey anti-goat IgG (4 mg/ml, Molecular Probes A-11055, RRID: AB_2534102). Sections were mounted on slides with Vectashield mounting medium containing DAPI (Vector Laboratories Inc. Cat# H-1200, RRID: AB_2336790).

2.2.3 Confocal Imaging and Analysis

Confocal images of containing stratum oriens (SO), stratum pyramidale (SP), stratum radiatum (SR) and stratum lacunosum-moleculare (SLM) layers in the CA1 hippocampus were taken with a Leica SP5 confocal laser-scanning microscope. High-resolution optical sections (1,024 x 1,024-pixel format) were captured with a 40x water-immersion and 1x zoom at 1-µm step intervals. All images were acquired under identical conditions. For the analysis of ephrin-B1 immunoreactivity, three adjacent projections from SR and SLM layers of the CA1 hippocampus were analyzed per each brain slice from at least three animals per group. Each z-stack was collapsed into a single image by projection, converted to a tiff file, encoded for blind analysis, and analyzed using Image J Software (RRID: nif-0000-30467). Cell area, integrated fluorescent intensity, and cell perimeter were determined for each GFAP-positive and ephrin-B1-positive cell (100–200 astrocytes, z-stacks at least 10 optical images, three mice per group, 2-3 brain slices per mouse). For the analysis of vGlut1, GAD65, and PSD95 immunolabeling, six sequential images were captured for selected area at 1-µm step intervals, each image in the series

was threshold-adjusted to identical levels (0-160 intensity) and puncta (0.5-10 μm^2) were measured using ImageJ software. Three adjacent areas from SR and SLM were imaged and analyzed per each hippocampus from four animals per group. Cell body labeling was excluded from the analysis. Statistical analysis was performed with one-way ANOVA followed by Tukey post-hoc analysis using GraphPad Prism 7 software (RRID: SCR_002798), data represent mean ± standard error of the mean (SEM).

2.2.4 Dendritic Spine Analysis

Dendritic spines were identified with GFP using transgenic Thy1-GFP-M male mice (Tg(Thy1-EGFP)MJrs/J, RRID: IMSR_JAX:007788), which were crossed with ERT2-Cre^{GFAP}*ephrin-B1*$^{flox/+}$ female mice (129S-*Efnb1*^{tm1Sor}/J, RRID: IMSR_JAX:007664) to obtain Thy1-GFP-ERT2-Cre^{GFAP}*ephrin-B1*$^{flox/y}$ (KO), or Thy1-GFP-ERT2-Cre^{GFAP} (WT) male mice expressing GFP in hippocampal neurons. Animals were anesthetized with isoflurane and transcardially perfused initially with 0.9% NaCl, followed by fixation with 4% PFA in 0.1 M PBS, pH 7.4. Brains were post-fixed for 2 h in 4% PFA in 0.1 M PBS, and 100 μm coronal sections were cut with a vibratome. CA1 hippocampal neurons were imaged using Leica SP5 confocal microscope. 10-15 GFP-expressing neurons were randomly selected per group, and dendrites were imaged using a 63x-oil immersion objective (1.2 NA), 1x zoom. Three-dimensional fluorescent images were created by the projection of each z-stack containing 50 high-resolution optical serial sections (1,024 x 1,024-pixel format) taken at 0.5 μm intervals in the X-Y plane. Quantifications of the spine density (spines per 10 μm dendrite), lengths (μm), volumes

(μm^3), and distances between spines were carried out using Neurolucida 360 software (MicroBrightField RRID: SCR_001775). Statistical analysis was performed with two-way ANOVA followed by Bonferroni's post-hoc analysis using GraphPad Prism 7 software (GraphPad Prism, RRID: SCR_002798), data represent mean ± SEM.

2.2.5 Synaptosome Isolation & Western Blot Analysis

Isolation of hippocampal synaptosomes was performed as previously described (Hollingsworth et al., 1985). Hippocampal tissues from P28 WT or KO mice were homogenized in 1 ml synaptosome buffer (in mM: 124 NaCl, 3.2 KCl, 1.06 KH_2PO_4, 26 $NaHCO_3$, 1.3 $MgCl_2$, 2.5 $CaCl_2$, 10 Glucose, 20 HEPES). Homogenates were first filtered through a 100 μm nylon net filter (NY1H02500, Millipore) and then through a 5 μm nylon syringe filter (SF15156, Tisch International). Homogenate flow through was collected and synaptosomes were spun down at 10,000 g, 4^{o}C, for 30 min. Synaptosomes were resuspended in 800 μl synaptosome buffer. To confirm synaptosome enrichment, levels of synapsin-1, PSD95, and histone deacetylase (HDAC I) were analyzed in tissue homogenates and synaptosome fractions with western blot analysis.

Isolated hippocampal synaptosome samples were centrifuged at 10,000 g, 4^{o}C, for 30 min, pellets were re-suspended in lysis buffer (50 mM Tris, 100 mM NaCl, 2% TritonX-100, 10 mM EDTA) containing 2% protease inhibitor cocktail (P8340, Sigma-Aldrich) and incubated for 2 h at 4^{o}C. Samples were added to 2X Laemmli Buffer (S3401, Sigma-Aldrich) and run on an 8-16% Tris-Glycine Gel (EC6045BOX, Invitrogen). Protein samples were transferred onto a nitrocellulose blotting membrane

(10600007, GE Healthcare). Blots were blocked with 5% milk in TBS (10 mM Tris, 150 mM NaCl, pH 8.0) followed by immunostaining with mouse anti-PSD95 (1.65 μg/ml, Invitrogen MA1-045, RRID: AB_325399), rabbit anti-GluA1 (1:100, Millipore AB1504, RRID: AB_2113602), rabbit anti-GluA2/3 (0.1 μg/ml, Millipore AB1506, RRID: AB_90710), rabbit anti-HDAC I (0.40 μg/ml, Santa Cruz Biotechnologies sc-7872, RRID: AB_2279709), rabbit anti-synapsin-1 (0.2 μg/ml, Millipore AB1543P, RRID: AB_90757), or mouse anti-GAPDH (0.2 μg/ml, Thermo Fisher Scientific 39-8600, RRID:AB_2533438) antibodies in 0.1% tween 20/TBS at 4^{o}C for 16 h. Secondary antibodies used were HRP conjugated donkey anti-mouse IgG (Jackson ImmunoResearch 715-035-150, RRID: AB_2340770) or HRP conjugated goat anti-rabbit IgG (Jackson ImmunoResearch 111-035-003, RRID: AB_2313567). Blots were incubated in ECL 2 Western Blotting Substrate (80196, Pierce) and a signal was collected with CL-XPosure film (34090, Pierce). Band density was analyzed by measuring band and background intensity using Adobe Photoshop CS5.1 software (RRID: SCR_014199). Statistical analysis was performed with a one-way ANOVA followed by Tukey post-hoc analysis using GraphPad Prism 7 software (RRID: SCR_002798), data represent mean ± SEM.

2.2.6 Extracellular Field Recordings

Early postnatal developing (P28) mice were used for electrophysiological experiments two weeks after the first tamoxifen injection. Animals were deeply anesthetized with isoflurane and decapitated. The brains were rapidly removed and immersed in ice-cold artificial cerebrospinal fluid (ACSF) with high Mg^{2+} and sucrose

concentration containing: (in mM) 3.5 KCl, 1.25 NaH_2PO_4, 20 D(+)-glucose, 185 sucrose, 26 $NaHCO_3$, 10 $MgCl_2$ and 0.50 $CaCl_2$, pH of 7.4, and saturated with 95% O_2/5% CO_2. Transverse hippocampal slices sectioned at 350 µm thick were prepared by using a vibrating blade microtome (LeicaVT1000s, Leica Microsystems; Buffalo Grove, IL, USA) in ice-cold slicing solution bubbled with 95% O_2/5% CO_2. Slices were then transferred into a holding chamber containing oxygenated ACSF (in mM: 124 NaCl, 3.5 KCl, 1.25 NaH_2PO_4, 10 D(+)-glucose, 26 $NaHCO_3$, 2 $MgCl_2$, and 2 $CaCl_2$, pH 7.4) and incubated for 1 h at 33°C, then kept at room temperature. For recordings, slices were transferred to a submersion recording chamber continuously perfused with oxygenated ACSF at a flow rate of 1 ml/min, at 33˚C. Slices were equilibrated in recording chamber for 10 min to reach a stable baseline response prior to running experimental protocols. Glass microelectrodes were pulled with a Sutter P-97 micropipette puller (Sutter Instrument, Novato, CA, USA; RRID: SCR_016842) with a tip resistance of 1-3 MΩ and filled with 3 M NaCl. Glass microelectrodes were positioned in the SP and SR areas of CA1 hippocampus for extracellular recording. Synaptic responses were evoked by stimulating Schaffer collaterals (SC) using a bipolar tungsten electrode (WPI, Sarasota, FL, USA). Potentials were amplified (Axoclamp-2B, Molecular Devices, Sunnyvale, CA, USA), digitized at a sampling rate of 10 kHz, and analyzed offline using pClamp 10.7 software (Molecular Devices; RRID: SCR_011323). All electrophysiological responses were digitally filtered at 1 kHz low-pass filter to improve signal-to-noise ratio.

Dendritic potentials typically consisted of a small presynaptic fiber volley (FV) followed by a negative field excitatory postsynaptic potential (fEPSP). The amplitude of

the FV reflects the depolarization of the presynaptic terminals and the fEPSP slope reflects the magnitude of the postsynaptic dendritic depolarization. Postsynaptic neuronal firing is represented by the amplitude of the population spike (PS). PSs were calculated as the voltage difference between two positive peaks and the most negative peak of the trace.

Input-output (I/O) curves were generated to examine basal synaptic transmission by incrementally increasing stimulation intensity, beginning at 0.10 mA and increasing stimulation by 0.10 mA until maximal somatic PS amplitudes were reached. Maximal PS amplitude was regarded as maximal neuronal output. Maximal fEPSP slope and PS response along with 30-50% of maximal fEPSP slope and PS were determined. Paired-pulse facilitation (PPF) was used to test for changes in presynaptic glutamate release probability. PPF was evoked by twin stimuli at 30% of maximal fEPSP slope. The two stimuli were separated by varying interpulse intervals: 20, 50, 100, 200, or 400 ms. PPF was calculated from the ratio of fEPSP2/fEPSP1 slope. To elicit paired-pulse inhibition (PPI), twin stimuli were provided at 100% of max PS response and at inter-pulse intervals of 6, 10, 20, 50, 100, or 200 ms. PPI was calculated from PS2/PS1 amplitude ratio. For long-term potentiation (LTP), SC were initially stimulated to evoke 30% maximal fEPSP slope for 10 min to obtain baseline response then SC were stimulated 2 trains of 100 pulses at 100 Hz, 20 s apart to induce LTP. LTP was sampled at 30 s intervals for 60 min post stimulation and potentiation was calculated by dividing the average slope of post-induction responses by the average slope of pre-induction baseline responses.

For electrophysiological data, two-way ANOVA was used followed by Bonferroni test to evaluate the effects of astrocytic ephrin-B1 deletion on the I/O curves, PPF, PPI, and LTP. In all electrophysiological recordings, the data represent mean ± SEM.

2.2.7 Whole-Cell Patch Voltage Clamp Recordings

Brain slice preparation for whole-cell patch clamp was similar as above; briefly, brains were rapidly removed and immersed in ice cold "slushy" artificial cerebrospinal fluid (ACSF) with high Mg^{2+} and sucrose concentration containing the following (in mM): 87 NaCl, 75 sucrose, 2.5 KCl, 0.5 $CaCl_2$, 7 $MgCl_2$, 1.25 NaH_2PO_4, 25 $NaHCO_3$, 10 glucose, 1.3 ascorbic, acid, 0.1 kynurenic acid, 2.0 pyruvate, and 3.5 MOPS with a pH of 7.4 and saturated with 95% O_2/5% CO_2. Transverse hippocampal slices (350 µm) were prepared by using a vibrating blade microtome (Campden 5100mz-Plus, Campden Instruments Ltd.) in high Mg^{2+}/sucrose ACSF solution bubbled with 95% O_2/5% CO_2. Slices were then incubated in a holding chamber containing oxygenated high Mg^{2+}/sucrose ACSF for 30 min at room temperature and then transferred into ACSF (in mM; 125 NaCl, 2.5 KCl, 2.5 CaCl2, 1.3 MgCl2, 1.25 NaH2PO4, 26 NaHCO3, 15 glucose 3.5 MOPS with a pH of 7.4) for an additional 30 min at room temperature. Slices were then transferred to a recording chamber continually perfused with oxygenated ACSF at a flow rate of 1 ml/min at 33˚C.

Whole-cell patch experiments were done blind as described in by Castañeda-Castellanos et al. (Castaneda-Castellanos et al., 2006). Electrical stimuli (0.1 Hz) were

delivered through a bipolar, Teflon®-coated tungsten electrode (FHC, Bowdin, ME, USA) placed in the CA3 Schaffer collaterals and in close proximity to the recording electrode. Tight-seal whole-cell recordings were obtained using pipettes made from borosilicate glass capillaries pulled on a Narishige PC-10 vertical micropipette puller (Narishige, Tokyo, Japan). Pipette resistance ranged from 3 to 4 MΩ and filled with an internal solution containing: (in mM) 130 CsOH, 130 D-gluconic acid, 0.2 EGTA, 2 $MgCl_2$, 6 CsCl, 10 Hepes, 2.5 ATP-Na, 0.5 GTP-Na, 10 phosphocreatine and 0.1% Biocytin for cellular post labeling, pH adjusted to 7.2-7.3 with CsOH, osmolarity adjusted to 300-305 mOsm with ATP-Na. Neurons were voltage-clamped at either -70 mV to measure AMPAR evoked responses or +40 mV to measure NMDAR evoked responses. 1 µM tetrodotoxin was added to isolate mEPSC responses. All excitatory postsynaptic currents (EPSCs) were recorded in the presence of 50 µM picrotoxin, a $GABA_A$ receptor antagonist, to block $GABA_A$-mediated currents. To measure inhibitory postsynaptic currents (IPSCs), neurons were voltage-clamped at 0 mV with 10 µM NBQX, an AMPA receptor antagonist, and 50 µM D-AP5, a NMDA receptor antagonist. EPSCs and IPSCs were recorded using an EPC-9 amplifier (HEKA Elektronik, Lambrecht, Germany), filtered at 1 kHz, digitized at 10 kHz, and stored on a personal computer using pClamp 10.7 software (Molecular Device) to run analysis. The series resistance was <25 MΩ and was compensated. Both series and input resistance were monitored throughout the experiment by delivering 5 mV voltage steps. If the series resistance changed more than 20% during the course of an experiment, the data was discarded. AMPA, NMDA-mediated EPSCs, IPSCs evoked responses, mEPSCs, and

mIPSCs were analyzed by Clampfit 10.7 software (Molecular Device). All averaged data were presented as means ± SEM. Statistical significance was determined by the Student's *t*-test using Prism 7 software (Graph Pad Software, Avenida, CA).

2.2.8 Fear Conditioning Behavior Test

A fear-conditioning paradigm was used to assess hippocampal dependent contextual learning as previously described (Anagnostaras et al., 2001; Koeppen et al., 2018). Two contexts were used to test contextual memory. Context A was an 18 X 18 cm rectangular clear plexiglass box with 16-grated steel bar flooring; trials in context A were in white light and the scent of Quatricide TB. Context B was in a cylinder with a diameter of 15 cm and a height of 20 cm with 2.5 X 2.5 cm, with checkered black and white walls; trials in context B were in altered light with fresh litter and the scent of Windex. Animals were allowed to acclimate in the behavioral room for 30 min before each testing day and handled for 2 min for 5 days prior to testing. On day one, the test mouse was placed in context A and habituated to the chamber for 10 min, 1 h after context A mice were habituated to context B for 10 min. The mouse was removed and separated from its home cage until all mice in that cage were habituated to both contexts. On day two, test mice were trained to associate an unconditioned stimulus (US; 0.6 mA scrambled foot shock) with a conditioned stimulus (CS; 9 kHz, 70 dB tone) in context A. Initially, test mice were placed in context A and given 3 minutes for habituation, then followed by a 30 s tone (CS), which co-terminated with a 2 s foot shock (US). The CS-US pairing occurred five times, with a pseudorandom interval between pairings. The test mouse, again, was

removed and separated from its home cage until all mice in that cage were trained. On day three, animals were tested for their associated memory of the context (in context A) and of the CS tone (in context B). For contextual recall, mice were placed in context A for 5 min with no sound and returned to home cage for 1 h before testing context B. For tone recall test, mice were placed in context B for a total of 6 min, with the CS tone playing for the final 3 min. Freezing behavior was measured as a percentage of time freezing using TopScan Software. To further understand mouse behavioral responses following fear conditioning, mouse behaviors were manually scored using six categories: stretch and attend posture (SAP), freezing, scanning, rearing, and in motion. Videos were scored at 10 s intervals during habituation in context A and B, training, context A recall, context B recall with no tone, and context B with tone, based on previous studies (Cruz et al., 1994; Rodgers and Johnson, 1995; Shin and Liberzon, 2010; Coimbra et al., 2017; Reinhard et al., 2019). GraphPad Prism 7 software (RRID: SCR_002798) was used to perform a one-way ANOVA followed by Tukey's post hoc analysis or *t*-test when appropriate, data represent mean ± SEM.

2.2.9 Open Field Behavior Test

Locomotor activity and anxiety was evaluated using a standard open field exploration test. The apparatus consisted of a 72 × 72 cm open field arena with 50-cm-high walls constructed from opaque acrylic sheets with a clear acrylic sheet for the bottom with a grid placed underneath it for scoring purposes. All testing was done in a brightly lit room (650 lux), between 9 am -2 pm. Prior to testing, mice were housed in a

room with a 12 hours light/dark cycle with *ad libitum* access to food and water. Mice were initially habituated to the testing room for at least 30 min before testing. During testing, animals were allowed to freely explore the open field for 10 min. The floor of the chamber was cleaned with 2-3% acetic acid, 70% ethanol, and water between tests to eliminate odor trails. Assessments of the digital recordings were done by blinded observers using TopScan Lite software (Clever Sys. Inc, Reston, VA 20190). Time spent in thigmotaxis and average velocity were scored by the program. A tendency to travel to the center and percent time spent in thigmotaxis was used as an indicator of anxiety (Yan et al., 2004; Yan et al., 2005). Average velocity and total line crosses were measured to score locomotor activity. Statistical analysis was performed using Student's *t*-test.

2.2.10 Social Novelty Behavior Test

Sociability and social memory were studied using a three-chamber test as described previously (Kaidanovich-Beilin et al., 2011). Briefly, a rectangular box contained three adjacent chambers 19 x 45 cm each, with 30 cm high walls and a bottom constructed from clear plexiglass. The three-chambers were separated by dividing walls made from clear plexiglass with openings between the middle chamber and each side chamber. Removable doors over these openings permitted chamber isolation or free access to all chambers. All testing was done in a brightly lit room (650 lux), between 9 am and 2 pm. Prior to testing, mice were housed in a room with a 12 hours light/dark cycle with *ad libitum* access to food and water. The cages were transferred to the behavioral room 30 min before the first trial began for habituation. The test mouse was

placed in the central chamber with no access to the left and right chambers and allowed to habituate to the test chamber for 5 min before testing began. Session 1 measured sociability; in session 1, another mouse (stranger 1) was placed in a wire cup-like container in one of the side chambers. The opposite side had an empty cup of the same design. The doors between the chambers were removed and the test mouse was allowed to explore all the three chambers freely for 10 min, while being video recorded from above. The following parameters were monitored: the duration of direct contact between the test mouse and the stranger mouse or the empty cup and the duration of entries into each chamber. Session 2 measured social memory; in session 2, a new mouse (stranger 2) was placed in the empty wire cup in the second side chamber. Stranger 1, now familiar mouse remained in the first side chamber. The test mouse was allowed to freely explore all three chambers for another 10 min and the same parameters were monitored. Placement of stranger 1 in the left or right side of the chamber was randomly altered between trials. Each testing session lasted 10 min and the session was recorded digitally from above. The floor of the chamber was cleaned with 2-3% acetic acid, 70% ethanol, and water between tests to eliminate odor trails. Assessments of the digital recordings were done using TopScan Lite software (Clever Sys. Inc, Reston, VA 20190). Statistical analysis was performed using two-way ANOVA followed by post-hoc with Bonferroni correction.

2.3 Results

Previous studies in the lab suggest that the changes in ephrin-B1 levels in astrocytes may influence trans-synaptic interaction between neuronal ephrin and its EphB receptors, affecting synapse formation *in vitro* (Koeppen et al., 2018). I reported that the overexpression of ephrin-B1 on astrocytes inhibited synapse formation in primary neuronal cultures, most likely by engulfing EphB-containing synaptic boutons. I also reported that astrocytic ephrin-B1 affects synapse maintenance *in vivo* (Koeppen et al., 2018). The goal of this study was to determine if deletion or overexpression of astrocytic ephrin-B1 during early postnatal development (P14-P28) would affect synapse formation and maturation in the developing hippocampus and E/I balance *in vivo*. Ephrin-B1 KO and OE was accomplished in astrocytes during P14-28 period of hippocampal synaptogenesis. Activity of CA1 hippocampal neurons was measured using both extracellular field recordings and whole-cell patch clamp electrophysiology to determine excitatory and inhibitory synaptic changes. To evaluate E/I circuit changes, I further analyzed dendritic spine density and morphology, and density of excitatory and inhibitory synapses by immunohistochemistry through the analysis of vGlut1/PSD95, vGlut1/PV and VGAT/gephyrin-positive puncta. To examine the functional significance of the synaptic changes in the developing hippocampus, mouse behaviors, such as sociability, social novelty, anxiety, hyperactivity and fear-associated memory were also evaluated in ephrin-B1 KO mice.

Ephrin-B1 loss in developing astrocytes enhances excitability of CA1 hippocampal neurons.

To determine if loss of astrocytic ephrin-B1 alters neuronal activity in the developing hippocampus acute hippocampal slices from P28 WT and KO mice were prepared for extracellular field recordings. To achieve tamoxifen-induced deletion of astrocytic ephrin-B1 during P14-28 period, P14 ERT2-Cre^{GFAP} (WT) and ERT2-Cre^{GFAP}*ephrin-B1*$^{flox/y}$ (KO) male littermates received tamoxifen intraperitoneally (IP; 0.5 mg in 5mg/ml of 1:9 ethanol/sunflower seed oil) once a day for 5 days and analyzed at P28 (Fig. 2.2A). Ephrin-B1 immunoreactivity was selectively disrupted in hippocampal astrocytes, but not neurons, of tamoxifen-treated KO as compared to tamoxifen-treated WT mice (Fig. 2.2A). Presynaptic FV amplitude, postsynaptic fEPSP slope, and somatic population spike (PS) amplitude of neuronal responses were recorded in SR and SP layers of CA1 hippocampus and input-output (I/O) curves were generated by incrementally increasing stimulation intensity of SC in CA3 hippocampus (Fig. 2.2B-D). Extracellular field recordings revealed that the loss of astrocytic ephrin-B1 increased the excitability of CA1 hippocampal neurons. Both, FV response amplitude (Fig. 2.2B; two-way ANOVA; stimulation intensity $F_{(14, 540)} = 89.41$; genotype $F_{(1, 540)} = 8.064$, $p = 0.0047$, $p < 0.0001$) and fEPSP slope were significantly higher in KO mice (Fig. 2.2C; two-way ANOVA; stimulation intensity $F_{(14, 386)} = 41.58$, $p < 0.0001$; genotype $F_{(1, 386)} = 39.26$, $p < 0.0001$), showing a significant difference with post hoc at a stimulation intensity of 1.1 ($t_{(386)} = 3.14$, $p = 0.0273$) and 1.3 mA ($t_{(386)} = 2.957$, $p = 0.0495$), PS response amplitude was also greatly enhanced in KO mice (Fig. 2.2D; two-way ANOVA;

stimulation intensity $F_{(14, 510)} = 42.41$, $p < 0.0001$; genotype $F_{(1, 510)} = 64.18$, $p < 0.0001$) with post hoc differences at stimulation intensity of 0.9 ($t_{(510)} = 3.611$, $p = 0.0050$), 1.1 ($t_{(510)} = 3.161$, $p = 0.0250$), and 1.3 mA ($t_{(510)} = 3.107$, $p = 0.0299$). Additionally, short-term plasticity was also enhanced in KO showing an increase in paired-pulse facilitation (PPF) at 100 ms (Fig. 2.2E; t-test; $t_{(41)} = 2.998$, $p = 0.0046$); however, paired-pulse inhibition (PPI) at 10 ms was unaffected (Fig. 2.2F; t-test; $t_{(18)} = 1.382$, $p = 0.1839$). NMDAR-dependent LTP was also unaffected following astrocytic ephrin-B1 deletion, as I observed similar potentiation at 0-10, 30-40, and 50-60 min post stimulation of Schaffer collaterals with 2 trains of 100 pulses in WT and KO hippocampal slices (Fig. 2.2G; two-way ANOVA; time $F_{(2, 72)} = 1.101$, $p = 0.3381$; gene $F_{(1, 72)} = 0.6301$, $p = 0.4299$).

These results show that hippocampal CA1 pyramidal neurons show enhanced excitability following astrocyte specific deletion of ephrin-B1 during early postnatal development, suggesting an alteration in E/I balance.

Enhanced evoked excitatory postsynaptic AMPAR- and NMDAR-mediated responses and higher mEPSC amplitude are detected in CA1 neurons of astrocyte-specific ephrin-B1 KO mice.

To determine the mechanism of enhanced hippocampal activity in the hippocampus of KO mice, whole-cell voltage clamp electrophysiology was used to measure spontaneous and evoked excitatory responses from CA1 pyramidal neurons of P28 WT and KO mice in the presence of $GABA_A$ receptor antagonist picrotoxin (Fig. 2.3). I observed a significant increase in both AMPAR- and NMDAR-mediated EPSCs in

KO mice compared to WT (Fig. 2.3C; WT AMPAR: 226.39 ± 30.41 vs KO AMPAR: 486.13 ± 103.18; $t_{(19)} = 2.5560$, p = 0.0193; WT NMDAR: 136.58 ± 37.27 vs KO NMDAR: 485.28 ± 97.18; $t_{(19)} = 4.10$, p = 0.0006). Interestingly, AMPAR/NMDAR ratio was not significantly different between WT and KO mice (Fig. 2.3D; WT: 2.54 ± 0.42; KO: 1.74 ± 0.43; $t_{(12)} = 0.9743$, p = 0.3491). No differences were observed in mEPSC frequencies between WT and KO mice (Fig. 2.3F-G; WT: 0.41 ± 0.05; KO: 0.51 ± 0.05; $t_{(9)} = 1.259$,p = 0.2398). In contrast, I observed a significant shift in cumulative probability distribution of mEPSC amplitude to a higher amplitude (Fig. 2.3H; K–S test, n=190 and 160 for WT and KO group, respectively, p < 0.0001, D=0.3119) and increased mEPSC average amplitude (Fig. 2.3I; WT: 7.41 ± 0.65; KO: 11.01 ± 1.37; $t_{(9)} = 2.208$, p = 0.0273). My results suggest enhanced postsynaptic excitatory responses in CA1 neurons following astrocyte-specific deletion of ephrin-B1 during P14-28 early postnatal period.

Overexpression of astrocytic ephrin-B1 in hippocampus CA1 affects AMPAR- and NMDAR-mediated responses and mEPSC amplitude.

Next I examined the effects of the overexpression of astrocytic ephrin-B1 in CA1 hippocampus during P14-28 period on excitatory activity using viral approach, I observed significantly reduced evoked AMPAR- and NMDAR-mediated responses in OE groups compared to WT (Fig. 2.4B; WT AMPAR: 467.74 ± 93.27 vs KO AMPAR: 372.52 ± 58.58; $t_{(23)} = 2.692$, p = 0.0130; WT NMDAR: 327.608 ± 30.51 vs KO NMDAR: 204.13 ± 9.09; $t_{(20)} = 0.0019$, p = 3.573), with no effect to AMPAR/NMDAR EPSC ratio (Fig.

2.4C; WT: 1.77 ± 0.23 vs KO 2.19 ± 0.33; $t_{(20)} = 0.9733$, p = 0.3426). Similar to KO mice, cumulative probability of inter-event interval (Fig. 2.4E; K–S test, n=550 and 360 for WT and KO group, respectively, p = 0.4819, D=0.1408) and average frequency of mEPSC were unchanged in OE group compared to WT (Fig. 2.4F; WT: 0.69 ± 0.07 vs KO: 0.56 ± 0.10; $t_{(12)} = 1.036$, p = 0.3206). However, KO mice exhibited significant leftward shift of cumulative probability of mEPSC amplitude (Fig. 2.4G; K–S test, n=550 and 360 for WT and KO group, respectively, p = 0.0145, D=0.1065) and a reduced mEPSC amplitude compared to their WT counterparts (Fig. 2.4H; WT: 10.30 ± 0.83 vs KO: 8.29 ± 0.41; $t_{(12)} = 1.821$, p = 0.0468). Together this further confirms that astrocytic ephrin-B1 negatively affects excitatory synaptic transmission in the developing hippocampus, such that loss ephrin-B1 in astrocytes enhances, but its overexpression reduces, excitatory responses in CA1 hippocampal neurons.

Excessive excitatory synapse formation is observed in CA1 hippocampus of developing KO mice

Next, I examined whether loss of ephrin-B1 from astrocytes would also affect the number of excitatory synapses in CA1 hippocampus by co-immunostaining against presynaptic vGlut1 and postsynaptic PSD95 (Fig. 2.5A, B). I observed a significant increase in vGlut1-positive puncta (Fig. 2.5C; WT: 15.11 ± 0.92 vs KO: 19.19 ± 0.38; $t_{(21)} = 4.238$, p = 0.0004), PSD95-positive puncta (Fig. 2.5D; WT: 5.91 ± 0.55 vs KO: 9.80 ± 1.11; $t_{(17)} = 2.801$, p = 0.0123) and vGlut1/PSD95 co-localization (Fig. 2.5E; WT: 5.69 ± 0.82; KO: 11.93 ± 1.06; $t_{(51)} = 3.784$, p = 0.0004) in the SR layer of CA1

hippocampus of KO mice compared to WT. Further, dendritic spine density was significantly higher in KO compared to WT (Fig. 2.5G; WT: 6.65 ± 0.24 vs KO: 7.68 ± 0.28; $t_{(31)} = 2.78$, $p = 0.0092$). Together, my results suggest that the loss of astrocytic ephrin-B1 results in excessive excitatory synapse formation on excitatory CA1 neurons, which may contribute to enhanced excitability.

Developmental astrocyte-specific deletion of ephrin-B1 does not affect synapse maturation.

To assess synapse maturation, spine morphology was measured. Spine length was comparable between WT and KO mice (Fig. 2.5H; WT: 3.33 ± 0.17 vs KO: 3.35 ± 0.16; $t_{(31)} = 0.0697$, $p = 0.9449$). Interestingly, KO mice had a greater proportion of spines with smaller heads (0-0.5 um^3; Fig. 2.5I; WT: 62.19 ± 2.28 vs KO: 76.41 ± 1.83; two-way ANOVA, Tukey's post hoc test, $p < 0.0001$) and a smaller percent of medium size spines (0.5-1.0 um^3; Fig. 2.5I; WT:28.01 ± 1.30 vs KO: 20.36 ± 1.68; two-way ANOVA, Tukey's post hoc test, $p = 0.0162$) but similar levels of large, mature spines (>1.0 um^3; Fig. 2.5I; WT: 6.54 ± 0.68 vs KO: 4.31 ± 0.52; two-way ANOVA, Tukey's post hoc test, $p = 0.9617$) compared to WT animals. In addition, the levels of synaptic AMPAR subunits GluA1 and GluA2/3 was analyzed in developing hippocampus of WT and KO mice. Crude synaptosomes were isolated from P28 hippocampi of WT and KO mice and analyzed with immunoblotting (Fig. 2.6A). Synaptic PSD95 levels (Fig. 2.6B; WT:1.11 ± 0.13 vs KO: 0.97 ± 0.07, t-test; $t_{(10)} = 0.9338$, $p = 0.3724$) and levels of AMPAR subunits GluA1 (Fig. 2.6C; WT: 0.96 ± 0.03 vs KO: 1.06 ± 0.06, t-test; $t_{(10)} = 1.085$, $p = 0.3036$)

and GluA2/3 (Fig. 2.6D; WT: 1.16 ± 0.15 vs KO: 1.12 ± 0.12, t-test; $t_{(10)} = 0.1792$, $p = 0.8613$) were not significantly different between WT and KO mice. These results are consistent with similar AMPAR/NMDAR EPSC ratio that was observed in WT and KO mice (Fig. 2.3D), indicating no differences in the functional maturation of excitatory synapses between WT and KO mice.

Inhibitory postsynaptic currents are reduced in CA1 neurons of astrocytic ephrin-B1 KO mice while overexpression enhances inhibitory transmission in CA1 hippocampus.

To determine if astrocytic ephrin-B1 affects inhibitory synapses, inhibitory post-synaptic currents (IPSCs) were recorded from CA1 hippocampal neurons in P28 WT and KO mice using whole-cell voltage clamp electrophysiology (Fig. 2.7A). In the presence of NMDAR and AMPAR blockers, D-AP5 and NBQX, I observed a significant decrease in evoked IPSC amplitude in CA1 hippocampal neurons of KO mice compared to WT (Fig. 2.7B; WT: 513.62 ± 68.05 vs KO: 314.76 ± 80.56; t-test; $t_{(20)} = 1.9$, $p = 0.0360$). My results show that loss of ephrin-B1 from astrocytes also affects inhibitory postsynaptic response in CA1 hippocampal neurons.

Conversely, to determine if overexpression astrocytic ephrin-B1 affects inhibitory synapses, inhibitory post-synaptic currents (IPSCs) were recorded from CA1 hippocampal neurons in P28 WT and OE mice using whole-cell voltage clamp electrophysiology (Fig. 2.7C. I observed a significant increase in evoked IPSC amplitude in CA1 hippocampal neurons of OE mice compared to WT (Fig. 2.7D; WT: 479.58 ±

69.99 vs OE: 877.56 ± 180.06; t-test; $t_{(19)}$; = 2.135 p = 0.0460). My results show that overexpression of ephrin-B1 from astrocytes has opposing effects on inhibitory postsynaptic response in CA1 hippocampal neurons compared to deletion of astrocytic ephrin-B1.

Changes in the PV-positive inhibitory neurons in CA1 hippocampus may contribute to impaired inhibition in KO mice.

To determine if astrocyte-specific deletion of ephrin-B1 affects the inhibitory drive onto CA1 hippocampal neurons, inhibitory synaptic sites were detected on GFP-expressing dendrites of CA1 excitatory neurons with immunostaining against VGAT and gephyrin (Fig. 2.8A, B). I observed no effect of ephrin-B1 deletion from developing astrocytes on VGAT (Fig. 2.8C; WT: 16.45 ± 0.81 vs KO: 11.54 ± 0.73; t-test; $t_{(53)}$ = 1.586, p = 0.1186) and gephyrin puncta (Fig. 2.8D; WT:14.27 ± 1.10 vs KO: 13.85 ± 0.89; t-test; $t_{(53)}$ = 1.945, p = 0.0571) along the dendrites of CA1 neurons in SR area of the hippocampus.

However, I observed a decrease in the density of PV-positive (PV+) inhibitory neurons in the CA1 hippocampus of KO mice compared to WT mice in SO (Fig. 2.9B; WT: 10.18 ± 1.45 vs KO 5.47 ± 0.87; $t_{(66)}$ = 2.889, p = 0.0052), SP (Fig. 2.9B; WT: 20.02 ± 1.67 vs KO: 11.79 ± 0.92; $t_{(66)}$ = 4.595, p < 0.0001), and SR (Fig. 2.9B; WT: 2.76 ± 0.70 vs KO 0.47 ± 0.12; $t_{(66)}$ = 4.727, p < 0.0001) layers of CA1 hippocampus. Interestingly, vGlut1-positive excitatory presynaptic boutons onto PV+ inhibitory neurons were also reduced in KO mice, specifically in the SO (Fig. 2.9D; WT: 21.82 ±

1.18 vs KO: 12.27 ± 0.93; t-test; $t_{(48)} = 5.536$, $p < 0.0001$) and SP (Fig. 2.9D; WT: 21.03 ± 0.55 vs KO: 11.78 ± 0.81; t-test; $t_{(67)} = 6.349$, $p < 0.0001$), but not in the SR (Fig. 2.9D; WT: 16.34 ± 3.53 vs KO: 15.06 ± 2.38; t-test; $t_{(20)} = 0.2142$, $p = 0.8325$) layers of CA1 hippocampus. The reduced excitatory drive onto PV+ inhibitory neurons in the CA1 hippocampus may contribute to reduced number of PV expressing cells and lower inhibitory activity, resulting in an overall increase in E/I balance in astrocyte-specific ephrin-B1 KO mice.

Interestingly, there was an overall increase in colocalization of VGAT and gephyrin (Fig. 2.10A, C; WT: 30.78 ± 2.61 vs KO: 51.91 ± 4.00; t-test; $t_{(53)} = 4.53$, $p < 0.0001$) and increased GAD65-positive puncta within the SR layer of CA1 hippocampus (Fig. 2.10B, D; WT: 5.19 ± 0.14 vs KO: 5.99 ± 0.21; t-test; $t_{(21)} = 3.139$, $p = 0.0050$), which may indicate increased inhibition of inhibitory neurons within CA1 hippocampus.

Astrocytic ephrin-B1 KO mice show impaired social behaviors, but no anxiety or hyperactivity and normal contextual learning.

To examine the functional significance of the synaptic changes in the developing hippocampus, mouse behaviors, such as social novelty and preference, anxiety and hyperactivity, as well as repetitive behaviors and fear-associated memory were also evaluated in ephrin-B1 KO mice. Social novelty and social preference were assessed using a three-chamber test. Mice were placed in a cage containing two side chambers and were tested in two 10 min sessions. In session one, an unfamiliar stranger mouse (S1) was placed in one of the side chambers, with the other chamber remaining empty (Fig.

2.11A). WT mice spent significantly more time in the chamber with S1 than the empty chamber (two-way ANOVA, Tukey's post hoc test, $p < 0.0001$) or the middle chamber (two-way ANOVA, Tukey's post hoc test, $p = 0.0002$); however, KO mice spent similar amount of time in each chamber, indicating impaired social preference (Fig. 2.11B). In session two, a novel mouse (S2) was placed in the empty chamber, while now familiar S1 mouse was remained in the same chamber. The test assessed social preferences by measuring time that mouse spent with either the familiar mouse (S1) or a novel mouse (S2) (Fig. 2.11A). WT mice spent significantly more time in the chamber with the novel mouse S2 than the familiar mouse S1 (two-way ANOVA, Tukey's post hoc test, $p = 0.0005$) or the middle chamber (two-way ANOVA, Tukey's post hoc test, $p = 0.0080$, Fig. 2.11C). However, KO mice spent the same amount of time in the chamber containing S1 mouse, S2 mouse, or the middle chamber, suggesting they could not discriminate between familiar and novel mouse.

Anxiety and hyperexcitability was assessed using an open field test by determining the time mice spent in thigmotaxis (near the walls) and the average velocity of the mice. Both WT and KO mice exhibited similar time spent in thigmotaxis (Fig. 2.11E; WT: 67.89 ± 3.24 vs KO: 66.14 ± 3.96; t-test, $t_{(15)} = 0.3455$, $p = 0.7345$), indicating no changes in anxious behavior following ephrin-B1 KO in astrocytes. Average velocity across the entire test was also similar between WT and KO mice (Fig. 2.11F; WT: 53.19 ± 1.73 vs KO: 49.98 ± 2.03; t-test, $t_{(15)} = 0.1.214$, $p = 0.2435$).

A fear-conditioning test was used to evaluate if loss of astrocytic ephrin-B1 in the developing hippocampus affects contextual hippocampal-dependent learning similar to

the adult hippocampus (Koeppen et al., 2018). In this paradigm, WT and KO were trained to associate an electric shock with a tone in a context (context A). Their ability to recall the context and tone was tested by measuring the amount of time freezing in context A without tone (context recall) and in context B with a tone (tone recall; Fig. 2.12A). Both WT and KO mice exhibited similar behaviors in all stages of the test, in habituation, training, context recall, context B without tone, and tone recall in context B (Fig. 2.12B-G). Long-term memory was also not affected by loss of ephrin-B1, as both contextual and tone memory recall remained intact 7 days following the training (Fig. 2.12H-K). Interestingly, manual analysis of mouse behaviors during each test revealed KO mice exhibited increased digging behavior, particularly during portions of the test with no fear association in context A habituation (Fig. 2.12K; WT: 0 ± 0 vs KO: 1.85 ± 0.76; t-test, $t_{(21)} = 2.341$, $p = 0.0292$), context B habituation(Fig. 2.12K; WT: 1.01 ± 0.64 vs KO: 9.26 ± 2.65; t-test, $t_{(21)} = 2.908$, $p = 0.0084$), and context B recall without tone (Fig. 2.12K; WT: 0 ± 0 vs KO: 6.48 ± 2.35; t-test, $t_{(21)} = 2.64$, $p = 0.0153$). Increased digging may be indicative of repetitive behavior (Kim et al., 2016).

2.4 Discussion

Interactions between neurons and astrocytes are essential for proper circuit formation, particularly during early postnatal development when synapses are rapidly forming and eliminated. The studies presented here suggest that astrocytic ephrin-B1 regulates hippocampal excitatory/inhibitory balance by influencing excitatory synapse formation during early postnatal development. First, I found that loss of ephrin-B1 in

astrocytes enhances excitability of CA1 hippocampal neurons, suggesting the changes in excitatory/inhibitory balance. While I observed increased evoked AMPAR- and NMDAR-mediated responses and increased excitatory synapse numbers and dendritic spines density in CA1 neurons of KO mice, overexpression of astrocytic ephrin-B1 resulted in reduced evoked AMPAR- and NMDAR-mediated EPSCs. Second, inhibitory transmission was decreased in CA1 neurons of KO mice, most likely due to lower density of PV-expressing inhibitory neurons and reduced excitatory innervation of PV cells. In contrast, enhanced inhibitory responses were recorded in CA1 neurons following ephrin-B1 overexpression in developing astrocytes. Third, loss of astrocytic ephrin-B1 during early postnatal development impaired mouse social behaviors, while triggering repetitive behaviors such as digging**.** Together, these studies implicate astrocytic ephrin-B1 in maintaining excitatory/inhibitory balance in the hippocampus during early postnatal development.

During the first weeks of postnatal development, hippocampal neurons undergo substantial synaptic alterations. At birth (P0-4), synapse numbers are low and dendrites extend filopodial-like protrusions with immature synapses (Steward and Falk, 1991; Fiala et al., 1998). Astrocytes start populating hippocampus around embryonic age (E) 18 - P0 (Miller and Gauthier, 2007; Reemst et al., 2016) and hippocampal astrocytes undergo significant changes during the first postnatal week (Yang et al., 2013; Reemst et al., 2016). During the second and third weeks (P15-28) after birth, synapse numbers dramatically increase (Steward and Falk, 1991; De Felipe et al., 1997). By the end of third week, synapses are found primarily on dendritic spines of hippocampal pyramidal

neurons, which represent postsynaptic sites of structurally mature synapses (Boyer et al., 1998). From the fourth week to adulthood, synapse formation is reduced allowing for maturation and refinement of synaptic circuits through synapse elimination. While hippocampus remains dynamic during in the adult brain, synaptic changes are less pronounced with overall average spine density and size remain constant (Steward and Falk, 1991; Harris et al., 1992; De Felipe et al., 1997). Coincident with synapse formation during early postnatal development, astrocytes begin to express specific synaptogenic proteins that can modulate synapse formation, maturation, and elimination. Expression of synapse-promoting proteins, such as thrombospondins and glypicans, is upregulated in astrocytes during the first two weeks of postnatal development (P0-14) and is downregulated in adult brain (Christopherson et al., 2005; Cahoy et al., 2008; Allen et al., 2012). Previous *in vitro* studies suggest that astrocytic ephrin-B1 may be involved in synapse removal (Koeppen et al., 2018). Therefore, this study, I investigated the role of astrocytic ephrin-B1 during P14-P28 postnatal period of synapse maturation and refinement, during which synapse elimination exceeds synapse formation and astrocytes continue to divide and expand in numbers. During this time, astrocytes also differentiate into more mature ones, characterized by morphology, expression profile, and electrophysiological properties (Yang et al., 2013).

Eph/ephrin signaling has been shown to modulate synapse development both *in vitro* and *in vivo* (Ethell et al., 2001; Henderson et al., 2001; Takasu et al., 2002; Henkemeyer et al., 2003; Liebl et al., 2003). Eph/ephrin-B signaling is involved in both presynaptic and postsynaptic formation and function. Presynaptic ephrin-Bs, specifically

ephrin-B1 and B2, interact with postsynaptic EphB2 to induce formation of functional presynaptic release sites on axons (Kayser et al., 2006; McClelland et al., 2009). Postsynaptically, Eph/ephrin-B signaling can affect synaptic plasticity, spinogenesis, glutamate receptor recruitment, and synapse density (Dalva et al., 2000; Ethell et al., 2001; Grunwald et al., 2001; Contractor et al., 2002; Henkemeyer et al., 2003; Grunwald et al., 2004; McClelland et al., 2010; Xu et al., 2011). Deletion of EphB1, 2, and 3 results in failure to form spines *in vitro* with development of abnormal, headless, or small-headed spines *in vivo* (Henkemeyer et al., 2003). In addition, ephrin-B2 reduces the number of filopodia-like protrusions and increases the number of spines that appear more mature in neuronal cultures, indicating Eph/ephrin-B signaling may be involved in the maturation and stabilization of spines. Increased expression of mature synapses enhances neural function; indeed, loss of ephrin-B2 in neurons reduces synaptic transmission (Essmann et al., 2008), whereas overexpression of ephrin-B3 enhances synaptic function (Aoto et al., 2007). However, the mechanism of astrocyte-neuron Eph/ephrin-B signaling may differ from neuron-neuron signaling. In contrast to neuronal Eph/ephrin-B signaling, I observed enhanced excitatory synapse number and function with the loss of astrocytic ephrin-B1 and conversely, reduced excitatory synapse numbers following the overexpression of ephrin-B1. It is possible that astrocytic ephrin-B1 can inhibit synapse formation by interfering with the interactions between axon terminals of CA3 neurons and postsynaptic dendrites of CA1 neurons. Astrocytic ephrin-B1 can also induce removal of excess synapses via phagocytic mechanisms. Eph/ephrin-B signaling was recently implicated in phagocytic-like mechanism by mediating trogocytosis of

neighboring connected cells to achieve efficient membrane scission and engulfment (Gong et al., 2019). Trogocytosis via Eph/ephrinB signaling can occur in both the forward and reverse direction. As astrocytes are involved in synapse elimination via phagocytosis (Chung et al., 2013), astrocytic elimination of excess synapses may be mediated by Eph/ephrin signaling such that astrocytic ephrin-B1 may contact neuronal Eph triggering reverse signaling to allow for astrocytes to engulf unwanted synapses. Indeed other previous work *in vitro* shows involvement of astrocytic ephrin-B1 signaling in the engulfment of synaptosomes (Koeppen et al., 2018). Here I provide an evidence that astrocytic ephrin-B1 may be playing a similar role during early postnatal development *in vivo*. The loss of astrocytic ephrin-B1 promotes excitatory synapse formation and in turn enhances excitatory synaptic function. Interestingly, despite increased excitatory synapse formation, loss of ephrin-B1 in developing astrocytes does not affect AMPAR/NMDAR EPSC ratio and the levels of synaptic AMPARs, suggesting no changes in synapse maturation.

In addition, decreased inhibitory transmission in CA1 pyramidal neurons may also contribute to their enhanced excitability in astrocyte-specific ephrin-B1 KO mice. Astrocytes co-cultured with developing neurons have been shown to significantly increase GABAergic synaptogenesis (Hughes et al., 2010) and increase amplitude and density of $GABA_A$ currents (Liu et al., 1996; Elmariah et al., 2005). Interestingly, neuronal cell bodies that were in direct contact with astrocytes exhibited higher amplitude and density of $GABA_A$ current (Liu et al., 1996). The increase in number of inhibitory presynaptic terminals, frequency of mIPSCs, and synaptic localization of $GABA_A$

receptor clusters was observed in neuronal co-cultures with astrocytes (Elmariah et al., 2005), but was not mediated by astrocyte-derived thrombospondins (Hughes et al., 2010). My studies show that the loss of astrocytic ephrin-B1 in the developing hippocampus leads to decreased IPSCs in CA1 hippocampal neurons potentially due to decreased number of PV-expressing inhibitory neurons in CA1 hippocampus (Fig. 10). Additionally, I observed a reduced number of vGlut1+ excitatory pre-synaptic boutons on PV cells in CA1 hippocampus of KO mice, suggesting decreased excitatory drive onto PV-expressing neurons, which may further reduce inhibition of CA1 pyramidal neurons. Ephrin-B has been implicated in the development of inhibitory neurons in the hippocampus (Talebian et al., 2018). Deletion of ephrin-B1, B2, and B3 in inhibitory neurons reduces number of PV, somatostatin, neuropeptide Y, and reelin-positive inhibitory neurons in the CA1 hippocampus (Talebian et al., 2018). Deletion of ephrin-B during embryogenesis affects the emergence and migration of interneurons thereby reducing the number of interneurons and increasing the excitation of cortical networks (Talebian et al., 2017). Inhibitory neurons, in particular PV-expressing interneurons, are generated during embryonic development in two waves between E9-E12 and E12-E16 from the medial ganglionic eminences (MGE) and caudal ganglionic eminences (CGE) (Butt et al., 2005; Miyoshi et al., 2010; Tricoire et al., 2011) and will invade the hippocampus by E14 (Tricoire et al., 2011). However, the expression of PV in interneurons is minimal until P12 and gradually increases until P30 (Nitsch et al., 1990; de Lecea et al., 1995). In addition, early studies in rats showed no evidence of inhibition prior to P18, after which it steadily increased to reach adult levels by P28 (Michelson and

Lothman, 1989). While excitatory responses in rat CA1 hippocampus were well established within 2 weeks following birth, the maturation of inhibitory processes was not evident until several weeks later. In my study, ephrin-B1 was deleted from astrocytes during P14-P28 period of PV cell maturation. As expression of PV is still increasing during this period in an activity dependent manner, the loss astrocytic ephrin-B1 may be affecting either (1) excitatory innervation of PV inhibitory neurons affecting the increase in PV expression or (2) the maturation of inhibitory neurons in the CA1 hippocampus during P14-P28 period.

The exact role of Eph/ephrin signaling in interneurons is still unknown; further investigation is required to determine how Eph/ephrin signaling mediates interneuron maturation and function, and specifically how astrocytes may contribute to these mechanisms. Interestingly, ephrin-B signaling in astrocytes have been shown to regulate neurogenesis in the DG of the hippocampus (Ashton et al., 2012). This neurogenesis may be impaired in early postnatal development with the loss of astrocytic ephrin-B1 such that interneuron migration may be reduced resulting in decreased PV expression. Eph/ephrin signaling is essential for cell migration during hippocampal neurogenesis (Chumley et al., 2007). EphB1 is found to regulate cell number, proliferation, and positioning of neural stem and progenitor cells in the DG (Chumley et al., 2007). However, ephrin-B1 overexpression only in CA1 hippocampal astrocytes during P14-P28 period resulted in increased IPSCs recorded from CA1 neurons, suggesting that the changes that I observe in my study are independent of neuronal differentiation in DG. Therefore, astrocytic

ephrin-B1 may be essential in maintaining proper E/I balance by influencing PV cell development in CA1 hippocampus during P14-P28 period.

I report that the loss of astrocytic ephrin-B1 enhanced excitatory function while also reducing inhibitory function. This E/I imbalance manifested behaviorally by impaired sociability and increased repetitive behaviors. Aberrant synaptogenesis has been linked to several neurodevelopmental disorders, such as autism spectrum disorder and epilepsy (Huttenlocher and Dabholkar, 1997; Lillis et al., 2015; Shen et al., 2016). Additionally, PV interneurons have been shown to have tight control over excitatory cell firing rhythms as PV interneurons can generate highly synchronized and fast inhibitory patterns (Hu et al., 2014). PV-expressing cells receive excitatory inputs from all major afferents therefore can provide both feedforward and feedback inhibition. In the CA1 hippocampus, PV neurons receive excitatory projections from CA3 cells, allowing for feedforward inhibition. This feedforward circuit restricts the magnitude and duration of afferent pyramidal cell excitatory postsynaptic potentials, thereby enhancing the temporal precision of pyramidal cell activation (Pouille and Scanziani, 2001). PV neurons also receive rhythmic feedback from excitatory cells, which provides temporal synchrony, which is necessary to generate network oscillations (Hu et al., 2014; Ognjanovski et al., 2017). Loss of PV interneurons may further contribute to the E/I imbalance and impaired social preference seen in astrocyte-specific ephrin-B1 KO mice. Indeed, loss of PV interneurons results in behavioral changes in mice. PV-depleted mice display similar core autism symptoms, including reduced social interactions and ultrasonic vocalizations, increased repetitive and stereotyped patterns of behaviors, seen with impaired reversal

learning, and increased seizure susceptibility (Wohr et al., 2015). It is interesting to note these PV-depleted mice exhibited no impairments with motor function and no anxiety-like or depression-like behaviors (Wohr et al., 2015). Blocking synaptic transmission of PV neurons specifically in the ventral hippocampus was also shown to impair social memory discrimination (Deng et al., 2019). My findings show that loss of astrocytic ephrin-B1 increased excitatory synaptogenesis and reduced PV expression in the CA1 hippocampus, which coincided with reduced sociability and increased repetitive digging behaviors but had no effect on anxiety or motor function. Together, this suggests that targeting astrocytic ephrin-B1 may be a potential avenue to repair PV cell functions and restore E/I imbalances in neurodevelopmental disorders.

The studies presented here suggest that astrocytic ephrin-B1 regulates E/I balance in the CA1 hippocampus during early postnatal development. During P14-P28 postnatal period, astrocytic ephrin-B1 is negatively regulating excitatory synapse formation as deletion of ephrin-B1 in astrocytes results in increased excitation, while overexpression of ephrin-B1 in astrocytes decreases excitation of CA1 neurons. Astrocytic ephrin-B1 may also affect inhibitory neuron maturation and function as loss of astrocytic ephrin-B1 reduces density of PV-expressing inhibitory neurons in the CA1 hippocampus and in turn impairs inhibition of CA1 pyramidal neurons. Conversely, overexpression of ephrin-B1 in astrocytes enhances inhibition of CA1 neurons. The deregulation of E/I balance in astrocyte-specific ephrin-B1 KO mice may contribute to observed changes in social behaviors of the mice. Not surprising, genetic studies have linked mutations associated with Eph/ephrin signaling with neurodevelopmental disorders, including autism spectrum

disorder (Sanders et al., 2012; Robichaux et al., 2014), characterized by dysfunctions in social interactions and repetitive behaviors, and increased seizure susceptibility. Imbalance of E/I balance is linked to many neurological diseases, including epilepsy and autism spectrum disorders (Gao and Penzes, 2015). Therefore, further understanding the role of astrocytic ephrin-B1 in establishing proper E/I balance during development may provide a potential target for treating neurodevelopmental disorders.

References

Allen, N.J., Bennett, M.L., Foo, L.C., Wang, G.X., Chakraborty, C., Smith, S.J., et al. (2012). Astrocyte glypicans 4 and 6 promote formation of excitatory synapses via GluA1 AMPA receptors. *Nature* 486(7403)**,** 410-414. doi: 10.1038/nature11059.

Allen, N.J., and Eroglu, C. (2017). Cell Biology of Astrocyte-Synapse Interactions. *Neuron* 96(3)**,** 697-708. doi: 10.1016/j.neuron.2017.09.056.

Anagnostaras, S.G., Gale, G.D., and Fanselow, M.S. (2001). Hippocampus and contextual fear conditioning: recent controversies and advances. *Hippocampus* 11(1)**,** 8-17. doi: 10.1002/1098-1063(2001)11:1<8::aid-hipo1015>3.0.co;2-7.

Aoto, J., Ting, P., Maghsoodi, B., Xu, N., Henkemeyer, M., and Chen, L. (2007). Postsynaptic ephrinB3 promotes shaft glutamatergic synapse formation. *J Neurosci* 27(28)**,** 7508-7519. doi: 10.1523/JNEUROSCI.0705-07.2007.

Araque, A., Parpura, V., Sanzgiri, R.P., and Haydon, P.G. (1999). Tripartite synapses: glia, the unacknowledged partner. *Trends Neurosci* 22(5)**,** 208-215.

Ashton, R.S., Conway, A., Pangarkar, C., Bergen, J., Lim, K.I., Shah, P., et al. (2012). Astrocytes regulate adult hippocampal neurogenesis through ephrin-B signaling. *Nat Neurosci* 15(10)**,** 1399-1406. doi: 10.1038/nn.3212.

Beattie, E.C., Stellwagen, D., Morishita, W., Bresnahan, J.C., Ha, B.K., Von Zastrow, M., et al. (2002). Control of synaptic strength by glial TNFalpha. *Science* 295(5563)**,** 2282-2285. doi: 10.1126/science.1067859.

Bonansco, C., and Fuenzalida, M. (2016). Plasticity of Hippocampal Excitatory-Inhibitory Balance: Missing the Synaptic Control in the Epileptic Brain. *Neural Plast* 2016**,** 8607038. doi: 10.1155/2016/8607038.

Boyer, C., Schikorski, T., and Stevens, C.F. (1998). Comparison of hippocampal dendritic spines in culture and in brain. *J Neurosci* 18(14)**,** 5294-5300.

Bush, J.O., and Soriano, P. (2009). Ephrin-B1 regulates axon guidance by reverse signaling through a PDZ-dependent mechanism. *Genes Dev* 23(13)**,** 1586-1599. doi: 10.1101/gad.1807209.

Butt, S.J., Fuccillo, M., Nery, S., Noctor, S., Kriegstein, A., Corbin, J.G., et al. (2005). The temporal and spatial origins of cortical interneurons predict their physiological subtype. *Neuron* 48(4)**,** 591-604. doi: 10.1016/j.neuron.2005.09.034.

Cahoy, J.D., Emery, B., Kaushal, A., Foo, L.C., Zamanian, J.L., Christopherson, K.S., et al. (2008). A transcriptome database for astrocytes, neurons, and oligodendrocytes: a new resource for understanding brain development and function. *J Neurosci* 28(1)**,** 264-278. doi: 10.1523/jneurosci.4178-07.2008.

Castaneda-Castellanos, D.R., Flint, A.C., and Kriegstein, A.R. (2006). Blind patch clamp recordings in embryonic and adult mammalian brain slices. *Nat Protoc* 1(2)**,** 532-542. doi: 10.1038/nprot.2006.75.

Christopherson, K.S., Ullian, E.M., Stokes, C.C., Mullowney, C.E., Hell, J.W., Agah, A., et al. (2005). Thrombospondins are astrocyte-secreted proteins that promote CNS synaptogenesis. *Cell* 120(3)**,** 421-433. doi: 10.1016/j.cell.2004.12.020.

Chumley, M.J., Catchpole, T., Silvany, R.E., Kernie, S.G., and Henkemeyer, M. (2007). EphB receptors regulate stem/progenitor cell proliferation, migration, and polarity during hippocampal neurogenesis. *J Neurosci* 27(49)**,** 13481-13490. doi: 10.1523/jneurosci.4158-07.2007.

Chung, W.S., Clarke, L.E., Wang, G.X., Stafford, B.K., Sher, A., Chakraborty, C., et al. (2013). Astrocytes mediate synapse elimination through MEGF10 and MERTK pathways. *Nature* 504(7480)**,** 394-400. doi: 10.1038/nature12776.

Clarke, L.E., and Barres, B.A. (2013). Emerging roles of astrocytes in neural circuit development. *Nat Rev Neurosci* 14(5)**,** 311-321. doi: 10.1038/nrn3484.

Coimbra, N.C., Paschoalin-Maurin, T., Bassi, G.S., Kanashiro, A., Biagioni, A.F., Felippotti, T.T., et al. (2017). Critical neuropsychobiological analysis of panic attack- and anticipatory anxiety-like behaviors in rodents confronted with snakes in polygonal arenas and complex labyrinths: a comparison to the elevated plus- and T-maze behavioral tests. *Braz J Psychiatry* 39(1)**,** 72-83. doi: 10.1590/1516-4446-2015-1895.

Contractor, A., Rogers, C., Maron, C., Henkemeyer, M., Swanson, G.T., and Heinemann, S.F. (2002). Trans-synaptic Eph receptor-ephrin signaling in hippocampal mossy fiber LTP. *Science* 296(5574)**,** 1864-1869. doi: 10.1126/science.1069081.

Cruz, A.P., Frei, F., and Graeff, F.G. (1994). Ethopharmacological analysis of rat behavior on the elevated plus-maze. *Pharmacol Biochem Behav* 49(1)**,** 171-176. doi: 10.1016/0091-3057(94)90472-3.

Dalva, M.B., Takasu, M.A., Lin, M.Z., Shamah, S.M., Hu, L., Gale, N.W., et al. (2000). EphB receptors interact with NMDA receptors and regulate excitatory synapse formation. *Cell* 103(6)**,** 945-956.

De Felipe, J., Marco, P., Fairen, A., and Jones, E.G. (1997). Inhibitory synaptogenesis in mouse somatosensory cortex. *Cereb Cortex* 7(7)**,** 619-634. doi: 10.1093/cercor/7.7.619.

de Lecea, L., del Rio, J.A., and Soriano, E. (1995). Developmental expression of parvalbumin mRNA in the cerebral cortex and hippocampus of the rat. *Brain Res Mol Brain Res* 32(1)**,** 1-13. doi: 10.1016/0169-328x(95)00056-x.

Deng, X., Gu, L., Sui, N., Guo, J., and Liang, J. (2019). Parvalbumin interneuron in the ventral hippocampus functions as a discriminator in social memory. *Proc Natl Acad Sci U S A* 116(33)**,** 16583-16592. doi: 10.1073/pnas.1819133116.

Elmariah, S.B., Oh, E.J., Hughes, E.G., and Balice-Gordon, R.J. (2005). Astrocytes regulate inhibitory synapse formation via Trk-mediated modulation of postsynaptic GABAA receptors. *J Neurosci* 25(14)**,** 3638-3650. doi: 10.1523/JNEUROSCI.3980-04.2005.

Essmann, C.L., Martinez, E., Geiger, J.C., Zimmer, M., Traut, M.H., Stein, V., et al. (2008). Serine phosphorylation of ephrinB2 regulates trafficking of synaptic AMPA receptors. *Nat Neurosci* 11(9)**,** 1035-1043. doi: 10.1038/nn.2171.

Ethell, I.M., Irie, F., Kalo, M.S., Couchman, J.R., Pasquale, E.B., and Yamaguchi, Y. (2001). EphB/syndecan-2 signaling in dendritic spine morphogenesis. *Neuron* 31(6)**,** 1001-1013. doi: 10.1016/s0896-6273(01)00440-8.

Fellin, T., Pascual, O., Gobbo, S., Pozzan, T., Haydon, P.G., and Carmignoto, G. (2004). Neuronal synchrony mediated by astrocytic glutamate through activation of extrasynaptic NMDA receptors. *Neuron* 43(5)**,** 729-743. doi: 10.1016/j.neuron.2004.08.011.

Fiala, J.C., Feinberg, M., Popov, V., and Harris, K.M. (1998). Synaptogenesis via dendritic filopodia in developing hippocampal area CA1. *J Neurosci* 18(21)**,** 8900-8911.

Fritschy, J.M. (2008). Epilepsy, E/I Balance and GABA(A) Receptor Plasticity. *Front Mol Neurosci* 1**,** 5. doi: 10.3389/neuro.02.005.2008.

Gao, R., and Penzes, P. (2015). Common mechanisms of excitatory and inhibitory imbalance in schizophrenia and autism spectrum disorders. *Curr Mol Med* 15(2)**,** 146-167. doi: 10.2174/1566524015666150303003028.

Gong, J., Gaitanos, T.N., Luu, O., Huang, Y., Gaitanos, L., Lindner, J., et al. (2019). Gulp1 controls Eph/ephrin trogocytosis and is important for cell rearrangements

during development. *J Cell Biol* 218(10)**,** 3455-3471. doi: 10.1083/jcb.201901032.

Grunwald, I.C., Korte, M., Adelmann, G., Plueck, A., Kullander, K., Adams, R.H., et al. (2004). Hippocampal plasticity requires postsynaptic ephrinBs. *Nat Neurosci* 7(1)**,** 33-40. doi: 10.1038/nn1164.

Grunwald, I.C., Korte, M., Wolfer, D., Wilkinson, G.A., Unsicker, K., Lipp, H.P., et al. (2001). Kinase-independent requirement of EphB2 receptors in hippocampal synaptic plasticity. *Neuron* 32(6)**,** 1027-1040.

Hama, H., Hara, C., Yamaguchi, K., and Miyawaki, A. (2004). PKC signaling mediates global enhancement of excitatory synaptogenesis in neurons triggered by local contact with astrocytes. *Neuron* 41(3)**,** 405-415.

Harris, K.M., Jensen, F.E., and Tsao, B. (1992). Three-dimensional structure of dendritic spines and synapses in rat hippocampus (CA1) at postnatal day 15 and adult ages: implications for the maturation of synaptic physiology and long-term potentiation. *J Neurosci* 12(7)**,** 2685-2705.

Henderson, J.T., Georgiou, J., Jia, Z., Robertson, J., Elowe, S., Roder, J.C., et al. (2001). The receptor tyrosine kinase EphB2 regulates NMDA-dependent synaptic function. *Neuron* 32(6)**,** 1041-1056.

Henkemeyer, M., Itkis, O.S., Ngo, M., Hickmott, P.W., and Ethell, I.M. (2003). Multiple EphB receptor tyrosine kinases shape dendritic spines in the hippocampus. *J Cell Biol* 163(6)**,** 1313-1326. doi: 10.1083/jcb.200306033.

Henneberger, C., Papouin, T., Oliet, S.H., and Rusakov, D.A. (2010). Long-term potentiation depends on release of D-serine from astrocytes. *Nature* 463(7278)**,** 232-236. doi: 10.1038/nature08673.

Hu, H., Gan, J., and Jonas, P. (2014). Interneurons. Fast-spiking, parvalbumin(+) GABAergic interneurons: from cellular design to microcircuit function. *Science* 345(6196)**,** 1255263. doi: 10.1126/science.1255263.

Hughes, E.G., Elmariah, S.B., and Balice-Gordon, R.J. (2010). Astrocyte secreted proteins selectively increase hippocampal GABAergic axon length, branching, and synaptogenesis. *Mol Cell Neurosci* 43(1)**,** 136-145. doi: 10.1016/j.mcn.2009.10.004.

Hussain, N.K., Thomas, G.M., Luo, J., and Huganir, R.L. (2015). Regulation of AMPA receptor subunit GluA1 surface expression by PAK3 phosphorylation. *Proc Natl Acad Sci U S A* 112(43)**,** E5883-5890. doi: 10.1073/pnas.1518382112.

Huttenlocher, P.R., and Dabholkar, A.S. (1997). Regional differences in synaptogenesis in human cerebral cortex. *J Comp Neurol* 387(2)**,** 167-178. doi: 10.1002/(sici)1096-9861(19971020)387:2<167::aid-cne1>3.0.co;2-z.

Kaidanovich-Beilin, O., Lipina, T., Vukobradovic, I., Roder, J., and Woodgett, J.R. (2011). Assessment of social interaction behaviors. *J Vis Exp* (48). doi: 10.3791/2473.

Kayser, M.S., McClelland, A.C., Hughes, E.G., and Dalva, M.B. (2006). Intracellular and trans-synaptic regulation of glutamatergic synaptogenesis by EphB receptors. *J Neurosci* 26(47)**,** 12152-12164. doi: 10.1523/JNEUROSCI.3072-06.2006.

Kim, H., Lim, C.S., and Kaang, B.K. (2016). Neuronal mechanisms and circuits underlying repetitive behaviors in mouse models of autism spectrum disorder. *Behav Brain Funct* 12(1)**,** 3. doi: 10.1186/s12993-016-0087-y.

Koeppen, J., Nguyen, A.Q., Nikolakopoulou, A.M., Garcia, M., Hanna, S., Woodruff, S., et al. (2018). Functional Consequences of Synapse Remodeling Following Astrocyte-Specific Regulation of Ephrin-B1 in the Adult Hippocampus. *J Neurosci* 38(25)**,** 5710-5726. doi: 10.1523/JNEUROSCI.3618-17.2018.

Kucukdereli, H., Allen, N.J., Lee, A.T., Feng, A., Ozlu, M.I., Conatser, L.M., et al. (2011). Control of excitatory CNS synaptogenesis by astrocyte-secreted proteins Hevin and SPARC. *Proc Natl Acad Sci U S A* 108(32)**,** E440-449. doi: 10.1073/pnas.1104977108.

Lee, E., Lee, J., and Kim, E. (2017). Excitation/Inhibition Imbalance in Animal Models of Autism Spectrum Disorders. *Biol Psychiatry* 81(10)**,** 838-847. doi: 10.1016/j.biopsych.2016.05.011.

Liebl, D.J., Morris, C.J., Henkemeyer, M., and Parada, L.F. (2003). mRNA expression of ephrins and Eph receptor tyrosine kinases in the neonatal and adult mouse central nervous system. *J Neurosci Res* 71(1)**,** 7-22. doi: 10.1002/jnr.10457.

Lillis, K.P., Wang, Z., Mail, M., Zhao, G.Q., Berdichevsky, Y., Bacskai, B., et al. (2015). Evolution of Network Synchronization during Early Epileptogenesis Parallels Synaptic Circuit Alterations. *J Neurosci* 35(27)**,** 9920-9934. doi: 10.1523/jneurosci.4007-14.2015.

Liu, Q.Y., Schaffner, A.E., Li, Y.X., Dunlap, V., and Barker, J.L. (1996). Upregulation of GABAA current by astrocytes in cultured embryonic rat hippocampal neurons. *J Neurosci* 16(9)**,** 2912-2923.

Mayford, M., Siegelbaum, S.A., and Kandel, E.R. (2012). Synapses and memory storage. *Cold Spring Harb Perspect Biol* 4(6). doi: 10.1101/cshperspect.a005751.

McClelland, A.C., Hruska, M., Coenen, A.J., Henkemeyer, M., and Dalva, M.B. (2010). Trans-synaptic EphB2-ephrin-B3 interaction regulates excitatory synapse density by inhibition of postsynaptic MAPK signaling. *Proc Natl Acad Sci U S A* 107(19)**,** 8830-8835. doi: 10.1073/pnas.0910644107.

McClelland, A.C., Sheffler-Collins, S.I., Kayser, M.S., and Dalva, M.B. (2009). Ephrin-B1 and ephrin-B2 mediate EphB-dependent presynaptic development via syntenin-1. *Proc Natl Acad Sci U S A* 106(48)**,** 20487-20492. doi: 10.1073/pnas.0811862106.

Michelson, H.B., and Lothman, E.W. (1989). An in vivo electrophysiological study of the ontogeny of excitatory and inhibitory processes in the rat hippocampus. *Brain Res Dev Brain Res* 47(1)**,** 113-122. doi: 10.1016/0165-3806(89)90113-2.

Miller, F.D., and Gauthier, A.S. (2007). Timing is everything: making neurons versus glia in the developing cortex. *Neuron* 54(3)**,** 357-369. doi: 10.1016/j.neuron.2007.04.019.

Miyoshi, G., Hjerling-Leffler, J., Karayannis, T., Sousa, V.H., Butt, S.J., Battiste, J., et al. (2010). Genetic fate mapping reveals that the caudal ganglionic eminence produces a large and diverse population of superficial cortical interneurons. *J Neurosci* 30(5)**,** 1582-1594. doi: 10.1523/jneurosci.4515-09.2010.

Moeller, M.L., Shi, Y., Reichardt, L.F., and Ethell, I.M. (2006). EphB receptors regulate dendritic spine morphogenesis through the recruitment/phosphorylation of focal adhesion kinase and RhoA activation. *J Biol Chem* 281(3)**,** 1587-1598. doi: 10.1074/jbc.M511756200.

Nitsch, R., Soriano, E., and Frotscher, M. (1990). The parvalbumin-containing nonpyramidal neurons in the rat hippocampus. *Anat Embryol (Berl)* 181(5)**,** 413-425. doi: 10.1007/bf02433788.

Nolt, M.J., Lin, Y., Hruska, M., Murphy, J., Sheffler-Colins, S.I., Kayser, M.S., et al. (2011). EphB controls NMDA receptor function and synaptic targeting in a subunit-specific manner. *J Neurosci* 31(14)**,** 5353-5364. doi: 10.1523/JNEUROSCI.0282-11.2011.

Ognjanovski, N., Schaeffer, S., Wu, J., Mofakham, S., Maruyama, D., Zochowski, M., et al. (2017). Parvalbumin-expressing interneurons coordinate hippocampal network dynamics required for memory consolidation. *Nat Commun* 8**,** 15039. doi: 10.1038/ncomms15039.

Pouille, F., and Scanziani, M. (2001). Enforcement of temporal fidelity in pyramidal cells by somatic feed-forward inhibition. *Science* 293(5532)**,** 1159-1163. doi: 10.1126/science.1060342.

Reemst, K., Noctor, S.C., Lucassen, P.J., and Hol, E.M. (2016). The Indispensable Roles of Microglia and Astrocytes during Brain Development. *Front Hum Neurosci* 10**,** 566. doi: 10.3389/fnhum.2016.00566.

Reinhard, S.M., Rais, M., Afroz, S., Hanania, Y., Pendi, K., Espinoza, K., et al. (2019). Reduced perineuronal net expression in Fmr1 KO mice auditory cortex and amygdala is linked to impaired fear-associated memory. *Neurobiol Learn Mem* 164**,** 107042. doi: 10.1016/j.nlm.2019.107042.

Robichaux, M.A., Chenaux, G., Ho, H.Y., Soskis, M.J., Dravis, C., Kwan, K.Y., et al. (2014). EphB receptor forward signaling regulates area-specific reciprocal thalamic and cortical axon pathfinding. *Proc Natl Acad Sci U S A* 111(6)**,** 2188-2193. doi: 10.1073/pnas.1324215111.

Rodgers, R.J., and Johnson, N.J. (1995). Factor analysis of spatiotemporal and ethological measures in the murine elevated plus-maze test of anxiety. *Pharmacol Biochem Behav* 52(2)**,** 297-303. doi: 10.1016/0091-3057(95)00138-m.

Sanders, S.J., Murtha, M.T., Gupta, A.R., Murdoch, J.D., Raubeson, M.J., Willsey, A.J., et al. (2012). De novo mutations revealed by whole-exome sequencing are strongly associated with autism. *Nature* 485(7397)**,** 237-241. doi: 10.1038/nature10945.

Segura, I., Essmann, C.L., Weinges, S., and Acker-Palmer, A. (2007). Grb4 and GIT1 transduce ephrinB reverse signals modulating spine morphogenesis and synapse formation. *Nat Neurosci* 10(3)**,** 301-310. doi: 10.1038/nn1858.

Shen, Y., Qin, H., Chen, J., Mou, L., He, Y., Yan, Y., et al. (2016). Postnatal activation of TLR4 in astrocytes promotes excitatory synaptogenesis in hippocampal neurons. *J Cell Biol* 215(5)**,** 719-734. doi: 10.1083/jcb.201605046.

Shin, L.M., and Liberzon, I. (2010). The neurocircuitry of fear, stress, and anxiety disorders. *Neuropsychopharmacology* 35(1)**,** 169-191. doi: 10.1038/npp.2009.83.

Sloniowski, S., and Ethell, I.M. (2012). Looking forward to EphB signaling in synapses. *Semin Cell Dev Biol* 23(1)**,** 75-82. doi: 10.1016/j.semcdb.2011.10.020.

Stellwagen, D., and Malenka, R.C. (2006). Synaptic scaling mediated by glial TNF-alpha. *Nature* 440(7087)**,** 1054-1059. doi: 10.1038/nature04671.

Steward, O., and Falk, P.M. (1991). Selective localization of polyribosomes beneath developing synapses: a quantitative analysis of the relationships between polyribosomes and developing synapses in the hippocampus and dentate gyrus. *J Comp Neurol* 314(3)**,** 545-557. doi: 10.1002/cne.903140311.

Südhof, T.C., and Malenka, R.C. (2008). Understanding synapses: past, present, and future. *Neuron* 60(3)**,** 469-476. doi: 10.1016/j.neuron.2008.10.011.

Takasu, M.A., Dalva, M.B., Zigmond, R.E., and Greenberg, M.E. (2002). Modulation of NMDA receptor-dependent calcium influx and gene expression through EphB receptors. *Science* 295(5554)**,** 491-495. doi: 10.1126/science.1065983.

Talebian, A., Britton, R., Ammanuel, S., Bepari, A., Sprouse, F., Birnbaum, S.G., et al. (2017). Autonomous and non-autonomous roles for ephrin-B in interneuron migration. *Dev Biol* 431(2)**,** 179-193. doi: 10.1016/j.ydbio.2017.09.024.

Talebian, A., Britton, R., and Henkemeyer, M. (2018). Abnormalities in cortical interneuron subtypes in ephrin-B mutant mice. *Eur J Neurosci* 48(2)**,** 1803-1817. doi: 10.1111/ejn.14022.

Tricoire, L., Pelkey, K.A., Erkkila, B.E., Jeffries, B.W., Yuan, X., and McBain, C.J. (2011). A blueprint for the spatiotemporal origins of mouse hippocampal interneuron diversity. *J Neurosci* 31(30)**,** 10948-10970. doi: 10.1523/jneurosci.0323-11.2011.

Ullian, E.M., Sapperstein, S.K., Christopherson, K.S., and Barres, B.A. (2001). Control of synapse number by glia. *Science* 291(5504)**,** 657-661. doi: 10.1126/science.291.5504.657.

Wohr, M., Orduz, D., Gregory, P., Moreno, H., Khan, U., Vorckel, K.J., et al. (2015). Lack of parvalbumin in mice leads to behavioral deficits relevant to all human autism core symptoms and related neural morphofunctional abnormalities. *Transl Psychiatry* 5**,** e525. doi: 10.1038/tp.2015.19.

Xu, N.J., and Henkemeyer, M. (2012). Ephrin reverse signaling in axon guidance and synaptogenesis. *Semin Cell Dev Biol* 23(1)**,** 58-64. doi: 10.1016/j.semcdb.2011.10.024.

Xu, N.J., Sun, S., Gibson, J.R., and Henkemeyer, M. (2011). A dual shaping mechanism for postsynaptic ephrin-B3 as a receptor that sculpts dendrites and synapses. *Nat Neurosci* 14(11)**,** 1421-1429. doi: 10.1038/nn.2931.

Yan, Q.J., Asafo-Adjei, P.K., Arnold, H.M., Brown, R.E., and Bauchwitz, R.P. (2004). A phenotypic and molecular characterization of the fmr1-tm1Cgr fragile X mouse. *Genes Brain Behav* 3(6)**,** 337-359. doi: 10.1111/j.1601-183X.2004.00087.x.

Yan, Q.J., Rammal, M., Tranfaglia, M., and Bauchwitz, R.P. (2005). Suppression of two major Fragile X Syndrome mouse model phenotypes by the mGluR5 antagonist MPEP. *Neuropharmacology* 49(7)**,** 1053-1066. doi: 10.1016/j.neuropharm.2005.06.004.

Yang, Y., Higashimori, H., and Morel, L. (2013). Developmental maturation of astrocytes and pathogenesis of neurodevelopmental disorders. *J Neurodev Disord* 5(1)**,** 22. doi: 10.1186/1866-1955-5-22.

Zimmer, M., Palmer, A., Kohler, J., and Klein, R. (2003). EphB-ephrinB bi-directional endocytosis terminates adhesion allowing contact mediated repulsion. *Nat Cell Biol* 5(10)**,** 869-878. doi: 10.1038/ncb1045.

Figure Legends

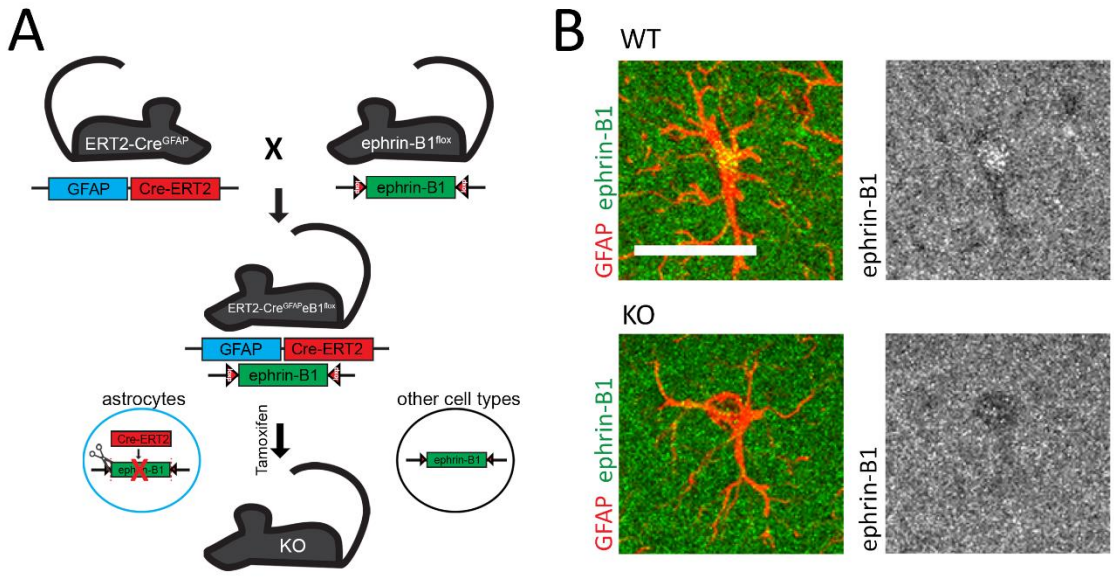

Figure 2.1 Deletion of astrocytic ephrin-B1 is achieved using a ERT2-Cre^{GFAP} mouse model. (A) Generation of ERT2-Cre^{GFAP}ephrin-B1$^{flox/y}$ mice. ERT2-Cre^{GFAP} male mice were crossed with ephrin-B1$^{flox/+}$ female mice to obtain ERT2-Cre^{GFAP}ephrin-B1$^{flox/y}$ (KO) mice. Tamoxifen was intraperitoneally injected to allow for specific deletion of astrocytic ephrin-B1 during P14-19 period. (B) Confocal images of GFAP (red) and ephrin-B1 (green) immunolabeling in the CA1 hippocampus in WT and KO mice.

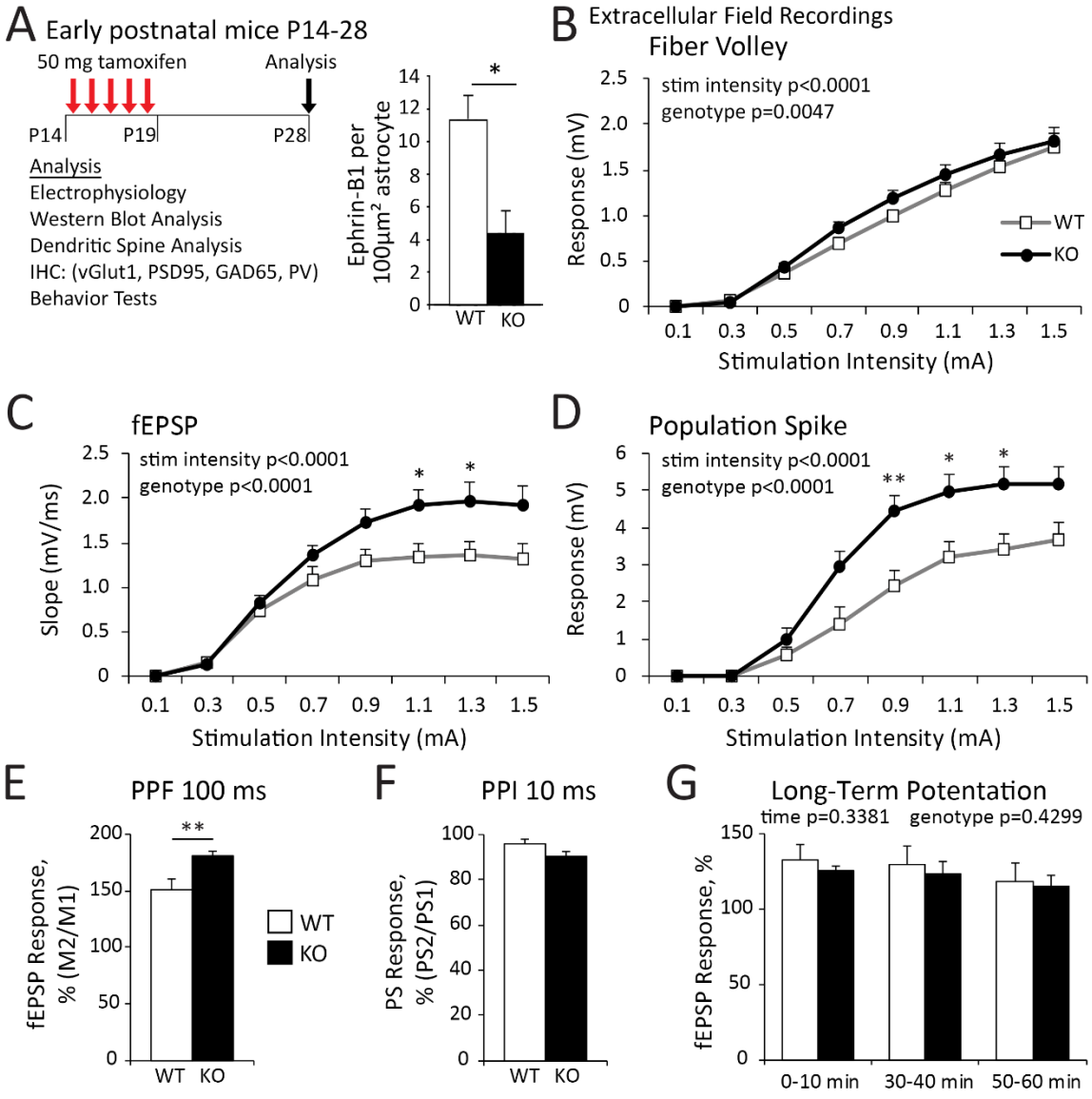
A Early postnatal mice P14-28
50 mg tamoxifen
Analysis
P14
P19
P28
Analysis
Electrophysiology
Western Blot Analysis
Dendritic Spine Analysis
IHC: (vGlut1, PSD95, GAD65, PV)
Behavior Tests
Ephrin-B1 per 100µm² astrocyte
WT
KO
B Extracellular Field Recordings
Fiber Volley
stim intensity p<0.0001
genotype p=0.0047
Response (mV)
Stimulation Intensity (mA)
C fEPSP
stim intensity p<0.0001
genotype p<0.0001
Slope (mV/ms)
Stimulation Intensity (mA)
D Population Spike
stim intensity p<0.0001
genotype p<0.0001
Response (mV)
Stimulation Intensity (mA)
E PPF 100 ms
fEPSP Response, % (M2/M1)
F PPI 10 ms
PS Response, % (PS2/PS1)
G Long-Term Potentation
time p=0.3381 genotype p=0.4299
fEPSP Response, %
0-10 min
30-40 min
50-60 min

Figure 2.2 Deletion of astrocytic ephrin-B1 results in functional synaptic changes in early postnatal CA1 hippocampal neurons. (A) Timeline of tamoxifen injection; 50 mg of tamoxifen was intraperitoneally injected at P14 for five days, experiments were performed at P28, fourteen days after initial injection. Graph shows expression of ephrin-B1 in hippocampal astrocytes of WT and KO mice. Expression of ephrin-B1 was significantly reduced in astrocytes of KO mice. (B-D) Input-output curves of CA1 neuronal FV amplitude (B), fEPSP slope (C), and PS amplitude (D) as a function of increasing stimulation intensity of Schaffer collaterals in hippocampal slices from P28 WT and KO mice. Deletion of astrocytic ephrin-B1 in early postnatal mice resulted in increased fEPSP slope (two-way ANOVA; stimulation intensity $F_{(14, 386)} = 41.58$, $p < 0.0001$; genotype $F_{(1, 386)} = 39.26$, $p < 0.0001$) and PS amplitude (two-way ANOVA; stimulation intensity $F_{(14, 510)} = 42.41$, $p < 0.0001$; genotype $F_{(1, 510)} = 64.18$, $p < 0.0001$) following stimulation of Schaffer collaterals (n = 6-9 mice; two-way ANOVA followed by Bonferroni post-test). (E) Graph shows paired-pulse facilitation (PPF) of the fEPSPs in response to twin pulses administered with a 100 ms inter-pulse interval; KO mice showed increased facilitation at 100 ms (t-test; $t_{(41)} = 2.998$, $p = 0.0046$). (F) Graph shows paired-pulse inhibition (PPI) of the PSs in response to twin pulses administered with a 10 ms inter-pulse interval in WT and KO mice with no differences in PPI between the groups (t-test; $t_{(18)} = 1.382$, $p = 0.1839$). (G) LTP magnitudes at 0-10, 30-40, and 50-60 min after LTP induction in WT and KO groups with no differences between the groups (two-way ANOVA; time $F_{(2, 72)} = 1.101$, $p = 0.3381$; genotype $F_{(1, 72)} = 0.6301$, $p = 0.4299$). Graph shows mean values and error bars represent SEM (n = 6-9 mice, student's t-test). Error bars represent SEM; * $p<0.05$, ** $p<0.01$.

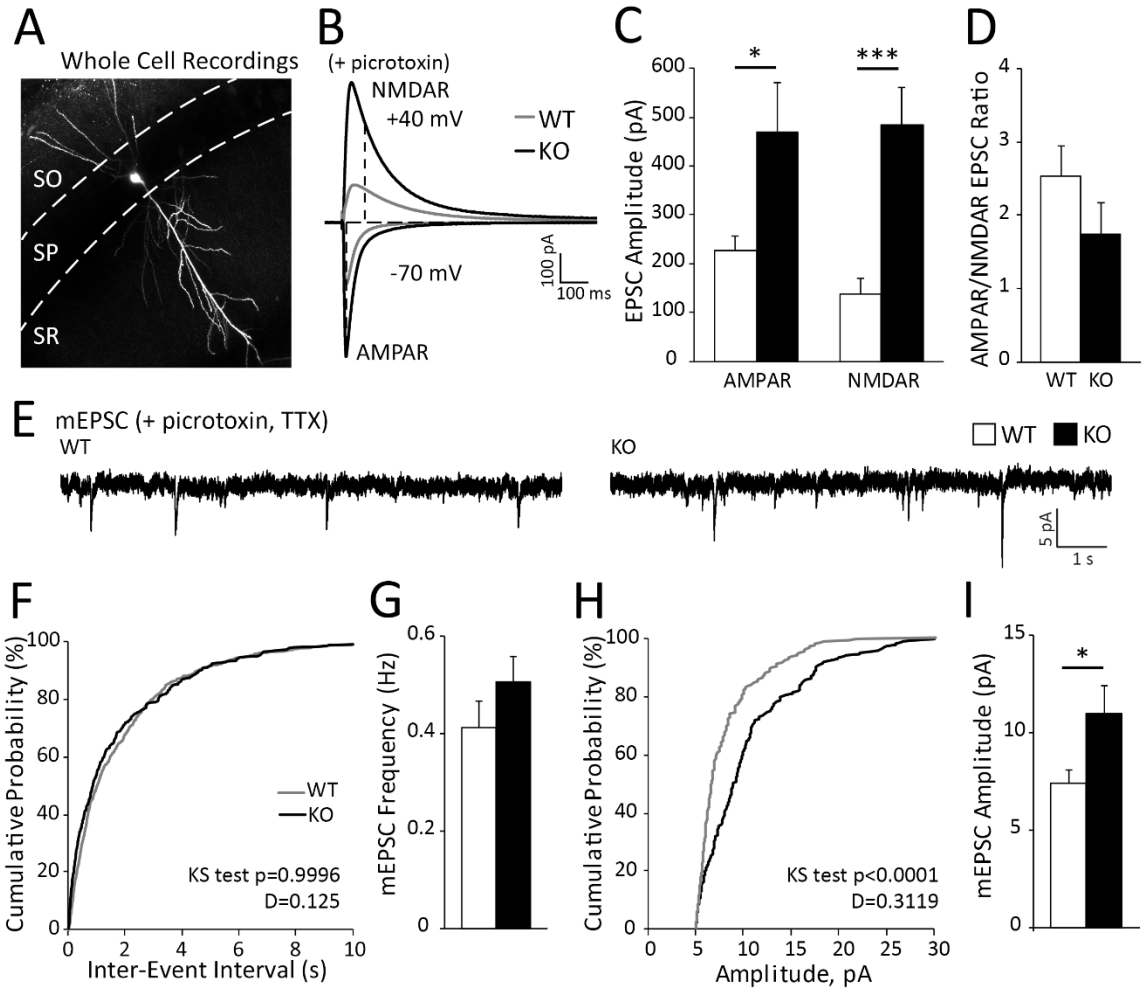
A
Whole Cell Recordings
SO
SP
SR
B
(+ picrotoxin)
NMDAR
+40 mV
WT
KO
-70 mV
100 pA
100 ms
AMPAR
C
EPSC Amplitude (pA)
*
***
AMPAR
NMDAR
D
AMPAR/NMDAR EPSC Ratio
WT KO
E
mEPSC (+ picrotoxin, TTX)
WT
KO
WT
KO
5 pA
1 s
F
Cumulative Probability (%)
WT
KO
KS test p=0.9996
D=0.125
Inter-Event Interval (s)
G
mEPSC Frequency (Hz)
H
Cumulative Probability (%)
KS test p<0.0001
D=0.3119
Amplitude, pA
I
mEPSC Amplitude (pA)
*

Figure 2.3 Loss of astrocytic ephrin-B1 during early postnatal development enhances both AMPAR and NMDAR-mediated responses but AMPAR/NMDAR EPSC ratio is unaffected. (A) Whole cell recordings were performed by blind cell patching of pyramidal cells in the CA1 hippocampus (example of biocytin filled neuron). (B) Representative traces of AMPAR- and NMDAR-evoked responses in WT (gray) and KO (black) P28 mice. (C, D) Graphs show amplitude and corresponding ratio of AMPAR- and NMDAR-mediated currents (n = 10-11 cells, 6-7 mice). Evoked AMPAR- and NMDAR-mediated currents were significantly increased (t-test; AMPAR $t_{(19)} = 2.556l$, $p = 0.0193$; NMDAR $t_{(19)} = 4.1$, $p = 0.0006$); however, ratio was unchanged (t-test; $t_{(12)} = 0.9743$, $p = 0.3491$). (E) Representative traces of mEPSCs in P28 WT and KO mice; recorded in the presence of TTX and picrotoxin (n = 5 mice). (F) The cumulative distribution of mEPSC interevent-intervals shows no differences between WT and KO mice. (G) Average frequency of mEPSCs was not significantly different between WT and KO mice (t-test; $t(9) = 1.259$, $p = 0.2398$), indicating potentially no effect on pre-synaptic activity. (H) The cumulative distribution of mEPSC amplitude shows a significant rightward shift (higher mESPC amplitude across the distribution) for KO (black) mice compared to WT (gray; K–S test, n=190 and 160 for WT and KO groups respectively, $p < 0.0001$, $D = 0.3119$). (I) Average amplitude of mEPSCs was higher in KO compared to WT mice (t-test; $t_{(9)} = 2.208$, $p = 0.0273$). Error bars represent SEM; * $p<0.05$, ** $p<0.01$.

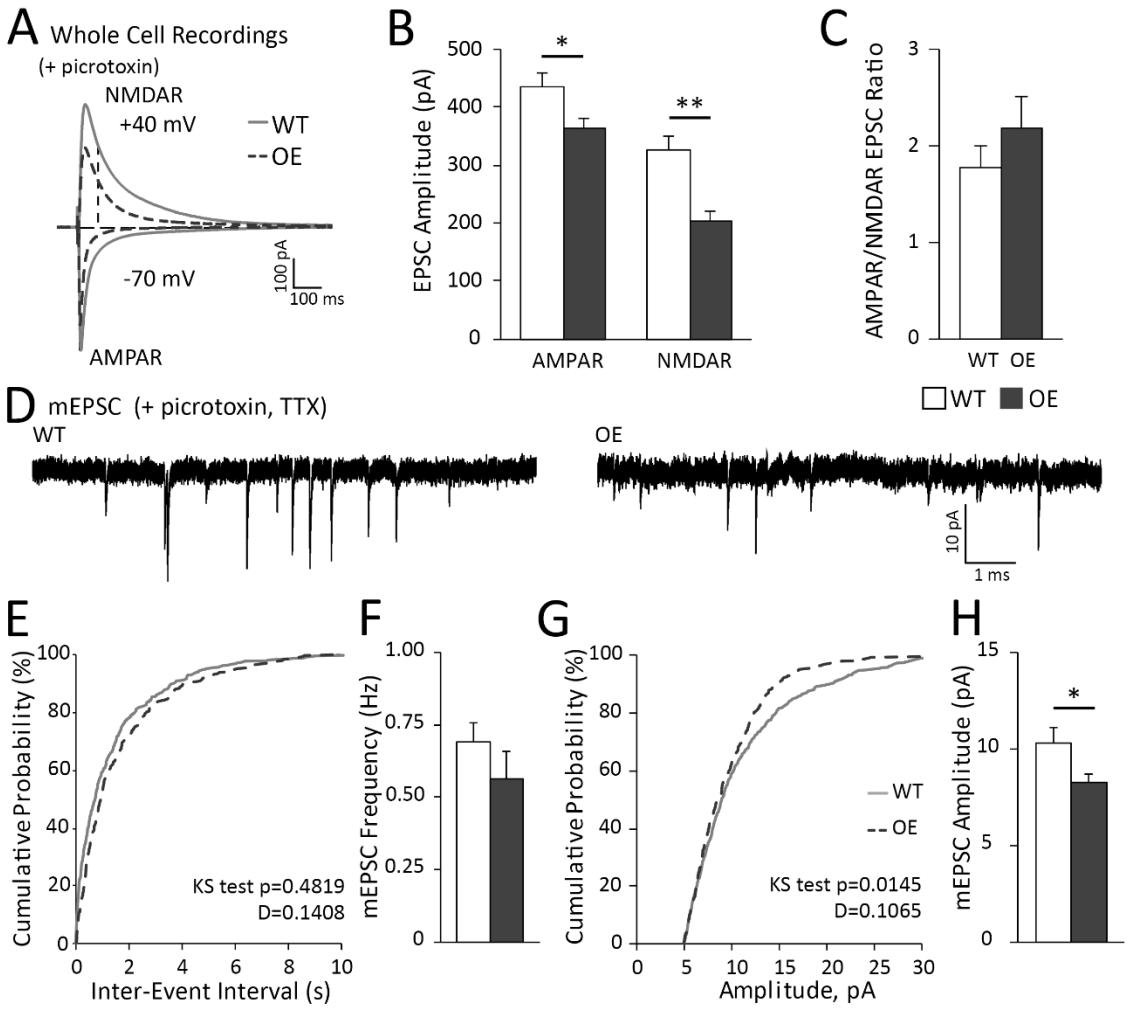
A Whole Cell Recordings
(+ picrotoxin)
NMDAR
+40 mV
WT
OE
-70 mV
AMPAR
100 pA
100 ms
B
EPSC Amplitude (pA)
500
400
300
200
100
0
*
**
AMPAR
NMDAR
C
AMPAR/NMDAR EPSC Ratio
3
2
1
0
WT OE
WT
OE
D mEPSC (+ picrotoxin, TTX)
WT
OE
10 pA
1 ms
E
Cumulative Probability (%)
100
80
60
40
20
0
0 2 4 6 8 10
Inter-Event Interval (s)
KS test p=0.4819
D=0.1408
F
mEPSC Frequency (Hz)
1.00
0.75
0.50
0.25
0
G
Cumulative Probability (%)
100
80
60
40
20
0
0 5 10 15 20 25 30
Amplitude, pA
WT
OE
KS test p=0.0145
D=0.1065
H
mEPSC Amplitude (pA)
15
10
5
0
*

Figure 2.4 Overexpression of astrocytic ephrin-B1 in the developing hippocampus reduced evoked AMPAR- and NMDAR-mediated responses. (A) Representative traces of AMPAR- and NMDAR-evoked responses in WT (gray) and OE (dotted dark gray) P28 mice recorded in the presence of picrotoxin to block GABAergic inhibition. (B, C) Graphs show amplitude and corresponding ratio in AMPAR- and NMDAR-mediated currents (n = 11-14 cells, 5 mice). Evoked AMPAR and NMDAR-mediated currents were significantly decreased (t-test; AMPAR $t_{(23)} = 2.692$, $p = 0.0130$; NMDAR $t_{(20)} = 3.573$, $p = 0.0019$); however, ratio was unchanged (t-test; $t_{(19)} = 0.9733$, $p = 0.3426$). (D) Representative traces of mEPSCs in P28 WT and OE mice; recorded in the presence of TTX and picrotoxin (n = 11-14 cells, 5 mice). (E) The cumulative distribution of mEPSC interevent-intervals in WT and OE mice (gray; K–S test, n = 550 for WT and 360 for OE groups respectively, $p = 0.4819$, $D = 0.1408$). (F) Average frequency of mEPSCs was not significantly different between WT and OE P28 mice (t-test; $t_{(12)} = 1.036$, $p = 0.3206$), indicating potentially no effect on pre-synaptic activity. (G) The cumulative distribution of mEPSC amplitude shows a significant leftward shift (smaller mESPC amplitude across the distribution) for OE (dotted dark gray) mice compared to WT (gray; K–S test, n = 550 for WT and 360 for OE groups respectively, $p = 0.0145$, $D = 0.1065$). (H) Average amplitude of mEPSCs was lower in OE compared to WT mice (t-test; $t_{(12)} = 1.821$, $p = 0.0468$). Error bars represent SEM; * $p<0.05$, ** $p<0.01$.

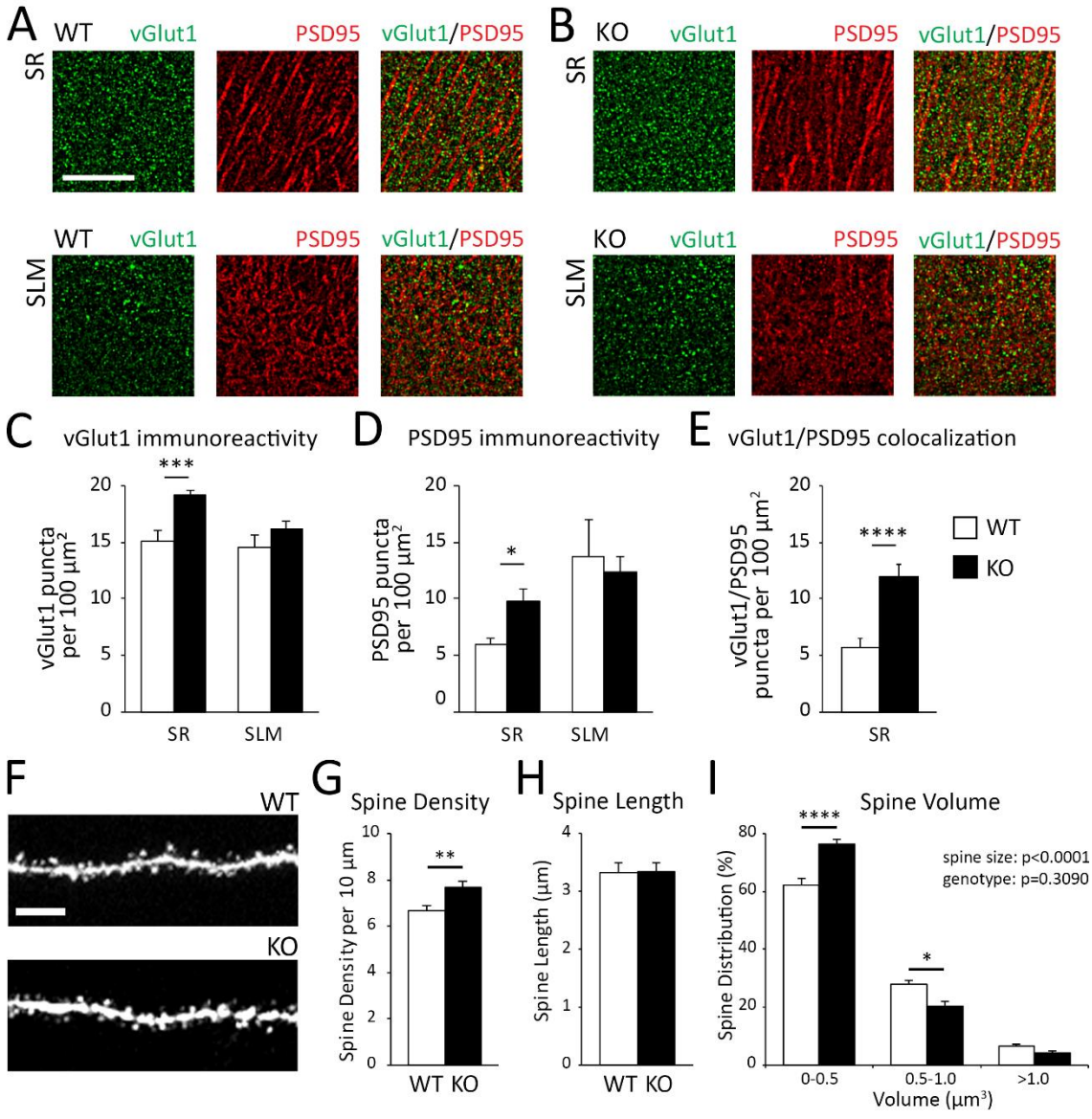
A
WT
vGlut1
PSD95
vGlut1/PSD95
SR
SLM
B
KO
C
vGlut1 immunoreactivity
vGlut1 puncta per 100 µm²
D
PSD95 immunoreactivity
PSD95 puncta per 100 µm²
E
vGlut1/PSD95 colocalization
vGlut1/PSD95 puncta per 100 µm²
WT
KO
F
G
Spine Density
Spine Density per 10 µm
H
Spine Length
Spine Length (µm)
I
Spine Volume
Spine Distribution (%)
spine size: p<0.0001
genotype: p=0.3090
0-0.5
0.5-1.0
>1.0
Volume (µm³)

Figure 2.5 Early postnatal astrocyte-specific deletion of ephrin-B1 resulted in increased number of excitatory synapses in CA1 hippocampus. (A-B) Confocal images of vGlut1 (green) and PSD-95 (red) immunolabeling in SR and SLM areas of CA1 hippocampus of WT and KO P28 mice (scale bar = 25 μm). (C-E) Graphs show density of vGlut1-positive puncta (C), PSD95-positive puncta (D), and vGlut1/PSD95 co-localization (E) per 100 μm^2 of SR and SLM areas in CA1 hippocampus of WT and KO mice (n=3-4 mice). KO mice showed a significant increase in the SR CA1 hippocampus in vGlut1-positive puncta (t-test; $t_{(21)} = 4.238$, $p = 0.0004$), PSD95-positive puncta (t-test; $t_{(17)} = 2.801$, $p = 0.0123$), and the colocalization of vGlut1 and PSD95 (t-test; $t_{(51)} = 3.784$, $p = 0.0004$). Graphs show mean values and error bars represent SEM; ***p<0.001, ****p<0.0001. (F) Confocal images of CA1 neurons expressing GFP in the SR area of CA1 hippocampus of WT and KO mice (scale bar = 10 μ). (G-I) Graphs show average density of dendritic spines per 10 μm dendrite (G), average spine length (H), and spine volume (I). There was a significant increase in average dendritic spine density in KO mice compared to WT mice (t-test; $t_{(31)} = 2.78$, $p = 0.0092$). There was a significantly increased proportion of dendritic spines with smaller heads (volume 0-0.5 μm^3), a decreased percent of medium size spines (volume 0.5-1.0 μm^3), and same percent of large, mature spines (volume >1.0 μm^3) observed in KO mice compared to WT mice (two-way ANOVA, spine size $F_{(2, 84)} = 726.7$, $p < 0.0001$; genotype $F_{(1, 84)} = 1.048$, $p = 0.3090$). Error bars represent SEM; *p < 0.05, **p < 0.01, ****p < 0.0001

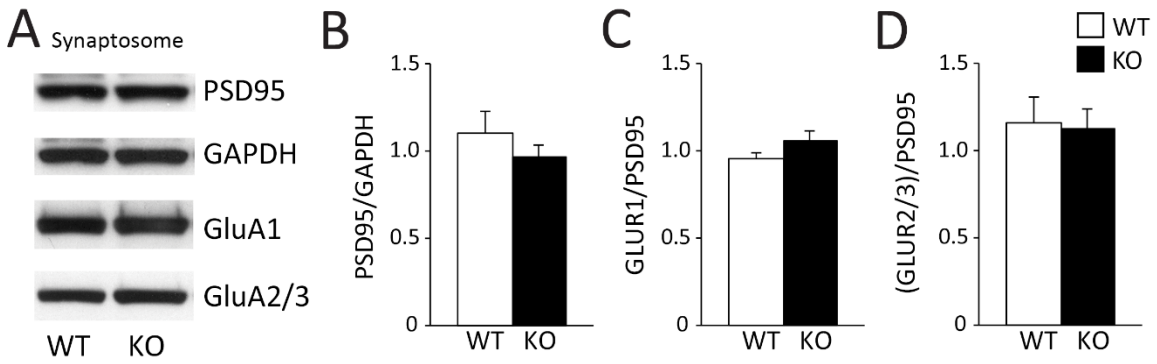

Figure 2.6 Hippocampal synaptic AMPAR levels are similar between P28 WT and KO mice. (A) Western blots show levels of PSD-95, GAPDH, and AMPAR subunits (GluA1 and GluA2/3) in synaptosomes isolated from hippocampus of P28 WT and KO mice. (B-D) Graphs show mean ratios of synaptic PSD-95 to GAPDH (B), and GluA1 (C), or GluA2/3 (D) levels to PSD-95 levels in synaptosomes isolated from P28 hippocampus of WT and KO mice. AMPAR levels at hippocampal synapses are similar in P28 WT and KO mice. Error bars represent SEM.

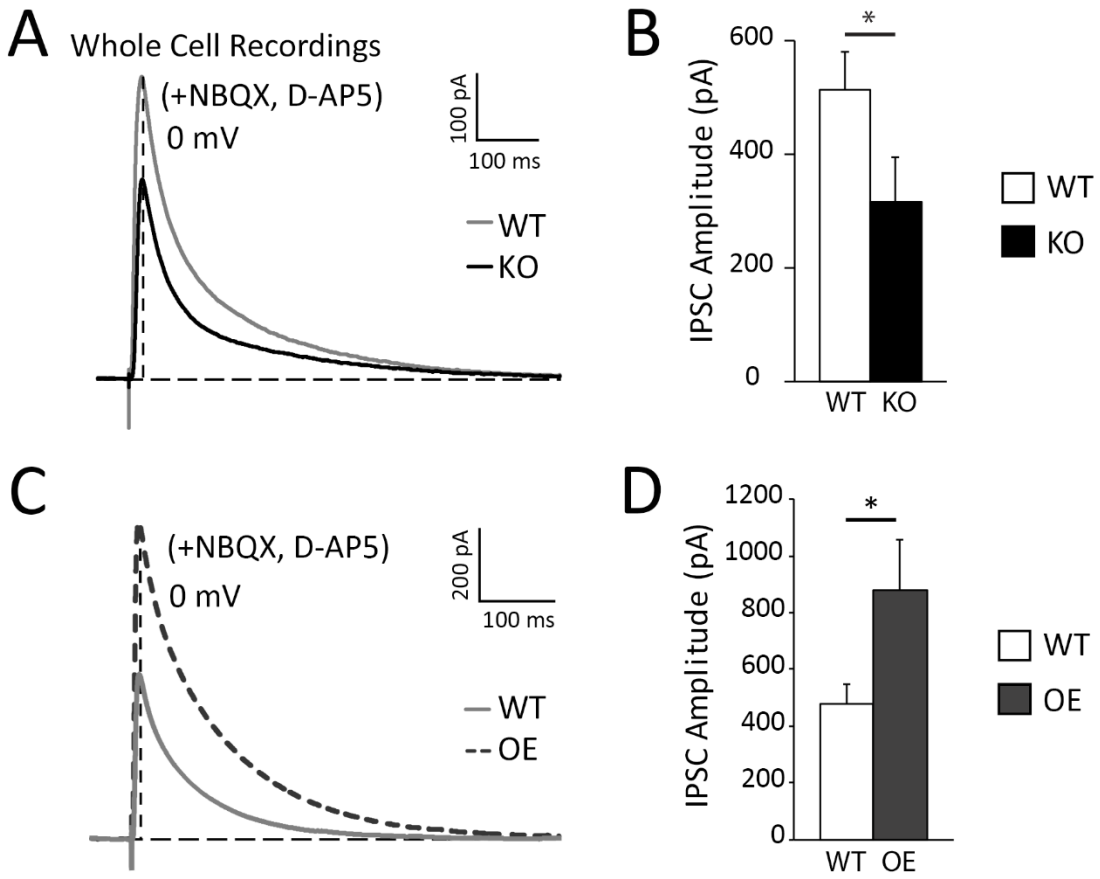

Figure 2.7 Inhibition is altered in CA1 hippocampal neurons following deletion or overexpression of astrocytic ephrin-B1 during early postnatal development. (A) Representative traces showing evoked IPSCs recorded in CA1 pyramidal neurons from P28 WT (gray) and KO (black). (B) Graph shows average amplitude of evoked IPSCs (n = 12-14 cells). Amplitude of evoked IPSCs is significantly decreased in CA1 neurons of P28 KO mice compared to WT mice (t-test; $t_{(20)}$; = 1.90, p = 0.0360). (C) Representative traces showing evoked IPSCs recorded in CA1 pyramidal neurons from P28 WT (gray) and OE (dotted dark gray) recorded in the presence of D-AP5 and NBQX to block AMPAR- and NMDAR-mediated currents. (D) Graph shows average amplitude of evoked IPSCs (n = 10- 11 cells, 6 mice). Amplitude of evoked IPSCs was significantly decreased in CA1 neurons of P28 OE mice compared to WT mice (t-test; $t_{(19)}$; = 2.135 p = 0.0460). Error bars represent SEM; * $p<0.05$.

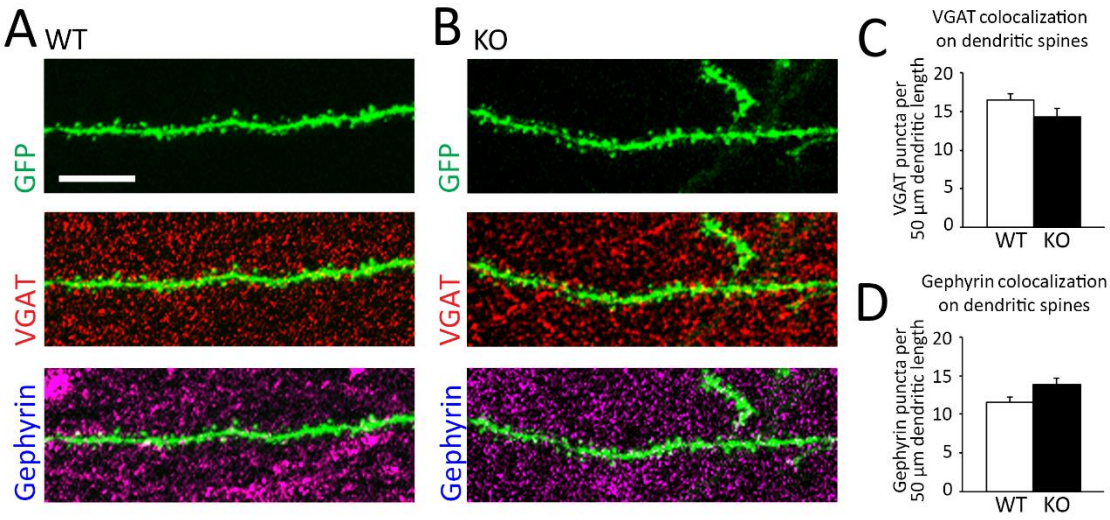

Figure 2.8 Inhibitory synaptic sites onto excitatory dendritic spines remain intact in KO developing mice. (A, B) Confocal images of the CA1 neurons expressing GFP (green) co-stained with VGAT (red) and gephyrin (purple) to visualize inhibitory synaptic sites on dendrites of CA1 hippocampal neurons (scale bar = 10 µm). (C) Graph shows colocalization of VGAT and GFP expressing dendritic spines (n = 2-4 mice). (D) Graph shows colocalization of gephyrin and GFP expressing dendritic spines.

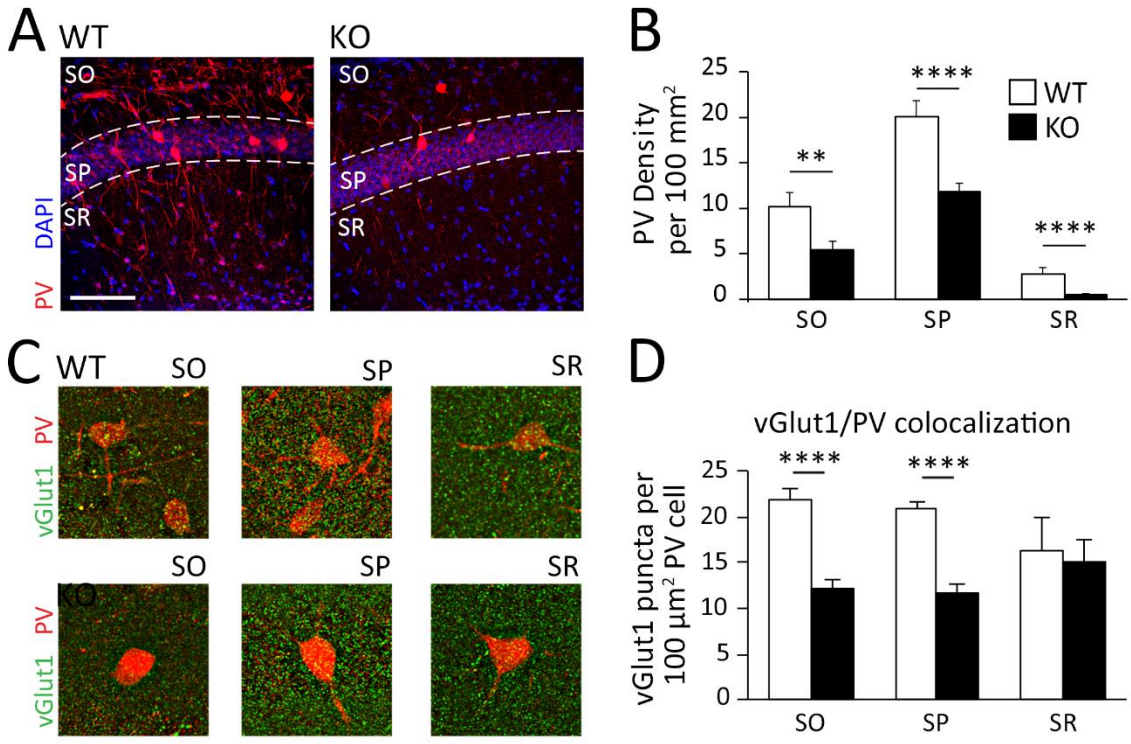

Figure 2.9 Parvalbumin inhibitory neurons are affected by the loss of astrocytic ephrin-B1 during postnatal development. (A) Confocal images of PV-expressing cells (red) with DAPI (blue) to indicate CA1 hippocampal layers, SO, SP, and SR. (B) Graph shows density PV-expressing neurons in SO, SP, and SR layers of CA1 hippocampus. KO mice exhibited decreased density of PV-expressing inhibitory neurons in all three layers (t-test; SO $t_{(66)} = 2.889$, $p = 0.0052$; SP $t_{(66)} = 4.595$, $p < 0.0001$; SR $t_{(66)} = 4.727$, $p < 0.0001$). (C) Confocal images of vGlut1 (green) and PV-expressing cells (red) in the SO, SP, and SR layers of the CA1 hippocampus (scale bar = 25 um). (D) Graph shows colocalization of vGlut1 puncta and PV immunoreactivity in the SO, SP, and SR layers of the CA1 hippocampus (n = 3 mice). KO mice exhibit decreased excitatory vGlut1-positive boutons on PV-expressing inhibitory neurons in the SO (t-test; $t_{(48)} = 5.536$, $p < 0.0001$) and SP (t-test; $t_{(67)} = 6.349$, $p < 0.0001$) of CA1 hippocampus.

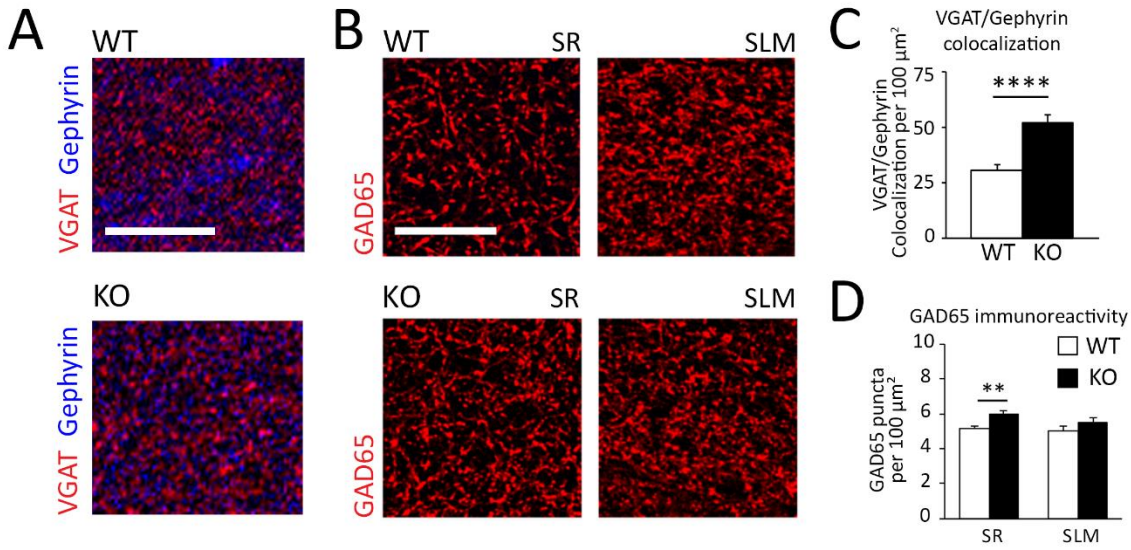

Figure 2.10 Inhibitory synapse number is increased with astrocytic ephrin-B1 deletion during early postnatal development. (A) Confocal images of CA1 SR region of hippocampus visualizing co-stain with VGAT (red) and gephyrin (blue) inhibitory synaptic sites (scale bar = 20 µm) (B) Confocal images of GAD65 (red) immunolabeling in SR and SLM areas of CA1 hippocampus of WT and KO P28 mice (scale bar = 25 µm). (C) Graph shows colocalization of VGAT and gephyrin in CA1 hippocampus; KO mice show significantly higher colocalization of VGAT and gephyrin (t-test; $t(53) = 4.53$, $p < 0.0001$). (D) Graph shows density of GAD65 puncta in the SR and SLM regions of the hippocampus. (n = 3 mice). GAD65 expression is significantly increased in P28 KO mice (t-test; $t_{(21)} = 3.139$, $p = 0.0050$). Error bars represent SEM; **p<0.01, ****p<0.0001.

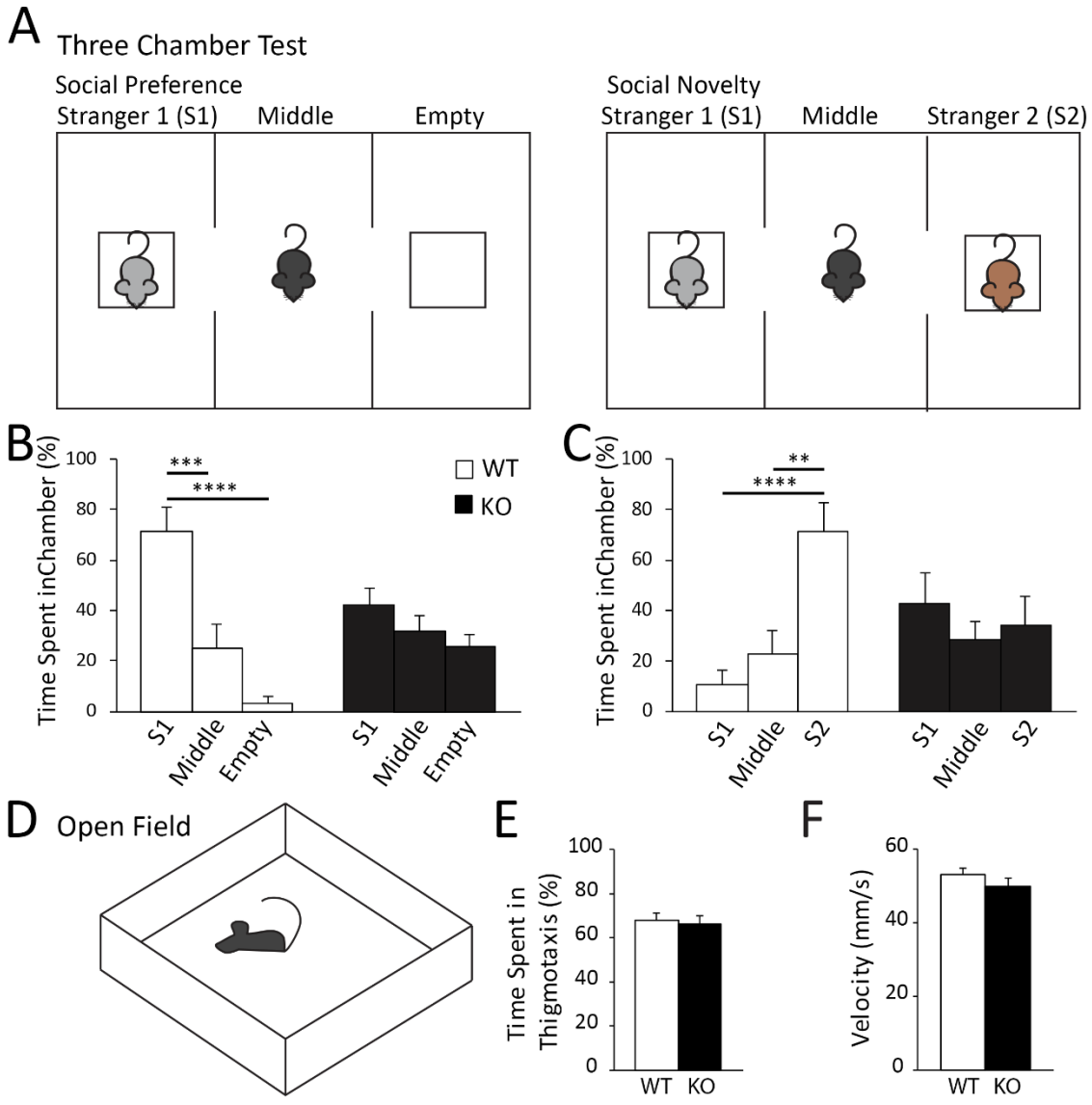
A
Three Chamber Test
Social Preference
Stranger 1 (S1)
Middle
Empty
Social Novelty
Stranger 1 (S1)
Middle
Stranger 2 (S2)
B
Time Spent inChamber (%)
WT
KO
***
****
S1
Middle
Empty
C
**
****
S2
D
Open Field
E
Time Spent in Thigmotaxis (%)
WT
KO
F
Velocity (mm/s)

Figure 2.11 Ablation of astrocytic ephrin-B1 during early postnatal development affected mouse social behaviors. (A) Diagram of three-chamber test for social preference and social novelty. Mice were placed in the middle chamber containing two side chambers and were tested in two 10 min sessions. During social preference test, an unfamiliar stranger mouse (S1) was placed in one of the side chambers, with the other chamber remaining empty. During social novelty test, an unfamiliar stranger mouse (S1) was remaining in the side chamber, while a novel mouse (S2) was placed in the empty chamber. (B) Graph shows time spent in either three chambers during social preference test. WT mice prefer spending time with S1 mouse compared to time in the middle (two-way ANOVA, Tukey's post hoc test, $p = 0.0002$) or empty chamber (two-way ANOVA, Tukey's post hoc test, $p < 0.0001$). KO mice show impaired sociability and spend the same amount of time in each chamber. (C) Graph shows time spent in each chamber during social novelty test. WT spend significantly more time with S2 mouse than with familiar S1 mouse (two-way ANOVA, Tukey's post hoc test, $p = 0.0005$), or in the middle chamber (two-way ANOVA, Tukey's post hoc test, $p = 0.0080$), indicating normal social memory. KO mice spend the same amount of time in S1, middle, or S2 chambers. (D) Schematics of open field test; during testing animals were allowed to freely explore the open field for 10 min while time spent in thigmotaxis and average velocity were measured. (E) Graph shows percent time spent in thigmotaxis with no significant differences between WT and KO mice (t-test, $t(15) = 0.3455$, $p = 0.7345$). (F) Graph shows average velocity of WT and KO mice (t-test, $t(15) = 0.1.214$, $p = 0.2435$).

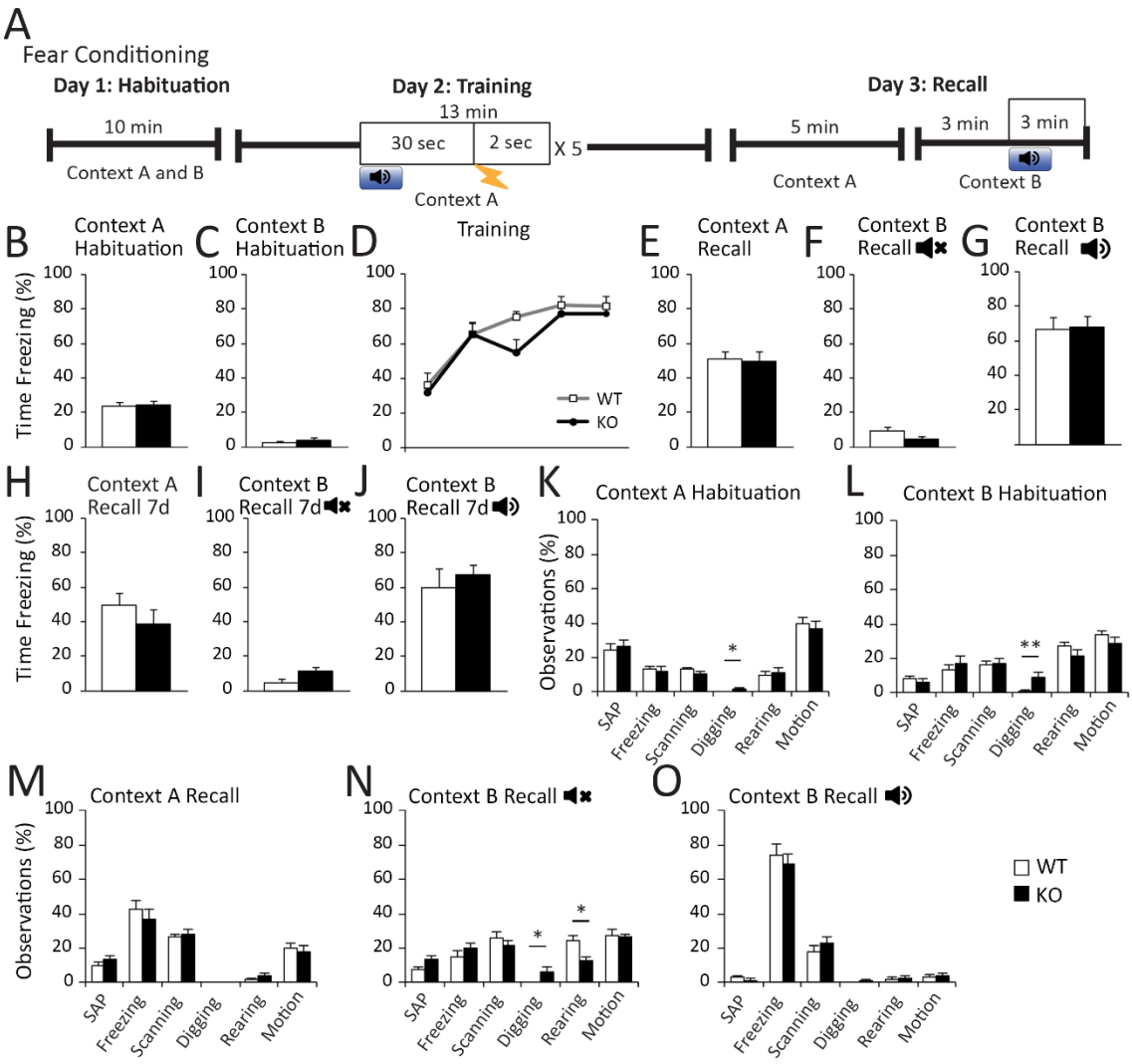
A
Fear Conditioning
Day 1: Habituation
10 min
Context A and B
Day 2: Training
13 min
30 sec
2 sec
X 5
Context A
Day 3: Recall
5 min
3 min
3 min
Context A
Context B
B Context A Habituation
C Context B Habituation
D Training
E Context A Recall
F Context B Recall
G Context B Recall
Time Freezing (%)
WT
KO
H Context A Recall 7d
I Context B Recall 7d
J Context B Recall 7d
K Context A Habituation
L Context B Habituation
Observations (%)
SAP
Freezing
Scanning
Digging
Rearing
Motion
M Context A Recall
N Context B Recall
O Context B Recall
WT
KO

Figure 2.12 Contextual memory is unaffected by the loss of astrocytic ephrin-B1 in developing hippocampus; however, ablation may cause increased repetitive behaviors. (A) Diagram of contextual fear learning paradigm; mice were habituated to contexts A and B for 10 min on day 1. On day 2 mice were placed in Context A and received 5 random 0.5-0.7 mA foot shocks for 2 s after a 30 s tone at 70 KHz. On day 3 mice were placed in Context A for 5 min; 1 h later mice were placed in Context B for 6 min and exposed to a 70 dB tone for the last 3 min. (B-G) Fear conditioning behavior during habituation in contexts A and B (B, C), training (D), and context A (E), context B without tone (F), and context B with tone (G) recall in P28 mice (n = 11 mice). (H-J) 7 d following recall test, animals are tested for long-term memory retention of contextual memory (H), context B without tone (I), and cued auditory memory (J). (K-L) Manual analysis of characteristic mouse behaviors during each behavior test: stretching/attending (SAP), freezing, scanning, rearing, and in motion. KO mice exhibit increased digging repetitive-like behaviors. Error bars represent SEM; * $p<0.05$.

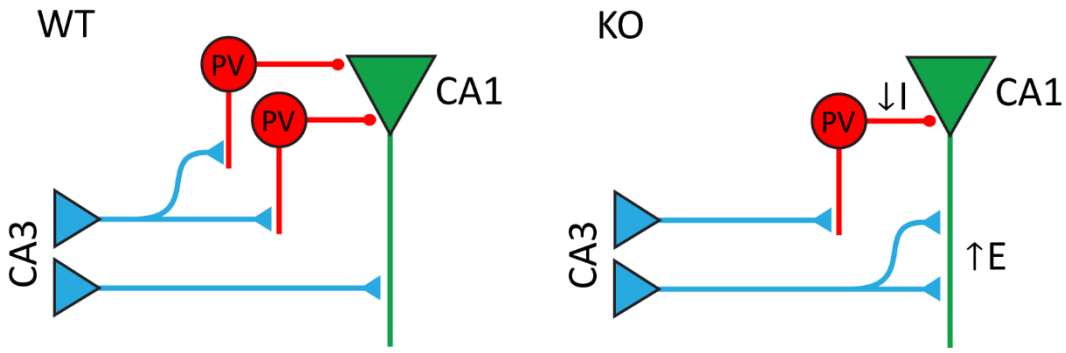

Figure 2.13 Model schematic of hippocampal circuitry in WT and KO mice. (A) Deletion of astrocytic ephrin-B1 affects E/I balance in the hippocampus by enhancing excitatory synaptogenesis onto CA1 pyramidal cells and reducing PV expression. Increased synapse formation of excitatory synapses induces increased excitatory function while reduction of PV-expressing neurons decreases inhibitory function onto CA1 pyramidal cells, thereby causing overall enhanced excitatory activity in the CA1 hippocampal pyramidal cells.

Chapter 3 : Astrocytic ephrin-B1 is involved in excitatory synapse maintenance in the adult hippocampus

Abstract

Astrocyte derived factors can control synapse formation and functions, making astrocytes an attractive target for regulating neuronal circuits and associated behaviors. Abnormal astrocyte-neuronal interactions are also implicated in neurodevelopmental disorders and neurodegenerative diseases associated with impaired learning and memory. However, little is known about astrocyte-mediated mechanisms that regulate learning and memory. Here, I propose astrocytic ephrin-B1 as a regulator of synaptogenesis in adult hippocampus. I found that astrocyte-specific ablation of ephrin-B1 in male mice triggers an increase in the density of immature dendritic spines and excitatory synaptic sites in the adult CA1 hippocampus. However, the prevalence of immature dendritic spines is associated with reduced number of mature spines and decreased evoked postsynaptic firing responses in CA1 pyramidal neurons, suggesting impaired maturation of these newly formed and potentially silent synapses or increased excitatory drive on the inhibitory neurons resulting in the overall decreased postsynaptic firing. My results suggest that astrocytic ephrin-B1 may compete with neuronal ephrin-B1 and mediate excitatory synapse elimination through its interactions with neuronal EphB receptors. My findings demonstrate that astrocytic ephrin-B1 regulates synaptogenesis by restricting new synapse formation in the adult hippocampus.

3.1 Introduction

Hippocampal circuits are highly plastic allowing for their essential role in the formation of new memories and life-long learning ((Milner et al., 1998; Neves et al., 2008). However, it is unclear how the circuits are regulated at the level of individual synapses. Neural activity can regulate synaptic strength, balancing between Hebbian and homeostatic type plasticity. In Hebbian plasticity, increased neural activity can increase synaptogenesis, and can be seen in adulthood (Zito and Svoboda, 2002). While homeostatic plasticity indicates that synapse form will occur if neural activity falls below a homeostatic set-point while activity exceeding the set-point will decrease the number of synapses (Butz and van Ooyen, 2013; Turrigiano, 2017). Formation of synapses can introduce either functional synapses or non-function, silent synapses, potentially allowing for circuit modification. Silent synapses contain NMDAR but not functional AMPARs; therefore, postsynaptically these synapses are silent at resting membrane potentials. Unsilencing with the recruitment of AMPARs can be achieved by potentiating synaptic transmission such that, in an activity-dependent manner, activation of NMDAR leads to appearance of functional AMPARs (Malenka and Nicoll, 1999; Malinow et al., 2000; Liao et al., 2001). During acquisition of new memories, hippocampal synapses undergo activity-dependent growth, elimination or maturation in a synapse-specific manner. In particular, CA1 hippocampal neurons have been implicated in contextual learning (Strekalova et al., 2003), which triggers a recruitment of AMPARs to specific dendritic domains of CA1 neurons (Matsuo et al., 2008), whereas ablation of synaptic NMDARs in the CA1 hippocampus was reported to impact learning (Tsien et al., 1996).

A single astrocyte can come into close association with approximately 2,000,000 synapses (Bushong et al., 2002); this close association allows for astrocytes to regulate synaptic formation, maturation, and pruning. Two methods by which astrocytes affect synapse is through either (a) secretion-factors or (b) contact-mediated factors. Several astrocyte-secreted factors, such as thrombospondin-1 (TSP-1), glypican, and hevin, have been shown to affect synapse formation and function by affecting synapse structure and recruiting of AMPARs (Ullian et al., 2001; Christopherson et al., 2005; Eroglu et al., 2009; Kucukdereli et al., 2011; Allen et al., 2012). Direct contact of astrocytes to synapses has also been shown to regulate synapse formation; neurons directly contacting astrocytes express robust synaptogensis, whereas neurons treated with only astrocyte-conditioned media formed fewer synapses (Ullian et al., 2001). In addition, astrocytes has been implicated to regulate synapse elimination via phagocytosis during synapse development (Lauterbach and Klein, 2006; Eroglu and Barres, 2010; Chung et al., 2013), allowing for refinement of functional circuits with increased neuronal transmission efficiency (Cowan et al., 1984; Luo and O'Leary, 2005). The hippocampus maintains a high level of synaptic plasticity in the adult brain, therefore can undergo synapse formation or elimination based on fluctuations of neuronal activity (Yasumatsu et al., 2008). Astrocytic pruning may contribute to persistent synaptic plasticity in the adult hippocampus by maintaining and refining neural circuits during learning and memory formation. Indeed, electron microscopy studies revealed neuronal debris in adult hippocampal astrocytes (Spacek and Harris, 2004).

Eph/ephrin signaling has been implicated in synapse formation and remodeling (Cowan and Henkemeyer, 2001; Ethell et al., 2001; Henderson et al., 2001; Takasu et al., 2002; Henkemeyer et al., 2003; Grunwald et al., 2004; Kayser et al., 2006; Segura et al., 2007; Kayser et al., 2008; Nikolakopoulou et al., 2016). Ephrin-B1 is a membrane-bound protein that acts as a ligand for EphB receptors. EphB/ephrin-B interactions activate bidirectional signaling in both cells expressing EphB receptor and ephrin-B (Bush and Soriano, 2009; Sloniowski and Ethell, 2012; Xu and Henkemeyer, 2012). Expression of ephrin-B1 is found in both astrocytes and neurons (Wang et al., 2005; Nikolakopoulou et al., 2016). However, how ephrin-B1 expression in astrocytes may influence synapse formation and maintenance is still unclear.

In vivo studies have demonstrated that astrocyte-specific ephrin-B1 deletion in the adult hippocampus of ERT2-Cre^{GFAP}*ephrin-B1*$^{\text{flox/y}}$ (KO) mice triggers an increase in the number of synaptic sites and immature dendritic spines in CA1 hippocampus (Koeppen et al., 2018). However, my studies show despite the increase in synapse numbers, there is reduced postsynaptic firing responses in the CA1 hippocampus and decreased number of functionally mature excitatory synapses. Astrocytic ephrin-B1 may compete with neuronal ephrin-B1 and trigger astrocyte-mediated elimination of EphB receptor-containing synapses via trans-endocytosis. Indeed, a deletion of synaptic EphB receptors impairs the ability of astrocytes expressing functional ephrin-B1 to engulf synaptosomes (Koeppen et al., 2018). My results suggest that astrocytic ephrin-B1 regulates synapse maintenance by restricting synapse formation in the adult hippocampus.

3.2 Materials & Methods

3.2.1 Mice

B6.Cg-Tg(*GFAP*-cre/ERT2)505Fmv/J (ERT2-Cre^{GFAP}, RRID: IMSR_JAX:012849) male mice were crossed with 129S-*Efnb1*^{tm1Sor}/J female mice (*ephrin-B1*$^{flox/+}$, RRID: IMSR_JAX:007664) to obtain ERT2-Cre^{GFAP}*ephrin-B1*$^{flox/y}$ (KO), or ERT2-Cre^{GFAP} (WT) male mice. Adult WT and KO littermates received tamoxifen intraperitoneally (IP; 1 mg in 5 mg/ml of 1:9 ethanol/sunflower seed oil solution) once a day for 7 consecutive days (Fig. 1A). I did not detect any changes in ephrin-B1 levels in astrocytes or neurons in ERT2-Cre^{GFAP}*ephrin-B1*$^{flox/y}$ non-injected or injected with sunflower seed oil without tamoxifen as previously reported (Nikolakopoulou et al., 2016). Ephrin-B1 immunoreactivity was analyzed in ERT2-Cre^{GFAP}*ephrin-B1*$^{flox/y}$ (KO) and ERT2-Cre^{GFAP} (WT) mice (Fig. 1B). Astrocyte-specific Cre expression was confirmed in tamoxifen-treated ERT2-Cre^{GFAP} using Rosa-CAG-LSL-tdTomato reporter mice (CAG-tdTomato, RRID:IMSR_JAX:007909; Fig. 1C). Ephrin-B1 immunoreactivity was observed in cell bodies and dendrites of CA1 neurons but not hippocampal astrocytes of tamoxifen-treated KO mice (Fig. 1C-G). There were no changes in ephrin-B1 levels in astrocytes and neurons of untreated and tamoxifen-treated WT animals. Genotypes were confirmed by PCR analysis of genomic DNA isolated from mouse tails. Mice were maintained in an AAALAC accredited facility under 12-h light/dark cycle and fed standard mouse chow. All mouse studies were done according to NIH and Institutional Animal Care and Use Committee guidelines.

3.2.2 Synaptosome Purification

Synaptosome purification was performed as previously described (Hollingsworth et al., 1985). Hippocampal tissues from adult WT or KO mice were homogenized in 1 ml synaptosome buffer (124 mM NaCl, 3.2 mM KCl, 1.06 mM KH_2PO_4, 26 mM $NaHCO_3$, 1.3 mM $MgCl_2$, 2.5 mM $CaCl_2$, 10 mM Glucose, 20 mM HEPES). Homogenates were filtered through a 100 μm nylon net filter (NY1H02500, Millipore) and 5 μm nylon syringe filter (SF15156, Tisch International). Homogenate flow through was collected and synaptosomes were spun down at 10,000 g, 4^{o}C, for 30 min. Synaptosomes were resuspended in 800 μl synaptosome buffer. To confirm synaptosome enrichment, levels of synapsin-1, PSD95, and histone deacetylase (HDAC I) were analyzed in tissue homogenates and synaptosome fractions with western blot analysis.

3.2.3 Western Blot Analysis

Tissue homogenate or purified synaptosome samples were centrifuged at 10,000 g, 4^{o}C, for 30 min, pellets were re-suspended in lysis buffer (50 mM Tris, 100 mM NaCl, 2% TritonX-100, 10 mM EDTA,) containing 2% protease inhibitor cocktail (P8340, Sigma-Aldrich) and incubated for 2 h at 4^{o}C. Samples were added to 2X Laemmli Buffer (S3401, Sigma-Aldrich) and run on an 8-16% Tris-Glycine Gel (EC6045BOX, Invitrogen). Protein samples were transferred onto a nitrocellulose blotting membrane (10600007, GE Healthcare). Blots were blocked with 5% milk in TBS (10 mM Tris, 150 mM NaCl, pH 8.0) followed by immunostaining with mouse anti-PSD95 (1.65 μg/ml, Invitrogen Cat# MA1-045, RRID: AB_325399), rabbit anti-GluA1 (1:100, Millipore

Cat# AB1504, RRID: AB_2113602), rabbit anti-GluA2/3 (0.1 μg/ml, Millipore Cat# AB1506, RRID: AB_90710), rabbit anti-HDAC I (0.40 μg/ml, Santa Cruz Biotechnologies Cat# sc-7872, RRID: AB_2279709), rabbit anti-synapsin-1 (0.2 μg/ml, Millipore Cat# AB1543P, RRID: AB_90757), or mouse anti-GAPDH (0.2 μg/ml, Thermo Fisher Scientific Cat# 39-8600, RRID:AB_2533438) antibodies in 0.1% tween 20/TBS at 4ºC for 16 h. Secondary antibodies used were HRP conjugated donkey anti-mouse IgG (Jackson ImmunoResearch Cat#715-035-150, RRID: AB_2340770) or HRP conjugated goat anti-rabbit IgG (Jackson ImmunoResearch Cat# 111-035-003, RRID: AB_2313567). Blots were incubated in ECL 2 Western Blotting Substrate (Pierce Cat# 80196) and a signal was collected with CL-XPosure film (34090, Pierce). Band density was analyzed by measuring band and background intensity using Adobe Photoshop CS5.1 software (RRID: SCR_014199). Statistical analysis was performed with a one-way ANOVA followed by Tukey post-hoc analysis using GraphPad Prism 6 software (RRID: SCR_002798), data represent mean ± SEM.

3.2.4 Extracellular Field Recordings

Adult mice (P90-110) were used for electrophysiological experiments two weeks after the first tamoxifen injection. Animals were deeply anesthetized with isoflurane and decapitated. The brains were rapidly removed and immersed in ice-cold artificial cerebrospinal fluid (ACSF) with high Mg^{2+} and sucrose concentration containing 3.5 mM KCl, 1.25 mM NaH_2PO_4, 20 mM D(+)-glucose, 185 mM sucrose, 26 mM $NaHCO_3$, 10 mM $MgCl_2$ and 0.50 mM $CaCl_2$ with a pH of 7.4 and saturated with 95% O_2/5% CO_2.

Transverse hippocampal slices (350 μm) were prepared by using a vibrating blade microtome (LeicaVT1000s, Leica Microsystems; Buffalo Grove, IL, USA) in ice-cold slicing solution bubbled with 95% O_2/5% CO_2. Slices were then transferred into a holding chamber containing oxygenated ACSF (124 mM NaCl, 3.5 mM KCl, 1.25 mM NaH_2PO_4, 10 mM D(+)-glucose, 26 mM $NaHCO_3$, 2 mM $MgCl_2$, and 2 mM $CaCl_2$ with a pH of 7.4) for 1 h at 33°C. Slices were then transferred to a submersion recording chamber continually perfused with oxygenated ACSF at a flow rate of 1 ml/min. Slices are allowed to equilibrate for approximately 10 min to reach a stable baseline response prior to running experimental protocols. Glass microelectrodes (tip resistance 1-3 MΩ, filled with 3 M NaCl) were positioned in the CA1 SP and SR area for extracellular recording. Synaptic responses were evoked by stimulating Schaffer collaterals with a bipolar tungsten electrode (WPI, Sarasota, FL, USA). Potentials were amplified (Axoclamp-2B, Molecular Devices, Sunnyvale, CA), digitized at a sampling rate of 10 kHz and analyzed offline using pClamp (Molecular Devices) software. All electrophysiological responses were digitally filtered at 1 kHz low-pass filter to improve signal-to-noise ratio.

Dendritic potentials typically consisted of a small presynaptic fiber volley (FV) followed by a negative field excitatory postsynaptic potential (fEPSP). The amplitude of the FV reflects the depolarization of the presynaptic terminals and the fEPSP slope reflects the magnitude of the postsynaptic dendritic depolarization. Postsynaptic neuronal firing is represented by the amplitude of the population spike (PS). PSs were calculated

as the voltage difference between two positive peaks and the most negative peak of the trace.

Several protocols were conducted to test for functional changes. To examine basal synaptic transmission, input-output (I/O) curves were generated by incrementally increasing stimulation intensity, beginning at 0.15 mA and increasing stimulation by 0.15 mA until maximal somatic PS amplitudes were reached. The maximal PS amplitude was regarded as maximal neuronal output. Maximal fEPSP slope and maximal PS response were determined, along with 30-50% of maximal fEPSP slope and PS. Paired-pulse facilitation (PPF) was used to test for changes in presynaptic glutamate release probability. PPF was evoked by two stimuli at 30% of maximal fEPSP slope. The two stimuli were separated by varying time differences (or interpulse intervals): 20, 50, 100, 200, or 400 ms. The second fEPSP was typically facilitated; PPF was calculated from the ratio of fEPSP2/fEPSP1 slope. To elicit paired-pulse inhibition (PPI), two stimuli were provided at 100% of max PS response and at inter-pulse intervals of 6, 10, 20, 50, 100, or 200 ms. PPI was calculated from PS2/PS1 amplitude ratio. For long-term potentiation (LTP), Schaffer collaterals were first stimulated to evoke 30% maximal fEPSP slope for at least 10 min to obtain baseline response. LTP was then induced by the stimulation of Schaffer collaterals with 2 trains of 100 pulses at 100 Hz, 20 s apart. LTP was sampled at 30 s intervals for 60 min post stimulation and potentiation was calculated by dividing the average slope of post-induction responses by the average slope of pre-induction baseline responses.

For electrophysiological data, I used two-way ANOVA followed by Bonferroni test to evaluate the effects of astrocytic ephrin-B1 deletion on the I/O curves, PPF, PPI, and LTP. In all electrophysiological recordings, the data represent mean ± SEM.

3.2.5 Whole-Cell Patch Clamp Electrophysiology

Adult mice (P90-110) were used for electrophysiological experiments two weeks after the first tamoxifen injection. Animals were deeply anesthetized with isoflurane and decapitated. The brains were rapidly removed and immersed in ice-cold artificial cerebrospinal fluid (ACSF) with high Mg^{2+} and sucrose concentration containing the following (in mM): 87 NaCl, 75 sucrose, 2.5 KCl, 0.5 $CaCl_2$, 7 $MgCl_2$, 1.25 NaH_2PO_4, 25 $NaHCO_3$, 10 glucose, 1.3 ascorbic, acid, 0.1 kynurenic acid, 2.0 pyruvate, and 3.5 MOPS with a pH of 7.4 and saturated with 95% O_2/5% CO_2. Transverse hippocampal slices (350 µm) were prepared by using a vibrating blade microtome (Campden 5100mz-Plus, Campden Instruments Ltd.) in ice-cold slicing solution bubbled with 95% O_2/5% CO_2. Slices were then transferred into a holding chamber containing oxygenated ACSF (in mM; 125 NaCl, 2.5 KCl, 2.5 CaCl2, 1.3 MgCl2, 1.25 NaH2PO4, 26 NaHCO3, 15 glucose 3.5 MOPS with a pH of 7.4) for 1 h at 33°C. Slices were then transferred to a submersion recording chamber continually perfused with oxygenated ACSF at a flow rate of 1 ml/min. Slices are allowed to equilibrate for approximately 10 min to reach a stable baseline response prior to running experimental protocols.

Whole-cell patch experiments were done blind as described in by Castañeda-Castellanos et al. (Castaneda-Castellanos et al., 2006). Electrical stimuli (0.1 Hz) were

delivered through a bipolar, Teflon®-coated tungsten electrode placed in the CA3 Schaffer collaterals and close proximity to the recording electrode. Tight-seal whole-cell recordings were obtained using pipettes made from borosilicate glass capillaries pulled on a Narishige PC-10 vertical micropipette puller (Narishige, Tokyo, Japan). Pipette resistance ranged from 3 MΩ to 5 MΩ, filled with an internal solution containing (in mM) 130 CsOH, 130 D-gluconic acid, 0.2 EGTA, 2 $MgCl_2$, 6 CsCl, 10 Hepes, 2.5 ATP-Na, 0.5 GTP-Na, 10 phosphocreatine and 0.1% Biocytin for cellular post labeling, pH adjusted to 7.2-7.3 with CsOH, osmolarity adjusted to 300-305 mOsm with ATP-Na. Neurons were voltage-clamped at either -70 mV to measure AMPAR evoked responses or +40mV to measure NMDA receptor evoked responses. 1 µM tetrodotoxin was added to isolate mEPSC responses. All excitatory postsynaptic currents (EPSCs) were recorded in the presence of 50 µM picrotoxin, a $GABA_A$ receptor antagonist, to block $GABA_A$-mediated currents. To measure inhibitory postsynaptic currents (IPSCs), neurons were voltage-clamped at 0 mV with 10 µM NBQX, an AMPA receptor antagonist, and 50 µM D-AP5, a NMDA receptor antagonist. EPSCs and IPSCs were recorded using an EPC-9 amplifier (HEKA Elektronik, Lambrecht, Germany), filtered at 1 kHz, digitized at 10 kHz, and stored on a personal computer using pClamp 10.7 software (Molecular Device) to run analysis. The series resistance was <25 MΩ and was compensated. Both series and input resistance were monitored throughout the experiment by delivering 5 mV voltage steps. If the series resistance changed more than 20% during the course of an experiment, the data was discarded. AMPA, NMDA-mediated EPSCs, IPSCs evoked responses, mEPSCs, and mIPSCs were analyzed by Clampfit 10.7 software (Molecular Device). All

averaged data were presented as means ± SEM. Statistical significance was determined by the Student's t-test using Prism 7.0 software (Graph Pad Software, Avenida, CA).

3.3 Results

It has been previously shown that the loss of astrocytic ephrin-B1 in adult mice resulted in increased excitatory synapses that appear to be immature (Koeppen et al., 2018); however, the effect of astrocytic ephrin-B1 on neuronal function was not explored. To determine if the increase in immature excitatory synapses due to loss of astrocytic ephrin-B1 does result in functionally immature synapses, synaptic AMPAR levels were analyzed in addition to measuring AMPAR and NMDAR evoked responses and mEPSCs at hippocampal pyramidal cells in the CA1. Inhibitory responses were recorded as well to confirm that astrocytic ephrin-B1 affects only excitatory synapses in the adult animal.

Experiments was performed in adult (P90-110) mice following tamoxifen-induced deletion of ephrin-B1 from astrocytes in ERT2-Cre^{GFAP}*ephrin-B1*$^{flox/y}$ mice. Adult ERT2-Cre^{GFAP} (WT) and ERT2-Cre^{GFAP}*ephrin-B1*$^{flox/y}$ (KO) male littermates received tamoxifen intraperitoneally (IP; 1 mg in 5mg/ml of 1:9 ethanol/sunflower seed oil) once a day for 7 days and analyzed 2 weeks after the first tamoxifen injection (Fig. 3.1A). Ephrin-B1 immunoreactivity was selectively disrupted in hippocampal astrocytes (Fig. 3.1B), but not neurons, of tamoxifen-treated KO as compared to tamoxifen-treated WT mice (Fig. 3.1B-G). Astrocyte-specific Cre expression was confirmed in tamoxifen-treated ERT2-Cre^{GFAP} mice using Rosa-CAG-LSL-tdTomato reporter (Fig. 3.1C).

Astrocyte-specific deletion of ephrin-B1 in the adult hippocampus triggers formation of synapses with reduced levels of AMPA receptors

To assess synapse maturation, I determined the levels of synaptic AMPAR subunits GluA1 and GluA2/3 in the adult hippocampus of WT and KO mice. Crude synaptosomes were isolated from P90-P120 hippocampi of WT and KO mice following tamoxifen treatment and analyzed with immunoblotting (Fig. 3.2A). A significant increase in synaptic PSD95 levels was observed in KO compared to WT group (Fig. 3.2D), most likely due to an overall increase in excitatory synapse number (Koeppen et al., 2018). However, I observed a significant decrease in the AMPAR/PSD95 ratio by assessing synaptic levels of AMPAR subunits GluA1 (Fig. 3.2B) and GluA2/3 (Fig. 3.2C). This is consistent with the increase in the proportion of immature dendritic spines with small heads (Koeppen et al., 2018) observed in KO mice as compared to WT mice, suggesting that some of the PSD95-positive synaptic sites may be potentially silent and are lacking AMPARs.

Impaired postsynaptic excitability is observed in CA1 hippocampal neurons following astrocyte-specific deletion of ephrin-B1.

Increased numbers of excitatory synapses may suggest an overall increase in excitatory drive in the CA1 hippocampus. Although greater in numbers, dendritic spines were structurally less mature in KO mice, showing a decrease in the proportion of dendritic spines with larger heads as compared to WT mice (Koeppen et al., 2018). Therefore, I next tested the excitability of CA1 hippocampal neurons in acute

hippocampal slices from adult KO and WT mice. To assess the effects of astrocytic ephrin-B1 deletion on basal synaptic transmission in CA1 hippocampus, synaptic responses were evoked in CA1 neurons by stimulating Schaffer collaterals with incrementally increased stimulation intensities. Input/output curves were generated by plotting presynaptic FV amplitude, postsynaptic fEPSP slope, or somatic population spike (PS) amplitude as a function of increasing stimulation intensity (Fig. 3.3B-D, Table 3.1). Surprisingly deletion of astrocytic ephrin-B1 did not affect presynaptic excitability, as I found no differences in the amplitude of the presynaptic FV between WT and KO groups (Fig. 3.3B). Although fEPSPs were not statistically different between the groups with potential trend towards reduced postsynaptic responses in KO animals as compared to WT group (Fig. 3.3C), there was a significant decrease in PS amplitude (Fig. 3.3D). In spite a decrease in baseline excitability, short-term plasticity was also unaffected by the deletion of astro-ephrin-B1, as I found no changes in PPF (Fig. 3.3E) and PPI (Fig. 3.3F) responses between WT and KO groups. NMDAR-dependent LTP was also unaffected following astrocytic ephrin-B1 deletion, as I observed similar potentiation at 0-10 min, 30-40 min, and 50-60 min post stimulation of Schaffer collaterals with 2 trains of 100 pulses in both WT and KO hippocampal slices (Fig. 3.3G).

Taken together my findings show that despite the increase in the number of excitatory synapses, CA1 pyramidal neurons showed a decrease in postsynaptic firing following astrocyte-specific deletion of ephrin-B1 in the adult hippocampus, suggesting impaired maturation of these newly formed and potentially silent synapses or increased

excitatory drive on the inhibitory neurons resulting in the overall decreased postsynaptic firing.

Whole-cell patch clamp reveals impaired AMPAR evoked responses in adult KO mice.

To resolve if loss of astrocytic ephrin-B1 induces formation of functionally immature synapses or increases excitatory drive onto inhibitory neurons, AMPAR and NMDAR responses were measured. Functionally immature synapses will have decreased AMPAR function and can be calculated by the ratio of AMPAR to NMDAR evoked responses. The AMPAR/NMDAR ratio gives a measure of the relative expression of AMPAR and NMDAR at the synapse. To calculate ratio of AMPAR and NMDAR on hippocampal pyramidal neurons, I measured AMPAR-mediated currents at -70 mV and NMDAR-mediated currents at +40 mV (Fig. 3.4B, C). AMPAR-mediated currents were significantly decreased in KO mice; however, NMDAR-mediated currents were not different between KO and WT mice (Fig.3.4C). The calculated AMPA/NMDA ratio shows that KO mice indeed have decreased AMPAR to NMDAR-mediated currents (Fig. 3.4D), indicating reduced AMPAR functionally and confirming the CA1 hippocampal pyramidal cells are indeed functionally immature.

The increase in functionally immature synapses following adult deletion of astrocytic ephrin-B1 is confirmed further by decreased frequency of mEPSCs (Fig. 3.4G) potentially due to decreased number contributing, mature synapses. Although average amplitude of mEPSC was not different between KO and WT mice (Fig. 3.4F), amplitude

distributions were skewed to smaller amplitudes in KO mice (Fig. 3.4H-I), potentially indicating decreased synaptic AMPAR expression is decreased in KO mice.

Inhibitory synapses are unaffected by the loss of astrocytic ephrin-B1

Inhibitory synapse activity on hippocampal CA1 pyramidal cells was measured at 0 mV in the presence of NBQX and D-AP5 to block AMPAR- and NMDAR-mediated currents, respectively. Evoked IPSCs was not significantly different between KO and WT mice (Fig. 3.5A-B), indicating that inhibitory synapses are not affected by astrocytic ephrin-B1 deletion.

3.4 Discussion

Hippocampal circuits are plastic by nature and underlies life-long learning and memory formation, reflected by ongoing synapse pruning and restructuring and is required for maintain synaptic homeostasis in the adult hippocampus (Maletic-Savatic et al., 1999; Spacek and Harris, 2004; Stevens et al., 2007; Schafer and Stevens, 2010; Paolicelli et al., 2011). Maintenance of synapse number can be regulated by formation of new synapses or removal of weak, potentially silent, synaptic connections and allowing for an opportunity for new connections to form. Together with previous work, I demonstrate here the role of astrocytes in maintaining hippocampal circuits in the adult mouse brain via astro-ephrin-B1, acting as a regulator of synaptic homeostasis in the adult hippocampus. My findings are consistent with the role of astro-ephrin-B1 as a negative regulator of synapse formation in the adult hippocampus, as astrocyte-specific

ablation of ephrin-B1 in adult mice triggers an increase in excitatory synapses that are functionally immature. These effects appear to be specific to excitatory changes as there was no changes to inhibitory function on hippocampal CA1 pyramidal cells with astrocytic ephrin-B1 loss. However, there may be effects on excitatory inputs onto inhibitory circuits as excitatory synapse formation can occur on both excitatory and inhibitory neurons. There may be increased excitatory drive onto inhibitory interneurons that may contribute to memory formation and recall. These results establish that astrocytic ephrin-B1 has a fundamental role in the formation of excitatory hippocampal synapses.

Ephrin-Bs bind to EphB receptors which are highly expressed on pre-synaptic CA3 fibers, specifically EphB1 and EphB2 receptors, and contact CA1 dendrites expressing ephrin-B ligands (Liebl et al., 2003; Grunwald et al., 2004). Astrocytic ephrin-B1 may interact with CA3 pre-synaptic EphB receptors and restrict the formation of new CA3 to CA1 connections by interfering with the interactions between pre-synaptic EphB receptors and dendritic ephrin-B, whereas reduced expression of astrocytic ephrin-B1 may promote synapse formation. Eph/ephrin signaling is implicated in synaptic development, function, and plasticity. Pre-synaptic EphB1 and EphB2 localized in CA3 axon terminals have been shown to serve as a ligand mediating trans-synaptic signaling and can induce either elimination/pruning at developing dendrites or spine maturation/synapse formation depending on interactions with either Grb4, Pick1, and syntenin (Xu et al., 2011). EphB receptors are also expressed post-synaptically on the dendrites of CA1 neurons and has been implicated in synapse development both *in vitro*

and *in vivo* (Ethell et al., 2001; Henderson et al., 2001; Takasu et al., 2002; Henkemeyer et al., 2003; Liebl et al., 2003). Loss of EphB receptors, specifically EphB1, B2, and B3, results in defects in spine formation. EphB1/EphB2-deficient neurons will expression increased protrusions of long, thin filopodia-like dendritic spines while triple EphB mutant mice will show decreased spine density and formation of abnormal headless or small-headed spines (Henkemeyer et al., 2003), potentially indicating that EphBs are essential for spine formation in hippocampal neurons. Post-synaptic EphB receptors has been shown to both clustering and recruitment of NMDARs and AMPARs to the postsynaptic sites (Dalva et al., 2000; Takasu et al., 2002; Kayser et al., 2006; Nolt et al., 2011; Hussain et al., 2015).

Astrocytic ephrin-B1 may also influence post-synaptic functions by disrupting post-synaptic EphB signaling; and I would expect an increase in synaptic strength in the adult hippocampus following the deletion of ephrin-B1 from astrocytes. Interestingly, despite an increase in synapse numbers, I observed reduced postsynaptic firing responses in the CA1 hippocampus of astrocyte-specific ephrin-B1 KO mice. Deletion of astro-ephrin-B1 in adult hippocampus had no effect on presynaptic fiber volley responses, but significantly reduced population spike amplitude in CA1 neurons following the stimulation of Schaffer collaterals. The postsynaptic nature of the observed changes is further supported by the fact that PPF is not affected by the deletion of astro-ephrin-B1, suggesting that the presynaptic release of glutamate is normal, while the population spike amplitude, or the postsynaptic neural firing strength, is reduced in astro-ephrin-B1 KO as compared to WT mice.

Despite the increase in synapse formation, synaptic strength is dictated by more than synapse number, as newly formed synapses may be initially post-synaptically silent characterized by the presence of NMDA but absence of AMPA receptors (Durand et al., 1996; Isaac, 2003). The abundance of immature silent synapses may explain the reduced postsynaptic responses observed in astro-ephrin-B1 KO mice in spite of the increase in the total number of synapses. Indeed, deletion of astro-ephrin-B1 resulted in a two-fold decrease in the synaptic levels of AMPARs. Neuronal ephrin-Bs have been found to stabilize and recruit both AMPA and NMDA receptors. Activation of ephrin-B2 signaling in cultured neurons have been shown to decrease AMPA receptor internalization by interacting with GRIP1, thereby stabilizing AMPA receptors and retention at the surface (Essmann et al., 2008). In addition, activation EphB2 enhances NMDA receptor function by clustering NMDA receptors and directly recruiting NR1 and associated subunits, such as NR2A-B (Dalva et al., 2000; Takasu et al., 2002). My results suggest that the loss of ephrin-B1 may lead to impaired ability of ephrin-B1 KO astrocytes to prevent an excessive formation of immature synapses in the adult hippocampus that may also compete for synaptic proteins with existing synapses.

Indeed, loss of astrocytic ephrin-B1 results in functionally immature excitatory synapses indicated by decreased AMPAR/NMDAR evoked response ratio and decreased frequency of mEPSCs. AMPA/NMDA amplitude ratio provides a rough indication of AMPA-silent synapses; if there is decreased AMPA/NMDA ratio response, then there is less functional contribution of AMPA to NMDA activity; with NMDA-mediated responses being similar between both WT and KO mice. mEPSC frequency was also

decreased with loss of astrocytic ephrin-B1 and may due to (i) decreased number of synapses contributing to these synapses or (ii) due to changes in spontaneous neurotransmitter release probability (Turrigiano et al., 1998). Despite the increase number of synapses, there is a decrease in frequency in astrocytic ephrin-B1 ablated mice potentially indicating functionally silent synapses. Pre-synaptically, there may be similar levels of quantal units of neurotransmitters released as amplitude of mEPSC was similar in WT and KO mice; however, there may be increased post-synaptic functional sites. Astrocytic ephrin-B1 may be maintaining the types of synapses formed; acting as a negative regulator on non-functional, immature excitatory synapses. Similarly, loss of neuronal ephrin-B3 results in reduced frequency but not amplitude of mEPSCs with an increase in dendritic spines (Xu et al., 2011).

Inhibitory function may also be affected by the loss of astrocytic ephrin-B1. The decrease in evoked postsynaptic firing of pyramidal cells with unchanged presynaptic and only trending, but not statistically significant, decrease of postsynaptic fEPSPs may indicate a larger role of inhibition. Increased excitatory input on inhibitory neurons and potentially an increased perisomatic inhibitory drive of CA1 pyramidal neurons may result in the overall decreased postsynaptic firing (Miles et al., 1996). This inhibitory drive can be mediated by PV-positive interneurons, which are activated by CA3 pyramidal neurons (Ylinen et al., 1995; Tukker et al., 2007; Oren et al., 2010) and play an important role in strengthening contextual memory (Donato et al., 2013; Donato et al., 2015). However, IPSC evoked responses were similar between WT and KO adult mice indicating no role of astrocytic ephrin-B1 on inhibitory synapse function. This is further

confirmed with morphological data; GAD65 puncta was similar in both WT and KO mice (Koeppen et al., 2018).

In contrast to ephrin-B1, glial expression of ephrin-A3 was shown to regulate glutamate transport in the hippocampus (Carmona et al., 2009; Filosa et al., 2009), potentially affecting excitatory activity at hippocampal pyramidal cells. Indeed, astrocytic ephrin-A3 can regulate synaptic functions through its interaction with synaptic EphA4 (Murai et al., 2003; Carmona et al., 2009; Filosa et al., 2009). Ephrin-A3 null mice exhibited impaired LTP (Filosa et al., 2009) potentially due to decrease glutamate available as GLT1 and GLAST levels, which play an essential role in glutamate homeostasis and modulation of hippocampal circuits, are increased levels in ephrin-A3 null mice (Carmona et al., 2009). In addition, loss of EphA4 results in spine irregularities as EphA4 may be responsible for spine retraction. It should be noted that EphA4 is highly promiscuous and can bind to both ephrin-As and ephrinBs (Bowden et al., 2009; Qin et al., 2010), whereas ephrin-B1 preferentially interacts with B type Eph receptor. The increased formation of new synapses following astrocyte-specific deletion of ephrin-B1 was not observed in ephrin-A3 KO mice (Carmona et al., 2009) indicating a different role of ephrin-B1 in astrocytes.

In summary, my studies demonstrate that astrocyte specific ephrin-B1 is a negative regulator of synaptogenesis by maintaining excitatory glutamatergic synapses in the adult hippocampus Therefore, astrocytic ephrin-B1 may be a potential target to manipulate new synapse formation or potentially prevent synapse loss in neurodegenerative diseases. Further understanding the role of astrocytic ephrin-B1 in

synaptogenesis may also provide insights into astrocyte-specific mechanisms underlying abnormal synapse development in neurodevelopmental and learning disorders.

References

Allen, N.J., Bennett, M.L., Foo, L.C., Wang, G.X., Chakraborty, C., Smith, S.J., et al. (2012). Astrocyte glypicans 4 and 6 promote formation of excitatory synapses via GluA1 AMPA receptors. *Nature* 486(7403)**,** 410-414. doi: 10.1038/nature11059.

Bowden, T.A., Aricescu, A.R., Nettleship, J.E., Siebold, C., Rahman-Huq, N., Owens, R.J., et al. (2009). Structural plasticity of eph receptor A4 facilitates cross-class ephrin signaling. *Structure* 17(10)**,** 1386-1397. doi: 10.1016/j.str.2009.07.018.

Bush, J.O., and Soriano, P. (2009). Ephrin-B1 regulates axon guidance by reverse signaling through a PDZ-dependent mechanism. *Genes Dev* 23(13)**,** 1586-1599. doi: 10.1101/gad.1807209.

Bushong, E.A., Martone, M.E., Jones, Y.Z., and Ellisman, M.H. (2002). Protoplasmic astrocytes in CA1 stratum radiatum occupy separate anatomical domains. *J Neurosci* 22(1)**,** 183-192.

Butz, M., and van Ooyen, A. (2013). A simple rule for dendritic spine and axonal bouton formation can account for cortical reorganization after focal retinal lesions. *PLoS Comput Biol* 9(10)**,** e1003259. doi: 10.1371/journal.pcbi.1003259.

Carmona, M.A., Murai, K.K., Wang, L., Roberts, A.J., and Pasquale, E.B. (2009). Glial ephrin-A3 regulates hippocampal dendritic spine morphology and glutamate transport. *Proc Natl Acad Sci U S A* 106(30)**,** 12524-12529. doi: 10.1073/pnas.0903328106.

Castaneda-Castellanos, D.R., Flint, A.C., and Kriegstein, A.R. (2006). Blind patch clamp recordings in embryonic and adult mammalian brain slices. *Nat Protoc* 1(2)**,** 532-542. doi: 10.1038/nprot.2006.75.

Christopherson, K.S., Ullian, E.M., Stokes, C.C., Mullowney, C.E., Hell, J.W., Agah, A., et al. (2005). Thrombospondins are astrocyte-secreted proteins that promote CNS synaptogenesis. *Cell* 120(3)**,** 421-433. doi: 10.1016/j.cell.2004.12.020.

Chung, W.S., Clarke, L.E., Wang, G.X., Stafford, B.K., Sher, A., Chakraborty, C., et al. (2013). Astrocytes mediate synapse elimination through MEGF10 and MERTK pathways. *Nature* 504(7480)**,** 394-400. doi: 10.1038/nature12776.

Cowan, C.A., and Henkemeyer, M. (2001). The SH2/SH3 adaptor Grb4 transduces B-ephrin reverse signals. *Nature* 413(6852)**,** 174-179. doi: 10.1038/35093123.

Cowan, W.M., Fawcett, J.W., O'Leary, D.D., and Stanfield, B.B. (1984). Regressive events in neurogenesis. *Science* 225(4668)**,** 1258-1265. doi: 10.1126/science.6474175.

Dalva, M.B., Takasu, M.A., Lin, M.Z., Shamah, S.M., Hu, L., Gale, N.W., et al. (2000). EphB receptors interact with NMDA receptors and regulate excitatory synapse formation. *Cell* 103(6)**,** 945-956.

Donato, F., Chowdhury, A., Lahr, M., and Caroni, P. (2015). Early- and late-born parvalbumin basket cell subpopulations exhibiting distinct regulation and roles in learning. *Neuron* 85(4)**,** 770-786. doi: 10.1016/j.neuron.2015.01.011.

Donato, F., Rompani, S.B., and Caroni, P. (2013). Parvalbumin-expressing basket-cell network plasticity induced by experience regulates adult learning. *Nature* 504(7479)**,** 272-276. doi: 10.1038/nature12866.

Durand, G.M., Kovalchuk, Y., and Konnerth, A. (1996). Long-term potentiation and functional synapse induction in developing hippocampus. *Nature* 381(6577)**,** 71-75. doi: 10.1038/381071a0.

Eroglu, C., Allen, N.J., Susman, M.W., O'Rourke, N.A., Park, C.Y., Ozkan, E., et al. (2009). Gabapentin receptor alpha2delta-1 is a neuronal thrombospondin receptor responsible for excitatory CNS synaptogenesis. *Cell* 139(2)**,** 380-392. doi: 10.1016/j.cell.2009.09.025.

Eroglu, C., and Barres, B.A. (2010). Regulation of synaptic connectivity by glia. *Nature* 468(7321)**,** 223-231. doi: 10.1038/nature09612.

Essmann, C.L., Martinez, E., Geiger, J.C., Zimmer, M., Traut, M.H., Stein, V., et al. (2008). Serine phosphorylation of ephrinB2 regulates trafficking of synaptic AMPA receptors. *Nat Neurosci* 11(9)**,** 1035-1043. doi: 10.1038/nn.2171.

Ethell, I.M., Irie, F., Kalo, M.S., Couchman, J.R., Pasquale, E.B., and Yamaguchi, Y. (2001). EphB/syndecan-2 signaling in dendritic spine morphogenesis. *Neuron* 31(6)**,** 1001-1013. doi: 10.1016/s0896-6273(01)00440-8.

Filosa, A., Paixao, S., Honsek, S.D., Carmona, M.A., Becker, L., Feddersen, B., et al. (2009). Neuron-glia communication via EphA4/ephrin-A3 modulates LTP through glial glutamate transport. *Nat Neurosci* 12(10)**,** 1285-1292. doi: 10.1038/nn.2394.

Grunwald, I.C., Korte, M., Adelmann, G., Plueck, A., Kullander, K., Adams, R.H., et al. (2004). Hippocampal plasticity requires postsynaptic ephrinBs. *Nat Neurosci* 7(1)**,** 33-40. doi: 10.1038/nn1164.

Henderson, J.T., Georgiou, J., Jia, Z., Robertson, J., Elowe, S., Roder, J.C., et al. (2001). The receptor tyrosine kinase EphB2 regulates NMDA-dependent synaptic function. *Neuron* 32(6)**,** 1041-1056.

Henkemeyer, M., Itkis, O.S., Ngo, M., Hickmott, P.W., and Ethell, I.M. (2003). Multiple EphB receptor tyrosine kinases shape dendritic spines in the hippocampus. *J Cell Biol* 163(6)**,** 1313-1326. doi: 10.1083/jcb.200306033.

Hollingsworth, E.B., McNeal, E.T., Burton, J.L., Williams, R.J., Daly, J.W., and Creveling, C.R. (1985). Biochemical characterization of a filtered synaptoneurosome preparation from guinea pig cerebral cortex: cyclic adenosine 3':5'-monophosphate-generating systems, receptors, and enzymes. *J Neurosci* 5(8)**,** 2240-2253.

Hussain, N.K., Thomas, G.M., Luo, J., and Huganir, R.L. (2015). Regulation of AMPA receptor subunit GluA1 surface expression by PAK3 phosphorylation. *Proc Natl Acad Sci U S A* 112(43)**,** E5883-5890. doi: 10.1073/pnas.1518382112.

Isaac, J. (2003). Postsynaptic silent synapses: evidence and mechanisms. *Neuropharmacology* 45(4)**,** 450-460. doi: 10.1016/s0028-3908(03)00229-6.

Kayser, M.S., McClelland, A.C., Hughes, E.G., and Dalva, M.B. (2006). Intracellular and trans-synaptic regulation of glutamatergic synaptogenesis by EphB receptors. *J Neurosci* 26(47)**,** 12152-12164. doi: 10.1523/JNEUROSCI.3072-06.2006.

Kayser, M.S., Nolt, M.J., and Dalva, M.B. (2008). EphB receptors couple dendritic filopodia motility to synapse formation. *Neuron* 59(1)**,** 56-69. doi: 10.1016/j.neuron.2008.05.007.

Koeppen, J., Nguyen, A.Q., Nikolakopoulou, A.M., Garcia, M., Hanna, S., Woodruff, S., et al. (2018). Functional Consequences of Synapse Remodeling Following Astrocyte-Specific Regulation of Ephrin-B1 in the Adult Hippocampus. *J Neurosci* 38(25)**,** 5710-5726. doi: 10.1523/JNEUROSCI.3618-17.2018.

Kucukdereli, H., Allen, N.J., Lee, A.T., Feng, A., Ozlu, M.I., Conatser, L.M., et al. (2011). Control of excitatory CNS synaptogenesis by astrocyte-secreted proteins Hevin and SPARC. *Proc Natl Acad Sci U S A* 108(32)**,** E440-449. doi: 10.1073/pnas.1104977108.

Lauterbach, J., and Klein, R. (2006). Release of full-length EphB2 receptors from hippocampal neurons to cocultured glial cells. *J Neurosci* 26(45)**,** 11575-11581. doi: 10.1523/JNEUROSCI.2697-06.2006.

Liao, D., Scannevin, R.H., and Huganir, R. (2001). Activation of silent synapses by rapid activity-dependent synaptic recruitment of AMPA receptors. *J Neurosci* 21(16)**,** 6008-6017.

Liebl, D.J., Morris, C.J., Henkemeyer, M., and Parada, L.F. (2003). mRNA expression of ephrins and Eph receptor tyrosine kinases in the neonatal and adult mouse central nervous system. *J Neurosci Res* 71(1)**,** 7-22. doi: 10.1002/jnr.10457.

Luo, L., and O'Leary, D.D. (2005). Axon retraction and degeneration in development and disease. *Annu Rev Neurosci* 28**,** 127-156. doi: 10.1146/annurev.neuro.28.061604.135632.

Malenka, R.C., and Nicoll, R.A. (1999). Long-term potentiation--a decade of progress? *Science* 285(5435)**,** 1870-1874. doi: 10.1126/science.285.5435.1870.

Maletic-Savatic, M., Malinow, R., and Svoboda, K. (1999). Rapid dendritic morphogenesis in CA1 hippocampal dendrites induced by synaptic activity. *Science* 283(5409)**,** 1923-1927. doi: 10.1126/science.283.5409.1923.

Malinow, R., Mainen, Z.F., and Hayashi, Y. (2000). LTP mechanisms: from silence to four-lane traffic. *Curr Opin Neurobiol* 10(3)**,** 352-357. doi: 10.1016/s0959-4388(00)00099-4.

Matsuo, N., Reijmers, L., and Mayford, M. (2008). Spine-type-specific recruitment of newly synthesized AMPA receptors with learning. *Science* 319(5866)**,** 1104-1107. doi: 10.1126/science.1149967.

Miles, R., Toth, K., Gulyas, A.I., Hajos, N., and Freund, T.F. (1996). Differences between somatic and dendritic inhibition in the hippocampus. *Neuron* 16(4)**,** 815-823. doi: 10.1016/s0896-6273(00)80101-4.

Milner, B., Squire, L.R., and Kandel, E.R. (1998). Cognitive neuroscience and the study of memory. *Neuron* 20(3)**,** 445-468.

Murai, K.K., Nguyen, L.N., Irie, F., Yamaguchi, Y., and Pasquale, E.B. (2003). Control of hippocampal dendritic spine morphology through ephrin-A3/EphA4 signaling. *Nat Neurosci* 6(2)**,** 153-160. doi: 10.1038/nn994.

Neves, G., Cooke, S.F., and Bliss, T.V. (2008). Synaptic plasticity, memory and the hippocampus: a neural network approach to causality. *Nat Rev Neurosci* 9(1)**,** 65-75. doi: 10.1038/nrn2303.

Nikolakopoulou, A.M., Koeppen, J., Garcia, M., Leish, J., Obenaus, A., and Ethell, I.M. (2016). Astrocytic Ephrin-B1 Regulates Synapse Remodeling Following Traumatic Brain Injury. *ASN Neuro* 8(1)**,** 1-18. doi: 10.1177/1759091416630220.

Nolt, M.J., Lin, Y., Hruska, M., Murphy, J., Sheffler-Colins, S.I., Kayser, M.S., et al. (2011). EphB controls NMDA receptor function and synaptic targeting in a subunit-specific manner. *J Neurosci* 31(14)**,** 5353-5364. doi: 10.1523/JNEUROSCI.0282-11.2011.

Oren, I., Hajos, N., and Paulsen, O. (2010). Identification of the current generator underlying cholinergically induced gamma frequency field potential oscillations in the hippocampal CA3 region. *J Physiol* 588(Pt 5)**,** 785-797. doi: 10.1113/jphysiol.2009.180851.

Paolicelli, R.C., Bolasco, G., Pagani, F., Maggi, L., Scianni, M., Panzanelli, P., et al. (2011). Synaptic pruning by microglia is necessary for normal brain development. *Science* 333(6048)**,** 1456-1458. doi: 10.1126/science.1202529.

Qin, H., Noberini, R., Huan, X., Shi, J., Pasquale, E.B., and Song, J. (2010). Structural characterization of the EphA4-Ephrin-B2 complex reveals new features enabling Eph-ephrin binding promiscuity. *J Biol Chem* 285(1)**,** 644-654. doi: 10.1074/jbc.M109.064824.

Schafer, D.P., and Stevens, B. (2010). Synapse elimination during development and disease: immune molecules take centre stage. *Biochem Soc Trans* 38(2)**,** 476-481. doi: 10.1042/bst0380476.

Segura, I., Essmann, C.L., Weinges, S., and Acker-Palmer, A. (2007). Grb4 and GIT1 transduce ephrinB reverse signals modulating spine morphogenesis and synapse formation. *Nat Neurosci* 10(3)**,** 301-310. doi: 10.1038/nn1858.

Sloniowski, S., and Ethell, I.M. (2012). Looking forward to EphB signaling in synapses. *Semin Cell Dev Biol* 23(1)**,** 75-82. doi: 10.1016/j.semcdb.2011.10.020.

Spacek, J., and Harris, K.M. (2004). Trans-endocytosis via spinules in adult rat hippocampus. *J Neurosci* 24(17)**,** 4233-4241. doi: 10.1523/JNEUROSCI.0287-04.2004.

Stevens, B., Allen, N.J., Vazquez, L.E., Howell, G.R., Christopherson, K.S., Nouri, N., et al. (2007). The classical complement cascade mediates CNS synapse elimination. *Cell* 131(6)**,** 1164-1178. doi: 10.1016/j.cell.2007.10.036.

Strekalova, T., Zorner, B., Zacher, C., Sadovska, G., Herdegen, T., and Gass, P. (2003). Memory retrieval after contextual fear conditioning induces c-Fos and JunB expression in CA1 hippocampus. *Genes Brain Behav* 2(1)**,** 3-10.

Takasu, M.A., Dalva, M.B., Zigmond, R.E., and Greenberg, M.E. (2002). Modulation of NMDA receptor-dependent calcium influx and gene expression through EphB receptors. *Science* 295(5554)**,** 491-495. doi: 10.1126/science.1065983.

Tsien, J.Z., Huerta, P.T., and Tonegawa, S. (1996). The Essential Role of Hippocampal CA1 NMDA Receptor–Dependent Synaptic Plasticity in Spatial Memory. *Cell* 87(7)**,** 1327-1338. doi: 10.1016/s0092-8674(00)81827-9.

Tukker, J.J., Fuentealba, P., Hartwich, K., Somogyi, P., and Klausberger, T. (2007). Cell type-specific tuning of hippocampal interneuron firing during gamma oscillations in vivo. *J Neurosci* 27(31)**,** 8184-8189. doi: 10.1523/JNEUROSCI.1685-07.2007.

Turrigiano, G.G. (2017). The dialectic of Hebb and homeostasis. *Philos Trans R Soc Lond B Biol Sci* 372(1715). doi: 10.1098/rstb.2016.0258.

Turrigiano, G.G., Leslie, K.R., Desai, N.S., Rutherford, L.C., and Nelson, S.B. (1998). Activity-dependent scaling of quantal amplitude in neocortical neurons. *Nature* 391(6670)**,** 892-896. doi: 10.1038/36103.

Ullian, E.M., Sapperstein, S.K., Christopherson, K.S., and Barres, B.A. (2001). Control of synapse number by glia. *Science* 291(5504)**,** 657-661. doi: 10.1126/science.291.5504.657.

Wang, Y., Ying, G.X., Liu, X., Wang, W.Y., Dong, J.H., Ni, Z.M., et al. (2005). Induction of ephrin-B1 and EphB receptors during denervation-induced plasticity in the adult mouse hippocampus. *Eur J Neurosci* 21(9)**,** 2336-2346. doi: 10.1111/j.1460-9568.2005.04093.x.

Xu, N.J., and Henkemeyer, M. (2012). Ephrin reverse signaling in axon guidance and synaptogenesis. *Semin Cell Dev Biol* 23(1)**,** 58-64. doi: 10.1016/j.semcdb.2011.10.024.

Xu, N.J., Sun, S., Gibson, J.R., and Henkemeyer, M. (2011). A dual shaping mechanism for postsynaptic ephrin-B3 as a receptor that sculpts dendrites and synapses. *Nat Neurosci* 14(11)**,** 1421-1429. doi: 10.1038/nn.2931.

Yasumatsu, N., Matsuzaki, M., Miyazaki, T., Noguchi, J., and Kasai, H. (2008). Principles of long-term dynamics of dendritic spines. *J Neurosci* 28(50)**,** 13592-13608. doi: 10.1523/jneurosci.0603-08.2008.

Ylinen, A., Bragin, A., Nadasdy, Z., Jando, G., Szabo, I., Sik, A., et al. (1995). Sharp wave-associated high-frequency oscillation (200 Hz) in the intact hippocampus: network and intracellular mechanisms. *J Neurosci* 15(1 Pt 1)**,** 30-46.

Zito, K., and Svoboda, K. (2002). Activity-dependent synaptogenesis in the adult Mammalian cortex. *Neuron* 35(6)**,** 1015-1017. doi: 10.1016/s0896-6273(02)00903-0.

Figures

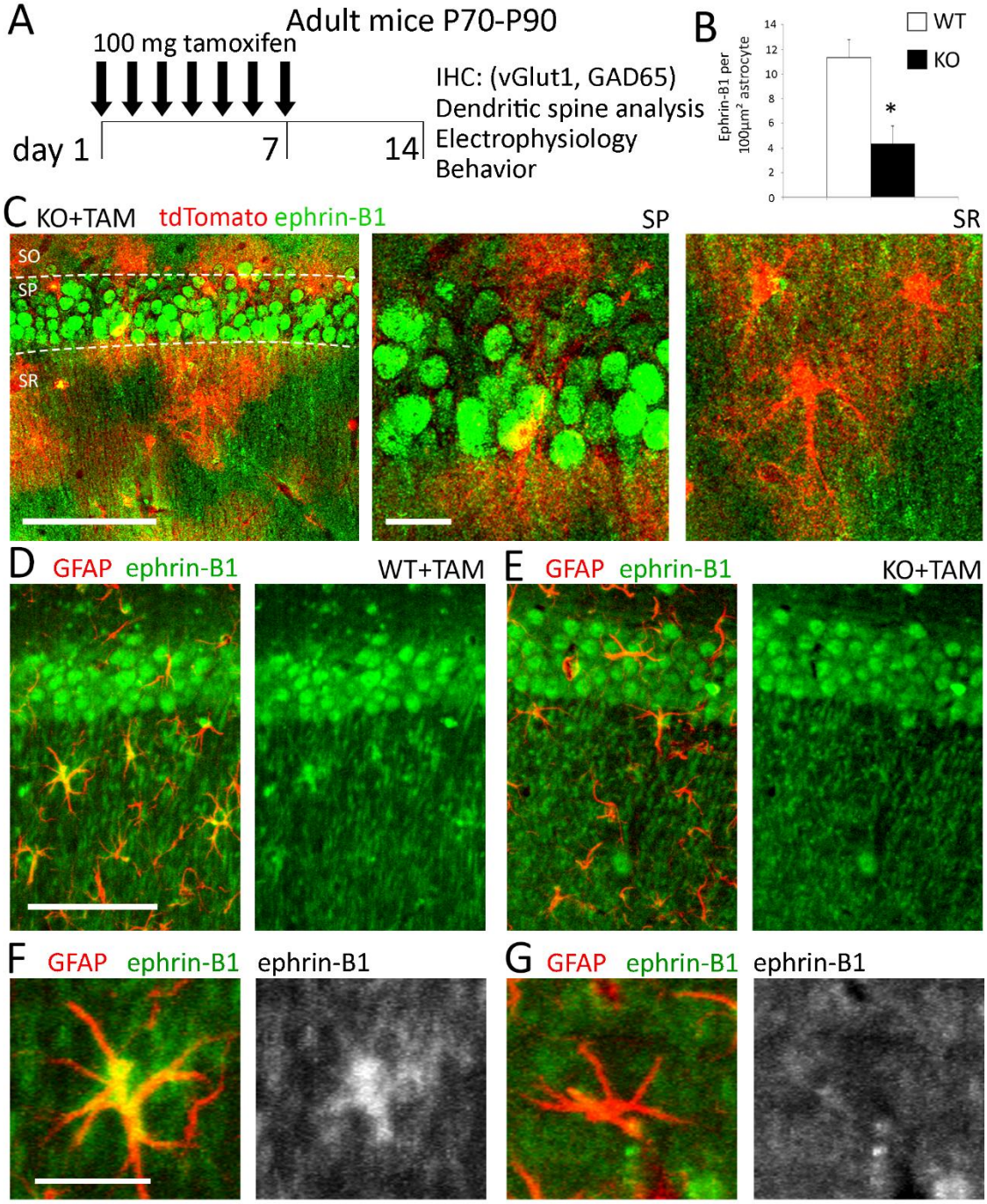
A
Adult mice P70-P90
100 mg tamoxifen
day 1
7
14
IHC: (vGlut1, GAD65)
Dendritic spine analysis
Electrophysiology
Behavior
B
WT
KO
Ephrin-B1 per 100μm² astrocyte
*
C KO+TAM tdTomato ephrin-B1
SO
SP
SR
SP
SR
D GFAP ephrin-B1
WT+TAM
E GFAP ephrin-B1
KO+TAM
F GFAP ephrin-B1
ephrin-B1
G GFAP ephrin-B1
ephrin-B1

Figure 3.1 Tamoxifen-induced deletion of ephrin-B1 in adult hippocampal astrocytes. (A) Adult male ERT2-Cre^{GFAP} and ERT2-Cre^{GFAP}ephrin-B1$^{flox/y}$ littermates (P90-110) were intraperitoneally (IP) injected with 1 mg of tamoxifen once a day for 7 consecutive days. Immunohistochemistry, spine labeling, electrophysiology, and behavior tests were performed 14 days after first injection. (B) Astrocytic ephrin-B1 immunoreactivity was significantly reduced in the hippocampus of KO as compared to WT mice (n=3 mice, t-test, * $p<0.05$). (C) Max projection confocal images of the CA1 hippocampus in tamoxifen injected ERT2-Cre^{GFAP}stop^{flox}tdTomato mice show tdTomato expression in astrocytes of stratum radiatum (SR), but not in CA1 neurons of the stratum pyramidal (SP) area. Ephrin-B1 immunoreactivity was detected in cell bodies (green, SP) and dendrites (green, SR) of CA1 neurons but not in tdTomato-positive astrocytes (red). Low magnification scale bar = 100 μm; high magnification scale bar = 20 μm (D-E) Max projection confocal images show GFAP (red) and ephrin-B1 (green) immunoreactivity in the CA1 hippocampus. Scale bar = 100 μm (F-G) High magnification images show ephrin-B1 immunoreactivity in astrocytes of WT but not KO mice. Ephrin-B1 is detected in dendrites of CA1 neurons verifying that deletion of ephrin-B1 is specific to astrocytes. Scale bar = 25 μm

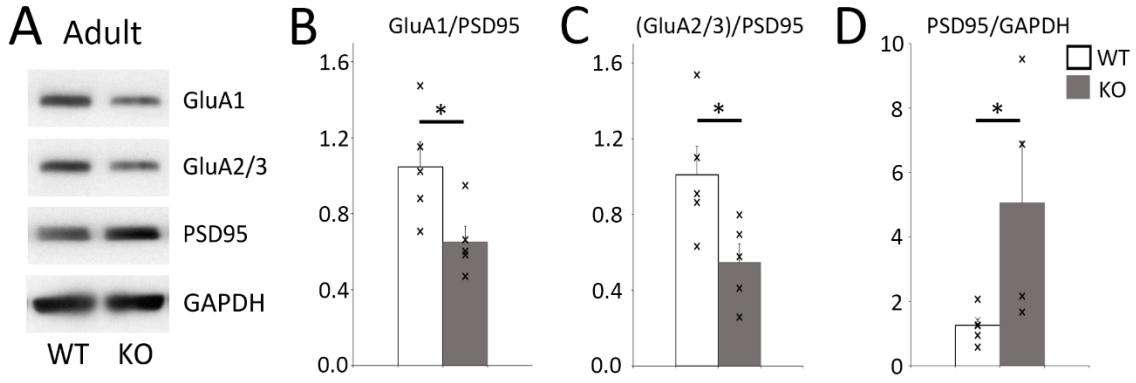

Figure 3.2 Synaptic AMPAR levels are decreased following loss of astrocytic ephrin-B1 in adult mice. (A) Western blots show levels of AMPAR subunits (GluA1 and GluA2/3), PSD95 and GAPDH in synaptosomes isolated from the hippocampus of WT and KO adult mice. (B-D) Graphs show ratios of synaptic GluA1 or GluA2/3 levels to PSD95 levels and PSD95 to GAPDH ratios in synaptosomes isolated from the hippocampus of WT and KO. Graphs show individual values (marked by x), mean values and error bars represent SEM (n=5 mice per group, t-test, *$p<0.05$). There was a significant increase in synaptic PSD95 levels in naïve KO compared to WT (WT: 1.252 ± 0.204 vs KO: 5.058 ± 1.895, $t(8) = 2.505$, $p=0.0366$). However, there was a significant decrease in AMPAR/PSD95 ratio assessed by synaptic GluA1 (WT: 1.04 ± 0.13 vs KO: 0.65 ± 0.079, $t(8) =2.564$, $p= 0.0335$, t-test) and GluA2/3 subunits (WT: 1.01 ± 0.15 vs KO: 0.54 ± 0.09, $t(8) =2.687$, $p=0.0276$).

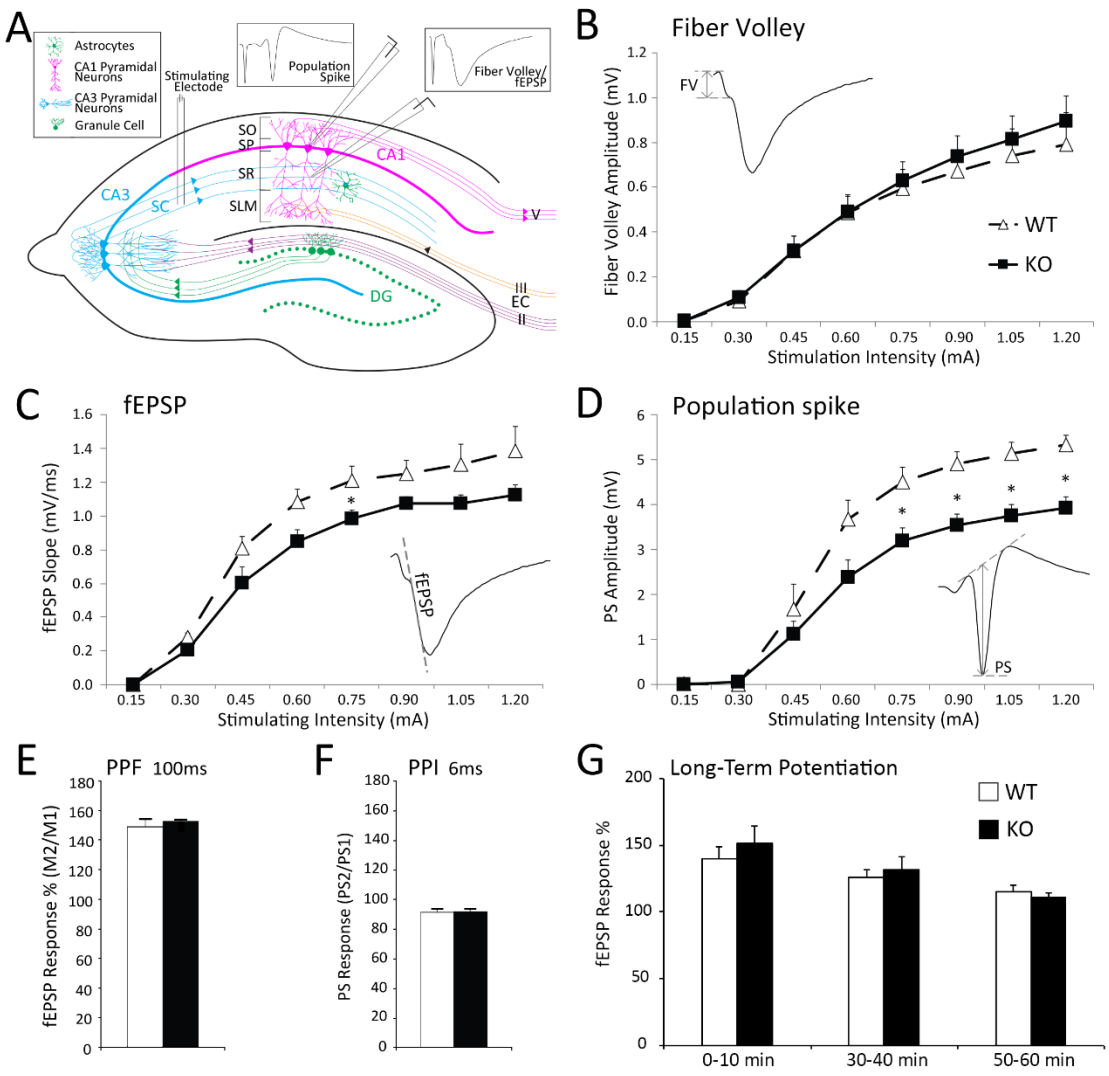
A
Astrocytes
CA1 Pyramidal Neurons
CA3 Pyramidal Neurons
Granule Cell
Stimulating Electode
Population Spike
Fiber Volley/ fEPSP
SO
SP
SR
SLM
CA1
CA3
SC
DG
V
III
EC
II
B
Fiber Volley
FV
Fiber Volley Amplitude (mV)
WT
KO
Stimulation Intensity (mA)
C
fEPSP
fEPSP Slope (mV/ms)
fEPSP
Stimulating Intensity (mA)
D
Population spike
PS Amplitude (mV)
PS
Stimulating Intensity (mA)
E
PPF 100ms
fEPSP Response % (M2/M1)
F
PPI 6ms
PS Response (PS2/PS1)
G
Long-Term Potentiation
WT
KO
fEPSP Response %
0-10 min
30-40 min
50-60 min

Figure 3.3 Functional synaptic changes in CA1 hippocampal neurons of astrocyte-specific ephrin-B1 KO adult mice. (A) Schematics of hippocampal circuit showing the placement of electrodes for extracellular stimulation and field potential recordings with the examples of stereotypical responses after stimulation. (B-D) Input-output curves were generated by plotting the amplitude of fiber volley (FV) presynaptic responses (B), fEPSP slope for postsynaptic dendritic responses (C), and population spike (PS) amplitude for postsynaptic neuronal responses (D) of CA1 hippocampal neurons as a function of the stimulation intensity of Schaffer collaterals in acute hippocampal slices from WT and KO adult mice. (B) There were no significant differences in pre-synaptic responses between the groups (n=6-8 mice, genotype × stimulation intensity interaction, $F(1, 112) = 1.072$, $p=0.3027$, two-way ANOVA followed by Bonferroni post-test). (C) Overall, fEPSP slope was not significantly different in KO animals compared to WT+TAM group with a trend towards lower fEPSPs in KO group (n=6-8 mice, genotype × stimulation intensity interaction, $F(18, 153) = 1.057$, $p=0.4007$, two-way ANOVA followed by Bonferroni post-test). (D) Population spike amplitude was significantly reduced in KO+TAM mice as compared to WT mice (n=6-8 mice, genotype × stimulation intensity interaction, $F(9, 99) = 4.882$, $p<0.001$, two-way ANOVA followed by Bonferroni post-test; *$p<0.05$). (E) Graph shows that fEPSP responses were facilitated following the second stimulus as compared to first stimulus at 100 ms stimulation interval in both WT and KO mice with no differences in PPF between the groups. Graphs show mean values and error bars represent SEM (n=6-8 mice, student's t-test). (F) Graph shows that the changes in PS amplitude between first and second stimulus at 6 ms stimulation interval were not significantly different between WT and KO groups. Graphs show mean values and error bars represent SEM (n=6-8 mice, student's t-test). (G) Graph shows that the potentiation was maintained 50-60 min after LTP induction in both WT and KO groups with no differences between the groups. Graph shows mean values and error bars represent SEM (n=6-8 mice, student's t-test).

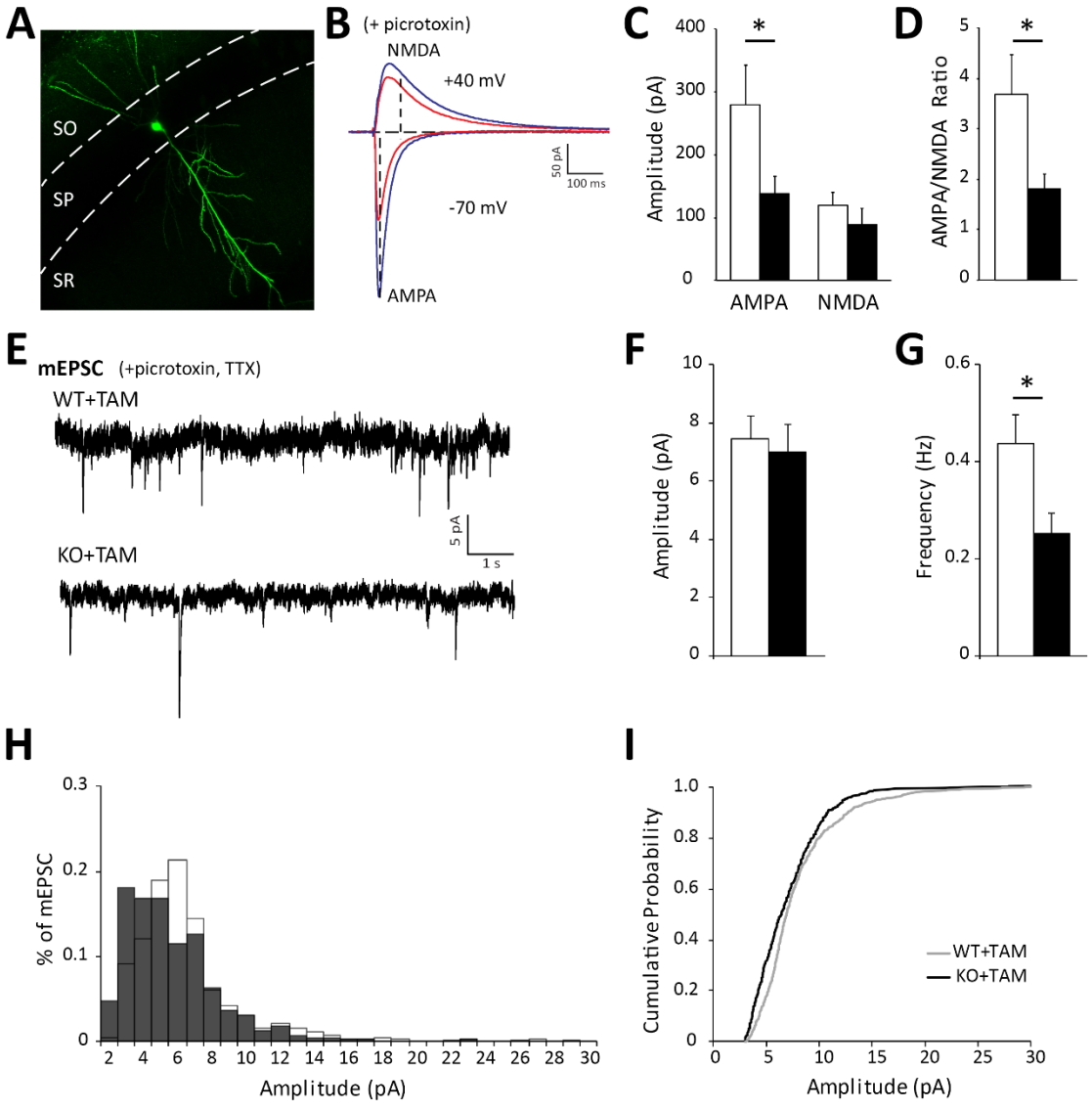
A
SO
SP
SR
B
(+ picrotoxin)
NMDA
+40 mV
50 pA
100 ms
-70 mV
AMPA
C
Amplitude (pA)
400
300
200
100
0
*
AMPA
NMDA
D
AMPA/NMDA Ratio
5
4
3
2
1
0
*
E
mEPSC (+picrotoxin, TTX)
WT+TAM
5 pA
1 s
KO+TAM
F
Amplitude (pA)
10
8
6
4
2
0
G
Frequency (Hz)
0.6
0.4
0.2
0
*
H
% of mEPSC
0.3
0.2
0.1
0
2 4 6 8 10 12 14 16 18 20 22 24 26 28 30
Amplitude (pA)
I
Cumulative Probability
1.0
0.8
0.6
0.4
0.2
0
0 5 10 15 20 25 30
Amplitude (pA)
WT+TAM
KO+TAM

Figure 3.4 Loss of astrocytic ephrin-B1 results in functionally immature excitatory synapses. (A) Whole cell recordings were performed by blind cell patching of pyramidal cells in the CA1 hippocampus (example of biocytin filled neuron). (B) Representative traces from whole-cell voltage-clamp recordings showing AMPAR- and NMDAR-mediated currents recorded in CA1 pyramidal neurons from adult WT (blue) and KO (red). (C, D) Amplitude and corresponding ratio of evoked AMPAR- and NMDAR-mediated currents (n=14-17 cells, 9-10 mice). Evoked AMPAR-mediated currents were significantly reduced in adult KO mice. (E) Representative 30s traces of mESPC in adult WT and KO; recorded in TTX and picrotoxin (n=6 mice). (F, G) Graphs show average amplitude (F) and average frequency (G) in WT and KO mice. (H) Distribution of mEPSC amplitudes between WT and KO mice (I) Cumulative probability curve of mEPSC amplitude in WT and KO mice. Error bars represent SEM; *$p<0.05$.

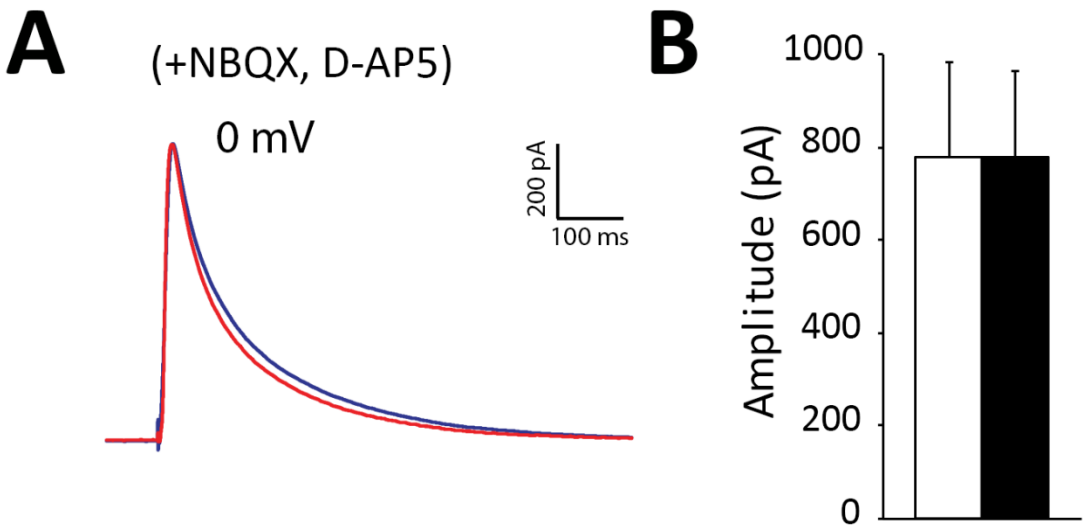

Figure 3.5 Astrocytic ephrin-B1 does not affect inhibitory synapses on hippocampal pyramidal CA1 neurons. (A) Representative traces showing evoked IPSCs recorded in CA1 pyramidal neurons from adult WT (blue) and KO (red). (B) Graph shows average amplitude of evoked IPSCs; KO mice had comparable evoked IPSC amplitude to WT mice, indicating astrocytic ephrin-B1 may not affect the functionality of inhibitory synapses (n=13-14 cells, 6 mice). Error bars represent SEM; *p<0.05.

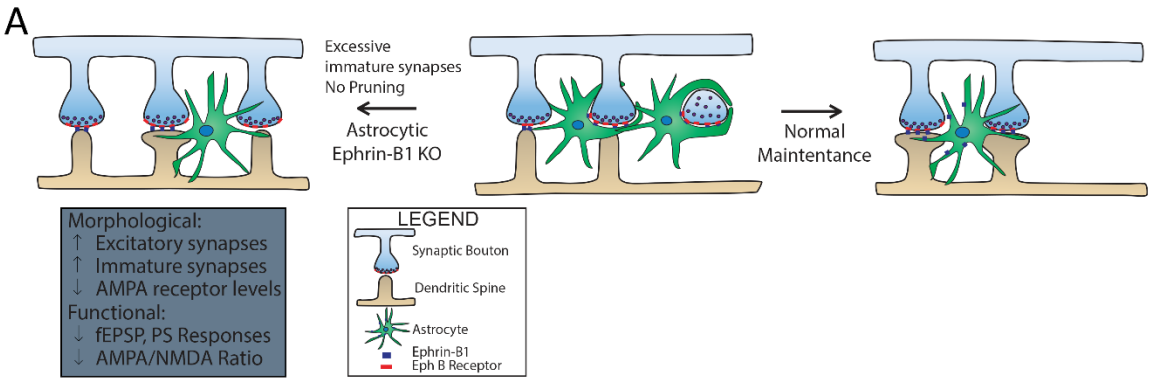

Figure 3.6 Astrocytic ephrin-B1 is a negative regulator of excitatory synapse formation. (A) Model detailing normal maintenance and loss of astrocytic ephrin-B1 during adulthood on formation of excitatory synapses. During normal maintenance, astrocytic ephrin-B1 is a negative regulator of synapse formation; astrocytic ephrin-B1 may be contacting unnecessary synapses and pruning these synapses away. Loss of astrocytic ephrin-B1 results in increased formation of immature synapses, resulting in reduced excitatory responses.

Table 3.1 Electrophysiological characteristics of CA1 hippocampal neurons in ERT2-Cre^{GFAP} and ERT2-Cre^{GFAP}ephrin-B1$^{flox/y}$ mice treated with tamoxifen. Table contains mean values and SEM of input-output curve. FV: F(1, 112) = 1.072, p=0.3027; EPSP: F(18, 153) = 1.057, p=0.4007; PS: F(9, 99) = 4.882, p<0.001, two-way ANOVA followed by Bonferroni multiple-comparison post-test; n = 6-8 mice.

Input-Output

	WT			**KO**		
SI (mA)	**FV (mV)**	**EPSP (ms/mV)**	**PS (mV)**	**FV (mV)**	**EPSP (ms/mV)**	**PS (mV)**
0.15	0.00 ± 0.00	0.00 ± 0.00	0.00 ± 0.00	0.00 ± 0.00	0.00 ± 0.00	0.00 ± 0.00
0.30	0.09 ± 0.01	0.28 ± 0.03	0.00 ± 0.00	0.11 ± 0.03	0.21 ± 0.5	0.04 ± 0.03
0.45	0.31 ± 0.03	0.81 ± 0.07	1.67 ± 0.56	0.31 ± 0.07	0.60 ± 0.10	1.11 ± 0.30
0.60	0.49 ± 0.04	1.09 ± 0.07	3.67 ± 0.43	0.49 ± 0.08	0.85 ± 0.07	2.38 ± 0.39
0.75	0.59 ± 0.05	1.21 ± 0.08	4.50 ± 0.34	0.63 ± 0.08	**0.99 ± 0.05***	**3.18 ± 0.31***
0.90	0.67 ± 0.05	1.25 ± 0.08	4.91 ± 0.27	0.74 ± 0.09	1.07 ± 0.04	**3.55 ± 0.25***
1.05	0.74 ± 0.05	1.31 ± 0.12	5.14 ± 0.25	0.81 ± 0.10	1.07 ± 0.05	**3.75 ± 0.26***
1.20	0.79 ± 0.05	1.39 ± 0.14	5.34 ± 0.20	0.90 ± 0.11	0.13 ± 0.06	**3.93 ± 0.26***

***p<0.05** depicts significance changes between WT and KO groups

Chapter 4 : Astrocytic ephrin-B1 regulates synapse formation during learning and memory

Abstract

Astrocytes play a fundamental role in synapse formation, pruning and plasticity, which are associated with learning and memory. However, the role of astrocytes in learning and memory is still largely unknown. Previous studies in the lab have showed that astrocyte-specific ephrin-B1 knock-out (KO) enhanced but ephrin-B1 overexpression (OE) in hippocampal astrocytes impaired contextual memory recall following fear conditioning. The goal of this study was to understand the mechanism by which astrocytic ephrin-B1influences learning; specifically, learning-induced remodeling of synapses and dendritic spines in the CA1 hippocampus using fear-conditioning paradigm. While I found a higher dendritic spine density and clustering on c-Fos-positive (+) neurons activated during contextual memory recall in both wild-type (WT) and KO mice, overall spine density and mEPSC amplitude were increased in CA1 neurons of KO compared to WT. In contrast, ephrin-B1 overexpression in hippocampal astrocytes impaired dendritic spine formation and clustering, specifically on c-Fos(+) neurons, coinciding with an overall decrease in vGlut1/PSD95 co-localization. Although astrocytic ephrin-B1 influenced learning-induced spine formation, the changes in astrocytic ephrin-B1 levels did not affect spine enlargement as no genotype differences in spine volume were observed between trained WT, KO and OE groups. My results suggest that a reduced formation of new spines rather than spine maturation in activated CA1 hippocampal neurons is most likely responsible for impaired contextual learning in OE mice due to abundantly high ephrin-B1 levels in astrocytes. The ability of astrocytic ephrin-B1 negatively influence new spine formation during learning can potentially

regulate new synapse formation at specific dendritic domains and underlie memory encoding.

4.1 Introduction

Hippocampal circuits are known for their plastic nature and play an important role in the formation of new memories and life-long learning (Milner et al., 1998; Neves et al., 2008). Contextual fear learning and retrieval relies on the hippocampus, particularly the CA1 region. This hippocampal-dependent learning requires activation of CA1 pyramidal neurons (Strekalova et al., 2003; Goshen et al., 2011), and promotes the growth and maturation of hippocampal synapses. Indeed, maturation of dendritic spines has been shown to be activity dependent, allowing for the recruitment of AMPARs and an increase in spine volume (Matsuo et al., 2008). In addition to promoting synapse maturation, experience has also been shown to modify hippocampal circuits through selective formation or removal of synapses (Lichtman and Colman, 2000; Draft and Lichtman, 2009; Holtmaat and Svoboda, 2009; Sala and Segal, 2014; Segal, 2017). Therefore, experience and learning can profoundly impact spine turnover rates (Yang et al., 2008; Holtmaat and Svoboda, 2009; Fu et al., 2012; Lai et al., 2012; Sala and Segal, 2014; Segal, 2017). Additionally, learning-induced spine changes are associated with selective spine clustering and formation of "hot spots" on dendrites (Fu et al., 2012; Frank et al., 2018; Lai et al., 2018), which are suggested to allow for efficient storage of information (Hayashi-Takagi et al., 2015; Frank et al., 2018). Most research has focused on neuron-neuron interactions; however, little is known about astrocyte-derived signals that regulate the synaptic remodeling during learning and memory.

Astrocytes play a critical role in maintaining, supporting, and directly modulating neuronal activity and function. Astrocytic processes encapsulate synapses allowing for

astrocytes to communicate with neurons. The interactions between astrocytes and synapses can regulate synaptogenesis and pruning, synaptic transmission and plasticity (Araque et al., 1999; Clarke and Barres, 2013; Chung et al., 2015; Allen and Eroglu, 2017). As these synaptic changes underlie the acquisition, retention, and retrieval of memory, astrocytes are well positioned to influence learning and memory (Nishiyama et al., 2002; Newman et al., 2011; Suzuki et al., 2011; Tadi et al., 2015; Gao et al., 2016; Adamsky et al., 2018). Activation of hippocampal astrocytes was recently suggested to enhance synaptic potentiation and acquisition of contextual fear memory (Adamsky et al., 2018). Astrocytes are also shown to regulate synapse formation, recruitment of AMPARs, and modulating synaptic functions through the release of gliotransmitters, such as glutamate (Fellin et al., 2004), thrombospondin (Christopherson et al., 2005), glypican (Allen et al., 2012), D-serine (Henneberger et al., 2010), and lactate (Alberini et al., 2018). Besides gliotransmission, astrocytes can communicate and affect synaptic functions through contact-mediated factors. Astrocytic contacts with neurons can direct synaptogenesis (Hama et al., 2004; Garrett and Weiner, 2009) and synapse elimination (Chung et al., 2013), which may allow for the refinement of memories.

Trans-synaptic Eph/ephrin-B interactions promote postsynaptic dendritic spine formation and maturation during development (Henderson et al., 2001; Henkemeyer et al., 2003; Kayser et al., 2006) and high levels of EphB receptors and ephrins are retained in the adult hippocampus (Grunwald et al., 2001; Liebl et al., 2003). Furthermore, the loss of EphA4 and EphB2 receptors are reported to affect associative memory in mice (Gerlai et al., 1999; Halladay et al., 2004; Willi et al., 2012; Dines et al., 2015).

Interestingly, EphB2 loss affects both short and long-term contextual fear conditioning memory formation, but only long-term memory depends on EphB2 forward signaling (Dines et al., 2015). Disruption of ephrin-B reverse signaling in neurons was also implicated in impaired hippocampal-dependent learning and memory in EphB2 KO mice (Grunwald et al., 2001). In addition, ephrin-B2 expression is upregulated in CA1 neurons but not the cortex or amygdala following fear conditioning without changes in levels of EphA4 receptor (Trabalza et al., 2012). While ephrin-B2 can activate both EphA4 and EphB receptors, ephrin-B1 is known for its high affinity for EphB but not EphA4 receptors. Deletion of neuronal ephrin-B1 was also responsible for impaired contextual recall in ephrin-B1 KO mice following fear conditioning (Arvanitis et al., 2014). Mutations in the *efnb1 gene* that encodes ephrin-B1 are associated with CranioFrontalNasal Syndrome, characterized by hypertelorism, frontonasal dysplasia, coronal craniosynostosis and mild learning disability (Twigg et al., 2004; Wieland et al., 2004). However, little is known about the role of astrocytic ephrin-B1. It was previously reported that deletion and overexpression of astrocytic ephrin-B1 in the adult CA1 hippocampus affects contextual memory (Koeppen et al., 2018), but the mechanism is still not clear.

My new findings suggest that astrocytic ephrin-B1 influences hippocampal-dependent contextual memory by regulating new dendritic spine formation and clustering on hippocampal neurons activated during memory recall, without affecting spine maturation. While I found that both wild type (WT) and astrocytic ephrin-B1 knock-out (KO) mice showed a significant increase in dendritic spine density and clustering on

activated c-Fos(+) neurons as compared to c-Fos(-) neurons following contextual recall, dendritic spine density remained higher in trained KO compared to WT, which coincided with a greater vGlut1/PSD95 co-localization and enhanced excitatory postsynaptic currents (EPSCs) in CA1 neurons of KO mice. In contrast, astrocytic ephrin-B1 overexpressing (OE) mice showed no increase in dendritic spine density and clustering on c-Fos(+) neurons compared to c-Fos(-) neurons, which coincided with an overall decrease in vGlut1/PSD95 co-localization. However, changes of ephrin-B1 levels in astrocytes did not affect spine enlargement, as no genotype differences in spine volume were observed between trained WT, KO and OE groups. My results suggest that the deficits in dendritic spine formation and clustering, but not spine maturation, may underlie impaired contextual memory recall in OE mice. These studies implicate astrocytic ephrin-B1 as a negative regulator of synapse formation in the activated hippocampal neurons during learning, which can influence contextual memory. Future studies will determine whether activity-dependent up-regulation or down-regulation of ephrin-B1 levels in selective astrocytes controls addition or removal of synapses on specific neurons or dendrites, which may potentially underlie memory encoding.

4.2 Materials & Methods

4.2.1 Mice

All animal care protocols and procedures were approved by the UC Riverside Animal Care & Use Program and done according to NIH and Institutional Animal Care and Use Committee guidelines; animal welfare assurance number A3439-01 is on file

with the Office of Laboratory Animal Welfare (OLAW). Mice were maintained in an AAALAC accredited facility under 12-h light/dark cycle and fed standard mouse chow. ERT2-Cre^{GFAP} male mice (B6.Cg-Tg(*GFAP*-cre/ERT2)505Fmv/J, RRID: IMSR_JAX:012849) were crossed with *ephrin-B1*$^{flox/+}$ female mice (129S-*Efnb1*^{tm1Sor}/J, RRID: IMSR_JAX:007664) to obtain ERT2-Cre^{GFAP}*ephrin-B1*$^{flox/y}$ (KO) or ERT2-Cre^{GFAP}*ephrin-B1*$^{+/y}$ (WT) male mice. Postnatal day (P) 70-90 adult WT and KO littermates received intraperitoneal (IP) injection of tamoxifen (TAM) (1 mg in 5 mg/ml of 1:9 ethanol/sunflower seed oil solution) once a day for 7 consecutive days. There were no detectable changes in ephrin-B1 levels in astrocytes or neurons of tamoxifen-injected WT mice (not shown). In tamoxifen-treated KO mice, ephrin-B1 immunoreactivity was observed only in neuronal cell bodies and dendrites of the CA1 hippocampus, but was significantly reduced by three fold in hippocampal astrocytes as previously reported (Nikolakopoulou et al., 2016; Koeppen et al., 2018). Genotypes were confirmed by PCR analysis of genomic DNA isolated from mouse tails.

4.2.2 Stereotaxic Microinjections

Expression of ephrin-B1 and tdTomato was induced in hippocampal astrocytes via adeno-associated viruses (AAV7) containing *AAV7.GfaABC1D.ephrin-B1.SV40* (AAV-ephrin-B1; viral titer at 7.56 X 10^{12} viral particles/ml) or *AAV7.GfaABC1D.tdTomato.SV40* (AAV-tdTomato; viral titer at 4.46 X 10^{12} viral particles/ml), respectively (both obtained from UPenn Vector Core, http://www.med.upenn.edu/gtp/vectorcore). Viral particles (VP) were concentrated with

Amicon ultra-0.5 centrifugal filter (UFC505024, Sigma-Aldrich), which was pretreated with 0.1% Pluronic F-68 non-ionic surfactant (24040032, Thermo Fisher). Mice were anesthetized with IP injections of ketamine/xylazine mix (80 mg/kg ketamine and 10 mg/kg xylazine). To ensure for adequate anesthesia, paw pad pinch test, respiratory rhythm, righting reflex, and/or loss of corneal reflex were assessed. Adult P70-90 Thy1-EGFP mice (RRID: IMSR_JAX: 007788) received craniotomies (1 mm in diameter) and VPs were stereotaxic injected into the dorsal hippocampus (2.5 mm posterior to bregma, 1.0 mm lateral to midline, and 1.2 mm from the pial surface). Control mice were bilaterally injected with 2 µl of 1.16 X 10^{13} VP/ml AAV-tdTomato, and experimental animals received bilateral injection of 1 µl of 3.78 X 10^{13} VP/ml AAV-ephrin-B1 + 1 µl of 2.32 X 10^{13} VP/ml AAV-tdTomato. Post-surgery, mice received 0.3 ml of buprenorphine by subcutaneous injection every 8 h for 48 h, as needed for pain. Animals were allowed to recover for 14 days prior to fear conditioning tests and/or immunohistochemistry. There was a significant four-fold increase in ephrin-B1 immunoreactivity in CA1 hippocampal astrocytes of mice injected with AAV-ephrin-B1 + tdTomato (OE) compared to AAV-tdTomato (WT) as previously reported (Koeppen et al., 2018). Mice showing bilateral hippocampal tdTomato expression were used for the analysis.

4.2.3 Fear Conditioning

A fear-conditioning paradigm was used to assess hippocampal dependent contextual learning as previously described (Anagnostaras et al., 2001; Koeppen et al.,

2018). Two contexts were used to test contextual memory. Context A was an 18 X 18 cm rectangular clear plexiglass box with 16-grated steel bar flooring; trials in context A were in white light and the scent of Quatricide TB. Context B was in a cylinder with a diameter of 15 cm and a height of 20 cm with 2.5 X 2.5 cm, with checkered black and white walls; trials in context B were in altered light with fresh litter and the scent of Windex. Animals were allowed to acclimate in the behavioral room for 30 min before each testing day and handled for 2 min for 5 days prior to testing. On day one, the test mouse was placed in context A and habituated to the chamber for 10 min, 1 h after context A mice were habituated to context B for 10 min. The mouse was removed and separated from its home cage until all mice in that cage were habituated to both contexts. On day two, test mice were trained to associate an unconditioned stimulus (US; 0.6 mA scrambled foot shock) with a conditioned stimulus (CS; 9 kHz, 70 dB tone) in context A. Initially, test mice were placed in context A and given 3 minutes for habituation, then followed by a 30 s tone (CS), which co-terminated with a 2 s foot shock (US). The CS-US pairing occurred five times, with a pseudorandom interval between pairings. The test mouse, again, was removed and separated from its home cage until all mice in that cage were trained. On day three, animals were tested for their associated memory of the context (in context A) and of the CS tone (in context B). For contextual recall, mice were placed in context A for 5 min with no sound and returned to home cage for 1 h before testing context B. For tone recall test, mice were placed in context B for a total of 6 min, with the CS tone playing for the final 3 min. Control mice were taken directly from their home cage in the vivarium and immediately perfused and did not undergo the fear conditioning paradigm.

For dendritic spine analysis and immunohistochemistry, 3-4 animals were euthanized and perfused 1 h after context A contextual recall only. Animals undergoing both context A and context B recall were euthanized and perfused 1 h after context B tone recall. Freezing behavior was measured as a percentage of time freezing using TopScan Software. GraphPad Prism 6 software (RRID: SCR_002798) was used to perform a one-way ANOVA followed by Tukey's post hoc analysis or t-test when appropriate, data represent mean ± SEM.

4.2.4 Immunohistochemistry

Animals were anesthetized with isoflurane and transcardially perfused first with 0.9% NaCl, followed by fixation with 4% paraformaldehyde (PFA) in 0.1 M phosphate-buffered saline (PBS), pH 7.4. Brains were post-fixed overnight with 4% PFA in 0.1 M PBS and sectioned into 100 µm coronal slices with a vibratome. Excitatory presynaptic boutons were labeled by immunostaining against vesicular glutamate transporter 1 (vGlut1) using rabbit anti-vGlut1 antibody (0.25 mg/ml, Invitrogen Cat# 482400, RRID: AB_2533843), postsynaptic sites were identified with mouse anti-postsynaptic density-95 (PSD95) antibody (1.65 µg/ml, Invitrogen Cat# MA1-045, RRID: AB_325399). Inhibitory sites were detected with mouse anti-glutamic acid decarboxylase 65 (GAD65) antibody (10 µg/ml, BD Pharmingen Cat# 559931, RRID: AB_397380). Parvalbumin (PV)-positive cells were identified with mouse anti-PV antibody (6 µg/ml, Sigma-Aldrich Cat# P3088, RRID: AB 477329). Activated neurons were detected with anti-c-Fos antibodies (40 µg/ml, Invitrogen Cat# PA1-37437, RRID: AB_1073599). The secondary

antibodies used were Alexa Fluor 594-conjugated donkey anti-mouse IgG (4 mg/ml, Molecular Probes Cat# A-21203, RRID: AB_141633), Alexa Fluor 647-conjugated donkey anti-rabbit IgG (4 mg/ml, Molecular Probes Cat# A-31573, RRID: AB_2536183), Alexa Fluor 647-conjugated donkey anti-goat IgG (4 mg/ml, Molecular Probes Cat# A-21447, RRID: AB_141844), or Alexa Fluor 488-conjugated donkey anti-goat IgG (4 mg/ml, Molecular Probes Cat# A-11055, RRID: AB_2534102). Sections were mounted on slides with Vectashield mounting medium containing DAPI (Vector Laboratories Inc. Cat# H-1200, RRID: AB_2336790).

4.2.5 Dendritic Spine Analysis

Dendritic spines were identified with GFP using transgenic Thy1-GFP-M mice (Tg(Thy1-EGFP)MJrs/J, RRID: IMSR_JAX:007788) for ephrin-B1 OE condition and Diolistic approach (Henkemeyer et al., 2003) in ephrin-B1 KO mice. Animals were anesthetized with isoflurane and transcardially perfused initially with 0.9% NaCl, followed by fixation with 4% PFA in 0.1 M PBS, pH 7.4. Brains were post-fixed for 2 h in 4% PFA in 0.1 M PBS, and 100 μm coronal sections were cut with a vibratome. Dendritic spines were labeled in ephrin-B1 KO mice and their WT counterparts using a DiOlistic approach (Henkemeyer et al., 2003) using fluorescent lipophilic dye 1,1'-dioctadecyl-3,3,3',3'-tetramethyl-indocarbocyanine perchlorate (DiO, D3898, Molecular Probes) coating tungsten particles. DiO was delivered by helium-powered ejection (Bio-Rad Helios Gene Gun System) into hippocampal slices and incubated in 0.1 M PBS for 72 h. CA1 hippocampal neurons were imaged using LSM 880 Airyscan Carl Zeiss

confocal microscope. 10-15 DiO-labeled or GFP-expressing neurons were randomly selected per group, and dendrites were imaged using a 63x objective (1.2 NA), 1x zoom. Three-dimensional fluorescent images were created by the projection of each z-stack containing 50-100 high-resolution optical serial sections (1,024 x 1,024-pixel format) taken at 0.5 µm intervals in the X-Y plane. Quantifications of the spine density (spines per 10 µm dendrite), lengths (µm), volumes (μm^3), and interspine intervals were carried out using Neurolucida 360 software (MicroBrightField RRID: SCR_001775). There was an overall higher density of spines in DiO-labeled compared to GFP expressing WT neurons, which was most likely due to a better detection of smaller spines with membrane dye DiO than GFP. There were about 60-70% of smaller spines in DiO labeled WT neurons compared to 50-55% of smaller spines in GFP-expressing WT neurons (Table 1). Therefore, comparisons were made only between DiO-expressing WT and KO groups or GFP-expressing WT and OE groups. Statistical analysis was performed with two-way ANOVA followed by Bonferroni's post-hoc analysis using GraphPad Prism 6 software (GraphPad Prism, RRID: SCR_002798), data represent mean ± SEM.

4.2.6 Electrophysiology

Brain slices were obtained from trained adult mice (P90-110) 1 h after recall test. Animals were deeply anesthetized with isoflurane and decapitated. Mouse brains were rapidly removed and immersed in ice-cold "slushy buffer" with high Mg^{2+} and sucrose concentration containing the following (in mM): 87 NaCl, 75 sucrose, 2.5 KCl, 0.5

$CaCl_2$, 7 $MgCl_2$, 1.25 NaH_2PO_4, 25 $NaHCO_3$, 10 glucose, 1.3 ascorbic, acid, 0.1 kynurenic acid, 2.0 pyruvate, and 3.5 MOPS with a pH of 7.4 and saturated with 95% O_2/5% CO_2. Transverse hippocampal slices (350 μm) were prepared by using a vibrating blade microtome (Campden 5100mz-Plus, Campden Instruments Ltd.) and transferred into a holding chamber containing oxygenated ACSF (in mM; 125 NaCl, 2.5 KCl, 2.5 CaCl2, 1.3 MgCl2, 1.25 NaH2PO4, 26 NaHCO3, 15 glucose 3.5 MOPS with a pH of 7.4) for 1 h at 33°C. Slices were then transferred to a submersion recording chamber continually perfused with oxygenated ACSF at a flow rate of 1 ml/min. Slices were allowed to equilibrate for approximately 10 min to reach a stable baseline response prior to running experimental protocols.

Blind whole-cell patch experiments was performed as described (Castaneda-Castellanos et al., 2006). Tight-seal whole-cell voltage clamp recordings were obtained using pipettes made from borosilicate glass capillaries pulled on a Narishige PC-10 vertical micropipette puller (Narishige, Tokyo, Japan). Pipette resistance ranged from 3 to 4 MΩ, filled with an internal solution containing (in mM) 130 CsOH, 130 D-gluconic acid, 0.2 EGTA, 2 $MgCl_2$, 6 CsCl, 10 Hepes, 2.5 ATP-Na, 0.5 GTP-Na, 10 phosphocreatine and 0.1% Biocytin for cellular post labeling, pH adjusted to 7.2-7.3 with CsOH, osmolarity adjusted to 300-305 mOsm with ATP-Na. The series resistance was <25 MΩ and was compensated, if the series resistance changed more than 20% during the course of an experiment, the data was discarded. For evoked EPSCs and IPSCs, electrical stimuli (0.1 Hz) were delivered through a bipolar, Teflon®-coated tungsten electrode placed in the SR region and close proximity to the recording electrode. Neurons were

voltage-clamped at either -70 mV to measure AMPAR evoked responses or +40 mV to measure NMDA receptor evoked responses. 1 µM tetrodotoxin was added to isolate mEPSC responses. All excitatory postsynaptic currents (EPSCs) were recorded in the presence of 50 µM picrotoxin, a $GABA_A$ receptor antagonist, to block $GABA_A$-mediated currents at 33˚C. To measure inhibitory postsynaptic currents (IPSCs), neurons were voltage-clamped at 0 mV with 10 µM NBQX, an AMPA receptor antagonist, and 50 µM D-AP5, a NMDA receptor antagonist at 33˚C. EPSCs and IPSCs were recorded using an EPC-9 amplifier (HEKA Elektronik, Lambrecht, Germany), filtered at 1 kHz, digitized at 10 kHz, and stored on a personal computer using pClamp 10.7 software (Molecular Device) to run analysis. AMPA, NMDA-mediated EPSCs, IPSCs evoked responses, and mEPSCs were analyzed by Clampfit 10.7 software (Molecular Device). All averaged data were presented as means ± SEM. Statistical significance was determined by the Student's t-test using Prism 7.0 software (Graph Pad Software, Avenida, CA).

4.3 Results

It was previously reported that the loss of astrocytic ephrin-B1 in adult mice resulted in enhanced contextual recall, while overexpression of astrocytic ephrin-B1 in the adult hippocampus impaired contextual memory recall (Koeppen et al., 2018). The goal of this study was to understand the mechanism by which astrocytic ephrin-B1 affects contextual fear conditioning memory, in particular how the deletion or overexpression of astrocytic ephrin-B1 affects remodeling of synapses and dendritic spines in the CA1 hippocampus following contextual learning. To accomplish this, astrocyte-specific

ephrin-B1 KO and ephrin-B1 OE mice, with corresponding WT counterparts, were trained in a fear condition paradigm to associate a context with an electric shock. Next day, the mice were placed in context A, in which they were trained, and their freezing was evaluated as a measure of contextual memory (Fig. 4.1). Dendritic spine clustering and neuronal activity were analyzed in the CA1 hippocampus of these mice 1 h after contextual memory recall. As specific memories are encoded in a sub-set of hippocampal neurons (Liu et al., 2012; Tonegawa et al., 2015), dendritic spine changes in CA1 hippocampal pyramidal neurons were further analyzed by identifying activated (c-Fos+) or not activated (c-Fos-) cells during contextual memory recall (Fig. 4.2).

Increased spine clustering is observed on c-Fos+ neurons in WT and KO mice, but not OE mice

It has been reported that spine density is significantly higher in trained KO compared to WT (Nguyen et al., 2019). To examine the effects of ephrin-B1 deletion in adult hippocampal astrocytes on remodeling of dendritic spines following contextual learning, coronal hippocampal sections were collected from WT and KO mice 1 h following contextual recall. Immunostaining was used against early immediate *gene c-fos* to identify CA1 neurons that were activated during memory recall. Dendritic spines were labeled with DiO to visualize dendritic spines in both c-Fos(+) and c-Fos(-) neurons. Interestingly, in addition to the effect of genotype further analysis showed a significant increase in the spine density on c-Fos(+) neurons as compared to c-Fos(-) neurons in KO. When spine morphology was analyzed, c-Fos(+) neurons in both WT and KO mice also

showed a significant decrease in smaller spines and an increase in larger spines (> 1.0 μm^3) with no effect of genotype. In addition, there was a small effect of training on spine length in c-Fos(+) neurons of WT mice with no effect of genotype. Overall higher spine density in KO compared to WT mice may explain enhanced contextual recall in KO (Fig. 4.1E, t-test $p<0.05$). The results suggest that increased number of dendritic spines may underlie enhanced contextual memory in astrocyte-specific ephrin-B1 KO mice. While new spine maturation is observed on c-Fos(+) neurons in both WT and KO mice, dendritic spine density remains higher in KO compared to WT mice.

Conversely, no significant differences were observed in overall spine density between trained OE and WT mice (Nguyen et al., 2019). To determine the effects of ephrin-B1 overexpression in adult hippocampal astrocytes on dendritic spine formation following contextual learning, coronal hippocampal sections were collected 1 h following contextual recall from Thy1-GFP mice containing hippocampal astrocytes expressing tdTomato (WT) or tdTomato with ephrin-B1 (ephrin-B1 OE). Immunostaining against early immediate *c-fos gene* to identify CA1 neurons that were activated during memory recall. Dendritic spines were visualized with GFP in both c-Fos(+) and c-Fos(-) neurons and astrocytes expressed td-Tomato. Further analysis showed a significantly higher spine density on c-Fos(+) neurons compared to c-Fos(-) neurons in trained WT but not OE mice. The impaired increase in spine density on c-Fos(+) neurons compared to c-Fos(-) neurons in OE mice may explain impaired contextual recall in OE mice (Fig. 4.1K, t-test $p<0.05$). In addition, a decreased proportion of smaller spines and an increased number of larger spines was seen on c-Fos(+) neurons compared to c-Fos(-) neurons, but there was

no genotype difference. No significant differences were also seen between trained WT and OE mice in synaptic GluA1 (Nguyen, et al., 2019). Taken together the results suggest that reduced spine density and impaired formation of spines on c-Fos+ CA1 hippocampal neurons may underlie the deficits in contextual recall in astrocyte-specific ephrin-B1 OE mice without affecting dendritic spine maturation.

To examine if new spines were added in a close proximity of neighboring spines, I analyzed interspine intervals (distances between neighboring spines) on c-Fos(+) and c-Fos(-) CA1 neurons in WT mice. As expected, I observed an overall reduction in interspine intervals between neighboring spines in c-Fos(+) neurons compared to c-Fos(-) neurons due to an increase in spine density. However, spines were not distributed uniformly as I found a specific increase in the percentage of spines with interspine interval less than 2.0 µm (which is a distance from the neighboring spine) on c-Fos(+) neurons compared to c-Fos(-) neurons (Suppl. Fig. 4B; WT c-Fos-: 50.91 ± 1.65 vs WT c-Fos+: 56.58 ± 1.00, $t_{(10)}$= 2.766 p = 0.019, t test). I further analyzed clusters of these spines that were less than 2.0 µm from each other in c-Fos(+) and c-Fos(-) neurons. There was an overall higher number of smaller spine clusters containing 3 spines in both c-Fos(+) and c-Fos(-) neurons (Fig. 4B; two-way ANOVA cluster size $F_{(4, 50)}$ = 69.19, p<0.0001). I also observed a significant increase in the number of the spine clusters on c-Fos(+) CA1 neurons compared to c-Fos(-) neurons in WT (Fig. 4B; two-way ANOVA; $F_{c\text{-}Fos}$ (1, 50) = 6.698, p = 0.0126), in particular smaller clusters containing 3 spines (WT c-Fos- (3): 3.42 ± 0.50 vs WT c-Fos+ (3): 4.59 ± 0.34; Bonferroni's post-hoc test, *p < 0.05). This suggests that spine formation occurs at specific locations, in a close proximity

to neighboring spines, on the dendrites of c-Fos(+) CA1 neurons activated during contextual recall.

Interestingly, I also observed a significant increase in number of spine clusters in c-Fos(+) neurons compared to c-Fos(-) neurons in ephrin-B1 KO mice (Fig. 4D, two-way ANOVA $F_{c\text{-}Fos}$ (1, 130) = 15.5, $p_{c\text{-}Fos}$ = 0.0001), specifically smaller clusters containing 3 spines (KO c-Fos- (3): 3.00 ± 0.41 vs KO c-Fos+ (3): 5.67 ± 0.80; Bonferroni's post-hoc test, **** $p < 0.0001$). In contrast, I observed no difference in the number of clusters between c-Fos(+) and c-Fos(-) CA1 neurons in ephrin-B1 OE mice (Fig. 4F; two-way ANOVA $F_{c\text{-}Fos}(1, 60) = 0.9948$, $p_{c\text{-}Fos} = 0.3226$). Astrocytic ephrin-B1 may affect up-regulation of dendritic spine density on c-Fos(+) neurons by impacting new spine formation at selective dendritic domains.

Excitatory responses were enhanced in CA1 hippocampal neurons of trained ephrin-B1 KO compared to WT mice

Changes in dendritic spine density may affect neuronal functionality; specifically, an increase in dendritic spine numbers in trained KO compared to WT may indicate an increase in excitatory responses. Whole-cell patch clamp experiments were conducted to determine if CA1 hippocampal pyramidal neurons in trained KO mice also show increased excitatory responses. Indeed, increased evoked excitatory responses were observed in CA1 hippocampal neurons of trained KO mice compared to WT mice by measuring both NMDAR and AMPAR currents (Fig. 4.5B; WT AMPAR: 527.65 ± 30.30 vs KO AMPAR: 713.52 ± 43.33, $t_{(398)} = 3.568$, $p = 0.0004$, *t* test; WT NMDAR: 186.36 ±

13.12; KO NMDAR: 307.43 ± 23.59, $t_{(373)} = 4.610$ $p < 0.0001$, *t* test). Interestingly, AMPAR/NMDAR ratio was not significantly different between trained WT and KO mice (Fig. 4.5C; WT: 2.40 ± 0.60; KO: 2.51 ± 0.48, $t_{(17)} = 0.149$, $p = 0.8829$, *t* test). Increased excitatory post-synaptic strength in trained KO mice was further confirmed by increased mEPSC amplitude (Fig. 4.5D, G, H; WT: 7.02 ± 0.62; KO: 14.08 ± 3.13, $t_{(13)} = 2.462$, $p = 0.0286$, *t* test), whereas no differences were observed in mEPSC frequencies between WT and KO trained mice (Fig 4.5D-F; WT: 0.81 ± 0.14; KO: 0.88 ± 0.29; $t_{(13)} = 0.238$, $p = 0.8157$, *t* test); together this suggests increased postsynaptic responsiveness in trained KO mice compared to WT mice.

4.4 Discussion

Astrocytes are well positioned to influence learning and memory consolidation by influencing dendritic spine formation and maturation in the adult hippocampus, but molecular mechanisms are not clear. My data suggest that astrocytic ephrin-B1 controls learning and memory consolidation during contextual fear conditioning by regulating new dendritic spine formation on activated CA1 hippocampal neurons. First, I found that the deletion of ephrin-B1 in astrocytes enhances learning-induced formation of new dendritic spines on CA1 hippocampal neurons, while its overexpression impairs new synapse formation. Second, ephrin-B1 overexpression in hippocampal astrocytes selectively affects dendritic spine formation and clustering on hippocampal neurons activated during contextual recall. Third, despite the changes to excitatory synapses, deletion or overexpression of ephrin-B1 in astrocytes does not affect the number of

inhibitory synapses in the CA1 hippocampus. Finally, deletion of ephrin-B1 in astrocytes does not affect learning-induced changes in spine volume, as I observed enlargement of dendritic spines in ephrin-B1 KO mice similar to their WT counterparts. My results suggest that the deficits in dendritic spine formation and clustering, but not spine enlargement, in particular on activated CA1 neurons may underlie impaired contextual memory recall in ephrin-B1 OE mice. These studies implicate astrocytic ephrin-B1 as a negative regulator of synapse formation in the hippocampus during learning, which can influence spatial memory.

One major finding of this study is that modulation of ephrin-B1 levels in astrocytes negatively affects the formation of new dendritic spines on activated CA1 hippocampal neurons following learning and contextual recall. Hippocampal excitatory neurons play an integral role in associative memory formation. Activation of CA1 pyramidal neurons is observed during contextual recall in mice (Ji and Maren, 2008). Several studies also report formation of new spines on hippocampal neurons during fear conditioning (Matsuo et al., 2008; Restivo et al., 2009; Giachero et al., 2013; Frank et al., 2018). Indeed, dendritic spines can be considered physical representation of memory (Matsuzaki et al., 2004; Holtmaat and Svoboda, 2009; Kasai et al., 2010). Acquisition of new memories facilitates hippocampal spine formation and spine maturation following contextual fear learning and memory recall, particularly more recent memories (Restivo et al., 2009; Giachero et al., 2013), coinciding with the increased synthesis and recruitment of GluR1 to mature mushroom-type spines in the adult hippocampus (Matsuo et al., 2008). The strong memory trace associated with the fear conditioned response is

consistent with an increase of total number of mature dendritic spines. Conversely, extinction of a fear memory induces spine loss, specifically dendritic spines that were formed during the learning phase (Lai et al., 2018). Further, reconditioning following extinction induces formation of new dendritic spines near the sites of spine formation that were induced during initial fear conditioning (Lai et al., 2018). In this study, I observed an increase in the number of spines on CA1 neurons in trained astrocytes-specific ephrin-B1 KO mice compared to their WT counterparts, suggesting that astrocytic ephrin-B1 may act as a negative regulator of new spine formation in the adult hippocampus during learning. Astrocytic ephrin-B1 may affect new synapse formation during learning by competing with neuronal ephrin-B for binding to neuronal EphB receptors. Loss of several EphB receptors is known to affect synapse and dendritic spine formation in the hippocampus (Ethell et al., 2001; Henkemeyer et al., 2003).

Another finding of this study is that there is a selective formation of new spines on activated CA1 hippocampal neurons in WT mice. These new spines form in a close proximity of neighboring spines resulting in an overall increase in the number of spine clusters containing three spines. This is consistent with the published work showing that there are hotspots or preferential dendritic regions for spine clustering of two or more spines following contextual fear conditioning (Frank et al., 2018). Clustering of dendritic spines with learning have been demonstrated in layer 5 pyramidal neurons of mouse primary motor cortex following motor learning tasks (Fu et al., 2012) and clusters of axon-dendritic contacts were also observed in vestibular systems of barn owl following prism adaptation (McBride et al., 2008). In this study, I see a selective increase in the

number of dendritic spines on activated c-Fos(+) CA1 hippocampal neurons in both WT and KO mice after contextual fear conditioning. However, the increase in spine density is impaired in OE group and I observed no difference in the number of spines and spine clusters between c-Fos(+) and c-Fos(-) CA1 neurons in the presence of ephrin-B1 overexpressing astrocytes. This is potentially due to reduced formation or increased elimination of dendritic spines on CA1 neurons, which most likely underlie impaired contextual recall in OE mice.

While the overexpression of ephrin-B1 in astrocytes affected spine numbers, the modulation of ephrin-B1 levels in astrocytes did not affect dendritic spine volume. Activity-dependent maturation of hippocampal synapses during memory formation was shown to promote structural changes to dendritic spines (Lichtman and Colman, 2000; Knott et al., 2006; Draft and Lichtman, 2009; Holtmaat and Svoboda, 2009) and to increase synaptic AMPA receptor levels in CA1 hippocampal neurons (Matsuo et al., 2008). Dendritic spines are diverse in structure and undergo activity-dependent morphological changes (Matsuzaki et al., 2004; Matsuo et al., 2008). The structural plasticity of hippocampal dendritic spines allows for spine maturation following learning and memory acquisition (Restivo et al., 2009; Giachero et al., 2013). Neuronal EphB receptors are shown to regulate dendritic spine maturation in hippocampal neurons (Ethell et al., 2001; Henkemeyer et al., 2003) and clustering of AMPARs (Kayser et al., 2006). Activation of EphB2 forward signaling can facilitate the recruitment of AMPARs to synaptic sites (Kayser et al., 2006; Hussain et al., 2015), and ephrin-B reverse signaling can antagonize the internalization of GluR2 subunit of AMPAR allowing for

the retention of AMPAR at the cell surface (Essmann et al., 2008). However, my studies show no changes in dendritic spine size between training WT and OE groups. Despite impaired increase in spine density and clustering on the dendrites of c-Fos(+) CA1 hippocampal neurons in OE mice, average size of dendritic spines was not significantly different between WT and KO or WT and OE groups.

Mature spines are larger in size and have larger postsynaptic densities (Harris et al., 1992), allowing for more AMPAR recruitment and anchorage (Ashby et al., 2006; Matsuzaki, 2007). As I observed no differences in dendritic spine size in both KO and OE mice compared to their WT counterparts, I also expected to see normal AMPAR recruitment. Indeed, I detected no differences in synaptic AMPAR levels between the groups, further confirming that the changes in astrocytic ephrin-B1 levels did not affect synaptic AMPAR levels. Although CA1 hippocampal neurons showed increased evoked AMPA and NMDAR responses in trained KO mice compared to their WT counterparts, the ratio of AMPAR/NMDAR currents was comparable between WT and KO mice suggesting that similar mature state of dendritic spines. It is most likely that mESPC amplitude is increased due to an overall increase in the number of functional dendritic spines/synapses on CA1 hippocampal neurons in KO compared to WT mice.

Increased AMPAR and NMDAR responses both contribute to enhanced synaptic strength and long-term potentiation (LTP), which is an essential mechanism underlying learning (Bliss and Collingridge, 1993). EphB2 was also shown to modulate synaptic transmission by regulating trafficking and function of NMDAR (Dalva et al., 2000; Henderson et al., 2001; Takasu et al., 2002; Nolt et al., 2011). The ability of synaptic

EphB2 receptor to regulate both AMPAR and NMDAR trafficking may influence hippocampal LTP and long-term depression (LTD; (Grunwald et al., 2001; Henderson et al., 2001). Indeed, EphB2 loss was shown to attenuate LTP (Grunwald et al., 2001; Henderson et al., 2001) and to impair LTD (Grunwald et al., 2001). While the loss of EphB2 function impairs long-term memory formation, photo-activation of EphB2 using optogenetics during fear conditioning learning enhances long-term memory (Alapin et al., 2018). Although in this study, I have not investigated the effects of astrocytic ephrin-B1 on LTP induction and consolidation, astrocytic ephrin-B1 may compete for binding to synaptic EphB2 and negatively affect LTP. Enhanced contextual memory and increased excitatory strength in CA1 neurons of KO mice may suggest that changes in astrocytic ephrin-B1 levels may potentially affect CA3 to CA1 LTP, which should be investigated in future studies.

Finally, I found no changes in inhibitory synapses in both ephrin-B1 KO and OE mice. Hippocampal dependent memory formation also requires input from local inhibitory neurons. In fact, ablation of $GABA_A$ receptor α5 subunit increased contextual recall (Crestani et al., 2002; Yee et al., 2004) and enhanced spatial learning in mice (Collinson et al., 2002). In addition, an inverse agonist to α5 subunit increased spatial learning (Chambers et al., 2004; Sternfeld et al., 2004). As $GABA_A$ receptor α5 subunit is highly expressed on hippocampal pyramidal neurons (Pirker et al., 2000; Rudolph and Mohler, 2006), changes in inhibitory cell activity may be potentially involved in the observed effects of ephrin-B1 KO or OE in astrocytes on memory consolidation. However, after deletion or overexpression of ephrin-B1 in the adult astrocytes, there was

no differences in overall numbers of GAD65 positive sites in the hippocampus of trained mice. Whole cell recording from CA1 hippocampal neurons also showed no differences in the amplitude or latency of evoked IPSCs between WT and KO mice. In addition, deletion of astrocytic ephrin-B1 did not affect the number of glutamatergic synapses on PV-positive inhibitory interneurons in trained KO mice compared to WT mice. Previous studies suggest involvement of hippocampal PV cells in learning and memory. While activation of hippocampal PV interneurons was suggested to contribute to reduced contextual recall after fear extinction (Caliskan et al., 2016), interneurons in CA3 hippocampus expressing high levels of PV were shown to receive higher excitatory input following fear conditioning and also play a role in memory consolidation (Donato et al., 2013; Donato et al., 2015). High-PV expressing interneurons were shown to exhibit a higher excitatory to inhibitory input ratio compared to low-PV expressing interneurons (Donato et al., 2015). Although in this study astrocytic ablation and overexpression of ephrin-B1 affected the overall number of excitatory sites in the CA1 hippocampus, there was no changes in excitatory innervation of PV neurons between KO and WT mice.

The studies presented here suggest that astrocytic ephrin-B1 regulates excitatory connections in the CA1 hippocampus during contextual memory formation in an activity dependent manner (Fig. 7). While deletion of ephrin-B1 in astrocytes does not affect formation of new spines on activated CA1 neurons, overexpression of ephrin-B1 in astrocytes impairs it, suggesting that ephrin-B1 is a negative regulator of learning-induced spine formation. Astrocytes have been shown to preferentially contact larger synapses and contribute to synapse stabilization and regulate synaptic activity (Haber et

al., 2006; Witcher et al., 2007). However, the role of astrocytes in the formation of new synapses in the adult hippocampus during learning has not been explored yet. I propose that ephrin-B1 plays an important role in astrocyte-mediated new synapse formation during learning. However, it is still unclear whether synaptic activity directly regulate levels of ephrin-B1 in astrocytes and if selective up-regulation or down-regulation of ephrin-B1 in some astrocytes may respectively suppress or facilitate new synapse formation at specific dendritic domains induced by local changes in synaptic activity during learning, and potentially underlie memory encoding.

References

Adamsky, A., Kol, A., Kreisel, T., Doron, A., Ozeri-Engelhard, N., Melcer, T., et al. (2018). Astrocytic Activation Generates De Novo Neuronal Potentiation and Memory Enhancement. *Cell* 174(1)**,** 59-71.e14. doi: 10.1016/j.cell.2018.05.002.

Alapin, J.M., Dines, M., Vassiliev, M., Tamir, T., Ram, A., Locke, C., et al. (2018). Activation of EphB2 Forward Signaling Enhances Memory Consolidation. *Cell Rep* 23(7)**,** 2014-2025. doi: 10.1016/j.celrep.2018.04.042.

Alberini, C.M., Cruz, E., Descalzi, G., Bessieres, B., and Gao, V. (2018). Astrocyte glycogen and lactate: New insights into learning and memory mechanisms. *Glia* 66(6)**,** 1244-1262. doi: 10.1002/glia.23250.

Allen, N.J., Bennett, M.L., Foo, L.C., Wang, G.X., Chakraborty, C., Smith, S.J., et al. (2012). Astrocyte glypicans 4 and 6 promote formation of excitatory synapses via GluA1 AMPA receptors. *Nature* 486(7403)**,** 410-414. doi: 10.1038/nature11059.

Allen, N.J., and Eroglu, C. (2017). Cell Biology of Astrocyte-Synapse Interactions. *Neuron* 96(3)**,** 697-708. doi: 10.1016/j.neuron.2017.09.056.

Anagnostaras, S.G., Gale, G.D., and Fanselow, M.S. (2001). Hippocampus and contextual fear conditioning: recent controversies and advances. *Hippocampus* 11(1)**,** 8-17. doi: 10.1002/1098-1063(2001)11:1<8::aid-hipo1015>3.0.co;2-7.

Araque, A., Parpura, V., Sanzgiri, R.P., and Haydon, P.G. (1999). Tripartite synapses: glia, the unacknowledged partner. *Trends Neurosci* 22(5)**,** 208-215.

Arvanitis, D.N., Behar, A., Drougard, A., Roullet, P., and Davy, A. (2014). Cortical abnormalities and non-spatial learning deficits in a mouse model of CranioFrontoNasal syndrome. *PLoS One* 9(2)**,** e88325. doi: 10.1371/journal.pone.0088325.

Ashby, M.C., Maier, S.R., Nishimune, A., and Henley, J.M. (2006). Lateral diffusion drives constitutive exchange of AMPA receptors at dendritic spines and is regulated by spine morphology. *J Neurosci* 26(26)**,** 7046-7055. doi: 10.1523/jneurosci.1235-06.2006.

Bliss, T.V., and Collingridge, G.L. (1993). A synaptic model of memory: long-term potentiation in the hippocampus. *Nature* 361(6407)**,** 31-39. doi: 10.1038/361031a0.

Caliskan, G., Muller, I., Semtner, M., Winkelmann, A., Raza, A.S., Hollnagel, J.O., et al. (2016). Identification of Parvalbumin Interneurons as Cellular Substrate of Fear

Memory Persistence. *Cereb Cortex* 26(5)**,** 2325-2340. doi: 10.1093/cercor/bhw001.

Castaneda-Castellanos, D.R., Flint, A.C., and Kriegstein, A.R. (2006). Blind patch clamp recordings in embryonic and adult mammalian brain slices. *Nat Protoc* 1(2)**,** 532-542. doi: 10.1038/nprot.2006.75.

Chambers, M.S., Atack, J.R., Carling, R.W., Collinson, N., Cook, S.M., Dawson, G.R., et al. (2004). An orally bioavailable, functionally selective inverse agonist at the benzodiazepine site of GABAA alpha5 receptors with cognition enhancing properties. *J Med Chem* 47(24)**,** 5829-5832. doi: 10.1021/jm040863t.

Christopherson, K.S., Ullian, E.M., Stokes, C.C., Mullowney, C.E., Hell, J.W., Agah, A., et al. (2005). Thrombospondins are astrocyte-secreted proteins that promote CNS synaptogenesis. *Cell* 120(3)**,** 421-433. doi: 10.1016/j.cell.2004.12.020.

Chung, W.S., Allen, N.J., and Eroglu, C. (2015). Astrocytes Control Synapse Formation, Function, and Elimination. *Cold Spring Harb Perspect Biol* 7(9)**,** a020370. doi: 10.1101/cshperspect.a020370.

Chung, W.S., Clarke, L.E., Wang, G.X., Stafford, B.K., Sher, A., Chakraborty, C., et al. (2013). Astrocytes mediate synapse elimination through MEGF10 and MERTK pathways. *Nature* 504(7480)**,** 394-400. doi: 10.1038/nature12776.

Clarke, L.E., and Barres, B.A. (2013). Emerging roles of astrocytes in neural circuit development. *Nat Rev Neurosci* 14(5)**,** 311-321. doi: 10.1038/nrn3484.

Collinson, N., Kuenzi, F.M., Jarolimek, W., Maubach, K.A., Cothliff, R., Sur, C., et al. (2002). Enhanced learning and memory and altered GABAergic synaptic transmission in mice lacking the alpha 5 subunit of the GABAA receptor. *J Neurosci* 22(13)**,** 5572-5580. doi: 20026436.

Crestani, F., Keist, R., Fritschy, J.M., Benke, D., Vogt, K., Prut, L., et al. (2002). Trace fear conditioning involves hippocampal alpha5 GABA(A) receptors. *Proc Natl Acad Sci U S A* 99(13)**,** 8980-8985. doi: 10.1073/pnas.142288699.

Dalva, M.B., Takasu, M.A., Lin, M.Z., Shamah, S.M., Hu, L., Gale, N.W., et al. (2000). EphB receptors interact with NMDA receptors and regulate excitatory synapse formation. *Cell* 103(6)**,** 945-956.

Dines, M., Grinberg, S., Vassiliev, M., Ram, A., Tamir, T., and Lamprecht, R. (2015). The roles of Eph receptors in contextual fear conditioning memory formation. *Neurobiol Learn Mem* 124**,** 62-70. doi: 10.1016/j.nlm.2015.07.003.

Donato, F., Chowdhury, A., Lahr, M., and Caroni, P. (2015). Early- and late-born parvalbumin basket cell subpopulations exhibiting distinct regulation and roles in learning. *Neuron* 85(4)**,** 770-786. doi: 10.1016/j.neuron.2015.01.011.

Donato, F., Rompani, S.B., and Caroni, P. (2013). Parvalbumin-expressing basket-cell network plasticity induced by experience regulates adult learning. *Nature* 504(7479)**,** 272-276. doi: 10.1038/nature12866.

Draft, R.W., and Lichtman, J.W. (2009). It's lonely at the top: winning climbing fibers ascend dendrites solo. *Neuron* 63(1)**,** 6-8. doi: 10.1016/j.neuron.2009.07.001.

Essmann, C.L., Martinez, E., Geiger, J.C., Zimmer, M., Traut, M.H., Stein, V., et al. (2008). Serine phosphorylation of ephrinB2 regulates trafficking of synaptic AMPA receptors. *Nat Neurosci* 11(9)**,** 1035-1043. doi: 10.1038/nn.2171.

Ethell, I.M., Irie, F., Kalo, M.S., Couchman, J.R., Pasquale, E.B., and Yamaguchi, Y. (2001). EphB/syndecan-2 signaling in dendritic spine morphogenesis. *Neuron* 31(6)**,** 1001-1013. doi: 10.1016/s0896-6273(01)00440-8.

Fellin, T., Pascual, O., Gobbo, S., Pozzan, T., Haydon, P.G., and Carmignoto, G. (2004). Neuronal synchrony mediated by astrocytic glutamate through activation of extrasynaptic NMDA receptors. *Neuron* 43(5)**,** 729-743. doi: 10.1016/j.neuron.2004.08.011.

Frank, A.C., Huang, S., Zhou, M., Gdalyahu, A., Kastellakis, G., Silva, T.K., et al. (2018). Hotspots of dendritic spine turnover facilitate clustered spine addition and learning and memory. *Nat Commun* 9(1)**,** 422. doi: 10.1038/s41467-017-02751-2.

Fu, M., Yu, X., Lu, J., and Zuo, Y. (2012). Repetitive motor learning induces coordinated formation of clustered dendritic spines in vivo. *Nature* 483(7387)**,** 92-95. doi: 10.1038/nature10844.

Gao, V., Suzuki, A., Magistretti, P.J., Lengacher, S., Pollonini, G., Steinman, M.Q., et al. (2016). Astrocytic beta2-adrenergic receptors mediate hippocampal long-term memory consolidation. *Proc Natl Acad Sci U S A* 113(30)**,** 8526-8531. doi: 10.1073/pnas.1605063113.

Garrett, A.M., and Weiner, J.A. (2009). Control of CNS synapse development by {gamma}-protocadherin-mediated astrocyte-neuron contact. *J Neurosci* 29(38)**,** 11723-11731. doi: 10.1523/JNEUROSCI.2818-09.2009.

Gerlai, R., Shinsky, N., Shih, A., Williams, P., Winer, J., Armanini, M., et al. (1999). Regulation of learning by EphA receptors: a protein targeting study. *J Neurosci* 19(21)**,** 9538-9549.

Giachero, M., Calfa, G.D., and Molina, V.A. (2013). Hippocampal structural plasticity accompanies the resulting contextual fear memory following stress and fear conditioning. *Learn Mem* 20(11)**,** 611-616. doi: 10.1101/lm.031724.113.

Goshen, I., Brodsky, M., Prakash, R., Wallace, J., Gradinaru, V., Ramakrishnan, C., et al. (2011). Dynamics of retrieval strategies for remote memories. *Cell* 147(3)**,** 678-689. doi: 10.1016/j.cell.2011.09.033.

Grunwald, I.C., Korte, M., Wolfer, D., Wilkinson, G.A., Unsicker, K., Lipp, H.P., et al. (2001). Kinase-independent requirement of EphB2 receptors in hippocampal synaptic plasticity. *Neuron* 32(6)**,** 1027-1040.

Haber, M., Zhou, L., and Murai, K.K. (2006). Cooperative astrocyte and dendritic spine dynamics at hippocampal excitatory synapses. *J Neurosci* 26(35)**,** 8881-8891. doi: 10.1523/jneurosci.1302-06.2006.

Halladay, A.K., Tessarollo, L., Zhou, R., and Wagner, G.C. (2004). Neurochemical and behavioral deficits consequent to expression of a dominant negative EphA5 receptor. *Brain Res Mol Brain Res* 123(1-2)**,** 104-111. doi: 10.1016/j.molbrainres.2004.01.005.

Hama, H., Hara, C., Yamaguchi, K., and Miyawaki, A. (2004). PKC signaling mediates global enhancement of excitatory synaptogenesis in neurons triggered by local contact with astrocytes. *Neuron* 41(3)**,** 405-415.

Harris, K.M., Jensen, F.E., and Tsao, B. (1992). Three-dimensional structure of dendritic spines and synapses in rat hippocampus (CA1) at postnatal day 15 and adult ages: implications for the maturation of synaptic physiology and long-term potentiation. *J Neurosci* 12(7)**,** 2685-2705.

Hayashi-Takagi, A., Yagishita, S., Nakamura, M., Shirai, F., Wu, Y.I., Loshbaugh, A.L., et al. (2015). Labelling and optical erasure of synaptic memory traces in the motor cortex. *Nature* 525(7569)**,** 333-338. doi: 10.1038/nature15257.

Henderson, J.T., Georgiou, J., Jia, Z., Robertson, J., Elowe, S., Roder, J.C., et al. (2001). The receptor tyrosine kinase EphB2 regulates NMDA-dependent synaptic function. *Neuron* 32(6)**,** 1041-1056.

Henkemeyer, M., Itkis, O.S., Ngo, M., Hickmott, P.W., and Ethell, I.M. (2003). Multiple EphB receptor tyrosine kinases shape dendritic spines in the hippocampus. *J Cell Biol* 163(6)**,** 1313-1326. doi: 10.1083/jcb.200306033.

Henneberger, C., Papouin, T., Oliet, S.H., and Rusakov, D.A. (2010). Long-term potentiation depends on release of D-serine from astrocytes. *Nature* 463(7278)**,** 232-236. doi: 10.1038/nature08673.

Holtmaat, A., and Svoboda, K. (2009). Experience-dependent structural synaptic plasticity in the mammalian brain. *Nat Rev Neurosci* 10(9)**,** 647-658. doi: 10.1038/nrn2699.

Hussain, N.K., Thomas, G.M., Luo, J., and Huganir, R.L. (2015). Regulation of AMPA receptor subunit GluA1 surface expression by PAK3 phosphorylation. *Proc Natl Acad Sci U S A* 112(43)**,** E5883-5890. doi: 10.1073/pnas.1518382112.

Ji, J., and Maren, S. (2008). Differential roles for hippocampal areas CA1 and CA3 in the contextual encoding and retrieval of extinguished fear. *Learn Mem* 15(4)**,** 244-251. doi: 10.1101/lm.794808.

Kasai, H., Fukuda, M., Watanabe, S., Hayashi-Takagi, A., and Noguchi, J. (2010). Structural dynamics of dendritic spines in memory and cognition. *Trends Neurosci* 33(3)**,** 121-129. doi: 10.1016/j.tins.2010.01.001.

Kayser, M.S., McClelland, A.C., Hughes, E.G., and Dalva, M.B. (2006). Intracellular and trans-synaptic regulation of glutamatergic synaptogenesis by EphB receptors. *J Neurosci* 26(47)**,** 12152-12164. doi: 10.1523/JNEUROSCI.3072-06.2006.

Knott, G.W., Holtmaat, A., Wilbrecht, L., Welker, E., and Svoboda, K. (2006). Spine growth precedes synapse formation in the adult neocortex in vivo. *Nat Neurosci* 9(9)**,** 1117-1124. doi: 10.1038/nn1747.

Koeppen, J., Nguyen, A.Q., Nikolakopoulou, A.M., Garcia, M., Hanna, S., Woodruff, S., et al. (2018). Functional Consequences of Synapse Remodeling Following Astrocyte-Specific Regulation of Ephrin-B1 in the Adult Hippocampus. *J Neurosci* 38(25)**,** 5710-5726. doi: 10.1523/JNEUROSCI.3618-17.2018.

Lai, C.S., Franke, T.F., and Gan, W.B. (2012). Opposite effects of fear conditioning and extinction on dendritic spine remodelling. *Nature* 483(7387)**,** 87-91. doi: 10.1038/nature10792.

Lai, C.S.W., Adler, A., and Gan, W.B. (2018). Fear extinction reverses dendritic spine formation induced by fear conditioning in the mouse auditory cortex. *Proc Natl Acad Sci U S A* 115(37)**,** 9306-9311. doi: 10.1073/pnas.1801504115.

Lichtman, J.W., and Colman, H. (2000). Synapse elimination and indelible memory. *Neuron* 25(2)**,** 269-278.

Liebl, D.J., Morris, C.J., Henkemeyer, M., and Parada, L.F. (2003). mRNA expression of ephrins and Eph receptor tyrosine kinases in the neonatal and adult mouse central nervous system. *J Neurosci Res* 71(1)**,** 7-22. doi: 10.1002/jnr.10457.

Liu, X., Ramirez, S., Pang, P.T., Puryear, C.B., Govindarajan, A., Deisseroth, K., et al. (2012). Optogenetic stimulation of a hippocampal engram activates fear memory recall. *Nature* 484(7394)**,** 381-385. doi: 10.1038/nature11028.

Matsuo, N., Reijmers, L., and Mayford, M. (2008). Spine-type-specific recruitment of newly synthesized AMPA receptors with learning. *Science* 319(5866)**,** 1104-1107. doi: 10.1126/science.1149967.

Matsuzaki, M. (2007). Factors critical for the plasticity of dendritic spines and memory storage. *Neurosci Res* 57(1)**,** 1-9. doi: 10.1016/j.neures.2006.09.017.

Matsuzaki, M., Honkura, N., Ellis-Davies, G.C., and Kasai, H. (2004). Structural basis of long-term potentiation in single dendritic spines. *Nature* 429(6993)**,** 761-766. doi: 10.1038/nature02617.

McBride, T.J., Rodriguez-Contreras, A., Trinh, A., Bailey, R., and Debello, W.M. (2008). Learning drives differential clustering of axodendritic contacts in the barn owl auditory system. *J Neurosci* 28(27)**,** 6960-6973. doi: 10.1523/jneurosci.1352-08.2008.

Milner, B., Squire, L.R., and Kandel, E.R. (1998). Cognitive neuroscience and the study of memory. *Neuron* 20(3)**,** 445-468.

Neves, G., Cooke, S.F., and Bliss, T.V. (2008). Synaptic plasticity, memory and the hippocampus: a neural network approach to causality. *Nat Rev Neurosci* 9(1)**,** 65-75. doi: 10.1038/nrn2303.

Newman, L.A., Korol, D.L., and Gold, P.E. (2011). Lactate produced by glycogenolysis in astrocytes regulates memory processing. *PLoS One* 6(12)**,** e28427. doi: 10.1371/journal.pone.0028427.

Nikolakopoulou, A.M., Koeppen, J., Garcia, M., Leish, J., Obenaus, A., and Ethell, I.M. (2016). Astrocytic Ephrin-B1 Regulates Synapse Remodeling Following Traumatic Brain Injury. *ASN Neuro* 8(1)**,** 1-18. doi: 10.1177/1759091416630220.

Nishiyama, H., Knopfel, T., Endo, S., and Itohara, S. (2002). Glial protein S100B modulates long-term neuronal synaptic plasticity. *Proc Natl Acad Sci U S A* 99(6)**,** 4037-4042. doi: 10.1073/pnas.052020999.

Nolt, M.J., Lin, Y., Hruska, M., Murphy, J., Sheffler-Colins, S.I., Kayser, M.S., et al. (2011). EphB controls NMDA receptor function and synaptic targeting in a subunit-specific manner. *J Neurosci* 31(14)**,** 5353-5364. doi: 10.1523/JNEUROSCI.0282-11.2011.

Pirker, S., Schwarzer, C., Wieselthaler, A., Sieghart, W., and Sperk, G. (2000). GABA(A) receptors: immunocytochemical distribution of 13 subunits in the adult rat brain. *Neuroscience* 101(4)**,** 815-850.

Restivo, L., Vetere, G., Bontempi, B., and Ammassari-Teule, M. (2009). The formation of recent and remote memory is associated with time-dependent formation of dendritic spines in the hippocampus and anterior cingulate cortex. *J Neurosci* 29(25)**,** 8206-8214. doi: 10.1523/jneurosci.0966-09.2009.

Rudolph, U., and Mohler, H. (2006). GABA-based therapeutic approaches: GABAA receptor subtype functions. *Curr Opin Pharmacol* 6(1)**,** 18-23. doi: 10.1016/j.coph.2005.10.003.

Sala, C., and Segal, M. (2014). Dendritic spines: the locus of structural and functional plasticity. *Physiol Rev* 94(1)**,** 141-188. doi: 10.1152/physrev.00012.2013.

Segal, M. (2017). Dendritic spines: Morphological building blocks of memory. *Neurobiol Learn Mem* 138**,** 3-9. doi: 10.1016/j.nlm.2016.06.007.

Sternfeld, F., Carling, R.W., Jelley, R.A., Ladduwahetty, T., Merchant, K.J., Moore, K.W., et al. (2004). Selective, orally active gamma-aminobutyric acidA alpha5 receptor inverse agonists as cognition enhancers. *J Med Chem* 47(9)**,** 2176-2179. doi: 10.1021/jm031076j.

Strekalova, T., Zorner, B., Zacher, C., Sadovska, G., Herdegen, T., and Gass, P. (2003). Memory retrieval after contextual fear conditioning induces c-Fos and JunB expression in CA1 hippocampus. *Genes Brain Behav* 2(1)**,** 3-10.

Suzuki, A., Stern, S.A., Bozdagi, O., Huntley, G.W., Walker, R.H., Magistretti, P.J., et al. (2011). Astrocyte-neuron lactate transport is required for long-term memory formation. *Cell* 144(5)**,** 810-823. doi: 10.1016/j.cell.2011.02.018.

Tadi, M., Allaman, I., Lengacher, S., Grenningloh, G., and Magistretti, P.J. (2015). Learning-Induced Gene Expression in the Hippocampus Reveals a Role of Neuron -Astrocyte Metabolic Coupling in Long Term Memory. *PLoS One* 10(10)**,** e0141568. doi: 10.1371/journal.pone.0141568.

Takasu, M.A., Dalva, M.B., Zigmond, R.E., and Greenberg, M.E. (2002). Modulation of NMDA receptor-dependent calcium influx and gene expression through EphB receptors. *Science* 295(5554)**,** 491-495. doi: 10.1126/science.1065983.

Tonegawa, S., Liu, X., Ramirez, S., and Redondo, R. (2015). Memory Engram Cells Have Come of Age. *Neuron* 87(5)**,** 918-931. doi: 10.1016/j.neuron.2015.08.002.

Twigg, S.R., Kan, R., Babbs, C., Bochukova, E.G., Robertson, S.P., Wall, S.A., et al. (2004). Mutations of ephrin-B1 (EFNB1), a marker of tissue boundary formation, cause craniofrontonasal syndrome. *Proc Natl Acad Sci U S A* 101(23)**,** 8652-8657. doi: 10.1073/pnas.0402819101.

Wieland, I., Jakubiczka, S., Muschke, P., Cohen, M., Thiele, H., Gerlach, K.L., et al. (2004). Mutations of the ephrin-B1 gene cause craniofrontonasal syndrome. *Am J Hum Genet* 74(6)**,** 1209-1215. doi: 10.1086/421532.

Willi, R., Winter, C., Wieske, F., Kempf, A., Yee, B.K., Schwab, M.E., et al. (2012). Loss of EphA4 impairs short-term spatial recognition memory performance and locomotor habituation. *Genes Brain Behav* 11(8)**,** 1020-1031. doi: 10.1111/j.1601-183X.2012.00842.x.

Witcher, M.R., Kirov, S.A., and Harris, K.M. (2007). Plasticity of perisynaptic astroglia during synaptogenesis in the mature rat hippocampus. *Glia* 55(1)**,** 13-23. doi: 10.1002/glia.20415.

Yang, Y., Wang, X.B., Frerking, M., and Zhou, Q. (2008). Spine expansion and stabilization associated with long-term potentiation. *J Neurosci* 28(22)**,** 5740-5751. doi: 10.1523/JNEUROSCI.3998-07.2008.

Yee, B.K., Hauser, J., Dolgov, V.V., Keist, R., Mohler, H., Rudolph, U., et al. (2004). GABA receptors containing the alpha5 subunit mediate the trace effect in aversive and appetitive conditioning and extinction of conditioned fear. *Eur J Neurosci* 20(7)**,** 1928-1936. doi: 10.1111/j.1460-9568.2004.03642.x.

Figures

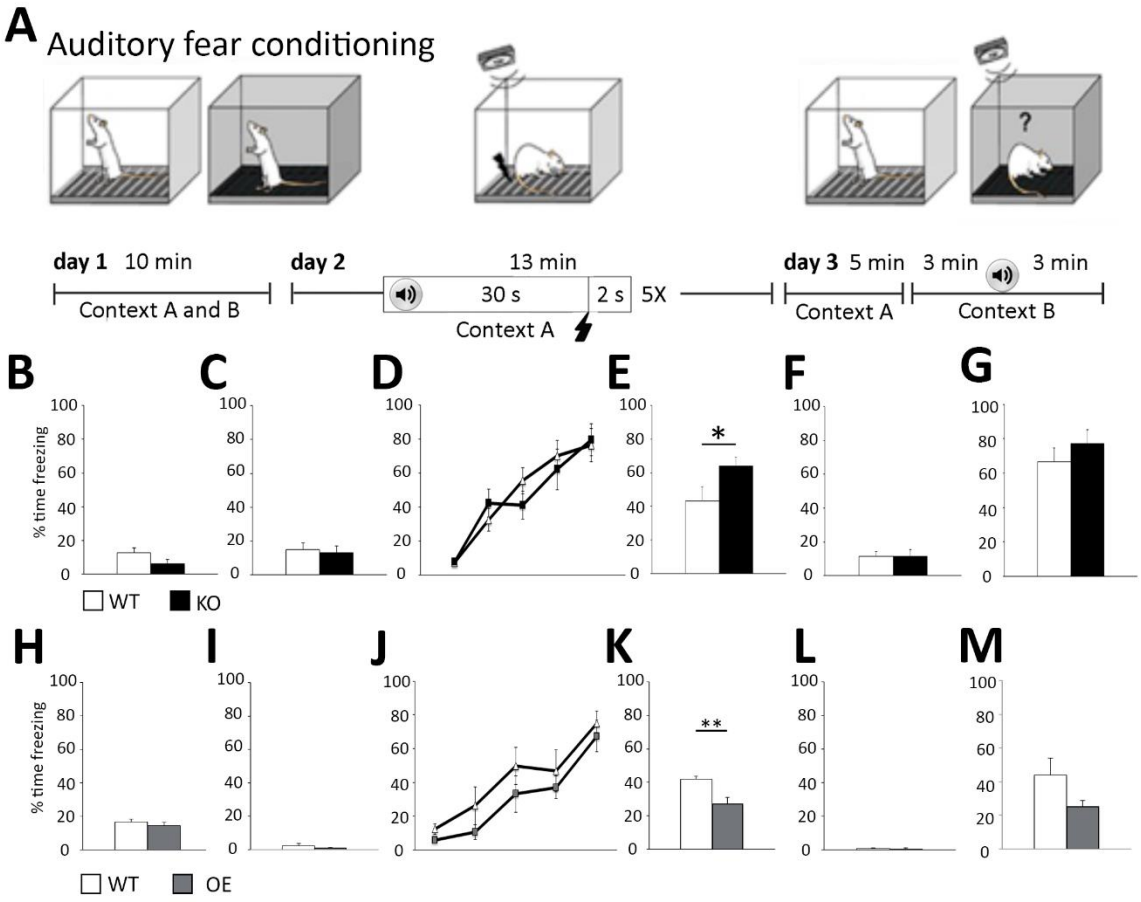
A
Auditory fear conditioning
day 1 10 min
Context A and B
day 2
13 min
30 s
2 s
5X
Context A
day 3 5 min
3 min
3 min
Context A
Context B
B
C
D
E
F
G
% time freezing
WT
KO
H
I
J
K
L
M
% time freezing
WT
OE

Figure 4.1 Fear conditioning paradigm. (A) Schematic representation of fear conditioning paradigm. Mice were habituated to contexts A and B for 10 min on day 1 with 1 h gap between context A and context B. On day 2, mice were placed in Context A and received 5 random 0.7 mA foot shocks for 2 s after a 30 s tone of 9 kHz at 70 dB, to train the mice to associate the tone with the foot shock. On day 3 mice were placed in Context A for 5 min, 1 h later mice were placed in Context B for 6 min and exposed to the same tone for the last 3 min. (B-G) Graphs show the percentage of time that KO mice and their corresponding WT mice freeze during each trial, including Context A habituation (B), Context B habituation (C), Context A training (D), Context A recall (E), Context B without tone (F), and with tone (G). KO mice show higher freezing than WT mice during Context A recall (n = 7–9 mice per group, t-test; $t_{(14)}$ = 2.389 *p = 0.0315). (H-M) Graphs show the percentage of time that OE mice and their corresponding WT mice freeze during each trial, including Context A habituation (H), Context B habituation (I), Context A training (J), Context A recall (K), Context B without tone (L) and with tone (M). Ephrin-B1 OE mice show reduced freezing compared to WT mice during Context A recall (n = 5 mice per group, astrocytic ephrin-B1 OE: 27.27 ± 3.57 vs control: 41.75 ± 2.04, $t_{(10)}$ = 3.522, p = 0.006, t test, **p = 0.01). Graphs show mean values and error bars represent SEM.

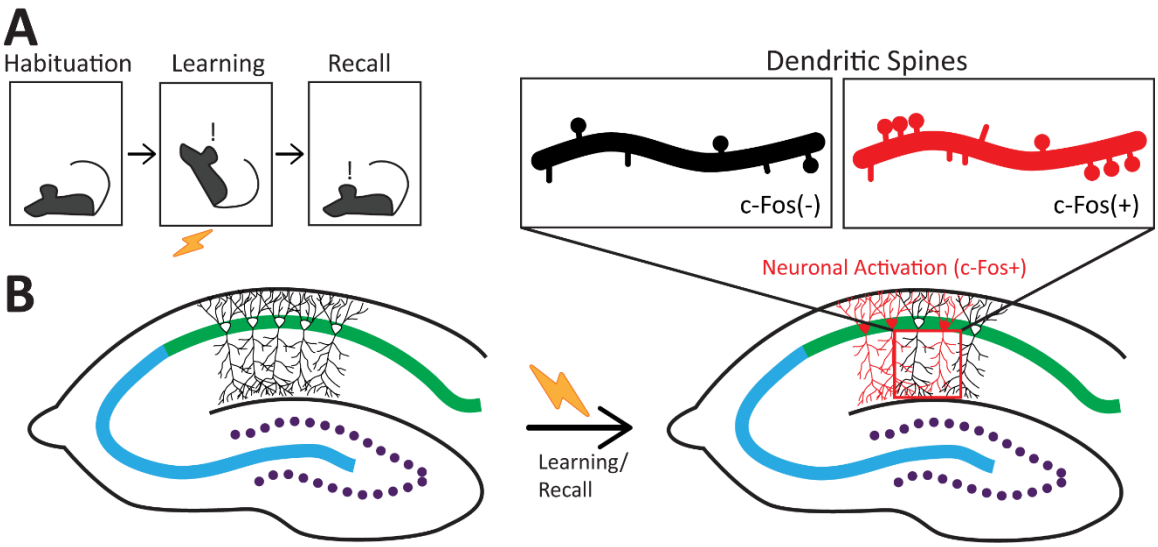

Figure 4.2 Activation of hippocampal CA1 neurons during contextual memory recall is identified with c-Fos+ expression. (A-B) During fear condition, contextual fear memories become encoded in a sub-set of hippocampal neurons and become re-activated during memory recall. Activated neurons during memory retrieval can be identified by c-Fos expression. Use of c-Fos expression can delineate the effects of astrocytic ephrin-B1 on synapse formation and maturation during learning and memory in activated (c-Fos+) and non-activated (c-Fos-) neurons.

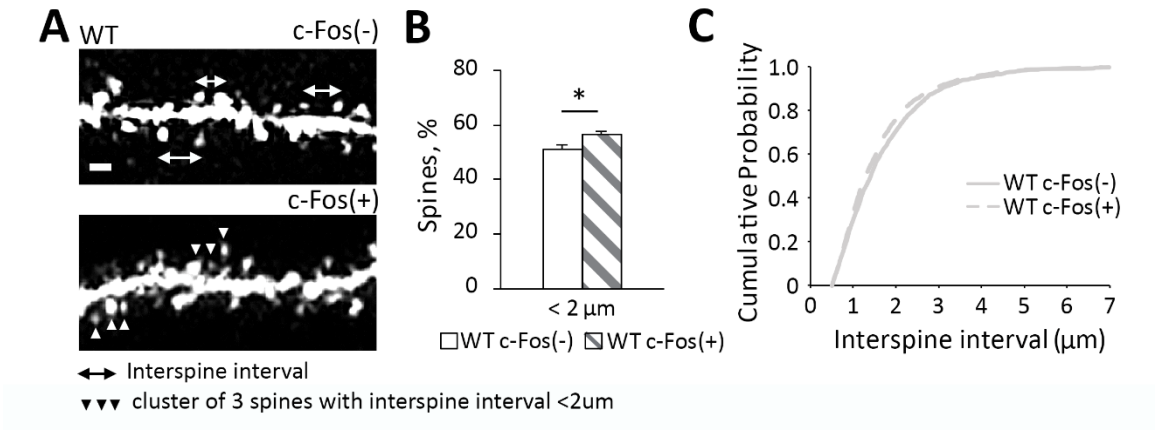

Figure 4.3 Clustered spines appear at an interspine interval less than 2 µm on activated neurons. (A) Confocal image of CA1 hippocampal dendrites of c-Fos(-) and c-Fos(+) cells in trained WT mice following fear conditioning; scale bar is 2 µm. White arrows indicate clusters containing 3 or more spines. (B) WT c-Fos(+) neurons had a significantly higher percent of spines that were located within 2.0 µm distance from neighboring spine (WT c-Fos(-): 50.91 ± 1.65 vs WT c-Fos(+): 56.58 ± 1.00, $t_{(10)}$ = 2.766 p = 0.019, t test) than WT c-Fos(-) neurons, suggesting an increased spine clustering in WT c-Fos(+) neurons. (C) Cumulative probability plot of distances between spines in WT c-Fos(-) and c-Fos(+) mice.

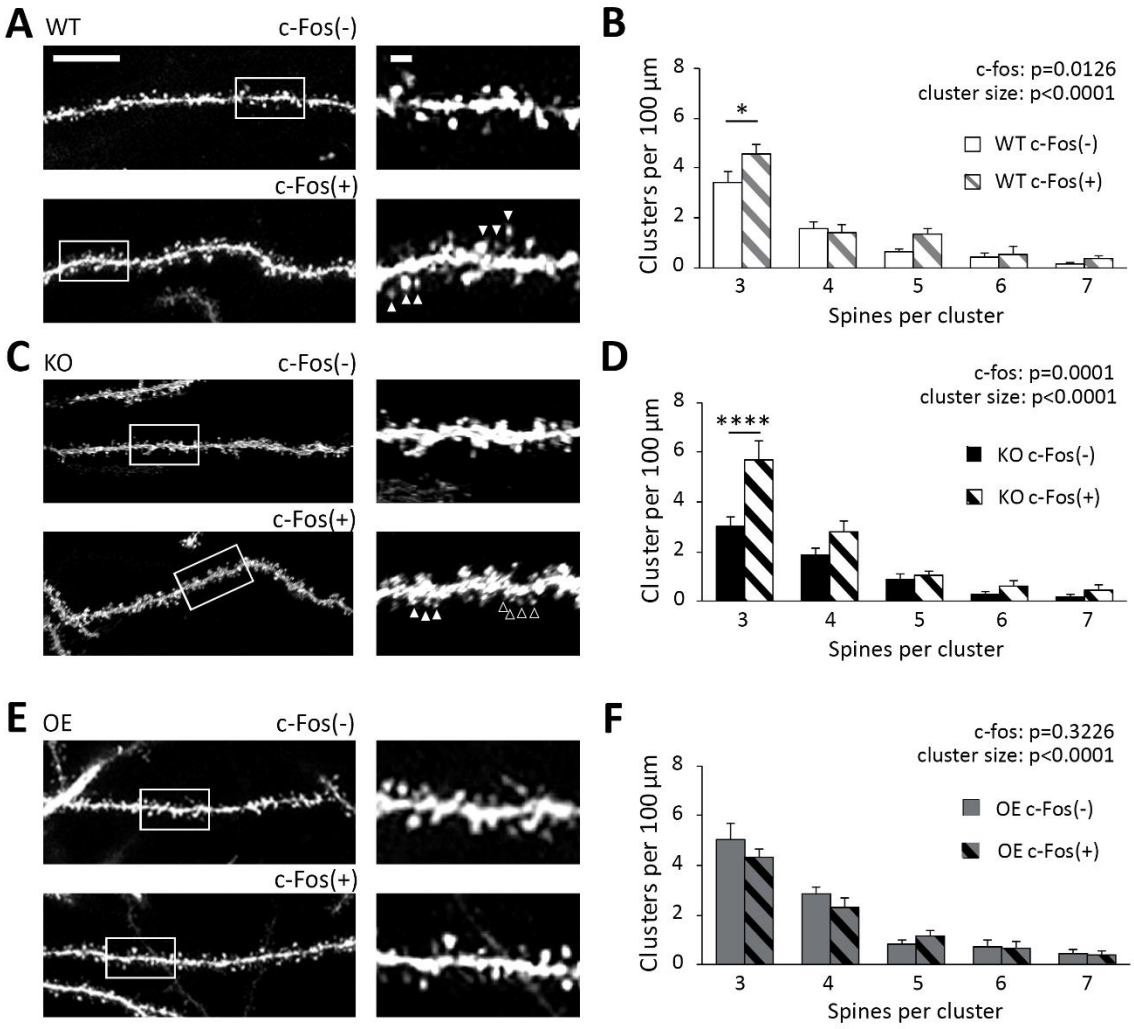
A
WT
c-Fos(-)
c-Fos(+)
B
c-fos: p=0.0126
cluster size: p<0.0001
*
WT c-Fos(-)
WT c-Fos(+)
Clusters per 100 µm
Spines per cluster
C
KO
c-Fos(-)
c-Fos(+)
D
c-fos: p=0.0001
cluster size: p<0.0001
****
KO c-Fos(-)
KO c-Fos(+)
Cluster per 100 µm
Spines per cluster
E
OE
c-Fos(-)
c-Fos(+)
F
c-fos: p=0.3226
cluster size: p<0.0001
OE c-Fos(-)
OE c-Fos(+)
Clusters per 100 µm
Spines per cluster

Figure 4.4 Increased spine clustering is observed on c-Fos(+) neurons in WT and KO mice, but not OE mice. (A, C, E) Confocal images of dendritic spines in c-Fos(-) or c-Fos(+) CA1 hippocampal neurons from WT (A), KO (C), and OE (E) mice 1 h after contextual recall; scale bar is 10 µm for low magnification images and 2 µm for high magnification images. (B, D, F) Graphs show number of clusters containing 3, 4, 5, 6, or 7 spines (< 2 µm apart) per cluster in c-Fos(-) or c-Fos(+) CA1 neurons from WT (B), KO (D) or OE (F) mice. (B) WT c-Fos(+) neurons had significantly higher number of clusters with 3 spines than WT c-Fos(-) neurons (cluster size $F_{(4, 50)} = 69.19$, $p < 0.0001$; c-Fos $F_{(1, 50)} = 6.698$, $p = 0.0126$; two-way ANOVA followed by Bonferroni's post hoc, *p = 0.0109). (D) There was a higher number of clusters with 3 spines in KO c-Fos(+) neurons compared to KO c-Fos(-) neurons (cluster size $F_{(4, 130)} = 45.77$, $p < 0.0001$; c-Fos $F_{(1, 130)} = 15.5$, $p = 0.0001$; two-way ANOVA followed by Bonferroni's post hoc, ****p < 0.0001). (F) There was no difference in the number of clusters with 3 spines between OE c-Fos(+) and OE c-Fos(-) neurons. Graphs show mean values and error bars represent SEM; *p < 0.05, ****p < 0.0001.

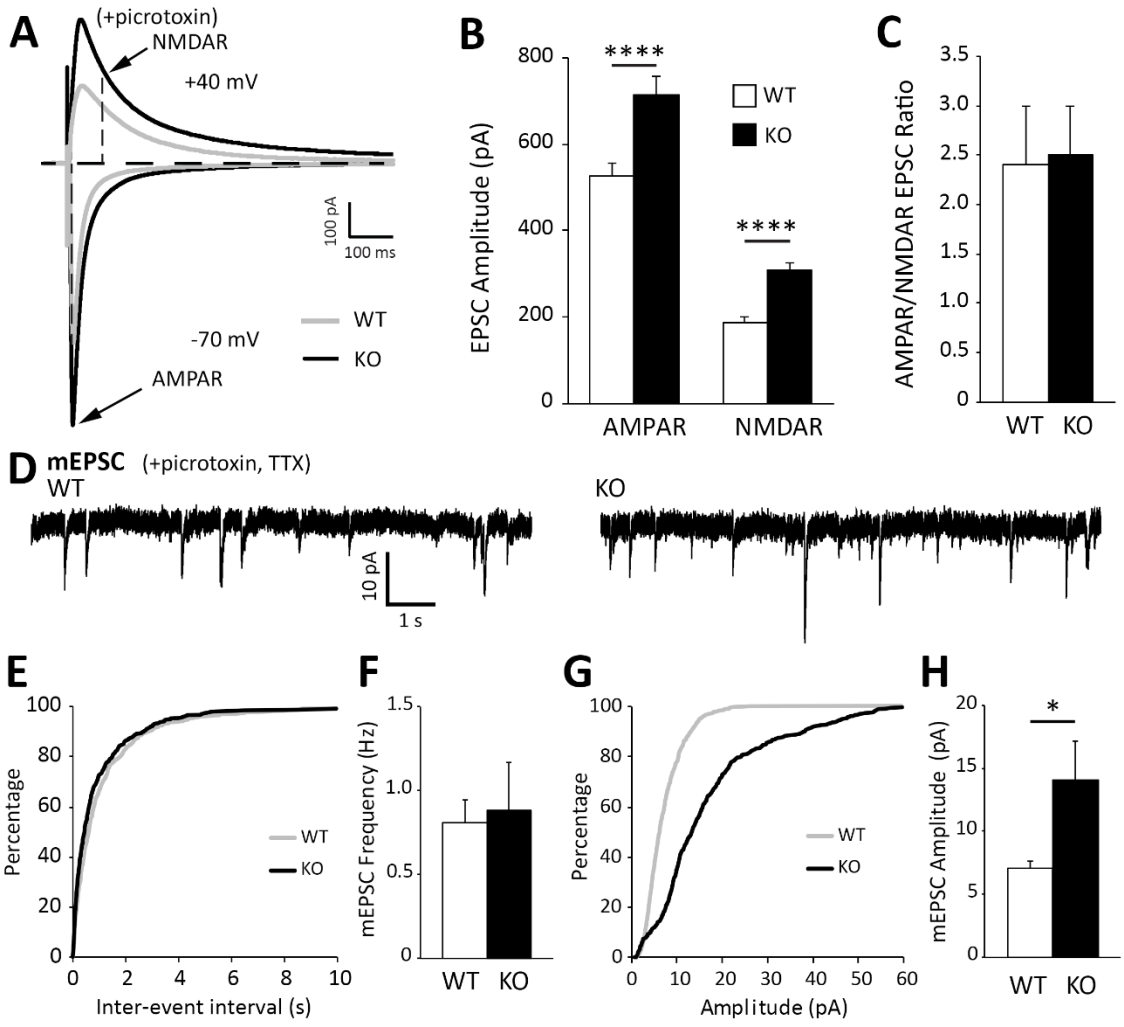
A
(+picrotoxin)
NMDAR
+40 mV
100 pA
100 ms
WT
KO
-70 mV
AMPAR
B
****
****
WT
KO
EPSC Amplitude (pA)
800
600
400
200
0
AMPAR
NMDAR
C
AMPAR/NMDAR EPSC Ratio
3.5
3.0
2.5
2.0
1.5
1.0
0.5
0
WT KO
D
mEPSC (+picrotoxin, TTX)
WT
KO
10 pA
1 s
E
Percentage
100
80
60
40
20
0
WT
KO
0 2 4 6 8 10
Inter-event interval (s)
F
mEPSC Frequency (Hz)
1.5
1.0
0.5
0
WT KO
G
Percentage
100
80
60
40
20
0
WT
KO
0 10 20 30 40 50 60
Amplitude (pA)
H
*
mEPSC Amplitude (pA)
20
15
10
5
0
WT KO

Figure 4.5 Excitatory post-synaptic responses are enhanced in CA1 hippocampal neurons from astrocytic ephrin-B1 KO mice compared to WT mice. (A) Representative traces of excitatory postsynaptic responses in CA1 hippocampal neurons in hippocampal slices from WT (grey) and KO (black) trained mice evoked by stimulating SR region in the presence of 50 µM picrotoxin, a $GABA_A$ receptor antagonist. Neurons were voltage-clamped at either -70 mV to measure AMPAR-mediated EPSCs or +40 mV to measure NMDAR-mediated EPSCs. (B, C) Graphs show average EPSC amplitude (B) and corresponding ratio of AMPAR- and NMDAR-mediated EPSCs (C) (n = 12-13 cells, 6 mice). Evoked AMPAR and NMDAR-mediated currents were significantly increased (AMPAR: $t_{(398)} = 3.568$, ***p = 0.0004; NMDAR: $t_{(373)} = 4.61$, p < 0.0001, t test, **** p < 0.0001); however, AMPAR/NMDAR EPSC ratio was unchanged ($t_{(17)} = 0.1495$, p = 0.8829, t test). (D) Sample recordings of mEPSCs from CA1 neurons in hippocampal slices from trained WT and KO mice; recorded in the presence of TTX and picrotoxin (n = 6 mice). (E) Cumulative probability curve of inter-event intervals between spikes in WT (grey) and KO (black). (F) Total average frequency of mEPSCs in WT and KO. (G) Cumulative probability curve of mEPSC amplitude in WT and KO. (H) Average amplitude of mEPSCs was significantly higher in KO compared to WT ($t_{(13)} = 2.462$, *p = 0.0286, t test). Error bars represent SEM; * p < 0.05, *** p < 0.001, ****p < 0.0001.

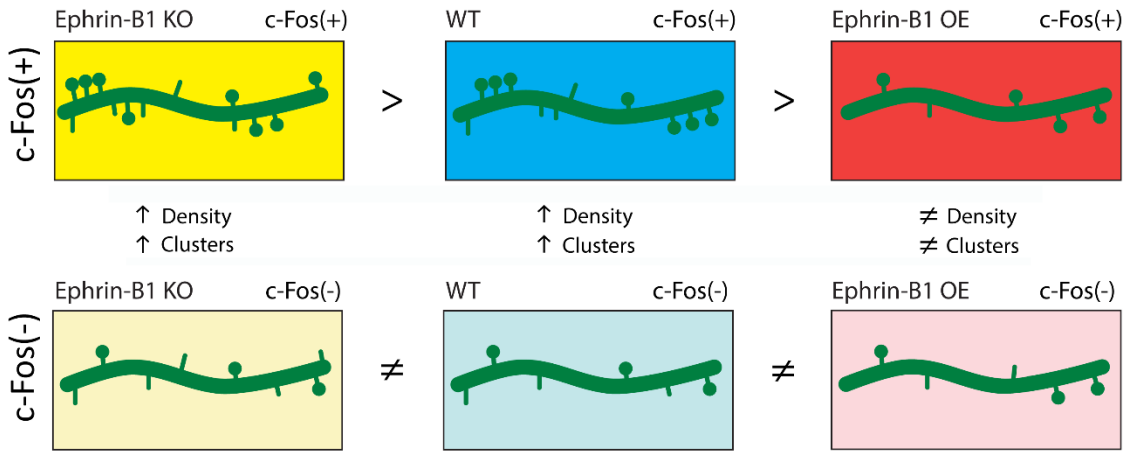

Figure 4.6 Schematic depiction of the effect of astrocytic ephrin-B1 KO or OE on dendritic spine formation following training. Astrocytic ephrin-B1 regulates excitatory connections in the CA1 hippocampus during contextual memory formation in an activity dependent manner. c-Fos(+) neurons activated during contextual memory recall show higher dendritic spines density and clustering compared to non-activated c-Fos(-) neurons in WT and KO mice. In contrast, no changes in dendritic spine density and clustering were observed between c-Fos(+) and c-Fos(-) neurons in CA1 hippocampus containing astrocytes that overexpress ephrin-B1 (OE). There was a higher number of spines on c-Fos(+) neurons of KO mice compared to WT mice, whereas a lower spine density was observed on c-Fos(+) neurons of OE mice compared to WT mice, coinciding with the enhanced or impaired memory recall, respectively. No differences were detected in spine density on non-activated c-Fos(-) neurons between WT, KO, and OE mice. All together these findings suggest that astrocytic ephrin-B1 is a negative regulator of learning-induced spine formation on activated CA1 neurons.

Table 4.1 Extended data table supporting Figure 4.4. Table shows the number of spine clusters with 3, 4, 5, 6 and 7 spines in c-Fos(-) and c-Fos(+) CA1 neurons of WT, KO, and OE mice. Statistical analysis of differences between c-Fos(-) and c-Fos(+) expression was performed using two-way ANOVA (c-Fos and cluster size as factors) with Bonferroni post hoc test: *P < 0.05, ****P < 0.001.

Spines per Cluster (Clusters per 100 µm dendritic length)					
	3	*4*	*5*	*6*	*7*
WT					
c-Fos(—) (n=6)	3.42 ± 0.46	1.56 ± 0.26	0.62 ± 0.13	0.42 ± 0.14	0.16 ± 0.06
c-Fos(+) (n=6)	4.59 ± 0.34	1.41 ± 0.29	1.36 ± 0.21	0.54 ± 0.30	0.38 ± 0.09
Statistics	t = 3.232 *p = 0.0109	t = 0.404 p > 0.999	t = 2.032 p = 0.2374	t = 0.333 p > 0.999	t = 0.593 p > 0.999
KO					
c-Fos(—) (n=15)	3.00 ± 0.41	1.84 ± 0.30	0.86 ± 0.26	0.28 ± 0.11	0.18 ± 0.08
c-Fos(+) (n=13)	5.67 ± 0.80	2.77 ± 0.48	1.04 ± 0.19	0.61 ± 0.19	0.45 ± 0.18
Statistics	t = 5.360 ****p < 0.0001	t = 1.853 p = 0.3306	t = 0.369 p > 0.999	t = 0.659 p > 0.999	t = 0.561 p > 0.999
OE					
c-Fos(—) (n=7)	5.03 ± 0.66	2.86 ± 0.27	0.84 ± 0.17	0.70 ± 0.28	0.46 ± 0.16
c-Fos(+) (n=7)	4.35 ± 0.29	2.32 ± 0.37	1.18 ± 0.18	0.66 ± 0.31	0.37 ± 0.16
Statistics	t = 1.503 p = 0.6906	t = 1.197 p > 0.999	t = 0.760 p > 0.999	t = 0.099 p > 0.999	t = 0.191 p > 0.999

Chapter 5 : Conclusion

The nervous system is comprised of hundreds of billions of neurons interconnected through synapses. Together these synaptic connections allow us to perceive and interact with the world. During development, it is essential that synapses undergo structural and functional modification to ensure neurons find the right partner and form the right connection. These connections continue to be maintained through adulthood, ensuring for proper function. Improper development can lead to neurodevelopmental disorders such as autism and intellectual disabilities. Additionally, improper maintenance of neural circuitry during adulthood can lead to psychiatric and neurodegenerative disorders, such as schizophrenia and Alzheimer's disease. Astrocytes come into close association with synapses, forming the tripartite synapse, and monitor and alter synaptic function. This interaction between astrocytes and neurons is essential for proper synapse development and function during both early postnatal development and adulthood.

This series of studies show that astrocytes expressing ephrin-B1 in the hippocampus are essential for proper synapse formation during early postnatal development, the maintenance of synapses during adulthood, and during learning and memory consolidation. During early postnatal development, astrocytic ephrin-B1 is essential for proper E/I circuitry formation in the hippocampus. In adulthood, loss of astrocytic ephrin-B1 impairs proper synapse maintenance, resulting in aberrant synaptogenesis. Interestingly, during learning and memory consolidation astrocytic ephrin-B1 selectively affects formation and clustering of synapses on neurons activated

during memory recall. Together, the main function of astrocytic ephrin-B1 is to negatively regulate synapse formation.

The hippocampus circuitry remains plastic throughout life therefore allowing for life-long learning (May, 2011; Lovden et al., 2013). During the first month of birth, the hippocampus undergoes intensive synaptic alterations. At birth, synapse numbers are still low and appear immature, containing synapses located mostly on dendritic shafts or small protrusions called filopodia (Steward and Falk, 1991; Fiala et al., 1998). During the second and third weeks, synaptogenesis occurs and dramatically increases synapse number (Steward and Falk, 1991; De Felipe et al., 1997). By the end of the third week synapses have become more mature and are primarily found on dendritic spines of hippocampal pyramidal neurons (Boyer et al., 1998). Synapse formation is then reduced during the fourth week after birth and onto adulthood. This synapse elimination allows for refinement and maturation of synaptic circuits. In adulthood, the hippocampus remains dynamic; however, the overall synaptic efficacies is more stationary as average spine density and size remain constant (Steward and Falk, 1991; Harris et al., 1992; De Felipe et al., 1997). During hippocampal circuit formation, mature astrocytes populate the hippocampus (Yang et al., 2013), and can express synapse-promoting proteins, such as glypican (Allen et al., 2012) and thrombospondin (Christopherson et al., 2005), to modulate synapse formation and maturation. Astrocytes can also affect synapse elimination to allow for synapse refinement (Chung et al., 2013). Together, astrocytes are an active player during all the steps of hippocampus circuitry formation and maintenance. From my studies, I focused on three periods: (1) early postnatal development when

synapse elimination exceeds synapse formation, (2) adulthood when synapse numbers remain stable, and (3) during learning and memory consolidation when synapses are most plastic.

Astrocytic ephrin-B1 negatively regulates synapse formation during early postnatal development, adulthood, and during learning and memory consolidation. However, it should be noted that astrocytic ephrin-B1 selectively inhibits synapse formation in an activity dependent manner. During learning and memory consolidation, hippocampal circuitry is dynamically altered such that acquisition of new memories facilitates synapse formation and maturation (Restivo et al., 2009; Giachero et al., 2013). I show that loss of astrocytic ephrin-B1 increased dendritic spine numbers on activated CA1 hippocampal pyramidal cells following training of a fear conditioning paradigm. Conversely, overexpression of astrocytic ephrin-B1 impaired synapse formation on activated CA1 neurons following training. Astrocytic ephrin-B1 may affect new synapse formation during learning by competing with neuronal ephrin-B for binding to neuronal EphB receptors. Loss of several EphB receptors is known to affect synapse and dendritic spine formation in the hippocampus (Ethell et al., 2001; Henkemeyer et al., 2003). Interestingly, formation of new dendritic spines on activated neurons occur in “hot-spots” or preferential dendritic regions essentially forming clusters of spines following learning (Frank et al., 2018). This phenomenon occurred in both WT and astrocytic ephrin-B1 deletion after contextual fear conditioning. However, as spine density was decreased in overexpression of astrocytic ephrin-B1, spine clusters did not form on activated neurons

during contextual recall. Together, this suggests that astrocytic ephrin-B1 is a negative regulator of learning-induced spine formation.

Following synapse formation, selective synapses will become matured. Maturation of synapses include larger dendritic spine size with larger postsynaptic densities (Harris et al., 1992), therefore allowing for more AMPAR recruitment and anchorage (Ashby et al., 2006; Matsuzaki, 2007). Although astrocytic ephrin-B1 negatively regulates synapse formation, it does not affect synapse maturation in early postnatal development, adulthood, or following learning and memory consolidation. During early postnatal development, loss of astrocytic ephrin-B1 increases excitatory synapse formation and in turn enhances synaptic function. However, AMPAR/NMDAR amplitude and levels of synaptic AMPARs is unaffected indicating no changes to synapse maturation. During adulthood, astrocyte-specific ablation of ephrin-B1 triggers an increase in the density of glutamatergic synapses and dendritic spines. However, synapse formation does not always correlate with an increase in synaptic strength, as newly formed synapses are often associated with silent post-synaptic spines that are usually smaller and are characterized by the presence of NMDA but absence of AMPA receptors (Isaac et al., 1995; Durand et al., 1996). In adult deletion of astrocytic ephrin-B1, there is an abundance of immature, potentially silent, synapses. The loss of astrocytic ephrin-B1 induces formation of these immature synapses. Unlike during development when there is greater synapse maturation processes occurring (Lohmann and Kessels, 2014) and higher expression of specific astrocytic synaptogenic proteins (Farhy-Tselnicker and Allen, 2018), maturation during adulthood occurs slower. Therefore, loss of astrocytic ephrin-

B1 induces synaptogenesis of immature excitatory synapses. Following learning and memory consolidation, there was no differences in dendritic spine size, synaptic AMPAR levels, and AMPAR/NMDAR amplitude ratio in both ablation and overexpression of astrocytic ephrin-B1 compared to their WT counterparts. The increased number of synapses following deletion of astrocytic ephrin-B1 could be a result of reduced engulfment of immature synapses by astrocytes, as primary astrocytes expressing ephrin-B1 engulf synaptosomes containing EphB receptors. Astrocytic ephrin-B1 may trigger the engulfment of synaptic sites through the activation of ephrin-B1 reverse signaling in astrocytes following its interaction with neuronal EphB receptor.

GABAergic inhibitory neurons populate the brain to modulate and efficiently control information flow within cortical circuits. The hippocampus comprises a large diversity of inhibitory neurons containing approximately 21 classes of inhibitory neuron subtypes (Klausberger and Somogyi, 2008). Hippocampal function, specifically memory formation, requires input from local inhibitory neurons. In fact, ablation of $GABA_A$ receptor α5 subunit increased contextual recall (Crestani et al., 2002; Yee et al., 2004) and enhanced spatial learning in mice (Collinson et al., 2002). An interesting finding was the role of astrocytic ephrin-B1 during early postnatal development versus adulthood. Loss of astrocytic ephrin-B1 during early postnatal development results in overall E/I imbalance due to both increased excitatory synaptogenesis and impaired inhibitory circuitry formation. In adulthood, ablation of astrocytic ephrin-B1 results in aberrant excitatory synaptogenesis. This potentially indicates astrocytic ephrin-B1 may affect hippocampal inhibitory neurons only during early postnatal development when inhibitory

circuitry is still being established. Inhibitory neurons are generated during embryonic development in two stages between E9-E12 and E12-E16 from the medial ganglionic eminences (MGE) and caudal ganglionic eminences (CGE) (Butt et al., 2005; Miyoshi et al., 2010; Tricoire et al., 2011) and will invade the hippocampus by E14 (Tricoire et al., 2011). In particular, PV-expressing inhibitory neurons are derived from the MGE and are generated in an early phase at E9.5-11.5 and a late phase at E13.5-15.5 (Donato et al., 2015). However, the expression of PV in interneurons is low until P12 and gradually increases until P30 (Nitsch et al., 1990; de Lecea et al., 1995). In addition, early studies showed no evidence of inhibition prior to P18 but will steadily increase to adult levels by P28 (Michelson and Lothman, 1989). Excitatory responses in rat CA1 hippocampus are established within two weeks following birth; however, the maturation of inhibitory processes was not evident until several weeks later. The loss of astrocytic ephrin-B1 during early postnatal development resulted in decreased expression of PV interneurons in the hippocampus. As expression of PV is still increasing during this period in an activity dependent manner, the loss astrocytic ephrin-B1 may be affecting either (1) excitatory innervation of PV inhibitory neurons affecting the increase in PV expression or (2) the maturation of inhibitory neurons in the CA1 hippocampus during P14-P28 period. Indeed, loss of astrocytic ephrin-B1 does reduce excitatory input onto PV-expressing inhibitory neuron, thereby decreasing overall PV expression. However, Eph/ephrin signaling has also been implicated in migration and neurogenesis in the hippocampus (Chumley et al., 2007; Ashton et al., 2012). Therefore, astrocytic ephrin-B1 may be

essential in maintaining proper E/I balance by influencing PV cell development in CA1 hippocampus during early postnatal development.

Behavioral deficits may manifest due to hippocampal circuit changes. Indeed, during early postnatal development, loss of astrocytic ephrin-B1 impaired E/I balance resulting in reduced sociability and increased digging repetitive-like behaviors. These behaviors may be a result of aberrant excitatory synaptogenesis, the loss of PV expression in the hippocampus, or a combination of both. Interestingly, these mice displayed two core autism symptoms: (1) reduced social interactions and (2) restricted repetitive patterns of behaviors (Kazdoba et al., 2016). Indeed, excessive synaptogenesis has been linked to several neurodevelopmental disorders, such as autism (Huttenlocher and Dabholkar, 1997; Guang et al., 2018). Additionally, PV interneurons play a role in social and repetitive behaviors. In a study, depletion of PV-expression in interneurons results in reduced social interactions and ultrasonic vocalizations, increased repetitive and stereotyped patterns of behaviors, seen with impaired reversal learning, and increased seizure susceptibility (Wohr et al., 2015). It is interesting to note these PV-depleted mice exhibited no impairments with motor function and no anxiety-like or depression-like behaviors (Wohr et al., 2015). Additionally, blocking synaptic transmission of PV neurons specifically in the ventral hippocampus was also shown to impair social memory discrimination (Deng et al., 2019). Interestingly, despite changes to social and repetitive behaviors, loss of astrocytic ephrin-B1 during early postnatal development does not affect learning and memory consolidation and recall. However, memory recall, specifically contextual recall, is enhanced when astrocytic ephrin-B1 is lost during adulthood.

Enhanced contextual recall may be due to the increase in synaptogenesis of immature excitatory synapses. Immature spines may represent potential sites for new memories (Matsuzaki, 2007), and mature following persistent stimulation of synapses during fear conditioning training. This new learned experience will modify the synaptic structure through selective stabilization of synapses and synthetization and recruitment of AMPARs into spines (Lichtman and Colman, 2000; Matsuo et al., 2008; Draft and Lichtman, 2009; Holtmaat and Svoboda, 2009). Indeed, following training, dendritic spine size increased and expressed higher levels of synaptic AMPAR and AMPAR function.

In summary, my studies demonstrate that astrocytic ephrin-B1 is essential for proper hippocampal circuit formation and maintenance. These findings establish the role of astrocytic ephrin-B1 as a negative regulator of synapse formation. It is interesting to note the differential effects following loss of astrocytic ephrin-B1 at different ages. Targeting astrocytic ephrin-B1 may be a potential avenue to repair E/I balance in neurodevelopmental disorder, while during adulthood, inhibition of astrocytic ephrin-B1 may be beneficial to reduce synapse loss in neurodegenerative diseases. Additionally, my studies focus only in a unidirectional astrocyte to neuron pathway. It is still unclear if synaptic activity can directly regulate astrocytic ephrin-B1 function. Continued studies of how astrocytic ephrin-B1 mediates circuit modifications may be imperative to understand how specific neurodevelopmental and neurodegenerative disorders begin. Taken all together, this still leaves exciting possibilities with potentially far reaching impact.

References

Allen, N.J., Bennett, M.L., Foo, L.C., Wang, G.X., Chakraborty, C., Smith, S.J., et al. (2012). Astrocyte glypicans 4 and 6 promote formation of excitatory synapses via GluA1 AMPA receptors. *Nature* 486(7403)**,** 410-414. doi: 10.1038/nature11059.

Ashby, M.C., Maier, S.R., Nishimune, A., and Henley, J.M. (2006). Lateral diffusion drives constitutive exchange of AMPA receptors at dendritic spines and is regulated by spine morphology. *J Neurosci* 26(26)**,** 7046-7055. doi: 10.1523/jneurosci.1235-06.2006.

Ashton, R.S., Conway, A., Pangarkar, C., Bergen, J., Lim, K.I., Shah, P., et al. (2012). Astrocytes regulate adult hippocampal neurogenesis through ephrin-B signaling. *Nat Neurosci* 15(10)**,** 1399-1406. doi: 10.1038/nn.3212.

Boyer, C., Schikorski, T., and Stevens, C.F. (1998). Comparison of hippocampal dendritic spines in culture and in brain. *J Neurosci* 18(14)**,** 5294-5300.

Butt, S.J., Fuccillo, M., Nery, S., Noctor, S., Kriegstein, A., Corbin, J.G., et al. (2005). The temporal and spatial origins of cortical interneurons predict their physiological subtype. *Neuron* 48(4)**,** 591-604. doi: 10.1016/j.neuron.2005.09.034.

Christopherson, K.S., Ullian, E.M., Stokes, C.C., Mullowney, C.E., Hell, J.W., Agah, A., et al. (2005). Thrombospondins are astrocyte-secreted proteins that promote CNS synaptogenesis. *Cell* 120(3)**,** 421-433. doi: 10.1016/j.cell.2004.12.020.

Chumley, M.J., Catchpole, T., Silvany, R.E., Kernie, S.G., and Henkemeyer, M. (2007). EphB receptors regulate stem/progenitor cell proliferation, migration, and polarity during hippocampal neurogenesis. *J Neurosci* 27(49)**,** 13481-13490. doi: 10.1523/jneurosci.4158-07.2007.

Chung, W.S., Clarke, L.E., Wang, G.X., Stafford, B.K., Sher, A., Chakraborty, C., et al. (2013). Astrocytes mediate synapse elimination through MEGF10 and MERTK pathways. *Nature* 504(7480)**,** 394-400. doi: 10.1038/nature12776.

Collinson, N., Kuenzi, F.M., Jarolimek, W., Maubach, K.A., Cothliff, R., Sur, C., et al. (2002). Enhanced learning and memory and altered GABAergic synaptic transmission in mice lacking the alpha 5 subunit of the GABAA receptor. *J Neurosci* 22(13)**,** 5572-5580. doi: 20026436.

Crestani, F., Keist, R., Fritschy, J.M., Benke, D., Vogt, K., Prut, L., et al. (2002). Trace fear conditioning involves hippocampal alpha5 GABA(A) receptors. *Proc Natl Acad Sci U S A* 99(13)**,** 8980-8985. doi: 10.1073/pnas.142288699.

De Felipe, J., Marco, P., Fairen, A., and Jones, E.G. (1997). Inhibitory synaptogenesis in mouse somatosensory cortex. *Cereb Cortex* 7(7)**,** 619-634. doi: 10.1093/cercor/7.7.619.

de Lecea, L., del Rio, J.A., and Soriano, E. (1995). Developmental expression of parvalbumin mRNA in the cerebral cortex and hippocampus of the rat. *Brain Res Mol Brain Res* 32(1)**,** 1-13. doi: 10.1016/0169-328x(95)00056-x.

Deng, X., Gu, L., Sui, N., Guo, J., and Liang, J. (2019). Parvalbumin interneuron in the ventral hippocampus functions as a discriminator in social memory. *Proc Natl Acad Sci U S A* 116(33)**,** 16583-16592. doi: 10.1073/pnas.1819133116.

Donato, F., Chowdhury, A., Lahr, M., and Caroni, P. (2015). Early- and late-born parvalbumin basket cell subpopulations exhibiting distinct regulation and roles in learning. *Neuron* 85(4)**,** 770-786. doi: 10.1016/j.neuron.2015.01.011.

Draft, R.W., and Lichtman, J.W. (2009). It's lonely at the top: winning climbing fibers ascend dendrites solo. *Neuron* 63(1)**,** 6-8. doi: 10.1016/j.neuron.2009.07.001.

Ethell, I.M., Irie, F., Kalo, M.S., Couchman, J.R., Pasquale, E.B., and Yamaguchi, Y. (2001). EphB/syndecan-2 signaling in dendritic spine morphogenesis. *Neuron* 31(6)**,** 1001-1013. doi: 10.1016/s0896-6273(01)00440-8.

Farhy-Tselnicker, I., and Allen, N.J. (2018). Astrocytes, neurons, synapses: a tripartite view on cortical circuit development. *Neural Dev* 13(1)**,** 7. doi: 10.1186/s13064-018-0104-y.

Fiala, J.C., Feinberg, M., Popov, V., and Harris, K.M. (1998). Synaptogenesis via dendritic filopodia in developing hippocampal area CA1. *J Neurosci* 18(21)**,** 8900-8911.

Frank, A.C., Huang, S., Zhou, M., Gdalyahu, A., Kastellakis, G., Silva, T.K., et al. (2018). Hotspots of dendritic spine turnover facilitate clustered spine addition and learning and memory. *Nat Commun* 9(1)**,** 422. doi: 10.1038/s41467-017-02751-2.

Giachero, M., Calfa, G.D., and Molina, V.A. (2013). Hippocampal structural plasticity accompanies the resulting contextual fear memory following stress and fear conditioning. *Learn Mem* 20(11)**,** 611-616. doi: 10.1101/lm.031724.113.

Guang, S., Pang, N., Deng, X., Yang, L., He, F., Wu, L., et al. (2018). Synaptopathology Involved in Autism Spectrum Disorder. *Front Cell Neurosci* 12**,** 470. doi: 10.3389/fncel.2018.00470.

Harris, K.M., Jensen, F.E., and Tsao, B. (1992). Three-dimensional structure of dendritic spines and synapses in rat hippocampus (CA1) at postnatal day 15 and adult ages: implications for the maturation of synaptic physiology and long-term potentiation. *J Neurosci* 12(7)**,** 2685-2705.

Henkemeyer, M., Itkis, O.S., Ngo, M., Hickmott, P.W., and Ethell, I.M. (2003). Multiple EphB receptor tyrosine kinases shape dendritic spines in the hippocampus. *J Cell Biol* 163(6)**,** 1313-1326. doi: 10.1083/jcb.200306033.

Holtmaat, A., and Svoboda, K. (2009). Experience-dependent structural synaptic plasticity in the mammalian brain. *Nat Rev Neurosci* 10(9)**,** 647-658. doi: 10.1038/nrn2699.

Huttenlocher, P.R., and Dabholkar, A.S. (1997). Regional differences in synaptogenesis in human cerebral cortex. *J Comp Neurol* 387(2)**,** 167-178. doi: 10.1002/(sici)1096-9861(19971020)387:2<167::aid-cne1>3.0.co;2-z.

Kazdoba, T.M., Leach, P.T., Yang, M., Silverman, J.L., Solomon, M., and Crawley, J.N. (2016). Translational Mouse Models of Autism: Advancing Toward Pharmacological Therapeutics. *Curr Top Behav Neurosci* 28**,** 1-52. doi: 10.1007/7854_2015_5003.

Klausberger, T., and Somogyi, P. (2008). Neuronal Diversity and Temporal Dynamics: The Unity of Hippocampal Circuit Operations. *Science* 321(5885)**,** 53-57. doi: 10.1126/science.1149381.

Lichtman, J.W., and Colman, H. (2000). Synapse elimination and indelible memory. *Neuron* 25(2)**,** 269-278.

Lohmann, C., and Kessels, H.W. (2014). The developmental stages of synaptic plasticity. *J Physiol* 592(1)**,** 13-31. doi: 10.1113/jphysiol.2012.235119.

Lovden, M., Wenger, E., Martensson, J., Lindenberger, U., and Backman, L. (2013). Structural brain plasticity in adult learning and development. *Neurosci Biobehav Rev* 37(9 Pt B)**,** 2296-2310. doi: 10.1016/j.neubiorev.2013.02.014.

Matsuo, N., Reijmers, L., and Mayford, M. (2008). Spine-type-specific recruitment of newly synthesized AMPA receptors with learning. *Science* 319(5866)**,** 1104-1107. doi: 10.1126/science.1149967.

Matsuzaki, M. (2007). Factors critical for the plasticity of dendritic spines and memory storage. *Neurosci Res* 57(1)**,** 1-9. doi: 10.1016/j.neures.2006.09.017.

May, A. (2011). Experience-dependent structural plasticity in the adult human brain. *Trends Cogn Sci* 15(10)**,** 475-482. doi: 10.1016/j.tics.2011.08.002.

Michelson, H.B., and Lothman, E.W. (1989). An in vivo electrophysiological study of the ontogeny of excitatory and inhibitory processes in the rat hippocampus. *Brain Res Dev Brain Res* 47(1)**,** 113-122. doi: 10.1016/0165-3806(89)90113-2.

Miyoshi, G., Hjerling-Leffler, J., Karayannis, T., Sousa, V.H., Butt, S.J., Battiste, J., et al. (2010). Genetic fate mapping reveals that the caudal ganglionic eminence produces a large and diverse population of superficial cortical interneurons. *J Neurosci* 30(5)**,** 1582-1594. doi: 10.1523/jneurosci.4515-09.2010.

Nitsch, R., Soriano, E., and Frotscher, M. (1990). The parvalbumin-containing nonpyramidal neurons in the rat hippocampus. *Anat Embryol (Berl)* 181(5)**,** 413-425. doi: 10.1007/bf02433788.

Restivo, L., Vetere, G., Bontempi, B., and Ammassari-Teule, M. (2009). The formation of recent and remote memory is associated with time-dependent formation of dendritic spines in the hippocampus and anterior cingulate cortex. *J Neurosci* 29(25)**,** 8206-8214. doi: 10.1523/jneurosci.0966-09.2009.

Steward, O., and Falk, P.M. (1991). Selective localization of polyribosomes beneath developing synapses: a quantitative analysis of the relationships between polyribosomes and developing synapses in the hippocampus and dentate gyrus. *J Comp Neurol* 314(3)**,** 545-557. doi: 10.1002/cne.903140311.

Tricoire, L., Pelkey, K.A., Erkkila, B.E., Jeffries, B.W., Yuan, X., and McBain, C.J. (2011). A blueprint for the spatiotemporal origins of mouse hippocampal interneuron diversity. *J Neurosci* 31(30)**,** 10948-10970. doi: 10.1523/jneurosci.0323-11.2011.

Wohr, M., Orduz, D., Gregory, P., Moreno, H., Khan, U., Vorckel, K.J., et al. (2015). Lack of parvalbumin in mice leads to behavioral deficits relevant to all human autism core symptoms and related neural morphofunctional abnormalities. *Transl Psychiatry* 5**,** e525. doi: 10.1038/tp.2015.19.

Yang, Y., Higashimori, H., and Morel, L. (2013). Developmental maturation of astrocytes and pathogenesis of neurodevelopmental disorders. *J Neurodev Disord* 5(1)**,** 22. doi: 10.1186/1866-1955-5-22.

Yee, B.K., Hauser, J., Dolgov, V.V., Keist, R., Mohler, H., Rudolph, U., et al. (2004). GABA receptors containing the alpha5 subunit mediate the trace effect in aversive and appetitive conditioning and extinction of conditioned fear. *Eur J Neurosci* 20(7)**,** 1928-1936. doi: 10.1111/j.1460-9568.2004.03642.x.